NORTHWESTERN UNIVERSITY

Identifying Molecular Pathways Linking Circadian Rhythms and Neurodegeneration

A DISSERTATION

SUBMITTED TO THE GRADUATE SCHOOL
IN PARTIAL FULFILLMENT OF THE REQUIREMENTS

for the degree

DOCTOR OF PHILOSOPHY

Field of Interdepartmental Biological Sciences (IBiS)

By
Fangke Xu

EVANSTON, ILLINOIS

June 2019

Abstract

Neurodegenerative diseases (NDs) commonly involve the accumulation and aggregation of neurotoxic proteins that impair and ultimately destroy specific neurons. Considerable evidence from human and animal studies indicates that many NDs show disrupted circadian and sleep as symptoms. Yet little is known about the molecular mechanisms by which genes cause NDs could impair circadian rhythmicity. In addition, it is unknown if circadian clocks, in turn, can modulate ND pathogenesis. To address the relationship between circadian clocks and neurodegenerative diseases, we performed a large-scale screen of genetic ND models in *Drosophila*, and found a several, including mutant *Htt* (mHtt; for Huntington's Disease; HD), *TDP43/FUS* (for amyotrophic lateral sclerosis; ALS) and mutant *ATNX3* (for spinocerebellar ataxia type 3; SCA3), that display poor circadian rhythmicity when they are expressed in circadian neurons. These models display a range of molecular and cellular phenotypes from loss of neuropeptide expression and cell loss.

To understand the basis of this poor rhythmicity, we analyzed the molecular and cellular impact of mHtt which resulted in poor behavioral rhythmicity and loss of a key subset of clock neurons. We also observed a dramatic reduction in the core clock component PERIOD. To determine if the clock-regulated mHtt effects, we examined cell loss under 10:10 cycles and found that this condition was neuroprotective but that this effect was gone in a per^{S} mutant, confirming a role of circadian timing. Similarly, we observed neuroprotective effects in mutants of the core clock activator *Clk* which was suppressed in double mutants also lacking the CLK repressor, PER. Thus, circadian clocks are not only a target of mHtt but may also be an important player in mediating mHtt-mediated pathogenesis.

To identify genes that mediate the effect of the clock on mHtt, we used a behavioral screen for HD suppressors, identifying clock-regulated genes that modify both pre-degenerative/functional and/or cell death effects of mHtt. As part of this screen, several novel pathways that mediate mHtt effects on behavior have been discovered including the RNA-binding

protein encoded by Ataxin2 (*Atx2*), involved in multiple NDs, and a co-chaperon, encoded by Hsp70/90 Organizing Protein (*Hop*) which is involved in multiple NDs. Overall, these studies reveal the clock-regulated molecular and cellular pathways that link mHtt to clock disruption.

Acknowledgment

Firstly, I would like to thank my advisor, Dr. Ravi Allada. After my first-year rotation, I join the lab without hesitation due to my interest in the project I was working, which later developed into this thesis. Ravi is a mentor who is very accurate about details in research. I need to think and search carefully in order to answer his questions in our meetings. During this process, I could already learn a lot even before I get to the answer. Ravi also pays great attention to the skills on how to make good presentations. There would always be emails and/or meetings following each lab meeting or other presentation, providing suggestions on how to make the presentations better. Because of the broad research topics all the other postdocs were focusing on in the lab, and also the diverse collaborations Ravi developed, I was exposed to many opportunities to learn new skills and techniques. All those details add up and make the lab a great environment to learn how to do research. I know there is still a lot to learn and improve, and I am sure that many pieces of the advice from Ravi will accompany my further scientific career, which I will benefit from for the long run.

I want to thank our previous research assistant professor in the lab, Dr. Valerie Kilman. Valerie was the first person I was working with in the lab. She always guided people who are new to the lab. Without her, I could not pick up the essential skills I need quickly. She was also like “the mom” to the lab since she knew how to solve anything. On a weekend when the cooling system broke down, Valerie came into the lab and rescued the dark room for behavior by removing the whole door. I still remember how saved I felt after I was panicking by myself for a while.

I want to thank my committees, Dr. Morimoto, Dr. Beitel, and Dr. Gallio providing me a lot of advice and feedback in my annual reviews. My presentations always run over time, and they were very patient and usually would offer me extra time squeezed from their busy schedule to let me finish. I appreciate all the help I got on my path to obtain my Ph.D.

The postdocs I worked most closely with are Jongbin, Daesung and Taichi. After I finished my preliminary screening for the ND genes, Ravi assigned we four as a group for some follow-up study. Daesung created a folder on the server for the data from that project at that time and named it “Fantastic Four”. From then, they became my mentors but also friends. Daesung is an expert on aging so we were in the same DARPA project at the beginning. He would always give me good suggestions on aging-related questions as well as on my presentations. Jongbin and Taichi were both from circadian labs and are the very skilled molecular biologists. I learned a lot of circadian knowledge and molecular experimental skills with their generous help. Daesung always kindly invite us to his home for holidays such as Thanksgiving and Christmas. I was not able to go back visit my own families often, but there were no holidays I feel lonely.

I want to thank Ela and Matt, two postdocs who had the most overlap time with me in the lab. Ela is a very organized researcher; even one-minute delay in her schedule would make her nervous. From her, I learned how to plan experiments ahead and efficiently. Although we do not have much time, I did learn a little tennis from Ela. Matt mostly worked in the darkroom on ePhys for most of the time, so we did not have many chances to talk at first. However, over time, besides he is always very critical in the lab meeting, I found him a very kind person. He would always come up with a solution if you went to him for help. I learned the will to take actions on things need to be resolved.

Evrim came to the lab later, but since he is a fan of Naruto, we became friends very soon. Evrim spent a long time in the circadian field, so we had a lot of discussions on circadian. He is also a critical person, which meant I got questioned on my data quite often and made me think about things I have not noticed.

More than 15 postdocs joined and left during the years I was in the lab. They are all outstanding researchers from either circadian or non-circadian fields, and they are all very nice

people to work with. I might not be able to thank everyone here one by one here, but I did learn different things from everyone.

I would also like to thank Tomas and Melanie, two Ph.D. students younger than me. They are both sweet and fun people who always try to bring more laughter to the lab. Tomas set the trend of dressing up for Halloween in the lab (although he stopped after two years). He is a great cook, so we enjoyed talking about cooking and baking a lot. He used to be one of the two people who work on sleep at a time. Without him, I would know much less about the sleep (although I still have very limited knowledge of the sleep). Melanie is a girl who is always energetic and excited about things. Since we both love music, I took advantage of her free entrance to music building practice rooms to enjoy playing some music.

I deeply thank my families, who supported me to come this far to pursue research. My grandpas were always excited to learn what I was working on and encouraged me to hold on to my enthusiasm for science. However, I am sorry for not being very helpful for most of the family issues while my mother and aunt took all the burdens during the past years.

Last but not least, I would like to thank my friends at NU and in Evanston. Yiwen, Angela, Baobao, Sali, Xiaobao, Han, Heeseon, Yunxiao, Liang and my IBiS peers who came to NU around a similar time as me. They always host home parties for holidays, which unites us like a family. Without them, I could not have much fun and warm time outside the lab. I also met many friends through Pokémon GO. Many of those friends turn into lifelong friends but no longer just friends in the game. My friends in China, in other countries and in other states in the US continuously send me postcards when they are traveling since they know I collect stamps and I do not leave campus. I have a wall full of postcards from all over the world by my desk now.

I am really grateful for meeting all the good mentors who guided me, all the excellent researchers I could learn from, all the good friends I could share laughter and tears. The years I spent at NU will become my precious memory forever.

List of Abbreviations

12:12 LD 12 hour light 12 hour dark LD cycle

10:10 LD 10 hour light 10 hour dark LD cycle

Aβ amyloid β

AD Alzheimer's disease

ALS amyotrophic lateral sclerosis

APP β amyloid protein precursor

APPL β amyloid protein precursor-like

ATX2 ATAXIN 2

AVP arginine-vasopressin peptide

BMAL1 brain and muscle arnt-like protein 1

cAMP cyclic adenosine monophosphate

CK2 casein kinase 2

CLK CLOCK

CrebA Cyclic-AMP Response Element Binding Protein A

CRY CRYPTOCHROME

CT Circadian Time

Ctrl Control

CWO CLOCKWORK ORANGE

CYC CYCLE

DBT DOUBLETIME

DD constant darkness

DN dorsal neuron

DN1a anterior dorsal neuron

DN1p posterior dorsal neuron

DNA deoxyribonucleic acid 9

DNC DUNCE

E cells Evening cells

EEG Electroencephalogram

eIF eukaryotic initiation factor

ER endoplasmic reticulum

FTD frontotemporal dementia

FUS Fused in Sarcoma

G3BP Ras GTPase-activating protein-binding protein

GABA gamma-Aminobutyric acid

GAL4 yeast transcription factor

GAL80 yeast transcription factor, inhibits GAL4 activity

$GAL80^{ts}$ yeast transcription factor, inhibits GAL4 activity at low temperature only

GFP Green Fluorescent Protein

HBE Hofbaur-Buchner eyelet

HD Huntington's Disease

Hel25E Helicase at 25E (UAP56)

hid head involution defective

Hip14 Huntingtin Interacting Protein 14

Hop Hsp70/90 Organizing Protein

Htt Huntingtin

KD knockdown

KO knock out

LD light/dark

LL constant light

lLNv large ventral-lateral neuron

LN lateral neuron

LNd dorsal-lateral neuron

LPN lateral posterior neuron

M cells Morning cells

mHtt Mutant *Htt*

NES nuclear export signal

NLS nuclear localization sequence

NREM sleep non-rapid eye movement sleep

OX overexpression

P-bodies processing bodies

PABP polyA binding protein

PD Parkinson's disease

PDF pigment dispersing factor

PDFR pigment dispersing factor receptor

PDP1e PAR-DOMAIN PROTEIN 1e

PER PERIOD

piRNA piwi-interacting RNA

PolyQ polyglutamine

RBP RNA-binding protein

REM sleep rapid eye movement sleep

RFP red fluorescent protein

RNA ribonucleic acid

RNP ribonucleoprotein

SCA spinocerebellar ataxia

SCN suprachiasmatic nucleus

SG stress granule

SGG SHAGGY

SLMB SUPERNUMERARY LIMBS

sLNv small ventral-lateral neuron

TDP43 Transactive response DNA-binding protein 43

TIA-1 T cell-induced antigen 1

TIM TIMELESS

TRiP Transgenic RNAi Project

TYF TWENTYFOUR

UAS upstream activating sequence

V1a/V1b vasopressin receptors 1a and 1b

VIP vasoactive intestinal peptide

VPAC2/VIPR VIP Receptor

VRI VRILLE

WT wild-type

ZT Zeitgeber Time

Table of Contents

List of Tables and Figures

Chapter 1: Introduction

Circadian (or ~24 h) rhythms are driven by internal biological clocks evident from single cell organisms to humans. The circadian clock controls many physiological processes including sleep and feeding behavior. Circadian disruptions have been shown to cause negative effects on general health. Circadian rhythm disruptions are often accompanied with neurodegenerative disorders and are increasingly seen as indicators of neurodegeneration. Yet, little is known about the interplay between circadian disruption and neurodegeneration. Do circadian rhythm disruptions occur because the clock circuitry is affected by neurodegeneration, or can circadian disruptions contribute to the pathogenesis of neurodegenerative diseases as well?

Here we study the interrelationship between Huntington's disease (HD) and circadian clocks using *Drosophila* as a model. HD is a neurodegenerative disease that exhibits robust circadian and sleep disruption. In this chapter, we will review the core properties of circadian rhythms and neurodegenerative diseases and what is known about the relationship between them. We will focus on HD models in *Drosophila* and will also discuss the underlying pathogenic mechanisms of HD.

1.1 Circadian Clocks Modulate Physiological Processes and Behavior

Circadian rhythms have four fundamental properties; they are free-running, have near 24 hr periodicity, synchronize to 24hr environmental cycles, and exhibit temperature compensation. Even in the absence of external environmental cues, rhythms are maintained by an endogenous molecular clock mechanism. The free-running period of this clock is typically around, but not exactly, 24 hr although this differs among species. Critically, the clock can be synchronized by environmental cues such as light, so that organisms can adjust to the 24 hr solar day. Lastly, the

circadian clock is temperature compensated, meaning that the period length is not significantly affected by temperature.

Circadian clocks are present throughout life from photosynthetic bacteria to humans. In higher organisms, clocks are found in most organs and tissues. Circadian rhythms regulate various behavioral and physiological processes. Around 40% of protein-coding genes are controlled by the clock, playing roles in many fundamental pathways (Zhang et al., 2014). Sleep is regulated by a homeostatic process and gated by the circadian clock, and clock gene mutants exhibit disrupted sleep/wake cycles. For example, *Drosophila per* mutants and hamster tau mutants (bearing a mutation in *CK1ε*) both display advanced activity onset (Konopka and Benzer, 1971; Lowrey et al., 2000). Similarly, a mutation in human *PER2* is related to a human sleep disorder, familial advanced sleep phase syndrome (FASPS) (Fu et al., 2001). Feeding behavior is also regulated by the clock in various organisms including mammals and flies (Arble et al., 2009; Sarov-Blat et al., 2000). A daily restricted feeding schedule is sufficient to entrain hepatic clocks (Stokkan et al., 2001). In mammals, body temperature displays a circadian-dependent oscillation pattern (Refinetti and Menaker, 1992), which is used as a marker of circadian phase. Blood pressure also exhibits a consistent daily pattern with two peaks in the morning and afternoon/early evening, and a decline during the night until the next morning (Smolensky et al., 2017).

1.2 Circadian Disruptions via Aberrant Environmental Cues or Genetic Mutations Affect Health

1.2.1 The Effects of Light Exposure Perturbations on Health

Circadian clocks can be disrupted or reset by environmental cues such as abnormal light input. Multiple studies have shown an increased risk for cancer among people who were exposed to light during the night (Davis et al., 2002; Stevens, 2005; Stevens and Rea, 2001). Circadian misalignment or disruption, such as shift work, also has negative effects on metabolism and

mental health (Courtet and Olie, 2012; Fonken et al., 2009; Gonnissen et al., 2012). Even aberrant light-dark cycles that do not disrupt the internal clock can elicit adverse effects. For example, when mice are exposed to an artificial light-dark cycle of just 7 hr, their core clock oscillations and activity rhythms continue to free-run with ~24 hr periodicity. Yet these mice exhibited increased depression-like symptoms, and impaired hippocampal long-term potentiation and learning (LeGates et al., 2012). It has also been shown that patients with weaker circadian rhythms treated with chemotherapy have a higher risk of neutropenia (Li et al., 2018). On the other hand, light exposure at a particular time point could be therapeutic. For example, a bright light treatment designed to delay the clock improves sleep and mood in Parkinson's disease patients with an advanced circadian phase (Rutten et al., 2012). In AD patients, correcting circadian rhythm impairments by light therapy can improve sleep-wake cycles and cognition (Hanford and Figueiro, 2013). Thus, light exposure can have adverse or beneficial effects in part depending on its impact on the circadian clock. Here, we will apply non-24 hr LD cycles to impact neurodegeneration.

1.2.2 The Effects of Clock Gene Perturbations on Health

In animal models, deletion or mutation of core clock genes has also been shown to have an adverse impact on health and disease. *Clock* mutant mice showed increased mortality after treated with low-dose radiation, which might be due to the up-regulation of pro-apoptotic genes in the absence of *Clock* (Antoch et al., 2008). *Cry2* knockout (KO) with MYC overexpression in the lymphoid cells develop tumors at an earlier age since CRY2 mediates MYC degradation (Huber et al., 2016). *Bmal1* KO mice display reduced lifespan and advanced aging. Those symptoms could be related to the increased oxidative stress observed in the *Bmal1* knockout mice (Kondratov et al., 2006). Age-dependent astrogliosis has been found in the cortex and hippocampus in *Bmal1* knockout or *Clock/Npas2* (*Bmal1*'s binding partners) double knockout mice but not in *Per1/Per2* double knockout mice, which suggests CLOCK/NPAS2/BMAL1 (redox-

related) target genes could be responsible for the aging phenotypes (Musiek et al., 2013). Human and mouse osteoarthritis cartilage showed disruption of *Bmal1* expression and *Bmal1* mutants also develop progressive cartilage degeneration (Dudek et al., 2016). *Clock* mutant mice develop metabolic syndromes and obesity (Turek et al., 2005). Mutations or polymorphisms in multiple circadian genes (*Per2/3* and *CSNK1δ*) are linked to sleep disorders (Takahashi et al., 2008). The $Per3^{5/5}$ mutation that leads to a long period in humans has also been reported to associate with early onset of bipolar disorder type I (Benedetti et al., 2008). Differential effects from specific clock gene disruptions may be explained by the fact that different mutations (e.g., activating vs. repressing) arrest the clock in different states. It is also possible that some of the differential effects may be the result of non-clock functions for the clock genes. For instance, BMAL1 also participates in translational control (Lipton et al., 2015). Here we use clock gene disruptions to assess the impact of circadian disturbance on neurodegeneration as well.

1.3 Neurodegenerative Diseases Result from the Progressive Accumulation of Toxic Proteins in Neurons

Neurodegeneration is frequently the result of the age-dependent accumulation of toxic proteins that impair, and then kill neurons. For example, HTT or ATXN1/2/3 containing expanded polyQ repeats accumulate in neurons in patients with Huntington's disease (HD) and spinocerebellum ataxia 1/2/3, respectively (Williams and Paulson, 2008). Amyloid beta (Aβ) and/or tau are accumulated in the neurons of patients with Alzheimer's disease (AD) (Bloom, 2014). Tau also contributes to frontotemporal dementia (FTD) (Seelaar et al., 2008). Parkinson's disease (PD) features the accumulation of α-synuclein (Jankovic, 2008).

Because neurodegeneration is irreversible in patients, it is crucial to identify these patients as early as possible. Preclinical symptoms such as circadian/sleep disorders could serve as criteria to screen potential ND patients and provide a marker for early intervention.

1.4 The Intricate and Bidirectional Relationship between Circadian Rhythms/Sleep Alterations and Neurodegenerative Diseases

While the field possesses a common view that neurodegenerative diseases lead to circadian and sleep disruption, detailed mechanisms of how the clock is affected and whether clock disruptions contribute to disease pathogenesis remain unclear. We will be reviewing the current knowledge on circadian/sleep disturbances occurring during multiple disease progression stages or even before other clinical symptoms in this section. Also, this section will summarize how could manipulation of circadian rhythms affect neurodegeneration shown by previous studies.

1.4.1 Neurodegenerative Diseases Lead to Sleep/Circadian Disturbances and Alterations in Clock Gene Expression

Altered or disrupted circadian rhythms or sleep often accompany neurodegenerative diseases (Musiek and Holtzman, 2016). Disturbance in sleep-wake activities has been identified in patients with AD, together with a delay in core body temperature (Satlin et al., 1995). The amount of amyloid beta in the cerebrospinal fluid of Alzheimer's patients correlates with the severity of sleep-wake disturbances (Roh et al., 2012). Loss of vasopressin and neurotensin neurons in the suprachiasmatic nucleus (SCN), and altered cortisol secretion have also been observed in AD patients (Giubilei et al., 2001; Stopa et al., 1999). The phase of the sleep/wake cycle is altered in FTD patients and a decrease in sleep has also been reported (Anderson et al., 2009; Merrilees et al., 2009, 2014; Selkoe, 2001). ALS patients frequently experience sleep-wake disturbances (Lo Coco et al., 2011). Meanwhile, Sleep and circadian defects were identified in a recent study demonstrating decreased circadian activity amplitude and REM sleep in mutant FUS knock-in rats for ALS (Zhang et al., 2018c). Sleep disorders have been reported for Parkinson's disease patients (Ferreira et al., 2006; Matsui et al., 2006; Porter et al., 2008; Stevens et al., 2004; Verbaan et al., 2007) as well as mouse models of the disease. For example, circadian activity

amplitude was significantly decreased in a PD mouse model (Kudo et al., 2011a). Patients at a later stage of PD had a significant alteration in melatonin secretion (Bordet et al., 2003) and the low level of melatonin is responsible for excessive daytime sleepiness (Videnovic et al., 2014). Patients with several SCAs (including SCA1/2/3/6), especially SCA3, experience sleep disorders (Chi et al., 2013; Pedroso et al., 2011). Besides REM sleep disruptions caused by motor behavior disorders, sleep spindle densities (distinctive electroencephalography (EEG) oscillations during NREM sleep) are decreased in SCA1/2/3 patients (Botta et al., 2016; Pedroso et al., 2011).

Huntington's disease has sleep and circadian symptoms in common with other NDs. An abnormal circadian activity profile has been found in HD patients (Morton et al., 2005; Wulff et al., 2010) and similar circadian disruption was observed in multiple mice models of HD (Fisher et al., 2013; Loh et al., 2013; Pallier et al., 2007). EEG recording reflected increases in both REM and non-REM sleep in the R6/2 mice (Kantor et al., 2013) while sleep changes including altered sleep phase and a decrease in REM sleep were found in HD patients (Arnulf et al., 2008; Goodman et al., 2011).

Cycling expression of core circadian genes is impaired in several neurodegenerative diseases. For example, phase differences in *Bmal1* and *Per2* expression have been reported in different brain regions in AD patients (Cermakian et al., 2011). *Bmal1* has been found with altered cycling expression in peripheral blood mononuclear cells or total leukocytes from PD patients (Breen et al., 2014; Cai et al., 2010). In HD, the *Bmal1* expression is decreased, and *Per1 and Per2* expressions tend to decrease at an earlier time point compared to the control in the mouse model of HD (Morton et al., 2005; Pallier et al., 2007). As previous data revealed, the standard view is that NDs would cause circadian and sleep disruption. To investigate this hypothesis, we will first test whether expressing different ND genes in fly circadian and sleep controlling neurons can cause circadian and sleep impairments (Chapter 2).

1.4.2 Sleep and Circadian Disruptions Manifest During Early Disease Stage or Prior to the Onset of Clinical Symptoms

One important aspect of the observations in ND patients with sleep/circadian symptoms is that the disruptions appear during the early stage of disease progression or even among individuals prior to the onset of their disease symptomatology. For example, preclinical AD patients with intact cognition lose their melatonin rhythms (Wu et al., 2003). Loss of rhythmic *Bmal1*, *Per1* and *Cry1* mRNA expression in the pineal gland was observed, together with a decrease of AVP mRNA in the SCN from both preclinical and clinical AD patients (Wu et al., 2006). REM sleep behavior disorder is considered a PD preclinical risk factor (Postuma et al., 2012; Trenkwalder, 1998). The absence of nocturnal blood pressure decline and impaired sleep quality/pattern have been found with early-stage or even premanifest HD patients (Cuturic et al., 2009; Diago et al., 2017; Goodman et al., 2011). An increase in delta power (from EEG recording) has been detected in early stage HD patients as well (Hunter et al., 2010). FUS mutation knock-in rats display disrupted sleep and circadian behavior prior to cognitive deficits (Zhang et al., 2018c). These data raise the question of whether circadian/sleep disruption might not only be a consequence of neurodegeneration but also a mediator of the disease pathogenesis at an early stage.

1.4.3 Manipulations of the Clock Influence Neurodegenerative Disease Pathogenesis

Not only does neurodegeneration impact circadian rhythms, but evidence also suggests a role for the circadian clock in neuronal survival and degeneration. Several groups investigated whether core clock gene mutants display aberrant neurodegeneration. In *Drosophila*, disruption of the circadian clock component *period (per)* accelerates neurodegeneration (as evidenced by brain vacuolization) in mutant flies predisposed to oxidative injury (Krishnan et al., 2012), although no direct access of cell dysfunction or death was documented. Inactivation of a kinase (*Doubletime*/DBT) that phosphorylates PER (and regulates periodicity in flies) enhances human

tau-induced retinal degeneration (Means et al., 2015). Mice lacking the core clock component *Bmal1* exhibited swollen presynaptic terminals together with the loss of normal synaptic vesicles (Musiek et al., 2013). These phenotypes are markers for astrogliosis, which is defined by an abnormal increase of astrocytes due to the trauma of nearby neurons, including neuronal death caused by NDs (Musiek et al., 2013). Astrogliosis was also observed in other circadian clock mutants, namely double knockouts of *Clock* and *Npas2* (*Bmal1*'s partners), but not in *Per1/Per2* double KO mice (Musiek et al., 2013). Reduction of *Bmal1* expression promoted neuronal death in cortical primary neuronal cultures and oxidative stress further exacerbated the phenotype (Musiek et al., 2013). Similarly, striatal lesions were larger in *Bmal1* hemizygous mice ($Bmal^{+/-}$) treated with 3-nitropropionic acid (a chemical inducer of oxidative injury and striatal neurodegeneration) (Musiek, 2015). While these data suggest that circadian clocks may contribute to neuronal survival, it is not clear if this would impact human ND models. In fact, loss of *per* failed to alter neurodegeneration, behavior or lifespan in flies expressing different pathogenic human Aβ isoforms (Chen et al., 2014; Long et al., 2014).

Manipulation of the sleep/wake cycle via drugs or light can improve ND related symptoms. Pharmacological management of the sleep-wake cycle in HD mouse models improved cognitive defects caused by HD (Pallier and Morton, 2009). Dysregulation of circadian rhythms through 20:4 LD cycles led to accelerated pathology in a mouse ALS model (SOD1 mutants) (Huang et al., 2018). Light treatment that improved sleep in AD patients also improved cognition (Hanford and Figueiro, 2013). In *Drosophila*, sleep deprivation increased amyloid beta levels while sleep induction decreased amyloid beta (Tabuchi et al., 2015).

Despite the association between circadian clocks and neurodegeneration, it remains unclear what the molecular mechanisms linking the clock to ND are. We aim to further explore specific pathways or mechanisms that mediate the effects of circadian rhythms on neurodegeneration. Due to the profound links between HD and circadian/sleep disruption, HD is

utilized as the primary model in our study focusing on circadian rhythms and neurodegeneration. We will address how mutant Huntingtin (mHTT) alters the clock and if manipulation of the clock affects mHTT toxicity in return in Chapter 3.

1.5 Huntington's Disease is a Fatal Motor Disease that Results from the Expansion of a Polyglutamine Repeat in the Huntingtin Protein

HD results from the inherited expansion of a polyglutamine (polyQ) repeat within the Huntingtin (HTT) protein that leads to striatal neuron death and progressive motor dysfunction. PolyQ disease is a class of neurodegenerative diseases caused by an expansion of CAG trinucleotide repeats in the affected genes (Ashley and Warren, 1995; Koshy and Zoghbi, 1997). Although different genes are affected in different polyQ diseases, they share some similarities in the disease pathology. Nonpathogenic forms of the genes involved in the diseases have a limited number of CAG repeats. When the repeat number exceeds a certain threshold, corresponding mutant proteins containing the expanded polyQ tracts accumulate and aggregate in the cells, impairing the normal cellular functions (Fan et al., 2014). The length of the repeat expansion is commonly correlated with the severity of the disease (Williams and Paulson, 2008). As the number of CAG repeats increases, patients experience earlier disease onset accompanied by more severe symptoms (Durr, 2010). Other polyQ diseases include spinocerebellar ataxias (SCA) types 1, 2, 3, 6, 7 and 17, for example. The toxicity from CAG repeats is not restricted to the proteins containing the polyQ tract but may also result from the RNA directly. It has been reported that RNAs containing CAG repeats partially contribute to the toxicity (de Mezer et al., 2011; Hsu et al., 2011; Li et al., 2008). The toxicity from RNA could be directly related to the hairpin structure formed by the triplet repeat (Nalavade et al., 2013; Todd and Paulson, 2010) or could be due to protein products from antisense repeat-associated non-ATG (RAN) translation (Banez-Coronel et al., 2015).

The human HTT gene encodes a large protein (3114 amino acid) in which the CAG repeats are located in the first exon (Truant et al., 2008). The HTT gene becomes pathogenic when the CAG repeat number exceeds 35 (Lee et al., 2012). The mutant HTT (mHTT) leads to disease pathogenesis with a mean age at onset between 30 and 50 (Roos, 2010). There is a positive correlation between the repeat length and the age of onset for HD (Andrew et al., 1993). The longer polyQ tract is also correlated with a higher propensity to form intraneuronal aggregates, which may contribute to or be associated with the HTT toxicity (Becher et al., 1998; Martindale et al., 1998; van Roon-Mom et al., 2006). Toxic mHTT then induces striatal neurodegeneration (Imarisio et al., 2008; Vonsattel et al., 1985). As a consequence, the major symptoms of HD are involuntary motor movements, chorea, as well as cognitive declines (Roos, 2010). Interestingly, psychiatric and circadian/sleep symptoms can develop prior to locomotor symptoms (Goodman et al., 2011; van Duijn et al., 2007), similar to what has been reported for other NDs as discussed above.

The subcellular localization of HTT appears to be important for its toxicity. Pathogenic HTT undergoes cleavage by caspase, calpains, and MMP-10 (Ross and Tabrizi, 2011). HTT is normally and mainly located in the cytoplasm, while aggregates formed by the N-terminus fragment of mHTT are located in both the cytoplasm and the nucleus (Lee et al., 2004b; Lunkes et al., 2002; Martindale et al., 1998; Saudou et al., 1998). The N-terminus fragment aggregates in the nucleus appear to be more toxic and are sufficient to induce disease symptoms (Benn et al., 2005; Gafni et al., 2004; Juenemann et al., 2011; Mangiarini et al., 1996; Truant et al., 2008). Moreover, the addition of a nuclear export signal (NES) to mHTT blocks striatal neuron apoptosis (Saudou et al., 1998). Aside from the toxicity of different deleterious mutant HTT species, loss of functional wild-type HTT due to the mutation could also contribute to disease pathogenesis. HTT has been shown to be involved in many regulatory pathways that are important for neuronal

survival, including vesicle trafficking and transcriptional regulation, which will be covered in detail in the next section.

Although HTT aggregates are a prominent hallmark observed in patients (Davies et al., 1997; DiFiglia et al., 1997), it is debatable whether aggregates observed in patients are directly linked to disease pathogenesis. On one hand, some studies reveal that decreasing or clearing aggregates, such as through autophagy pathways and chaperone proteins, could rescue degeneration (Jana et al., 2000b; Tsunemi et al., 2012), indicating aggregates are toxic and cause neuronal death. On the other hand, some studies suggest that aggregate formation is not correlated with cell death, but the reduction of soluble pathogenic HTT would rescue degeneration (Arrasate et al., 2004; Lu and Palacino, 2013; Miller et al., 2010). In addition, using higher resolution microscopy, small aggregate species have been found alongside the diffusible form and large inclusions of HTT (Sahl et al., 2012). The different subspecies of HTT aggregates might play a role in the pathogenesis in different ways (Li et al., 2016). Therefore, it is likely that certain pathways or modifiers could suppress the pathogenic phenotypes resulting from one subspecies of pathogenic HTT but not another.

1.6 Mutant Huntingtin Induces Toxicity Via Multiple Pathways

Studies of mHtt toxicity have identified a number of pathways through which it may work. We propose to find pathways controlled by the circadian rhythms that modulate mHTT toxicity. Therefore, we will be reviewing pathways through which mHTT can induce toxicity in this section.

PolyQ expansion in *HTT* leads to protein misfolding, consequently results in toxic aggregation and perturbed protein homeostasis (Labbadia and Morimoto, 2013; Williams and Paulson, 2008). This activates multiple stress pathways in order to clear or reduce aggregation (Lim and Yue, 2015). Activation of heat shock response (HSR) is thought to reduce mHTT/polyQ protein toxicity. Indeed, chemical inducers for HSR (by activating heat shock transcription factor

1 (HSF1)) reduce mHTT (and other polyQ proteins) induced neurodegeneration and/or aggregation (Fujikake et al., 2008; Sittler et al., 2002; Waza et al., 2005). Besides, overexpression of multiple chaperons/heat shock proteins including HSP70, HSP60, HSP110, HSP40,HSP27 and STIP1 (as known as, *Hsp70/90 organizing proteins, Hop*) suppresses mHTT/polyQ protein toxicity (Chan et al., 2000; Hay et al., 2004; Kuo et al., 2013; Nollen et al., 2004; Zourlidou et al., 2007) while knocking down many of those genes enhances the toxicity in warm, fly, mouse or human cell cultures (Brehme et al., 2014; Wolfe et al., 2013; Zhang et al., 2010b). However, other studies suggest that HSP proteins can increase mHTT toxicity. A few studies have demonstrated that HSP90 facilitates mHTT aggregation and inhibition of HSP90 reduced HTT level (Baldo et al., 2012; He et al., 2017; He et al., 2016). Activation of HSF1 lowered the threshold concentration for HTT to form aggregates (Bersuker et al., 2013). Down-regulation of other heat shock genes, including *Stip1* and *Hsc70-4* (heat shock cognate protein), reduces protein toxicity of tau or mutant ATNX3 and HTT (Butzlaff et al., 2015; Vossfeldt et al., 2012; Zhang et al., 2010b), which is consistent with some of our results in Chapter 3. Toxic polyQ protein aggregation can be cleared through autophagy as well (Martin et al., 2015; Pandey et al., 2007). Polymorphism in *ATG7* significantly increases the age of onset for HD and activation of autophagy pathway reduces mHtt toxicity (Metzger et al., 2010; Ravikumar et al., 2004; Sarkar et al., 2008; Sarkar et al., 2009). However, mHTT interferes cargo degradation in the autophagy pathway (Wong and Holzbaur, 2014).

As noted, the nuclear mHTT are more toxic and the inclusions are found even prior to neurological phenotype onset and correlated with the severity of symptoms (Davies et al., 1997). The polyQ region is commonly involved in transcription activation (Mitchell and Tjian, 1989) and polyQ containing proteins are more likely to play a role in transcription regulations (Schaefer et al., 2012). Recent real-time imaging confirmed the interactions between both pathogenic and nonpathogenic HTT with different transcriptional factors, suggesting the role HTT' play on

transcription in general (Li et al., 2016). Therefore, the expanded polyQ region of mHtt may induce toxicity via transcriptional dysregulation prior to the disease onset. TAF(II)130, a transcription factor, could bind to HTT polyQ stretches and lead to suppression of CREB dependent transcription activation (Shimohata et al., 2001). Other studies demonstrated that mHTT decreases CRE-mediated transcription and cAMP signaling can partially rescue the cell death induced by pathogenic polyQ HTT. (Wyttenbach et al., 2001). Wild-type HTT interacts with neuron restrictive silencer element (NRSE) and suppresses its inhibitory activity, thus enabling the transcription of brain-derived neurotrophic factor (BDNF). This interaction is compromised in mutant HTT, which leads to neuronal loss in the striatum due to insufficient transcription of BDNF (Zuccato et al., 2001; Zuccato et al., 2003). Pathogenic polyQ HTT represses the transcription of genes activated by p53, which might result from the interaction between pathogenic polyQ HTT and p53 (Bae et al., 2005; Steffan et al., 2000). It also has been shown that HDAC inhibitors can arrest neurodegeneration caused by mHTT (Mielcarek et al., 2011; Wyttenbach et al., 2001), providing a direction for therapeutic treatment via regulating impaired gene expression in HD.

Subcellular compartment localization of mHTT, including mitochondria and ER, implies it might induce toxicity in other organelles besides nucleus (Jonas, 2014; Ueda et al., 2016). Mutant HTT caused aberrant mitochondrial fission and blocked mitochondrial protein import (Manczak and Reddy, 2015; Song et al., 2011; Yano et al., 2014). Mutant Htt located in the ER membrane and led to ER morphology defects (Ueda et al., 2016). The mitochondrial and ER dysfunctions result from mHtt educe abnormal calcium capacities (Brustovetsky, 2016; De Mario et al., 2016; Panov et al., 2002). Wild-type HTT has been found on the membranes of different type of vesicles including endosome, autophagic vesicles, and trafficking vesicles (Atwal et al., 2007; Caviston and Holzbaur, 2009). HTT might play a role in both microtubule and actin-based vesicle trafficking (Caviston et al., 2007; Pal et al., 2006). Size decreases in perinuclear component and secretory apparatus, reduced perinuclear recycling endosomes, and absence of clustered mitochondria

were observed in *HTT* KO ES cells (Atwal et al., 2007; Caviston and Holzbaur, 2009; Hilditch-Maguire et al., 2000). These data imply the potential functions of wild-type HTT in subcellular organelles that mHTT fails to fulfill leads to HD pathogenesis.

Genes regulated by the clock and involved in pathways mentioned above at the same time could have higher potentials to link circadian rhythms and mHtt toxicity modulation. We identified and will elucidate more on one of the modifier candidates, *Hop*, which complies with both criteria in Chapter 3.

1.7 Drosophila Is A Valid Genetic Model to Study Human Diseases

Drosophila melanogaster, the fruit fly, has been used as a model organism for more than a hundred years, aiding basic biology and biomedical research. In general, *Drosophila* is a great model organism to conduct experiments with because of its shorter life cycle and lifespan. Flies are easier to maintain, and it is also relatively easy to achieve a larger progeny population compared to mammal organisms. Despite its small brain, the fruit fly shows many types of complex behaviors, including learning and memory formation, courtship, aggression, and sleep. A variety of technologies to manipulate gene expression have been established in flies. Transgenic techniques combined with the UAS-Gal4 system, enable human disease genes expression in flies. Given that fly has a shorter lifespan, the phenotypes can be observed or measured faster. For example, fly models expressing human neurodegenerative disease transgenes display similar symptoms to human patients including shortened lifespan, locomotor deficiency, and neuronal dysfunction, or cell death (Bilen and Bonini, 2005b; Stephenson, 2013). But these phenotypes develop during a much shorter period (usually within a month) in the fly compared to mammals. Therefore, after establishing the disease models with measurable phenotypes, fly models are more ideal to be used for large-scale genetic screening. With all the

established knowledge and reagents from the previous studies, *Drosophila* provides us with a powerful platform to perform our screenings.

Many human disease-related genes have homologs or orthologs in flies (Reiter et al., 2001). And genes identified from a forward genetic screening for fly genes involved in neural development and signaling showed strong enrichment in human homologs (93% of the fly genes had human homologs) indicating the conservation between fly and mammals, especially for neuroscience (Yamamoto et al., 2014). In addition, around one-third of the fly homologs have been associated with human disease (Yamamoto et al., 2014). Owing to the complexity of the human genome and the myriad of genes that can be involved in the same disease between individuals, human genome-wide association studies (GWAS) becomes an expedient method for identifying disease-related genes. More than 60% of the disease-related genes that have been discovered through GWAS showed conservation with *Drosophila* genes (Wangler et al., 2017). The conservation between fly and human disease-causing genes, together with other aforementioned advantages, legitimate *Drosophila* as a model for drug screening as well (Fernandez-Hernandez et al., 2016).

Aside from the molecular conservation, the fly has privileges at the cellular level as a model organism. Although the *Drosophila* brain has very different anatomy from human, their neurons share plenty of similarities at the cellular level, making them especially useful in the study of neuroscience (Ugur et al., 2016). Sub-groups of neurons in fly brains follow a functional organization in a similar way to sub-structures in the human brain but the total number of neurons involved in a certain function is much smaller. For example, the approximately 150 circadian neurons in each fly are equivalent to the human suprachiasmatic nucleus (SCN) (Helfrich-Forster et al., 2007; Shafer et al., 2006), which contains around 15,000 neurons (Abruzzi et al., 2017). This makes Drosophila a resealable organism for research that simultaneously possesses both complexity and simplicity.

1.8 Valid *Drosophila* Neurodegenerative Disease Models Have Been Established by Expression of Human Genes Involved in Neurodegenerative Diseases

Genetic diseases could result from two types of mutations of genes: gain-of-function and loss-of-function. Gain-of-function mutations in genes could lead to excess accumulation of toxic protein products and/or overactivation of pathways, while loss-of-function mutations result in misregulation of pathways the affected genes are critically involved in. When modeling different diseases in the flies, diseases due to loss-of-function mutations could be recapitulated by knocking down fly homolog genes or generating loss-of-function mutants. Diseases caused by gain-of-function mutations could be simulated by overexpressing toxic human pathogenic genes or fly homologs utilizing the Gal4-UAS system. Moreover, overexpression of human pathogenic genes can be used to study more complex cases, in which toxic proteins contribute to the disease pathogenesis through gain-of-function (toxic protein accumulation) and loss-of-function (since the original function is disrupted due to aggregation) at the same time.

Mutations in certain genes that are associated to the disease pathogenesis have been discovered for many NDs and then modeled in flies, such as *SOD1*, *TDP43*, and *FUS* for ALS, alpha-synuclein, *PRKN* and *PINK1* for PD, tau, Aβ, and *PSEN* for AD, *HTT* for HD. Transgenic lines expressing wild-type or mutant forms of these genes have been successfully established to study those NDs, which are incorporated into our study. What genes are selected for our study and how each gene contributes to pathogenesis for each ND are discussed in more details in Chapter 2. Expression of human ND related genes with pan-neuronal drivers commonly leads to locomotor defects and shortened lifespan, which recapitulate the most basic disease features of many NDs. Other features including cognitive defects and sleep/wake cycle disturbance are also observed in fly models. For example, TDP43 and FUS overexpression with motor neuron driver lead to morphology defects in larvae motor neuron accompanied with locomotor deficiencies

(Chen et al., 2011; Watson et al., 2008). ATXN3Q78 overexpression cause lethality (Vossfeldt et al., 2012). Pan-neuronal expression of Aβ42 impairs memory in Drosophila (Chiang et al., 2010).

To study the effect of ND-related genes on sleep and circadian rhythms, I systematically screened ~120 ND genes in brain regions regulating circadian rhythms and sleep in *Drosophila.* We found human *TDP43* and *FUS* for ALS pathogenesis, human *PSEN* and fly mutant *Psn* related to AD, polyQ disease gene mutant *ATXN3* or *HTT*, HTT interacting gene *Hip14* and GGGGCC repeat related to both ALS and FTD cause circadian defects.

1.9 *Drosophila* Models for Huntington's Disease Identify Novel and Conserved Mechanisms for mHtt Toxicity

Drosophila HD models recapitulate behavioral, cellular and molecular features of the human disease. As discussed above, the primary gene involved in HD pathogenesis is HTT. Both full length and N-term fragment mHTT transgenic lines have been established and studied in flies. Overexpressing human mHTT in the fly nervous system results in similar phenotypes as in human patients, such as age-dependent locomotor deficiency and shortened lifespan manifest (Gonzales and Yin, 2010; Lee et al., 2004a; Romero et al., 2008; Weiss et al., 2012). Sleep defects and circadian neuron degeneration, similar to HD patients and mouse models of HD, have been reported in the fly with m*HTT* expressed (Gonzales and Yin, 2010; Gonzales et al., 2016; Sheeba et al., 2010). Pan-neuronal drivers have an advantage in eliciting phenotypes resembling HD patients, yet quantification of neurodegeneration is not easy to be accomplished in those flies due to broadly affected neurons. Expressing ND genes in the Drosophila compound eye, using GMR-GAL4, is a powerful way to access neuronal degeneration in the fly (Huber et al., 2016). Overexpression of human m*HTT* transgenes leads to visible and quantifiable degenerative eye morphology phenotypes such as rough eye, pigment loss, and ommatidium disorganization (Lee et al., 2004b; Romero et al., 2008; Wyttenbach et al., 2001; Zhang et al., 2010b). Eye morphology

has been used in the search for modifiers for mHtt toxicity. (Doumanis et al., 2009; Kaltenbach et al., 2007; Zhang et al., 2010b). However, the eye is not a tissue affected in HD. Thus, the neuronal dysfunction in the eye cannot be related to the disease phenotypes. By expressing m*HTT* in circadian GAL4s and testing its effects on sleep, circadian rhythms and neurodegeneration, we hope to generate a more valid *Drosophila* Huntington model that more closely resemble phenotypes observed in patients and mammalian models.

Fly *Htt* is an ortholog for human *HTT* and both genes are involved in similar pathways (Schaefer et al., 2012). Human mHTT overexpression in flies and fly *Htt* knock-down both affected axonal transport (Gunawardena et al., 2003). Meanwhile, overexpression of wild-type HTT rescues the axonal transport defects caused by mHTT overexpression in the fly (Zala et al., 2013). *Htt* RNAi disrupted the spindle positions in fly neuroblasts and fly HTT overexpression could rescue spindle disorientation caused by *HTT* siRNA in mice (Godin et al., 2010). These data suggest the existence of conserved *Huntingtin* functions between fly and mammals, where the molecular and cellular defects caused by human mHTT overexpression could depict actual pathogenic biological processes.

Conserved molecular pathways involved in mHTT pathogenesis have been identified in the fly. For example, chemical or genetical inhibition of histone deacetylases (HDACs) reduces HD pathogenesis in both flies and mammals (Bardai et al., 2013; Ferrante et al., 2003; Hockly et al., 2003; Pallos et al., 2008; Steffan et al., 2001). Activation of either mTor dependent or independent autophagy pathways reduces mHTT toxicity (Ravikumar et al., 2004; Sarkar et al., 2008; Sarkar et al., 2009).

Proteins that interact with HTT, such as *HTT Interacting Protein 14 (Hip14)*, may also mediate mHTT toxicity. *Hip14* encodes a palmitoyl acyltransferase that catalyzes palmitoylation modification on membrane proteins (Smotrys and Linder, 2004). Increased cell death in the striatum together with motor coordination deficiency has been observed in *Hip14*-/- mutant mice

(Singaraja et al., 2011). Since HIP14 shares a large portion of protein interactors with HTT (Butland et al., 2014) and *Hip14*-/- mutants showed similar neurology defects as HD mouse models, Hip14 becomes one of the targets to study HD pathogenesis. Fly *Hip14* regulates synaptic vesicle trafficking (Ohyama et al., 2007b; Stowers and Isacoff, 2007). Although *Hip14* has been implicated in HD, its role in *Drosophila* HD models has not been defined nor has its role in mediating mHtt -dependent sleep/circadian defects been determined. As part of our screen to identify sleep/circadian ND models, we examine the function of Hip14 in circadian rhythms and mHtt toxicity in Chapter 2.

1.10 The Drosophila Circadian Clock Consists of a Conserved Transcriptional Feedback Loop that is Modified Post-transcriptionally

The molecular clock is regulated by transcriptional feedback loops that keep the timing of 24 hours (Allada and Chung, 2010a). In *Drosophila*, the core clock consists of three feedback loops (Tomioka and Matsumoto, 2010) (Figure 1.1). Oscillators in the main transcriptional feedback loop are *Clock* (*Clk*), *Cycle* (*cyc*), *Period* (*per*) and *Timeless* (*tim*) (Lee et al., 1999). CLK and CYC are transcription factors and form a heterodimer, which binds to E-box promoters to initiate the transcription of target genes including *per* and *tim* (Allada et al., 1998; Rutila et al., 1998). PER and TIM interact with each other, relocating from the cytoplasm to the nucleus, to inhibit the transcriptional activity of CLK and CYC (Lee et al., 1999; Rutila et al., 1998). PER/TIM stability and localization are regulated by posttranslational modifications (phosphorylation/dephosphorylation) through kinases CK2, SGG, DBT, NMO and phosphatases PP1 and PP2A (Chiu et al., 2011; Fang et al., 2007; Kim and Edery, 2006; Kloss et al., 1998; Kloss et al., 2001; Lin et al., 2002; Martinek et al., 2001; Price et al., 1998; Sathyanarayanan et al., 2004; Yu et al., 2011). In a second loop, CLK and CYC initiate the transcription of *Vrille* (*Vri*) and *Pdp1ε* (*Pdp1*). VRI is a transcription repressor, which binds to the V/P box resides in *Clk*

promoter and represses *Clk* transcription (Cyran et al., 2003; Glossop et al., 2003; Zheng et al., 2009). PDP1ε binds to the same site as VRI but activate *Clk* transcription after VRI dissociates the V/P box(Cyran et al., 2003). *Clockwork orange* (*cwo*) consists of the third feedback loop. CLK and CYC initiate the transcription of *cwo*. CWO is another transcription repressor, which can reduce CLK/CYC activated transcription by competing at binding sites (E-box) with CLK and CYC (Kadener et al., 2007; Lim et al., 2007; Matsumoto et al., 2007). Outside the core feedback loops, light input is sensed by a blue light photoreceptor encoded by *Cryptochrome* (*cry*) (Ceriani et al., 1999; Emery et al., 1998). CRY mediates the degradation of TIM upon light activation (Emery et al., 2000; Stanewsky et al., 1998). This feedback loop mechanism generates specifically phased, 24 hr oscillations in gene expression (Panda et al., 2002).

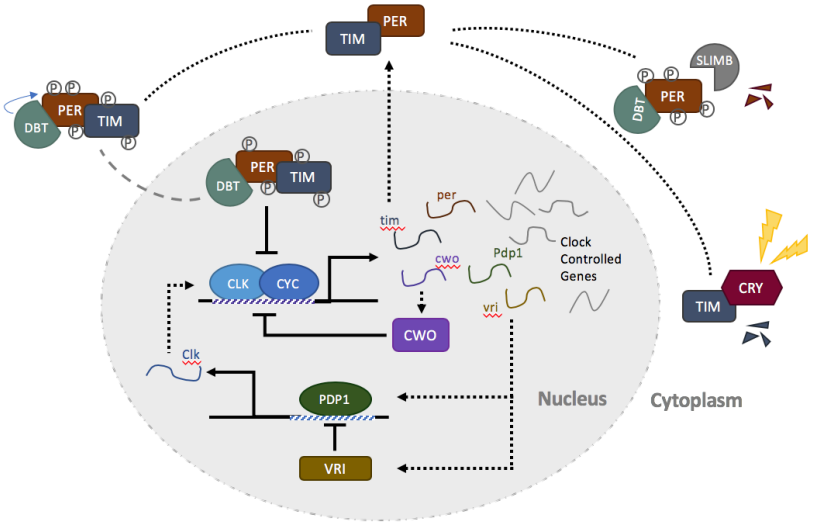

Figure 1.1. Transcriptional Feedback Loop in Drosophila Circadian Neurons

The transcriptional feedback loop is highly conserved among organisms, from plants to mammals. For example, mammalian CLOCK and BMAL1 share the similar functions as fly CLK and CYC to initiate transcription in the first loop (Gekakis et al., 1998). The CLOCK/BMAL1 heterodimer activates transcriptions of *mPer*s (mammalian *Per1*, *Per2* and *Per3*) and m*Cry*s (*Cry1* and *Cry2*) (Griffin et al., 1999; Reppert and Weaver, 2002; Shearman et al., 2000; Zheng

et al., 2001; Zheng et al., 1999). mPER/mCRY heterodimer, in turn, inhibits the transcription activity of CLOCK/BMAL1 (Reppert and Weaver, 2002). Casein kinase I epsilon/delta (CKIε/*δ*) phosphorylates mPER and mCRY to mediate the inhibition of CLOCK/BMAL1(Lee et al., 2001) or phosphorylates mPER for its degradation (Akashi et al., 2002). The second transcriptional feedback loop consists of *RevErb* and *Ror*. CLOCK/BMAL1 initiating the transcription of *RevErb/Ror* (Guillaumond et al., 2005). ROR binds to the retinoic acid-related orphan receptor response elements (ROREs) in the BMAL1 promoter to activate the transcription of *Bmal1* while REVERB binds to the same sites to repress the transcription (Guillaumond et al., 2005).

In addition to the canonical transcriptional feedback mechanisms and key phosphorylation steps that regulate the molecular clock, other post-transcriptional and post-translational mechanisms also participate in regulating the molecular clock. For example, mRNA stability of many clock genes is affected by post-transcriptional regulations in their 3'-UTRs in different organisms, ranging from plants to animals (Kojima et al., 2011). *Atx2* and its binding partners, *tyf* and *Lsm12,* interact with the translation initiation complex to activate PER translation (Lee et al., 2017; Lim and Allada, 2013a; Lim et al., 2011a; Zhang et al., 2013). *Atx2* has also been found to be involved in *me31B (DDX6)* and *Not1* dependent gene silencing, which also affects circadian rhythms but in a *per* independent manner (Lee et al., 2017). Mammalian *Atxn2* KO showed unstable rhythmicity although without decreases in PER1 and PER2 levels in the SCN (Pfeffer et al., 2017). Proteins in the ubiquitin-proteasome pathway, such as SCF^{Fbxl3} (for CRY) in the mouse, USP8 (for CLK) and SLIMB (for PER) in the fly, are responsible for degradation of clock proteins (Busino et al., 2007; Ko et al., 2002; Luo et al., 2012). As a part of our genetic screen for mHtt-induced arrhythmicity, we also discovered novel genes that impact circadian rhythms in the absence of mHtt. These candidate circadian clock genes will be described in Appendix 2 and 3.

1.11 *Drosophila* Pacemaker Neurons Form an Interconnected Network of Distinct Clusters Important for Circadian Behavior

The *Drosophila* circadian clock is typically assessed behaviorally by measuring locomotor activity under 12 hr light: 12 hr dark (LD) and constant darkness (DD) conditions. By recording the locomotion activities of a fly throughout the day under different LD conditions, a profile of activity distribution can be generated and used to study circadian rhythms (Hamblencoyle et al., 1989). For wild-type flies in regular light-dark conditions 12 hours light and 12 hours dark, 12:12 LD), the activity profile will exhibit a rhythmic pattern, which peaks around both light on and light off time (Hamblencoyle et al., 1989). After being released into constant darkness (DD) without any light stimulus (free running), this pattern will be maintained by the internal molecular clock for days but with a gradual decay in rhythm amplitude (Ashmore and Sehgal, 2003).

Circadian behavior depends on the oscillations of the core clock gene within a neuronal network of ~150 neurons (Kaneko et al., 1997a). These clock neurons are classified into subgroups according to their functions and/or gene expression specificity (mostly neurotransmitters and their receptors) (Figure 1.2) (Kaneko et al., 1997b; Muraro et al., 2013; Yoshii et al., 2009). Different subgroups of neurons are responsible for morning and/or evening activities. The four small lateral ventral neurons (sLNvs) and four large lateral ventral neurons (lLNvs) in each hemisphere are critical for morning behavior (Helfrich-Forster, 1998; Shafer and Taghert, 2009; Stoleru et al., 2004), and lateral dorsal neurons (LNds) and the 5th sLNv are critical for evening behavior (Nitabach and Taghert, 2008; Picot et al., 2007; Stoleru et al., 2004). CRY in LNvs enables these neurons to sense light input directly (Yoshii et al., 2008). LNvs also receive light input from the compound eye and HB eyelet (Malpel et al., 2002; Muraro and Ceriani, 2015). DN1, DN2, and DN3 are the three major groups of circadian neurons on the dorsal side. Pigment dispersing factor (PDF) is a neuron peptide secreted by LNvs (Renn et al., 1999b). PDF null mutants or genetic ablation of LNvs resulted in arrhythmic under DD and advanced evening peak

under LD (Renn et al., 1999b). LNvs communicate with LNds and DN1 through PDF signaling (Flourakis et al., 2015; Seluzicki et al., 2014b; Stoleru et al., 2004). Arousal in the morning is controlled by communication between LNvs and DN1s (Zhang et al., 2010a), though DN1 may also participate in promoting siestas during the middle of the day as well as nighttime sleep (Collins et al., 2012; Flourakis et al., 2015; Zhang et al., 2010c). PDF signaling is important for synchronization between different groups of neurons and maintaining the rhythmic behavior under constant darkness (Lin et al., 2004; Yoshii et al., 2009). Nevertheless, it has been shown that one single sLNv expressing PDF will be sufficient to maintain a fly's rhythmicity (Helfrich-Forster, 1998). Here we focus on this core set of PDF pacemaker neurons.

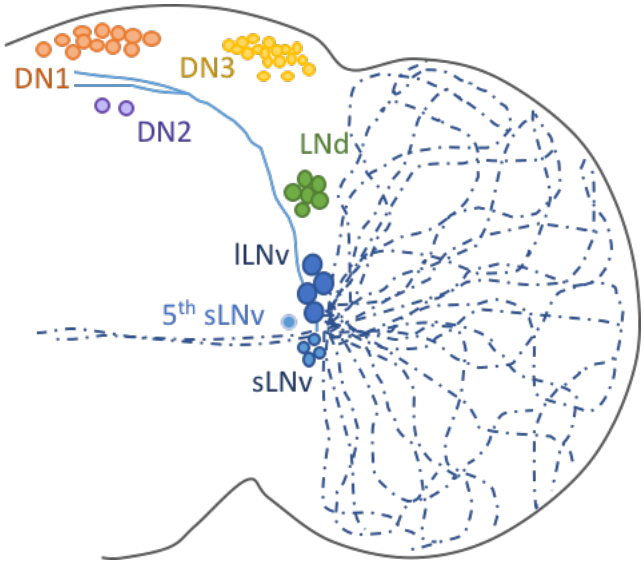

Figure 1.2. Organization of *Drosophila* Circadian Neuron Network

1.12 The Application of *Drosophila* Models to Understand the Link Between Circadian Clocks and Mutant Huntingtin Toxicity

As mentioned above, fly HD models also display sleep and circadian disturbance similar to what is observed in HD patients. Expression of two polyQ pathogenic transgenes, mHTT and SCA3, in fly circadian neurons specifically affected one subgroup circadian neurons, the sLNvs

(Kadener et al., 2006; Sheeba et al., 2010; Sheeba et al., 2008). Small LNvs lost their immunoreactivity to PDF antibody and the flies become arrhythmic (Renn et al., 1999b). Gonzales and Yin reported that flies with mHTT expression decreased nighttime sleep and increased daytime sleep and sleep was more fragmented (Gonzales and Yin, 2010). These phenotypes resemble the circadian and sleep disruption in HD patients (Morton et al., 2005). Besides, fly *Htt* RNAi caused a similar effect on sleep (Gonzales and Yin, 2010), which suggests that loss of endogenous HTT may work in a similar way as overexpression of human mHTT in *Drosophila*. The comparable phenotypes of fly HD models and human HD patients for sleep and circadian disruption serves as the basis for understanding how mHTT impacts circadian clocks in the flies.

Chapter 2: Disordered Circadian Rhythms in *Drosophila* Neurodegenerative Disease Models

2.1 Summary

Progressive accumulation and aggregation of neurotoxic proteins that impair specific neurons commonly result in neurodegenerative diseases (NDs). Considerable evidence stems from human and animal studies indicates that disturbances in normal circadian rhythms and sleep are found as symptoms for many NDs. However, the detailed mechanisms through which ND genes affect the clock is not clear yet. To further elucidate the mechanistic relationship between circadian clocks and NDs, we first aimed to identify ND genes that generate circadian or sleep-related phenotypes when expressed in neurons controlling circadian and sleep in the model of *Drosophila*. Multiple ND genes, including mutant *Htt* (*mHtt* for HD), *TDP43/FUS* (for ALS) and mutant *Atx3* (for SCA3) display circadian defects in rhythmicity or period length when they are expressed in circadian neurons. When we further investigated how they affect circadian rhythms, we that found most of them cause degeneration of at least one sub-group of circadian neurons and may affect circadian gene expression in different ways.

2.2 Introduction

The aggregation of deleterious proteins is a common cause of neurodegenerative diseases (Ross and Poirier, 2004). It is thought that toxic protein species can accumulate during the presymptomatic phase. Once the oligomers and/or aggregates pass a concentration threshold, they impair neuronal function. This is believed to cause the initial symptomatology. Continued toxicity and dysfunction then lead to irreversible cell death. A challenge in neurodegenerative diseases is the early detection of the disease process, prior to cell death. This is when therapeutic interventions may still reverse the neurotoxic process. (Pedroso et al., 2011)

Circadian and sleep disorders are commonly observed in neurodegenerative diseases including AD (Harper et al., 2005; Satlin et al., 1995), PD (Bordet et al., 2003; Kudo et al., 2011a), FTD (Anderson et al., 2009; Merrilees et al., 2009, 2014), HD (Morton, 2013; Musiek and Holtzman, 2016) and several SCAs (Botta et al., 2016; Pedroso et al., 2011). Researchers want to know whether circadian and/or sleep symptoms are consequences of degeneration in regions of the brain that control circadian/sleep, or indicators that could identify pre-clinical stage degeneration. A decrease in VIP and AVP positive neurons has been described in AD and HD patients (van Wamelen et al., 2013; Zhou et al., 1995). However, another study has shown that the reduction in circadian rhythms is correlated with a higher risk of developing incident dementia or mild cognitive impairment (Tranah et al., 2011). Moreover, sleep and circadian disruptions have been found in HD, PD and AD preclinical patients (Cuturic et al., 2009; Diago et al., 2017; Goodman et al., 2011; Postuma et al., 2012; Trenkwalder, 1998; Wu et al., 2003; Wu et al., 2006). ALS patients usually experience disrupted sleep due to respiratory insufficiency caused by motor neuron degeneration (Hardiman, 2011). However, sleep-wake disturbances have also been found in patients without respiratory dysfunction (Lo Coco et al., 2011; Lo Coco et al., 2010). Mutant *FUS* KI mice have been shown to have altered sleep and circadian activity patterns (Zhang et al., 2018c). This finding suggests that circadian symptoms are associated with multiple NDs and might be the clinical pathogenesis. Therefore, we propose using circadian and sleep phenotypes as readouts to detect neuronal dysfunction.

The fruit fly *Drosophila* has been used to model many human neurodegenerative diseases (Bilen and Bonini, 2005a). Its short life cycle, ability to produce vast number of progenies, and the abundant genetic tools available to manipulate gene expression give it many advantages as a model organism. To study the circadian and/or sleep phenotypes in human neurodegenerative diseases in *Drosophila*, we first need to verify which ND models exhibit similar circadian/sleep phenotypes in fly and human patients. The stock collection of *Drosophila* models of human

disease from the Bloomington Drosophila Stock Center provides an adequate testing pool of ND genes. This will be discussed in detail in the following sections. The diseases are modeled in flies by expressing different transgenic lines with the GAL4-UAS system. Many NDs that are caused by the accumulation of pathogenic proteins can be simulated in flies by overexpressing the human pathogenic genes. Examples include mutant *HTT*, *TDP43*, and *ATXN3*. Pathogenesis due to gene loss-of-function is achieved by knocking down fly homologs in human disease-related genes, such as *Fmr1* and *pink1*. The genes included in our screening, and for which disease models, will be described in the following sections.

We expressed or knocked down several genes involved in ALS. *Superoxide dismutase 1 (SOD1)* was the first gene identified as being linked to ALS. It is still unclear whether mutated SOD1s contributes to ALS pathogenesis through loss-of-function or through gain-of-function, but hypotheses have been proposed and tested for both (Chen et al., 2013; Paez-Colasante et al., 2015). Therefore, we included overexpression of human mutant SOD1 and fly Sod1, as well as fly Sod1 RNAi, in our screening (Watson et al., 2008). The overexpression of human wild-type or mutant SOD1 in fly motor neurons leads to reduced climbing activity (Watson et al., 2008). *TAR DNA-binding protein 43* (*TDP43*) and *Fused in Sarcoma* (*FUS*) both encode nucleus RNA binding proteins. Mutations in *TDP43* and *FUS* lead to the mislocalization and accumulation of TDP43 and FUS in the cytoplasm, which is toxic to the neurons (Barmada et al., 2010; Kwiatkowski and Vanderburg, 2009). TDP43/FUS overexpression with various Gal4s induces neurodegeneration in multiple tissues including motor neurons. It also retards larvae locomotor activity (Chen et al., 2011; Li et al., 2010). The overexpression of human wild-type or mutant SOD1, wild-type or mutant TDP43/FUS and fly Sod1 RNAi were included in our screening. In addition to the mutations in coding regions described above, a hexanucleotide repeat expansion of GGGGCC in the non-coding region of *C9ORF72* has been observed in 23.5% cases of familial ALS (DeJesus-Hernandez et al., 2011). The dipeptide products containing arginine generated though repeat-

associated, non-ATG (RAN) translation was able to induce neurodegeneration and shorten the lifespan in flies (Mizielinska et al., 2014). The expression of GGGGCC repeats has been found to cause retinal degeneration and shorter lifespans in flies, while the expression of the same number of repeats disrupted by stop codons in the middle did not show any phenotypes (Mizielinska et al., 2014).

Disrupted sleep and circadian rhythms have also been implicated in Alzheimer's disease, and we tested multiple fly AD models for this. AD pathology is characterized by the accumulation of plaques formed by beta-amyloid (Aβ) and neurofibrillary tangles (NFT) formed by tau (Benilova et al., 2012; Giacobini and Gold, 2013). Aβ42 is the product of the cleavage of the amyloid precursor protein (APP) by beta secretase (beta-site APP-cleaving enzyme, BACE) and gamma secretase (presenilin, PSEN) (Selkoe, 2001). The overexpression of human APP and BACE was sufficient to deposit Aβ42 in flies (Fossgreen et al., 1998; Greeve et al., 2004). In addition, the loss-of-function mutation of fly PSN decreased the toxicity due to the co-overexpression of human APP and BACE. Meanwhile, the overexpression of PSN with mutations corresponding to those found in the familial AD (FAD) patients enhanced the toxicity (Greeve et al., 2004). These data suggest fly PSN are able to process human APP into toxic Aβ fragments. We were able to cleave the fly homologs of APP and APPL with fly BACE. This led to amyloid deposits as well (Carmine-Simmen et al., 2009). Directly expressing human Aβ42 in flies led to neurodegeneration and decreased lifespan, while Aβ42 with FAD mutations exhibited more severe toxicity (Crowther et al., 2005; Finelli et al., 2004; Iijima et al., 2004). The overexpression of human tau in flies induced neurodegeneration as well (Jackson et al., 2002; Wittmann et al., 2001). Based on the previous models, we included overexpression/co-overexpression of the human APP, BACE, PSEN (wildtype and mutant), fly PSN (wildtype and mutant), and fly APP homolog in our screening.

Autosomal-dominant familial frontotemporal dementia (FTD) shares several pathogenic genes with other NDs. For example, mutations in tau account for ~10% of familial FTD cases

(Seelaar et al., 2008; Whitwell et al., 2012). GGGGCC expansion in *C9ORF72* that has been found in familial ALS is also found in 11.7% cases of familial FTD(DeJesus-Hernandez et al., 2011). TDP43 is found in tau-negative inclusions in FTD patients' brains (Arai et al., 2006; Neumann et al., 2006).

The neuropathology feature for PD is the Lewy bodies found in the patients. These are mainly composed of alpha-synuclein (Spillantini et al., 1997). The overexpression of human wild-type and mutant alpha-synuclein results in decreased dopaminergic neurons, which recapitulates the feature of PD patients (Feany and Bender, 2000). Besides alpha-synuclein, mutations in PTEN-induced kinase 1, PINK1 and parkin (PARK2) and DJ-1 have been associated with the autosomal recessive form or sporadic form of PD (Wood-Kaczmar et al., 2006). Dopaminergic neuron degeneration and locomotor defects have been found in fly *Pink1* and *park* mutants, together with mitochondrial dysfunction and excessive oxidative stress. These are thought to be triggers in PD-like pathogenesis (Clark et al., 2006; Dodson and Guo, 2007; Park et al., 2006; Yang et al., 2006). Therefore, the wild-type and mutant alpha-synuclein overexpression as well as *Pink1*, *park* and *DJ-1* RNAi were incorporated in our screening to represent the pathology for PD.

Valid HD models have been established for *Drosophila* by expressing human mHtt with different numbers of polyQ expansion. There are different forms of mHtt transgenes in different lengths. Full-length Htt expression cause shortened lifespan, locomotor defects, as well as retinal degeneration, but in a milder manner (Burr et al., 2014; Romero et al., 2008). The N-terminus fragments of mHtt, which are more correlated with the disease symptoms (Gafni et al., 2004; Juenemann et al., 2011; Mangiarini et al., 1996; Truant et al., 2008), display neuronal degeneration in various tissues with different drivers. Degenerative phenotypes include decreases in lifespan, locomotor ability, retinal and mushroom body degeneration, aggregate formation and defects in axonal transport (Agrawal et al., 2005; Gunawardena et al., 2003; Lee

et al., 2004b; Sinadinos et al., 2009; Steffan et al., 2001; Zhang et al., 2010b). N-term fragment expression in circadian neurons causes the degeneration of a sub-group of circadian neurons and reduced rhythmicity (Prakash et al., 2017; Sheeba et al., 2010). Meanwhile, both full length and N-term fragments induced decreases in sleep (Gonzales and Yin, 2010). In order to elucidate whether different mHtt transgenes exhibit similar circadian and sleep phenotypes, we included mHtt transgenes that have been, and have not been tested, with circadian and sleep in our screening.

Huntingtin Interacting Protein14 (*HIP14*) is a conserved gene whose loss-of-function phenocopies HD features in mammals, and thus represents a potential HD model (Singaraja et al., 2008). *HIP14* encodes a palmitoyl acyltransferase that catalyzes palmitoylation modification, mainly on membrane proteins (Smotrys and Linder, 2004). *HIP14*$^{-/-}$ mice showed increased cell death in the striatum, and also motor coordination deficiencies (Singaraja et al., 2011). There are two potential ways HIP14 could contribute to HD pathogenesis: 1. The decreased interaction between HIP14 could impair the HIP14's enzyme activity, causing deficits in the palmitoylations of HIP14 targets that could be linked to HD (Huang et al., 2011; Sanders and Hayden, 2015; Singaraja et al., 2002; Singaraja et al., 2011). This is also supported by the fact that HIP14 shares a large portion of protein interactors with Htt (Butland et al., 2014). 2. HTT is palmitoylated by HIP14, and the palmitoylation is critical for its functions that mHtt lacks (Yanai et al., 2006). Fly *Hip14* shares some of the conserved functions in regulating proteins involved in vesicle trafficking with human *HIP14* (Huang et al., 2004; Ohyama et al., 2007a; Singaraja et al., 2002; Stowers and Isacoff, 2007). Nevertheless, whether the loss-of-function of fly *Hip14* affects circadian/sleep as does mHtt, or affects mHtt toxicity, has yet to be determined. Thus, our screening further tests the circadian-related features of fly *Hip14*.

In addition to mHtt, we also examined the impact of other ND genes with expanded polyQ repeats. Spinocerebellar ataxias type 3 is another ND caused by CAG triplet expansion in ATXN3

(Kawaguchi et al., 1994). The concept of modeling SCA3 in flies is comparable to HD; it is done primarily through the overexpression of human ATXN3 with the expanded polyQ tract. ATXN3Q78 overexpression was able to induce retinal degeneration, and shortened lifespan (Vossfeldt et al., 2012; Warrick et al., 1998). ATXN3Q78 also caused degeneration of a subgroup of circadian neurons and decreased clock gene expression when expressed with a broad circadian Gal4 (timGAL4) (Kadener et al., 2006). It has been discovered that toxicity from CAG repeat-containing RNAs is another mechanism by which CAG triplet expansion contributes to the pathogenesis for polyQ diseases such as SCA and HD (de Mezer et al., 2011; Li et al., 2008; Nalavade et al., 2013). In addition to mHTT and mATXN3 protein overexpression, we also incorporated reagents that remained as RNAs after overexpression. This was done to test whether mHTT and mATXN3 protein are able to induce circadian/sleep phenotypes, and whether RNA toxicity is involved.

To address the role of ND genes in sleep and circadian rhythms, we expressed these genes in a core set of PDF circadian pacemaker neurons and in the mushroom bodies—a fly homolog of the mammalian cortex and hippocampus, previously implicated in sleep regulation(Joiner et al., 2006; Krashes et al., 2007). ND genes are commonly deleterious and can also cause development defects if expressed early and broadly. Behavior assay for sleep and circadian typically takes 12 days. Therefore, no massive lethality would have happened in the first month. This is preferable, especially if there is the need to test aged flies. To obtain enough adult flies with decent viability, we chose drivers that were more restricted to circadian/sleep neurons for our ND gene screening. To see the circadian-related phenotypes, we used PdfGAL4. PdfGAL4 drives gene expression in PDF positive neurons (aka PDF positive sLNvs and lLNvs mentioned in Chapter 1)(Renn et al., 1999b). Loss of PDF positive neurons leads to abolished morning anticipation, advanced evening phase during LD, and decreased rhythmicity under DD (Renn et al., 1999a). Therefore, we expected to see similar phenotypes if the ND transgenes had degenerated the LNvs. The mushroom bodies (MB) are a tissue that consists of around 2,500

Kenyon cells that have been identified as centers for sleep regulation in flies (Joiner et al., 2006; Pitman et al., 2006). The Kenyon cells were classified into subgroups depending on which lobe they project into (Tanaka et al., 2008). 247GAL4 was selected to express ND genes in the mushroom bodies. 247GAL4 induced a strong expression in cells projecting into alpha, beta and gamma lobes (Aso et al., 2009). It has been shown that when blocking synaptic transmission in neurons covered by 247GAL4, flies experience reduced sleep in the morning (Pitman et al., 2006). For ND genes that may disrupt neuronal function in the MB, we would expect to see reduced sleep. Had any of the ND genes we screened exhibited circadian/sleep phenotypes, we would have continued to look further into their effects at the cellular and molecular levels (e.g. circadian/sleep neuron number and circadian gene level).

2.3 Material and Methods

Whole Mount Immunostaining

Adult brains were dissected in PBS (137mM NaCl, 2.7mM KCl, 10mM Na_2HPO_4 and 1.8mM KH_2PO_4) within 10 minutes per genotype/time point. The brains were then fixed in 3.7% formalin solution for 30 minutes. For most primary antibodies, with the exception of anti-Clk, brains were washed with 0.3% PBSTx 4 times before primary antibody incubation. Primary antibodies were diluted in 0.3% PBSTx with 5% normal goat serum, and brains were incubated at 4℃ overnight. After primary antibody incubation, the brains were washed at room temperature 4X for 30 minutes with 0.3% PBSTx. Secondary antibodies were diluted in 0.3% PBSTx with 5% normal goat serum, and incubation was performed at 4℃ overnight or at room temperature for 2 hours. For anti-Clk staining, 0.3% PBST was replaced by 0.5% PBST for all steps, and primary antibody incubation was performed at 4℃ for 2 days without GNS. The following primary antibodies and dilutions were used: mouse anti-PDF (1:800, DSHB, C7), rabbit anti-PDF (1:1,000, from Nitabach

Lab), mouse anti-GFP (1:500), rabbit anti-GFP (1:1,000, life technologies), rabbit anti-PER (1:8,000, from Rosbash Lab), goat anti-Clk (1:500, Santa Cruz Biotechnology, dC-17). Secondary antibody dilution was performed as follows: anti-mouse Alexa594 (1:800, life technologies), anti-mouse Alexa488 (1:800, life technologies), anti-rabbit Alexa594 (1:800, life technologies), anti-rabbit Alexa488 (1:800, life technologies), anti-rabbit Alexa647 (1:800, life technologies).

Locomotor Activity Recording and Circadian/Sleep Data Analysis

Behavior data recording, processing, plotting and analysis were conducted, as previously described (Pfeiffenberger et al., 2010a, b). Fly locomotor activity was recorded from the Drosophila Activity Monitoring (DAM) data collection system for 5LD and 7DD at 25°C. Data were then extracted with DAM File Scan (Trikinetics). Rhythmicity was measured by power - significance (P-S). The two parameters were calculated by ClockLab using chi-square periodogram, based on the data from the 7DD. Flies with P-S below 10 were considered arrhythmic and thus eliminated from the average period calculation. Flies lacking rhythmic power are considered as completely arrhythmic and are assigned with P-S=0 but are included in the average rhythmicity calculation. Activity profiles were plotted with either Counting Macro or ClockLab. Morning and evening Index were calculated with normalized activity given by output from Counting Macro. Morning Index = sum of normalized activities 3hr before the light was turned on / sum of normalized activities 6hr before the light was on. Evening Index = sum of normalized activities 3hr before the light was turned off / sum of normalized activities 6hr before the light went off (Seluzicki et al., 2014b). Sleep data was also acquired from the DAM data collection system and then extracted with DAM File Scan. Data was processed, as previously described, using Counting Macro (Pfeiffenberger et al., 2010c). Behavior testing for young flies was done with flies eclosed within 3 days, by the 1st day of the behavior run. Old flies used for behavior test were also collected during a similar time window as the young flies, then were aged on regular food,

25C 12:12 LD for 3 weeks prior to loading. They were entrained from the embryonic stage under 12:12 LD cycles.

To look for candidates in the screening, we first performed T-tests between each ND gene and the control from the same behavior run to identify any significant differences. As the PdfGAL4 and 247GAL4 controls displayed wide variance between different runs, especially after aging, the hits that could show significant difference were dependent on which batch of control they had been compared to. To avoid this issue, we used a Z-score calculated based on all of the lines that had been screened as a population to determine the significance.

Fly Stocks

RNAi lines used for screening were acquired from Bloomington Stock Center, unless indicated otherwise. PdfGAL4 and 247GAL4 were from our laboratory (previously obtained from other circadian laboratories which had generated them but had either kept or isogenized them in our lab for several years). UAS-HttQ0/128 were kindly provided by Dr. Littleton. UAS-HttQ25/46/72/103-eGFP were kindly provided by Dr. Perrimon. TDP and FUS wild-type and mutant overexpression lines were kindly provided by Dr. Wu. CAG RNA overexpression reagents were kindly provided by Dr. Bonini. Some of the UAS-Aβ40/42 lines were kindly provided by Dr. Crowther. The rest of the human ND lines were acquired from Bloomington Stock Center or human disease fly collection.

2.4 Results

2.4.1 Screening *Drosophila* Neurodegenerative Disease Models for Circadian or Sleep Phenotypes

As noted previously, we expressed ND genes in PDF circadian pacemaker neurons and in the mushroom bodies. In order to achieve this, we chose PdfGAL4 to test for circadian phenotypes, and 247GAL4 to test for sleep phenotypes. PdfGAL4 drives the expression of

transgenes in PDF positive LNvs (large and small LNvs) (Renn et al., 1999b), and small LNvs control the rhythmicity of behavior under constant darkness (Renn et al., 1999a). Therefore, reductions in rhythmicity are expected if ND genes degenerate LNvs. 247GAL4 drives expression in most neurons in the alpha, beta and gamma lobes of mushroom bodies (Aso et al., 2009). Sleep decreased in the morning when the synaptic transmission was blocked in neurons which were included in 247GAL4 driven expression (Pitman et al., 2006). Total sleep under LD may have been reduced had the ND genes disrupted those neurons. Because of the progressive nature of neurodegenerative disease, it was likely that we would see phenotypes in flies at a later age only. Alternatively, there might have been age-dependent changes in either circadian or sleep. Thus, we decided to perform the preliminary screening with flies at two different ages. The first group of flies was loaded for the behavior test within 3 days after their eclosion. The second group of flies was collected during a similar time frame, aged on regular food under 12:12 LD for 21 days, and then loaded for behavior testing. In addition to looking at the circadian and sleep parameters at each age independently, we also compared the changes between the different age groups. For the preliminary screening, 8 flies per genotype were tested. For hits that showed a significant difference, more replicates were tested to confirm the reproducibility.

We screened 8 models and found several lines that had resulted in either reduced rhythmicity (~15 genes) as scored as rhythmic power (Power-Significance; P-S), or as circadian period length (1 gene). In order to uncover circadian phenotypes, we analyzed the rhythmicity and period length under DD by using the average power minus the average significance for the PdfGAL4 driven ND gene expressing flies. The distributions of rhythmicity and period of ND genes screened are shown in Figure 2.1. Overall, there are more genotypes with lower rhythmicity in the older flies than in the young group (Figure 2.1A vs. 1B left panel). Also, the older age group tended to have more genotypes than the young (Figure 2.1A vs. 1B right panel). Several interesting candidates exhibited low rhythmicity at both ages or age-dependent rhythmicity decreases. For

example, most of the TDP43 and FUS (WT or mutant) overexpression lines caused a severe reduction in rhythmicity in both young and old flies. Similar phenotypes were observed for MJDQ78 (ATXN3Q78) and HTTQ128 overexpression, indicating those proteins are toxic to LNvs. However, alpha-synuclein and Aβ42 (labeled in blue) overexpression do not significantly impact the rhythmicity, although these transgenes have been described as causing neurodegeneration when they are expressed with GAL4s targeting other neurons/tissues (Auluck et al., 2002; Burr et al., 2014). These data suggest that there is some specificity in toxic ND genes to circadian neurons. The most striking age-dependent phenotype came from *Hip14* RNAi. *Hip14* knockdown caused a lengthening in the period and a decrease in the rhythmicity, in an age-dependent fashion. The following sections will focus on further tests for these candidates (labeled in red).

We examined sleep in flies expressing ND genes in the MB but results from our initial hits were not reproducible on retesting. For preliminary sleep phenotypes, we used the average total sleep during both light and dark phases for four days as the primary parameters for 247GAL4 driven ND gene expressing flies. The distributions of the total LD sleep for the ND genes screened are shown in Figure 2.2. There were no notable changes in the overall distribution of total sleep when comparing the old and the young flies. Among the genes tested in young and old flies, several showed prominent changes in total sleep among all the genes. These phenotypes were not reproducible. Therefore, we did not follow-up on the sleep phenotypes. For each gene that was tested, we then analyzed the changes between the two age groups in the rhythmicity, period, and sleep amount (detailed data can be found in Appendix 1).

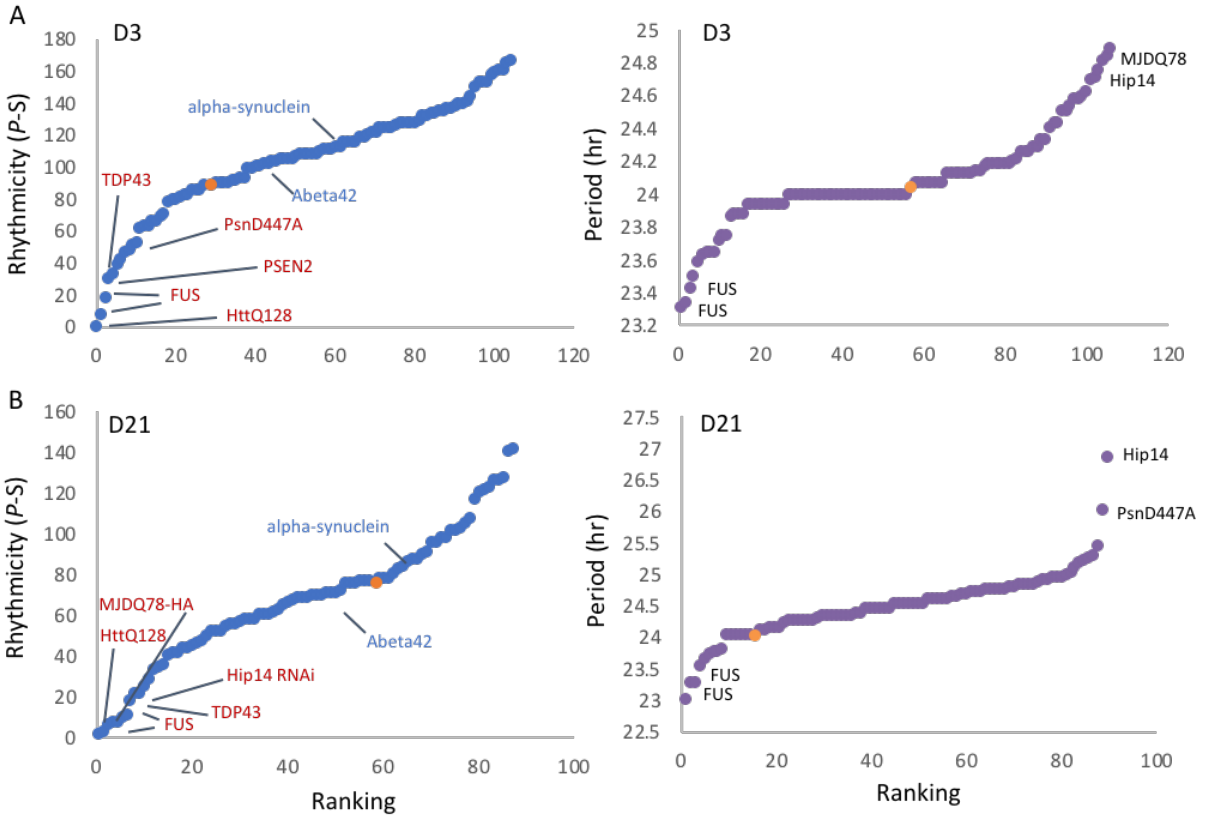

Figure 2.1. Identifying Genes for Human Neurodegenerative Disease with Circadian Phenotypes

A. The overexpression and RNAi lines of genes related to multiple neurodegenerative diseases were crossed with the PdfGAL4 driver. Adult flies were collected within 3 days after eclosion, and loaded for behavior. Average P-S (left) and average period (right) for each genotype were plotted. Orange circles represent average rhythmicity in the control flies (PdfGAL4 under control (W1118) background). B. For the same batch of flies collected in A, some were kept under 25C, 12:12 LD conditions for 3 weeks, and then loaded for behavior. Average P-S (left) and average period (right) of each genotype was plotted. Orange circles represent the average period for the control flies (PdfGAL4 under control (W1118) background).

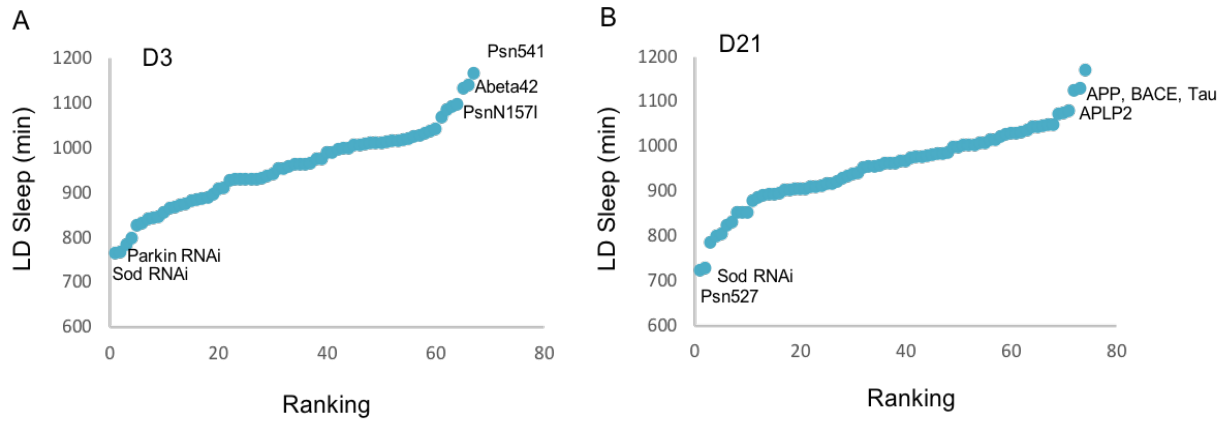

Figure 2.2. Identifying Genes for Human Neurodegenerative Disease with Sleep Phenotypes

A. The overexpression and RNAi lines of genes related to multiple neurodegenerative diseases were crossed with 247GAL4 driver. Adult flies were collected within 3 days after eclosion and loaded for behavior. Average sleep during 4 days of LD cycles for each genotype was plotted. The orange circles represent the control flies' average sleep (247GAL4 under control (W1118) background). B. For the same batch of flies collected in A, some were kept under 25C, 12:12 LD conditions for 3 weeks, and then loaded for behavior. The average sleep during 4 days of LD cycles for each genotype was plotted. The orange circles represent the average sleep of control flies (247GAL4 under control (W1118) background).

2.4.2 The Overexpression of Wild-Type or Pathogenic Mutant *TDP43* and *FUS* Leads to Arrhythmicity, Reduced PDF Expression, and Loss of PDF Neurons

Two genes that have been linked to familial ALS (*TDP43,* and *FUS),* exhibited the most severe circadian phenotypes. The overexpression of either wild-type or mutant TDP43 and FUS caused reduced rhythmicity, in both young and old flies (Figure 2.1). *TDP34* and *FUS* both encoded a DNA/RNA binding protein. TDP43 and FUS were primarily in the nucleus, but translocated to the cytoplasm and form aggregates during ALS pathogenesis (Mackenzie et al., 2010). For the D3 flies, TDP43-WT-RFP overexpression led to a more than 50% reduction in the rhythmicity, while three WT and mutant FUS lines (FUS-WT-RFP #4, FUS-WT-RFP #9 and FUS-P525L-RFP #8a) each caused even more severe decreases (Table 2.1). The arrhythmicity phenotypes were further enhanced in the aged flies, except for the line FUS-WT-RFP #9, which had already displayed the most significant reduction, even in the young flies (Table 2.1).

In order to predict more detailed molecular/cellular defects from behavior, we analyzed the behavior profile in more detail. Our data revealed that TDP43 and FUS overexpression imitated the phenotypes observed in flies lacking PDF signaling. Those phenotypes included advanced evening peaks in both LD and DD, and decreased morning anticipation in flies that had impaired PDF signals, such as Pdf or Pdfr mutants and flies lacking lNvs due to *hid* expression (LNvs) (Hyun et al., 2005; Renn et al., 1999b). The D3 TDP43-WT-RFP expressing flies exhibited a typical behavior eduction under the LD, and the onset of evening peak was similar to the wild type control. A decrease in rhythmicity was found under DD, especially after DD3 (Figure 2.3A, indicated by the red arrow). The evening peak during the subjective night was indistinguishable from the control (Figure 2.3A, indicated by the blue arrow). For the eductions of aged flies, TDP43-WT expression resulted in an advanced evening peak and reduced morning anticipation under LD (Figure 2.3B, indicated by the red arrow). Overall, rhythmicity displayed a more arrhythmic

Age	Genotype	Period	P-S	n	R%
D3	Pdf>RFP	24.8±0.1	109±22	8	100%
	Pdf>TDP43-WT-RFP	24.0±0.2	39±13***	6	83%
	Pdf>FUS-WT-RFP #4	23.6±0.1	42±8***	8	88%
	Pdf>FUS-WT-RFP #9	23.5±0.0	8±5***	8	25%
	Pdf>FUS-P525L-RFP #8a	24.0±0.1	32±10***	8	88%
D21	Pdf>RFP	25.2±0.2	51±10	7	100%
	Pdf>TDP43-WT-RFP	23.8±0.3	20±4***	8	63%
	Pdf>FUS-WT-RFP #4	25±0.3	8±4***	8	25%
	Pdf>FUS-WT-RFP #9	23.3±0.3	7±3***	8	25%
	Pdf>FUS-P525L-RFP #8a	24.0±1.0	10±6***	8	29%

Table 2.1. The Overexpression of Human Wild-type TDP43 and Human Wild-type or Mutant FUS in PDF Positive LNvs Causes Low Rhythmicity in Young and Old Flies

Rhythmicity (P-S), period, and % rhythmic flies (%R) are indicated for various genotypes including flies expressing a different version of TDP43 or FUS driven by PdfGAL4. Flies were collected within the first 3 days after eclosion. T-tests were performed between RFP controls and other pathogenic transgenes (*:p<0.05 **:p<0.01, ***:p<0.005).

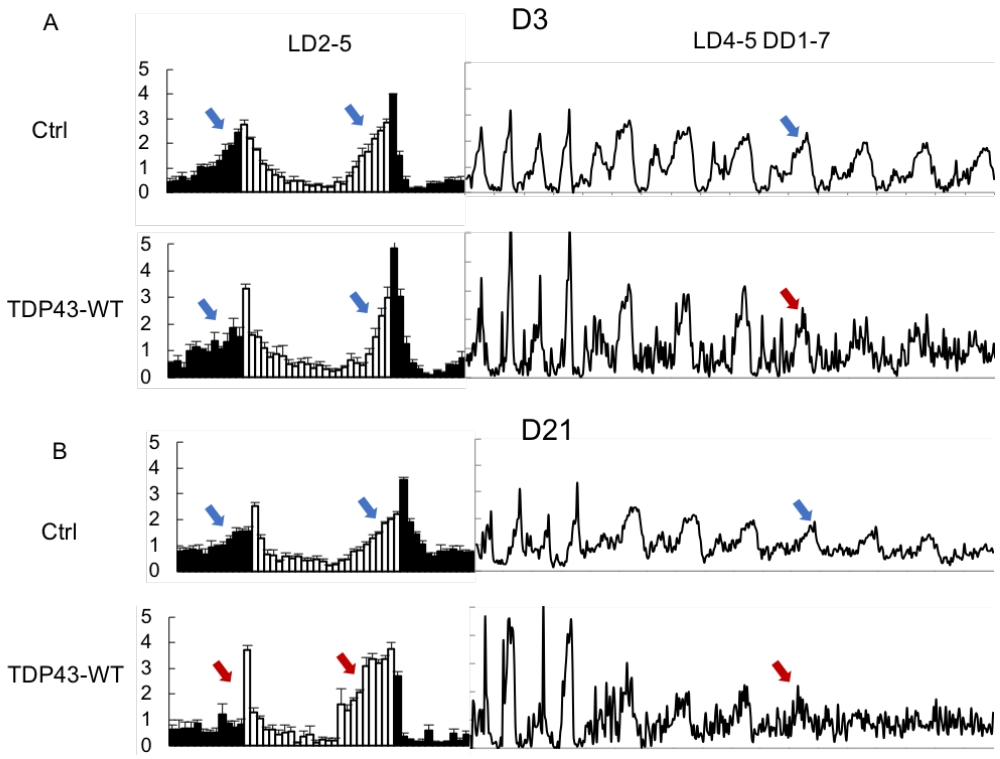

Figure 2.3. The Overexpression of Human Wild-Type TDP43 in PDF Positive Neurons Causes Low Rhythmicity in Young and Old Flies

A. The locomotor activity profile of control (Ctrl, upper) or wild-type TDP43 overexpression (TDP43-WT, lower) flies during the 2nd to 5th LD (left), the 1st DD (middle) and the 4th to 5th LD followed by 1st to 7th DD (right) are plotted. Flies eclosed within 3 days were loaded as the young fly group. B. The older flies collected from the same crosses (as flies used in A) were aged for another 3 weeks under 25C, 12:12 LD before loading. Flies with WT TDP43 overexpression in PDF positive neurons showed decreased rhythmicity under DD. The decreases in evening peak under LD and DD are indicated by the red arrows (compared to the behavior pattern in the control and young TDP43 expressing flies indicated by the blue arrows).

pattern under DD. The subjective evening peak under DD was also advanced under DD (Figure 2.3B, indicated by the red arrow). These behavioral features in aged flies resembled what has been found in flies lacking PDF signaling. This could indicate a more progressive loss of PDF neurons.

To examine whether the age-dependent changes in circadian behavior profile were associated with the loss of LNvs, we performed PDF staining at 3 different ages. Flies after one day of eclosion (D1) were tested to identify any developmental defects. D5 flies and D21 flies were examined to represent the D3 and D21 flies tested for behavior. Since the TDP43-WT construct was tagged with RFP, LNvs could also be visualized by the RFP signal in the nucleus. As shown in Figure 2.4A, most of the large and small LNvs possessed a clear cytoplasmic PDF staining and a clear nucleus signal from TDP43 in the D1 flies. By D5, the PDF signal in the lLNv had noticeably decreased, while the cell bodies were still evidenced by the RFP signal from TDP43. By D21, PDF signal had decreased more in both lLNvs and sLNvs. Some LNvs were also unable to be visualized by the RFP signal. This suggests that the LNvs were degenerating, not only losing PDF signal.

In addition to the staining in the PDF neurons, dorsal projections from sLNvs were another marker to test the presence of PDF signaling. We found that when PDF signals began to decrease in the sLNvs by D5, dorsal projections had already been weakly stained (Figure 2.4B). The PDF staining was similarly impaired at D21 (Figure 2.4B). Moreover, there was abnormal morphology in the branching, manifest in both the young and old flies. Overall, the loss of PDF signal in the cell was more in concert with the age-dependent behavioral changes, while the cell bodies remained (labeled by nucleus signals), even after the flies had become arrhythmic. These data imply that the circadian behaviors tend to reflect the neuronal function, rather than suggesting that the presence of the cells and behavioral phenotypes could have resulted from circadian gene disruption prior to cell death.

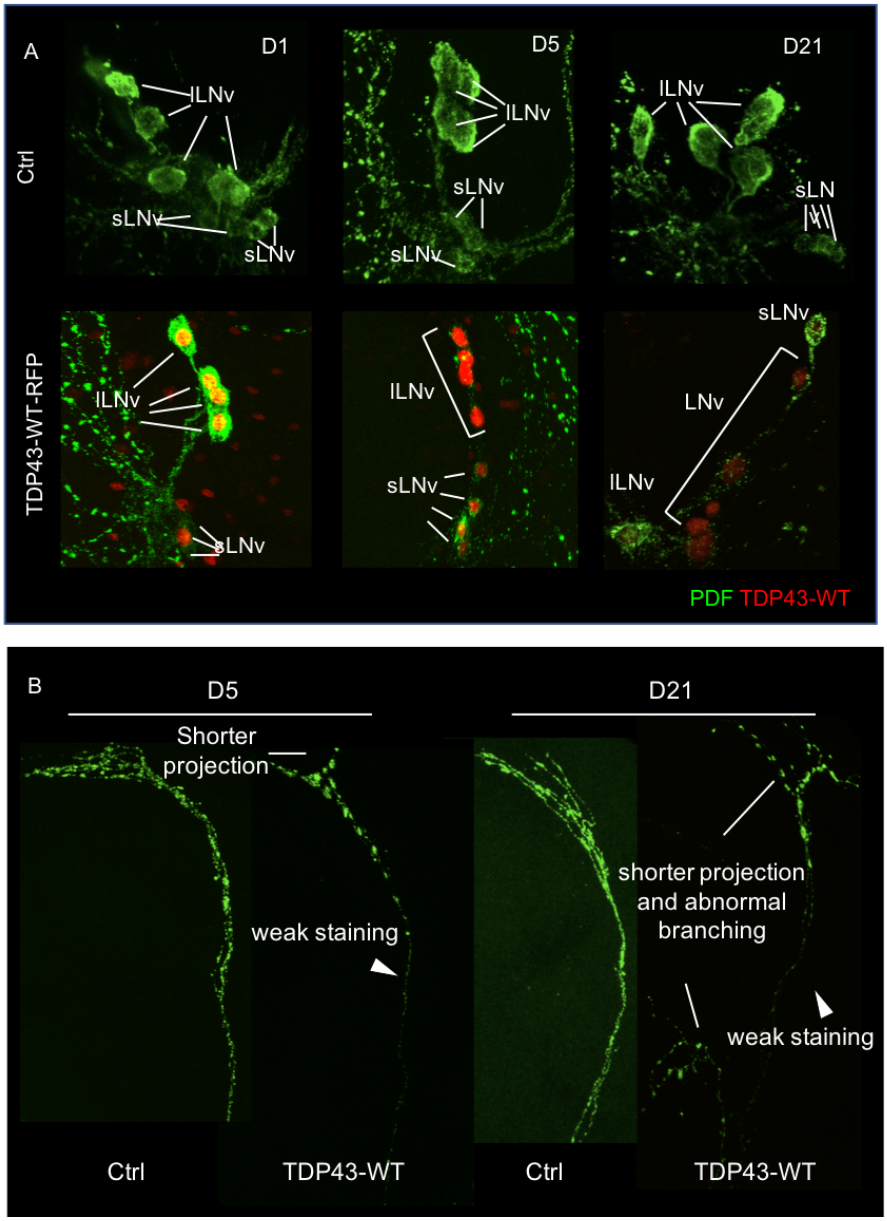

Figure 2.4. The Overexpression of Human TDP43 Reduces PDF, and Alters sLNv Dorsal Projections

A. Adult control (Ctrl, upper) or wild-type TDP43 overexpression (TDP43-WT, lower) flies were collected on the 1st day of eclosion. Flies were kept under 25C, 12:12 LD for 1 day (left), 5 days (middle) and 21 days (right), then, were dissected at ZT1. All brains were stained with PDF antibody (shown in green). TDP43-WT is tagged with RFP (shown in red). WT TDP43 overexpression flies showed reductions in PDF staining and number of LNvs. B. Adult control (Ctrl, left) and wild-type TDP43 overexpression (TDP43-WT, right) flies were collected on the 1st day of eclosion. Flies were kept under 25C, 12:12 LD for 5 days, and were dissected at ZT1 on the 5th day. B. Flies from the same batch as flies used in panel A were kept under 25C, 12:12 LD for 21 days, and were dissected at ZT1 on the 21st day. All brains were stained with PDF antibody (shown in green). WT TDP43 overexpression flies had shorter dorsal projections (from sLNvs) with weaker PDF staining. Abnormal branching was also observed.

Since by D21 most PDF neurons were still evidenced by the RFP signal, we then asked whether the cells will eventually lose the RFP signals due to neuronal degeneration after longer aging. To address this, we aged the flies expressing TDP43-WT and mGFP driven by PdfGAL4 (as an additional marker) for 45 days. These flies lost most signals from TDP43-RFP, PDF or mGFP. Only one LNv remained with PDF and RFP signal, yet it still lacked the mGFP signal (Figure 2.5A). There was massive loss of PDF signal in both projections in the optical lobes from the large LNvs and the dorsal projections from the small LNvs. This is indicated by the orange arrows (the white arrows signify the control). This further corroborates the degeneration of the LNvs.

Since FUS overexpression also exhibits less rhythmicity than TDP43, we also examined LNvs with PDF staining. FUS-WT-RFP #4 overexpression led to a reduction in rhythmicity at D3. This decreased further at D21 (Table 2.1). FUS-WT-RFP #4 did not affect PDF or RFP signal from FUS at D1. At D5, a slight decrease in PDF signal in a few sLNvs was observed in both FUS-WT-RFP #4 and FUS-WT-RFP #9 expressing flies (Figure 2.6A). By D20, we observed that some LNvs had lost their PDF signals but remained visible by the RFP tagged FUS. Meanwhile, several of the LNvs were invisible when all the flies exhibited poor behavioral rhythms. Fewer LNvs were stained with PDF by D20 in the FUS-WT-RFP #9 expressing flies than in the FUS-WT-RFP #4, suggesting #9 might have been a stronger expression line (similarly suggested by the behavior data). These data are coincident with the TDP43 overexpression results which showed that behavior phenotype became evident earlier than the cell body disappearance.

2.4.3 The Expression of Arginine-Containing Dipeptide Proteins Translated from GGGGCC Repeats Leads to Arrhythmicity

The other transgene that significantly reduced rhythmicity was the overexpression of hexanucleotide (GGGGCC) repeat. GGGGCC repeat expansion in the non-coding region of

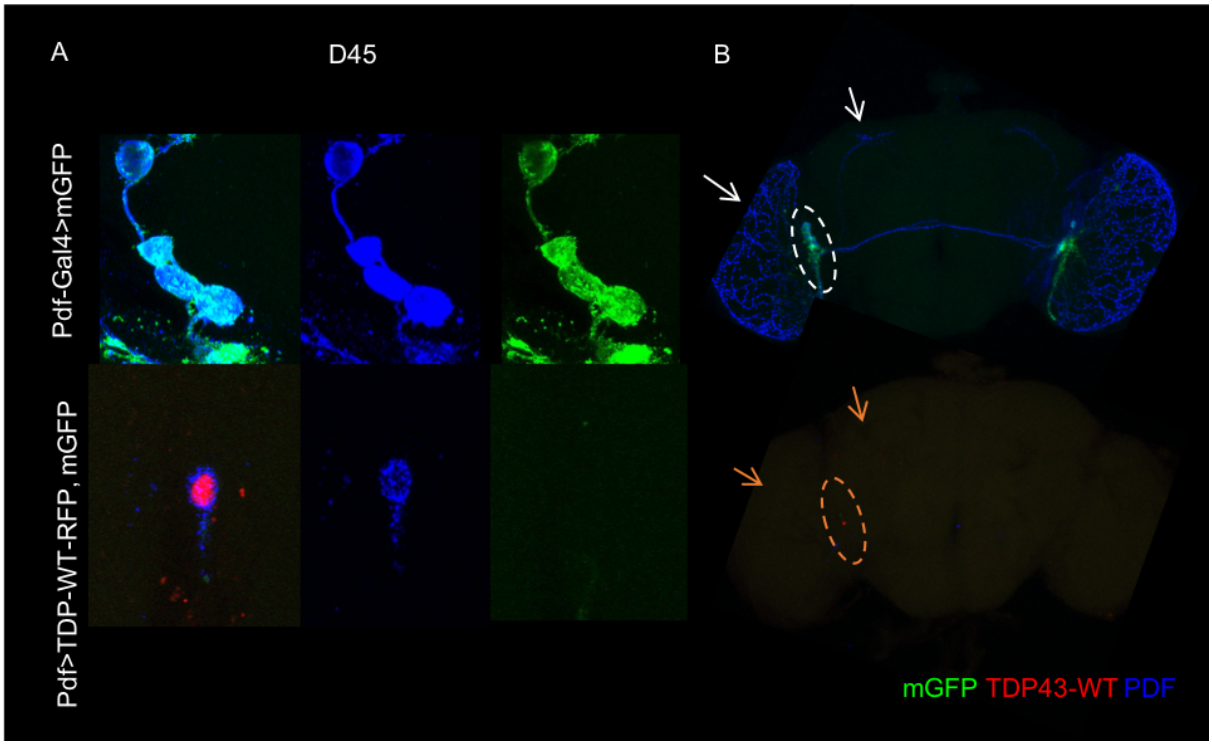

Figure 2.5. The Overexpression of Human Wild-Type TDP43 Results in Loss of Both Large and Small LNvs in Aged Flies

Adult control (Pdf>mGFP, upper) and wild-type TDP43 overexpression (Pdf>TDP43-WT, mGFP, lower) flies were collected on the 1st day of eclosion. Flies were kept under 25C, 12:12 LD for 45 days, then, were dissected at ZT1. All brains were stained with PDF antibody (shown in blue). TDP43-WT was tagged with RFP (shown in red) and cell bodies were labeled with PdfGAL4 driven mGFP (shown in green). A. Zoom in view of LNvs in the dashed white and orange circles in panel B. WT TDP43 overexpression in flies caused loss of most of the PDF staining, TDP43-RFP, and mGFP signals, in both small and large LNvs. B. The white arrows indicate the dorsal projection from the sLNvs and the projections from the lLNvs into the optical lobe in the control brains which are missing in the WT-TDP43 expressing brains (indicated by the orange arrows).

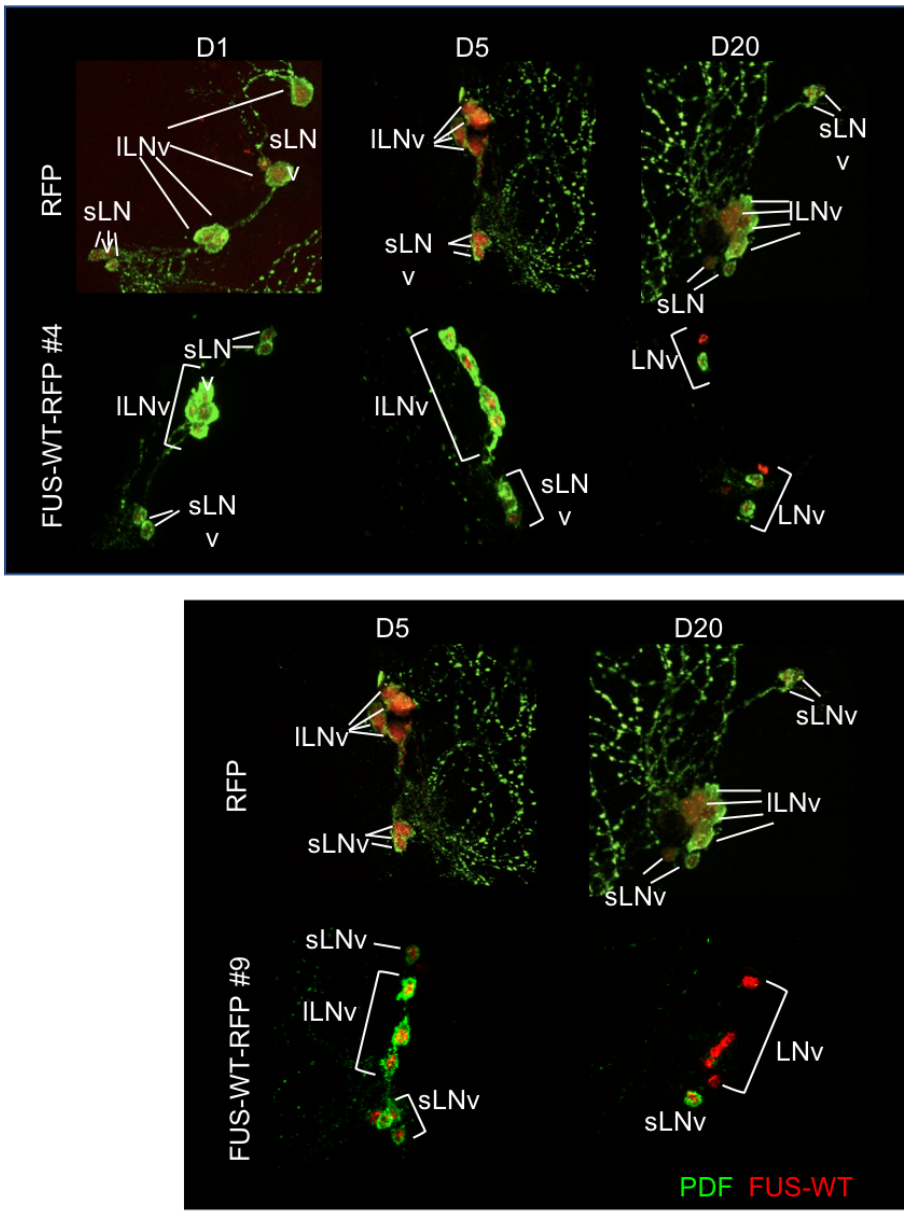

Figure 2.6. The Overexpression of Human FUS Reduces PDF, Prior to PDF Neuron Degeneration

A. Adult control (Pdf>RFP, upper) and wild-type TDP43 overexpression (Pdf>FUS-WT #4, lower) flies were collected on the 1st day of eclosion. Flies were kept under 25C, 12:12 LD for 1 day (left), 5 days (middle) and 20 days (right), then were dissected at ZT1. All brains were stained with PDF antibody (shown in green). FUS-WT was tagged with RFP (shown in red). WT FUS overexpression reduced PDF staining and number of LNvs in the older flies. B. Adult control (Pdf>RFP, upper) and wild-type TDP43 overexpression (Pdf>FUS-WT-RFP #9, lower) flies were collected on the 1st day of eclosion. Flies were kept under 25C, 12:12 LD for 5 days (left) and 20 days (right), then were dissected at ZT1. All brains were stained with PDF antibody (shown in green). FUS-WT was tagged with RFP (shown in red). WT FUS overexpression flies showed decreased PDF staining and number of LNvs in older flies. White arrows indicate the weaker projection staining coming from the lLNvs to the optical lobe.

C9ORF72 has been found in familial ALS (DeJesus-Hernandez et al., 2011). We tested GGGGCC repeats, GGGGCC repeats with stop codon disruption ("RNA only", RO), and different dipeptide products (poly-proline-alanine(PA)/glycine-alanine(GA)/proline-arginine(PR)/glycine-arginine (GR)) with behavior assay. GGGGCC36 decreased the rhythmicity while all the GGGGCC RO reagents with either the same or higher repeat number (36/108/288) did not affect the rhythmicity when expressed in the PDF neurons (Table 2.2). For the dipeptide products translated from different ORFs, only the arginine-rich dipeptides reduce the rhythmicity. Our data implies that arginine-rich dipeptides are toxic to PDF neurons. This is consistent with the degeneration from the eye or pan-neuronal expression of the arginine-rich dipeptides in a previous study (Mizielinska et al., 2014).

2.4.4 The Expression of Human *Presenilin2* (*PSEN2*) Or *Drosophila* Mutant *Psn* (*Psn-D447A*) Leads to Arrhythmicity and PDF+ sLNv Loss

For AD-related models, we specifically observed the phenotypes related to *Presenilin 2* which encode the gamma secretase involved in processing the amyloid precursor protein (APP) into pathogenic Aβ42 peptides (Kumar-Singh et al., 2006). Mutations in PSEN2 will result in an increased ratio for toxic Aβ species (Riazanskaia et al., 2002). We found that the overexpression of human PSEN2 leads to partial arrhythmicity in both young and aged flies (Table 2.3, average P-S around 30).

Psn-D447A is a dominant negative mutation of *Drosophila Presenilin*, a homolog for human *PSEN* (Bier, 2005). Fly PSN is able to process human APP as well as fly APPL, then generate toxic human or fly Aβ fragments (Carmine-Simmen et al., 2009; Greeve et al., 2004). The overexpression of a mutant form of fly *Presenilin* (*Psn-D447A*) caused a slight decrease in rhythmicity in the young flies, and a further decrease in the aged flies (Table 2.3). However, we did not observe circadian phenotypes for Aβ models, including flies expressing human Aβ42 or

Pdf-G4 X	Period	P-S	n	R%
GGGGCC 3	24.1±0.2	120±13	9	100%
GGGGCC 36	22.5	3±3***	6	17%
GGGGCC RO 36	24.6±0.1	65±14	8	100%
GGGGCC RO 108	24.7±0.1	116±16	9	100%
GGGGCC RO 288	24.34±0.1	101±14	7	100%
poly PA PO 36	24.2±0.1	100±17	10	100%
poly PA PO 100	24.2±0.1	107±13	10	100%
poly GA PO 36	24.2±0.1	106±13	10	100%
poly GA PO 100	24.6±0.1	112±10	10	100%
poly PR PO 36	27.0±3.5	5±3***	7	29%
poly PR PO 100	22.5	2±2***	10	10%
poly GR PO 36	24.1±1.0	17±9***	7	86%
poly GR PO 100	23.2±0.2	13±7***	10	30%

Table 2.2. The Overexpression of Dipeptide Products Containing Arginine from GGGGCC Repeats Leads to Arrhythmicity

Rhythmicity (P-S), period, and % rhythmic flies (%R) are each indicated for various genotypes including flies expressing different transgenes driven by PdfGAL4. Flies were collected within the first 3 days after eclosion. T-tests were performed between the controls (GGGGCC3) and other pathogenic transgenes (*:p<0.05 **:p<0.01, ***:p<0.005).

Age	Genotype	Period	P-S	n	R%
D3	Pdf-Gal4 Ctrl	24.4±0.1	108±6	14	100%
	Pdf>PSEN2	23.8±0.1	30±12***	8	50%
	Pdf>Psn-D447A	24.3±0.1	51±12***	8	88%
D21	Pdf-Gal4 Ctrl	24.7±0.1	37±7	15	80%
	Pdf>PSEN2	24.3±0.1	32±9	7	71%
	Pdf>Psn-D447A	26.0±0.2	33±5	6	100%

Table 2.3. The Overexpression of Human PSEN2 and Fly Mutant PSN (D447A) in PDF Neuron Lowers Rhythmicity

Rhythmicity (P-S), period, and % rhythmic flies (%R) are each indicated for various genotypes including flies expressing different transgenes driven by PdfGAL4. Flies were collected within the first 3 days after eclosion. D21 flies were aged for 21 days prior to the test. T-tests were performed between the controls (PdfGAL4 Ctrl) and other pathogenic transgenes, at the same age (*:p<0.05 **:p<0.01, ***:p<0.005).

Aβ42 with familial mutations or co-expression of APP and BACE which could have been processed APP into Aβ. Aβ42 and mutant Aβ42 deposits amyloid plaques in fly brains and causes degeneration in other neurons (Crowther et al., 2005). However, they do not cause circadian defects with PdfGAL4, or degenerate LNvs (Chen et al., 2014). This accords with our data.

Examination of the PDF neurons found a selective reduction or loss of PDF (or PDF neurons) in the small LNv, but not the large LNv, in PSEN2 expressing flies. To elucidate whether the circadian defect was related to the presence of the LNvs, we imaged the LNvs with PDF staining at different ages. There were fewer sLNvs with positive PDF signals, even at very young ages (D1 and D5, Figure 2.7). At the age of D20, sLNvs were mostly absent, while the lLNvs were still present. This suggests that sLNvs are more vulnerable to PSEN2 induced toxicity. In both cases when human and fly Presenilin were overexpressed to induce arrhythmicity, the human APP was not co-expressed. A previous study has demonstrated that fly PSN can also process the fly homolog of the human APP, APPL, and lead to the formation of toxic amyloid-like deposits (Carmine-Simmen et al., 2009). Thus, it remains unclear whether the toxicity is related to the processing of fly endogenous APPL, or is due to an unknown function of Presenilin in circadian control. However, the similarity between human and fly Presenilin overexpression induced circadian defects suggests that there might be a conserved mechanism.

2.4.5 The Overexpression of Human *Ataxin3* (*ATXN3*) Leads to Arrhythmicity and PDF Neuron Loss

The expression of two polyQ disease genes, HTT and ATXN3 each caused arrhythmicity (Figure 2.1). Since the next chapter will focus on circadian phenotype caused by HTT, the focus of this chapter will be phenotypes from ATXN3. ATXN3 is the pathogenic gene for SCA3, also known as Machado-Joseph Disease. ATXN3 normally contains 12-37 CAG repeats, which became 61-84 in affected patients (Kawaguchi et al., 1994; Paulson et al., 1997). C-term fragments of ATXN3 containing 27 and 78 polyQ, corresponding to the normal and pathogenic

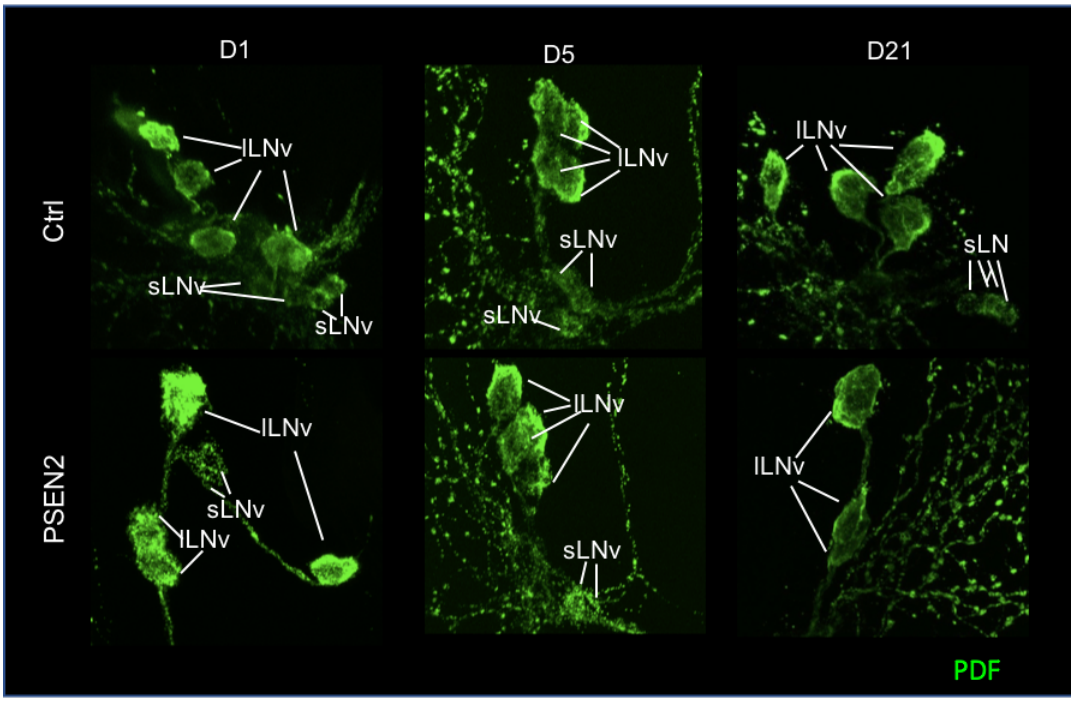

Figure 2.7. The Overexpression of Human PSEN2 Reduces PDF Positive Small LNvs Number

Representative images for control fly brains (Ctrl, upper) and fly brains expressing human PSEN2 overexpression (PSEN2, lower) are shown. Flies were collected within 1 day of eclosion. Flies were kept under 25C, 12:12 LD for 1 day (left), 5 days (middle) and 21 days (right), and then were dissected at ZT1. All brains were stained with PDF antibody (shown in green). PSEN2 overexpression reduced the number of sLNvs in older flies.

ATXN3, were incorporated into our screening. ATXN3Q78 decreased the rhythmicity in aged flies (Table 2.4). However, in addition to ATXN3Q78, the control ATXN3Q27 also reduced the rhythmicity in aged flies (Table 2.4). To further demonstrate whether all LNvs had been affected by ATXN3Q27/78 overexpression, we tested the brains with PDF staining. By D25, although most lLNvs were stained, less than 4 sLNvs remained in ATXN3Q27 expressing flies (Figure 2.8). In the ATXN3Q87 expressing flies, partial reductions in both sLNv and lLNv cell number were observed. The absence of sLNv in ATXN3Q27 expressing flies coincided with the reduced P-S in the aged flies. However, the difference in the affected subgroup of LNvs needs to be confirmed with a large sample size with more careful quantification since a previous study has reported that only sLNv are affected by ATXN3Q78 (but tested at a different age) (Kadener et al., 2006). Taken together, these results suggest that ATXN3 overexpression decreases rhythmicity and PDF positive LNvs, regardless of the length of the polyQ tract.

2.4.6 The Expression of Non-coding CAG Repeats Does Not Cause Behavioral Arrhythmicity

CAG repeats may be toxic via non-coding RNA mechanisms. CAG repeats have been predicted to form a hairpin structure, and this structure is found in HTT transcripts (de Mezer et al., 2011; Sobczak et al., 2003). The overexpression of CAG repeats that cannot be translated into proteins still causes neurodegeneration in flies. This confirms the RNA toxicity of CAG repeats *in vivo* (Lawlor et al., 2011; Li et al., 2008). We also tested CAG repeat overexpression and found that it does not decrease rhythmicity when expressed in PDF neurons, in either young or aged flies (Table 2.5). The expression of CAG RNA with the broader and stronger circadian driver timGAL4 also failed to cause arrhythmicity (Table 2.6). These data suggest that RNA toxicity might not contribute to the pathogenesis of polyQ gene-induced neurodegeneration in the PDF neurons.

Age	Genotype	Period	P-S	n	R%
D3	Pdf>ATXN3Q27	24.1±0.3	46±13	8	88%
	Pdf>ATXN3Q78	23.9±0.2	81±10	8	100%
D21	Pdf>ATXN3Q27	NA	$0±0^{\#\#\#}$	7	0%
	Pdf>ATXN3Q78	23.3±0.3	$8±4^{\#\#\#}$	5	40%

Table 2.4. The Overexpression of Human ATXN3 in PDF Neurons Reduces Rhythmicity in Older Flies

Rhythmicity (P-S), period, and % rhythmic flies (%R) are indicated for various genotypes including flies expressing different transgenes driven by PdfGAL4. Flies were collected within the first 3 days after eclosion. D21 flies were aged for 21 days prior to the test. T-tests were performed between D3 and D21 flies for the same genotypes (#:p<0.05 ##:p<0.01, ###:p<0.005).

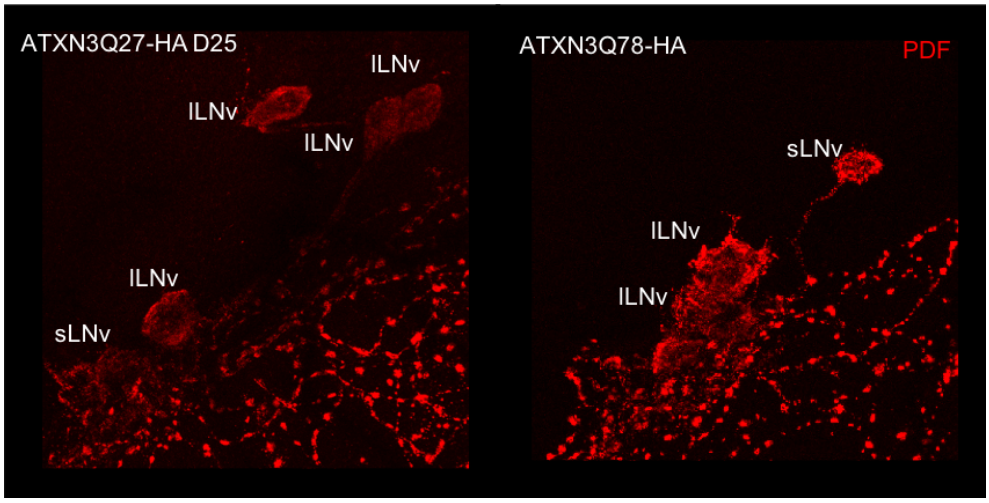

Figure 2.8. The Overexpression of Human Mutant ATXN3 Causes the Degeneration of PDF Positive LNvs

Representative images for fly brains expressing control ATXN3 overexpression (ATXN3Q27-HA, left) and mutant ATXN3(ATXN3Q78-HA, right) are shown. Flies were collected within 1 day of eclosion. They were kept under 25C, 12:12 LD for 25 days, then were dissected at ZT1. All brains were stained with PDF antibody (shown in red).

2.4.7 The Knockdown of *Hip14* Reduces the Rhythmicity and Lengthens the Period, in an Age-Dependent Manner

RNAi mediated knockdown of the HD-related gene *Hip14* resulted in an age-dependent period lengthening and a reduction in rhythmic power. A slight increase in the period (around 1hr) was observed in young flies (D3), while there were no significant changes in the rhythmicity (Table 2.6). However, the aged flies (D21) had a longer extension in the period accompanied by a strong decrease in rhythmicity. The decrease in rhythmicity was partially ameliorated by the overexpression of YFP tagged fly *Hip14* (Hip14-YFP), and the period was rescued to 25.2hr, closer to the period of the control flies. To maximize the phenotype, we then tested *Hip14* RNAi with a broader circadian driver with stronger expression in the PDF neurons (timGAL4). *Hip14* knocked down with timGAL4 decreased the rhythmicity even more (Table 2.6). Thus, the overexpression of Hip14 (UAS-Hip14.O) can significantly improve arrhythmicity.

Since the period and rhythmicity were strongly affected, we then asked whether there were any molecular changes in the core clock by assaying oscillations of the core clock component PER. PER staining was performed to test the core clock oscillation in LNvs in the *Hip14* RNAi flies. Flies at the age of D30 were used, since this age corresponds to the end of the behavior test for the aged flies when flies are more arrhythmic. However, for the peak and trough time for PER (ZT1 and 13), we did not observe any significant changes in the PER intensities or phase (Figure 2.9) under LD entrainment. Since the defects could be more evident under DD without the light input as a cue, we stained PER in the Hip14 RNAi flies on the second subjective morning (CT24). By CT24, we observed a mild, but significant, decrease in PER intensity among the lLNvs (data not shown).

Age	Genotype	Period	P-S	n	R%
D3	Pdf>CAG0	24.9±0.3	93±19	8	88%
	Pdf>CAG250	24.3±0.1	103±14	11	100%
D7	Pdf>CAG0	25.9±0.2	80±14	6	100%
	Pdf>CAG250	24.8±0.1	71±12	12	92%
D14	Pdf>CAG0	25.5±0.2	97±6	8	100%
	Pdf>CAG250	24.8±0.2	72±12	6	100%
D21	Pdf>CAG0	24.8±0.1	142±10	7	100%
	Pdf>CAG250	24.5±0.0	80±11	6	100%
D3	tim>CAG0	24.4±0.2	83±19	8	88%
	tim>CAG250	24.6±0.1	84±16	9	89%

Table 2.5. The Overexpression of CAG Repeats RNA Derived from Genes Does Not Cause Behavioral Arrhythmicity

Rhythmicity (P-S), period, and % rhythmic flies (%R) are indicated for various genotypes including flies expressing different lengths of CAG repeat in UTR region of the transgene driven by PdfGAL4 and timGAL4. Flies were collected within the first 3 days after eclosion. Flies with PdfGAL4 driven CAG repeat expression were tested right after collection (D3), or after aging for 1/2/3 weeks (D7/D14/D21). Flies with timGAL4 driven CAG repeat expression were tested right after collection (D3). T-tests were performed between controls with no repeat and pathogenic transgenes (*:p<0.05 **:p<0.01, ***:p<0.005).

Genotype	Period	P-S	n	R%
Pdf-Gal4/Ctrl (TRiP) (D3)	24.0±0.0	108±10	15	100%
Pdf-Gal4/+; Hip14 RNAi (TRiP)/+ (D3)	25.0±0.2*	70±8	15	100%
Pdf-Gal4/+;U-Hip14-YFP/Hip14 RNAi (TRiP) (D3)	24.9±0.4	94±12	8	100%
Pdf-Gal4/Ctrl (TRiP) (D21)	24.0±0.0	121±10	16	100%
Pdf-Gal4/+; Hip14 RNAi (TRiP)/+ (D21)	29.5±1.0***	13±4***	14	21%
Pdf-Gal4/+;U-Hip14-YFP/Hip14 RNAi (TRiP) (D21)	25.2±0.5#	40±13$	6	83%
tim-Gal4/Ctrl (TRiP) (D3)	24.3±0.1	80±9	8	100%
tim-Gal4; Hip14 RNAi (TRiP)/+ (D3)	25.4±0.2*	12±6***	8	50%
tim-Gal4; Hip14 RNAi (TRiP)/U-Hip14.O (D3)	24.6±0.3###	61±11###	7	100%

Table 2.6. Knocking Down of *Hip14* with PdfGAL4 Lengthens the Period while Knocking Down of Hip14 with timGal4 Reduces Rhythmicity

Hip14 RNAi was driven by either PdfGAL or timGALl4. A T-test was applied between different genotypes. * indicates the significance of period or P-S comparing the Hip14 RNAi to the control (GAL4 only) flies (*:p<0.05 **:p<0.01, ***:p<0.005). # indicates the significance of the period or P-S comparing Hip14 RNAi rescued by Hip14 overexpression to Hip14 RNAi only flies (#:p<0.05 ##:p<0.01, ###:p<0.005, $:p=0.05).

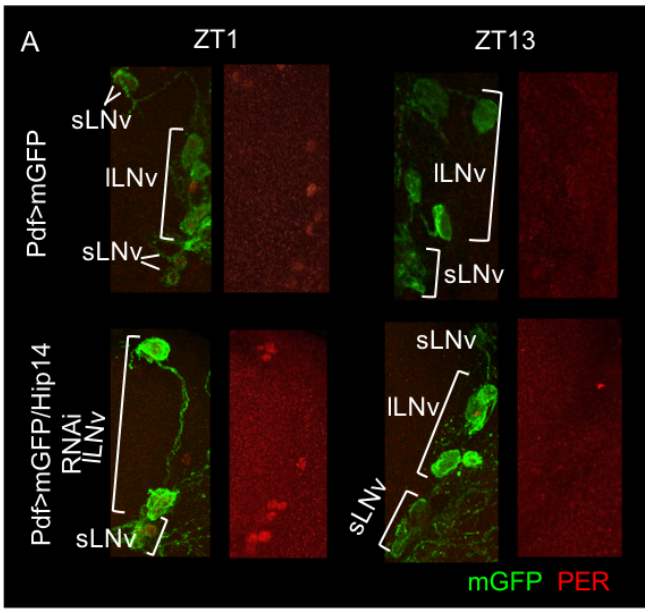

Figure 2.9. *Hip14* Knock Down with PdfGAL4 Does not Reduce PDF Positive sLNv, and PER is Not Affected under LD, but does Decrease in lLNvs under DD

Flies expressing mGFP in the PDF neurons in the wild-type control background (Pdf>mGFP) and expressing *Hip14* TRiP RNAi line (Pdf>mGFP/Hip14 RNAi) were used for dissection. Flies were entrained to 12:12 LD prior to dissection, and dissection was done at ZT1 and ZT13, at D30. sLNvs and lLNvs are labeled with mGFP (green). Brains are stained with PER antibody (red).

2.4.8 The Knockdown of *Hip14* Impairs Dorsal Projection Morphology and Elevates PDF Intensity in Dorsal Terminals

Given the potential role of HTT/HIP14 in synaptic transmission (Ohyama et al., 2007a; Romero et al., 2008), we asked whether it is possible that *Hip14* affects PDF signaling by controlling PDF release in the dorsal terminals, which are also under clock control (Fernandez et al., 2008; Sivachenko et al., 2013). To examine the morphology and PDF levels in the dorsal terminals, we imaged dorsal projections with PDF staining in both young and aged flies. Dorsal projections in the *Hip14* RNAi flies were similar to the control flies (Figure 2.10A) right after eclosion (D1), suggesting *Hip14* RNAi does not cause developmental defects. However, we observed striking morphology in the dorsal projections by D30 (Figure 2.10B). More branches and puncta were formed when *Hip14* was knocked down. The morphology and intensity of PDF in dorsal terminals each exhibited cycling patterns with higher intensity and more branches in the morning (ZT1), and lower intensity and fewer branches at night (ZT13) (Kula et al., 2006; Sivachenko et al., 2013). Control flies had a normal cycling pattern when comparing ZT1 to ZT13, while no cycling could be seen in the *Hip14* RNAi flies (Figure 2.10B).

To further elucidate whether the defects in PER and PDF in dorsal terminals had mediated the behavioral defects, we overexpressed core genes together with *Hip14* RNAi. PER overexpression, as well as ATX2 (since ATX2 activates PER translation (Lim and Allada, 2013a; Zhang et al., 2013)), was tested due to the observation of decreased PER levels under DD. The overexpression of PDFR was tested to verify the role of PDF signaling in Hip14 mediated circadian regulation. Significant rescue was found in the period by PDFR and ATX2 overexpression for both young and aged flies (Table 2.7). Due to the decreased rhythmicity in the aged (D21) *Hip14* RNAi and *Hip14* RNAi,ATX2 overexpressing flies, there was wide variation in the period. We were

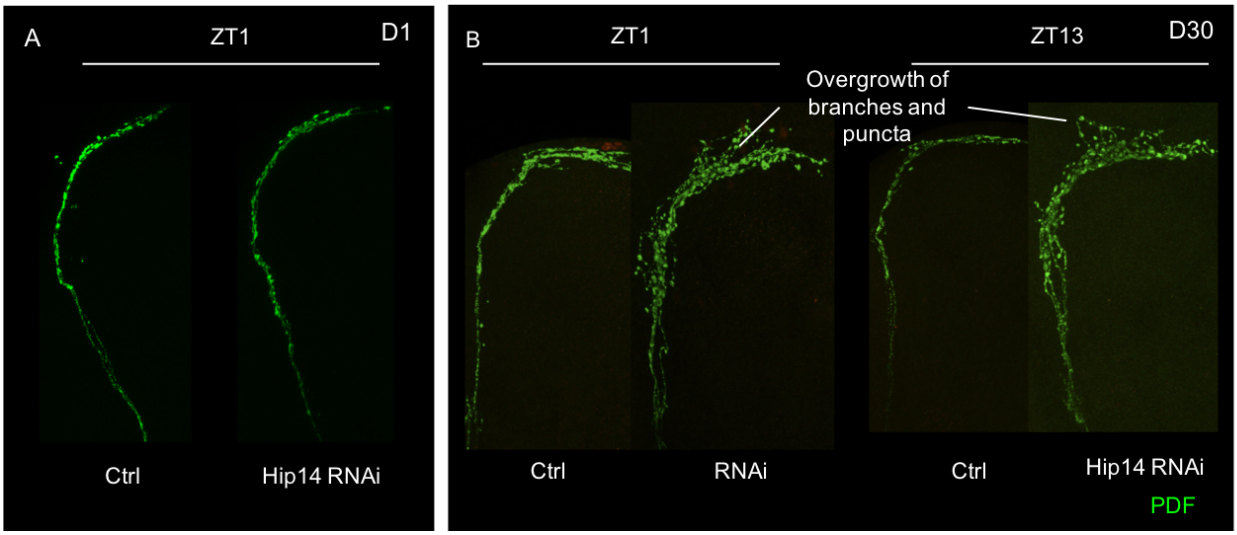

Figure 2.10. *Hip14* Knockdown with PdfGAL4 Leads to Overgrowth of Dorsal Projection Branches from sLNv in Aged Flies

A. Flies expressing *Hip14* RNAi (Pdf>Hip14 RNAi) in the PDF neurons, or only in the wild-type control background (PdfGAL4 Ctrl), were used for dissection. They were entrained to 12:12 LD prior to dissection and the dissection was conducted at ZT1, at the age of D1. Dorsal projections from sLNv were stained with PDF antibody. B. Flies expressing Hip14 RNAi (Pdf>Hip14 RNAi) in the PDF neurons or only in the wild-type control background (PdfGAL4 Ctrl) were used for dissection. Flies were entrained to 12:12 LD prior to dissection, and dissection was conducted at ZT1 and ZT13, at the age of D30. Dorsal projections from sLNv were stained with PDF antibody.

Age	Pdf-Gal4; Hip14 RNAi TRiP X	Period	P-S	n	R%
D3	Ctrl	25.5±0.1	75±8	8	100%
D21	Ctrl	26.6±0.5	28±11	8	63%
D3	UAS-PDFR	24.8±0.2***	92±13	7	100%
D21	UAS-PDFR	25.1±0.1$	69±15	7	100%
D3	UAS-ATX2	24.4±0.1***	30±12	8	63%
D21	U-ATX2	25.0±0.2*	23±10	12	50%
D3	Ctrl	25.1±0.2	104±8	8	100%
D14	Ctrl	26.0±0.2	52±12	5	100%
D3	UAS-PER16	25.3±0.1	79±16	7	100%
D14	UAS-PER16	25.6±0.1	83±21	4	100%

Table 2.7. PDFR and ATX2 Overexpression Reduces the Period Lengthening Due to *Hip14* Knockdown in Young Flies

The rhythmicity (P-S), period, and % rhythmic flies (%R) are indicated for various genotypes including flies expressing *Hip14* RNAi in the PDF neurons with overexpression of several circadian genes (UAS-PDFR or ATX2 or PER16) in the wild-type control background (ctrl). Flies were collected within the first 3 days after eclosion and were tested right after collection (D3) or after aging for 2-3 weeks (D14/D21). A t-test was applied between different genotypes. * indicates the significance for the period, comparing Hip14 RNAi with clock gene overexpression to *Hip14* RNAi flies at the same age (*:p<0.05 **:p<0.01, ***:p<0.005, $:p=0.05).

unable to conclude whether or not the period was reliable, based on the sample size used. However, since all of the young *Hip14* RNAi and *Hip14* RNAi with PDFR overexpression flies had P-S over 40 (a more stringent criterion for rhythmic flies), the rescue in the period within this age group should be reliable. A potential issue with conducting the behavior test at the age of D14 is that the *Hip14* RNAi flies had yet to show enough reduction in rhythmicity or lengthening of periods. Thus, the failure to show sufficient rescue by PER overexpression might not have been accurate. Behavior done at D14 should be repeated at D21 to confirm the results. To demonstrate whether the morphology defects of dorsal terminals can also be ameliorated by PDFR and ATX2 overexpression, we imaged the brains with PDF staining at D25. We did find less branching of the projections in both *Hip14* RNAi with PDFR and ATX2 overexpression flies, compared to the *Hip14* RNAi flies (Figure 2.11). Nevertheless, this conclusion should be verified with better quantification methods.

2.4.9 HIP14 Overexpression Suppresses Circadian Arrhythmicity Caused by Pathogenic Htt

Given that loss of *Hip14* has been implicated in HD pathogenesis, we also explored whether HIP14 overexpression could suppress mHtt induced arrhythmicity. Loss-of-function of *HIP14* has been identified as an alternative mechanism of HD pathogenesis. Evidence supporting this view includes 1. *Hip14* KO mice developed neurology and physiology degeneration similar to those of the mHtt mice models (Singaraja et al., 2011). 2. mHTT failed to potentiate the enzyme activity of HIP14 while wild-type HTT could. This would have led to the misregulation of proteins regulated by palmitoylations (Huang et al., 2011; Sanders and Hayden, 2015). Therefore, we hypothesized that the overexpression of fly HIP14 might rescue the toxicity from mHtt.

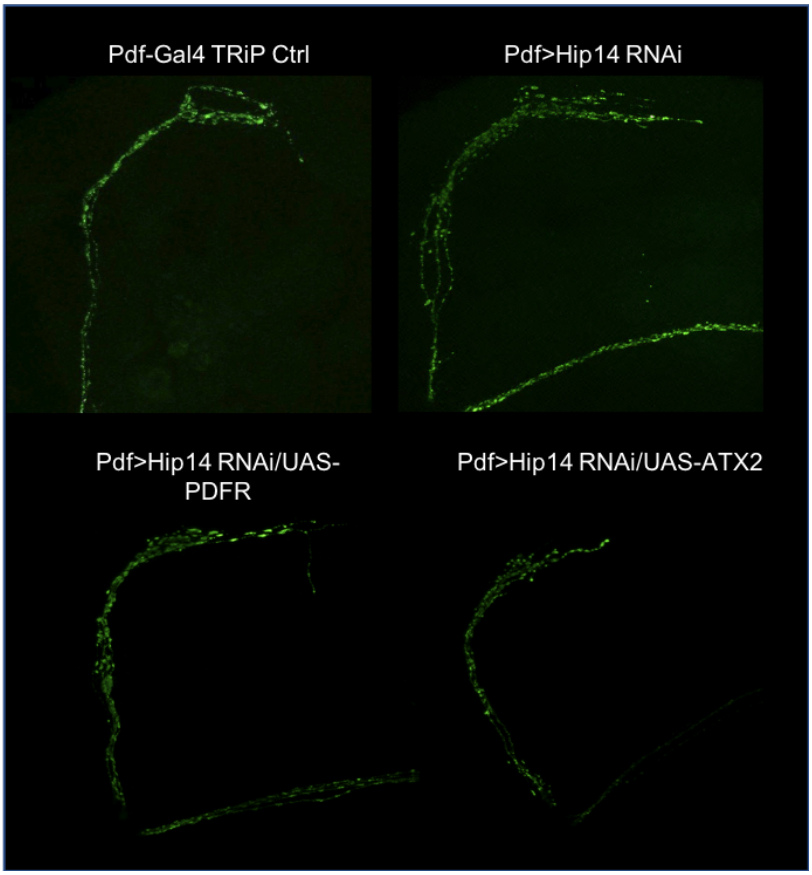

Figure 2.11. PDFR and ATX2 Overexpression Suppressed Morphology Defects in Dorsal Projections Due to *Hip14* Knockdown

Flies with only PdfGAL4 (PdfGAL4 TRiP Ctrl), as well as flies expressing *Hip14* RNAi in the PDF neurons with overexpression of PDFR or ATX2 (Pdf>Hip14/UAS-PDFR or ATX2) in the wild-type control background (Pdf>Hip14), were used for dissection at D25. Flies were entrained to 12:12 LD prior to dissection, and dissection was conducted around ZT1. Dorsal projections were stained with PDF (green). Morphology defects in *Hip14* RNAi flies are labeled.

We first tested the two HIP14 overexpressions with two mHtt transgenes with behavior assay. Both HIP14 overexpressing lines rescued arrhythmicity in HttQ128 expressing flies (Figure 12.2A). However, they may have improved arrhythmicity for HttQ103 expressing flies (Figure 12.2B), yet we cannot confirm the results were statistically significant since p was exactly .05. In addition, *Hip14* RNAi did not enhance the arrhythmic caused by HttQ103. Of note, HIP14 had a stronger interaction with the 548 amino acid N-term fragment of Htt, but miniscule interaction with the shorter fragment consisting of 224 amino acid (Sanders et al., 2014). The HttQ128 transgene contained the 548 amino acids while the HttQ103 transgene contained only the first exon (Lee et al., 2004a; Zhang et al., 2010b). Thus, it is possible that although HttQ128 might have had a weaker interaction with HIP14 than HttQ0, the interaction could have still been stronger than that of HttQ103. This resulted in higher functional overexpressed HIP14.

Next, we tested whether HIP14 overexpression also suppressed mHtt-induced sLNv cell loss. No rescue in sLNv numbers was found, suggesting that HIP14 might rescue the neuronal function of LNvs (Figure 2.13A). There was also no effect on HttQ46 aggregation with both HIP14 overexpression lines. This was consistent with the behavior data for HttQ103 (Figure 2.13B).

2.5 Discussion

This section has identified a range of circadian rhythm phenotypes across a broad range of many (but not most) neurodegenerative disease models. While many of these lines share reduced rhythmicity as a phenotype, differences in the underlying cell-type specificity and molecular phenotypes suggest distinct mechanisms that may reflect the differences observed in human diseases.

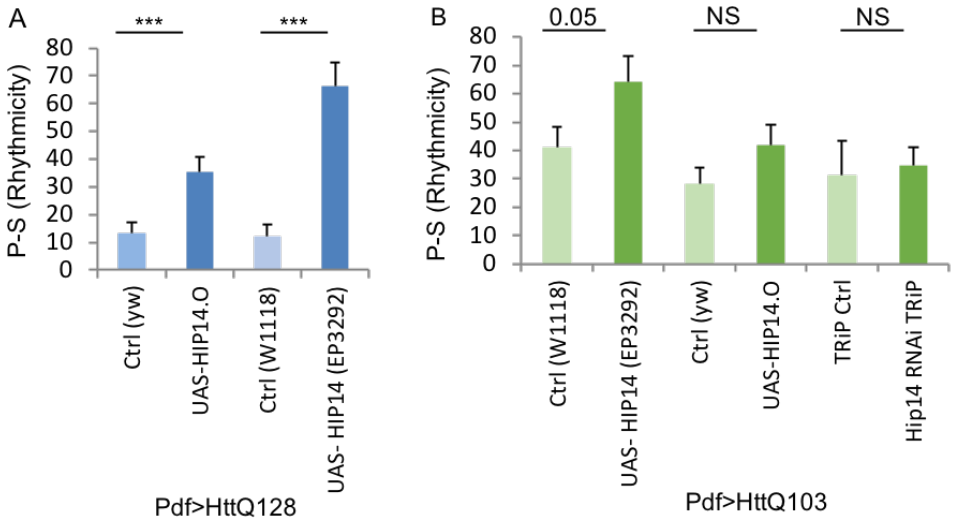

Figure. 2.12. HIP14 Overexpression Rescue was Arrhythmicity Induced by HttQ128, but not HttQ103

A. Rhythmicity (P-S) is indicated for various genotypes including flies expressing HttQ128 in PDF neurons in two different wild-type control backgrounds (Ctrl(W1118) and Ctrl(yw)), and expressing two different HIP14 overexpression lines (UAS-HIP14.O and UAS-HIP14 (EP3292); n=18-44 ; *p<0.05 **p<0.01, ***:p<0.005). B. A. Rhythmicity (P-S) is indicated for various genotypes including flies expressing HttQ128 in PDF neurons in three different wild-type control backgrounds (Ctrl(W1118), Ctrl(yw), and TRiP Ctrl), and expressing two different HIP14 overexpression lines (UAS-HIP14.O and UAS-HIP14 (EP3292)) or the *Hip14* RNAi line (n=14-27 ; *p<0.05 **p<0.01, ***:p<0.005, NS: not significant).

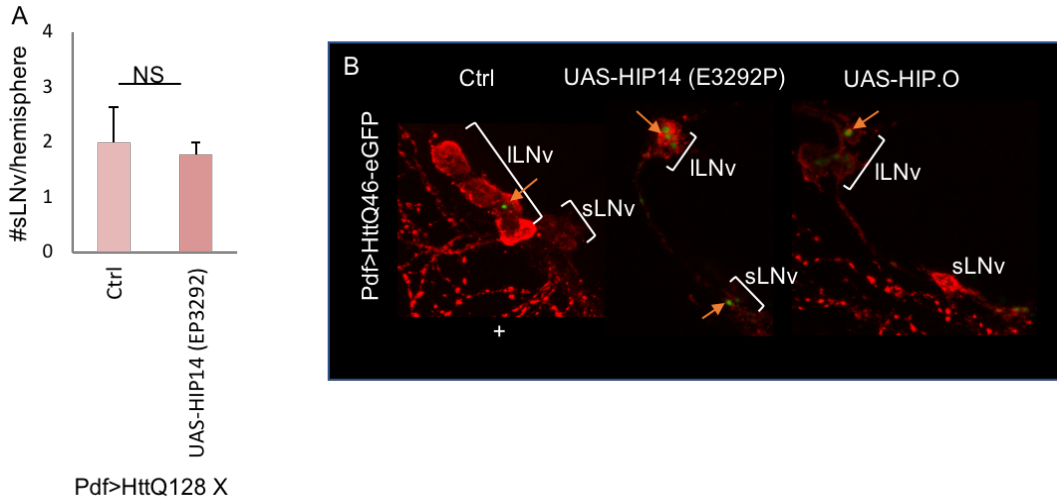

Figure 2.13. HIP14 Overexpression Does Not Rescue PDF Positive sLNv Number or Suppress Aggregation

A. The number of sLNv present per brain hemisphere at age day 5 is indicated for various genotypes, where either HIP14 (UAS-HIP14 (EP3292)) or wild-type control (Ctrl) and HttQ128 are expressed is shown (n=5-23; *p<0.05 **p<0.01, ***p<0.005, NS: not significant). B. Representative images of LNvs (sLNv and lLNv) expressing HttQ46-eGFP at day 30 are shown in the wild-type control background (Ctrl) or with HIP14 overexpression (UAS-HIP14 (EP3292) and UAS-HIP14.O). Sample aggregates are indicated by the orange arrows.

2.5.1 Different Neurodegeneration Genes Variously Impact Circadian Behavior, PDF levels, and PDF Neurons

Although we identified multiple ND genes that reduce rhythmicity and the number of PDF neurons, they do not appear to have identical effects. *TDP43* and *FUS* are both ND genes whose toxicity is not dependent on polyQ expansion. The overexpression of *TDP43* and *FUS* reduces rhythmicity and PDF positive LNv number. Unlike the case for mHTT overexpression (discussed in more detail in Chapter 3) or PSEN overexpression where only sLNvs degenerate, *TDP43* and *FUS* lead to the degeneration of both sLNvs and lLNvs. These data suggest that although multiple ND genes are toxic to the LNvs, the underlying mechanisms of why they are toxic are different. One way to take advantage of the non-polyQ ND models is to use them as an additional behavioral model to test whether modifiers found for polyQ expansion dependent ND could affect non-polyQ dependent degeneration.

Discrepancies also existed between the behavior phenotypes caused by different ND genes. Although small and large LNvs were both PDF-positive circadian neurons, the circadian phenotypes resulting from the absence of sLNvs only, or both sLNvs and lLNvs, were different. The loss of both sLNvs and lLNvs caused by *TDP43 or FUS* overexpression resembled the phenotypes observed from Pdf01 mutant and Pdf>hid flies in reduced morning anticipation, advanced evening peaks, and partial arrhythmicity under DD (as mentioned in the introduction section (Renn et al., 1999a)). However, the loss of sLNv only, such as what is caused by mHtt and *Presenilin,* leads to more severe arrhythmicity under DD, but no other distinct phenotypes under LD (Prakash et al., 2017). These discrepancies in LD phenotypes might be applicable to differentiating subgroup LNv degeneration.

The differences in the timing of arrhythmicity onset may imply what circadian genes/functions are first affected. Arrhythmicity induction by mHtt occurs in parallel with the disappearance of PDF positive sLNvs. Most of the flies were arrhythmic by the end of the DD,

while fewer than one sLNv on average remained at the corresponding age when we examined the PDF staining (data shown in Chapter 3). However, arrhythmicity elicited by FUS happened earlier than the absence of PDF signal in the LNvs. Especially for line FUS-WT-RFP #9, advanced evening peak and severe arrhythmicity under DD (data not shown) could be observed in the young flies, while most of the LNvs were still positive with PDF staining. These data suggest that some ND genes might impair PDF expression while simultaneously disrupting the other circadian gene expression or general cellular functions. Meanwhile, other ND genes may affect other circadian genes or cellular functions, prior to PDF signal decrease.

In summary, different ND genes induce degeneration in different circadian neurons and display different impacts on behavior. They might also impact different circadian genes or cellular functions in a distinct order.

2.5.2 Neurodegeneration Genes Might Cause Toxicity in PDF Neurons Differently Than in Other Neurons

ND genes that cause degeneration in other neuronal tissues may not degenerate LNvs. For example, we did not observe any Aβ42 transgenes (wild-type or mutant) that exhibited strong behavior phenotypes, although they did cause retinal degeneration (Iijima et al., 2004). Alpha-synuclein, which is found in PD, also did not show circadian phenotypes when expressed with PdfGAL4. However, the same transgenic lines reduced dopaminergic neurons when expressed with DcdGAL4, and decreased rhythmicity when expressed with THGAL4 (both Gal4s drive expression in dopaminergic neurons) (Feany and Bender, 2000)(data not shown, from Dr. Lee).

In addition, even for the ND genes that elicit degeneration in other tissues/neurons and LNv, detailed phenotypes might vary. For example, TDP43 overexpression leads to neuronal death when expressed in mushroom bodies and motor neurons. It has also been found to be mislocalized to cytoplasm prior to cell death, indicating that the cytoplasmic aggregates are toxic

(Li et al., 2010). In contrast, we did not observe any mislocalization of TDP43 until all the LNvs had degenerated (losing both PDF signal and RFP signal from TDP43). This suggests that the degeneration is more likely due to the malfunction of nuclear TDP43 in the LNvs. ATXN3 is another example of genes that show different toxicities in LNvs and other tissues. ATXN3Q78 is the pathogenic version that causes retinal degeneration, while ATXNQ27 serves as the non-toxic control in the eye (Warrick et al., 1998). However, arrhythmicity and LNv degeneration with ATXN3Q27 was observed as well. ATXN3Q27 is still less toxic than ATXNQ78, since the circadian defects only develop after aging. However, these data imply that the toxicity from ATXN3 might not have been restricted to aggregation results from the polyQ expansion; it might have also come from the function of ATXN3 in the LNvs.

2.5.3 Lack of Reliable Sleep Phenotypes when Expressing Neurodegeneration Genes in the Mushroom Bodies

We aimed to identify both circadian and sleep phenotypes for the ND genes with two different drivers targeting neurons controlling circadian and sleep, respectively. However, most of the consistent and reproducible results came from the PdfGAL4 driven ND gene screen for circadian phenotypes. This can partially be explained by the sleep data being inconsistent when lacking controlled genetic backgrounds. Although the 247GAL4 driver was isogenized, and we used virgins from 247GAL4 to make all the crosses, the ND transgenic lines were generated in different labs. Thus, they probably had different genetic backgrounds. Therefore, when we tried to replicate the initial hits, we were unable to find any reproducible data, owing to the large variation between runs.

In addition, it is known that 247GAL4 can drive expression in MB neurons that project into alpha, beta, and gamma lobes (Aso et al., 2009). Blocking synaptic transmission in these neurons initially was thought to be sleep-reducing (Pitman et al., 2006). However, the MB is a complex

structure and contains many types of neurons. Later studies have shown that some neurons can be sleep-promoting, while others can be wakefulness-inducing (Sitaraman et al., 2015). A non-specific MB driver like 247GAL4 may lead to over-expression in neurons that have opposite effects in sleep regulation. Drivers targeting more specific MB neuron subgroups for more unified functions in sleep regulation would be helpful for data interpretation.

2.5.4 Unique Age-dependent Circadian Phenotypes Caused by *Hip14* Knockdown

Hip14 knockdown displays a strong age-dependent circadian phenotype, which has not previously been described. Wild-type flies tend to have a longer period and less rhythmicity after being aged for at least 30 days (Umezaki et al., 2012). The PDF levels in mall LNvs and dorsal projections decreased after 40 days of aging (Umezaki et al., 2012). The age-dependent phenotypes from *Hip14* RNAi could have been due to the decrease in PDF signaling during the natural aging process. In addition, recent deep sequencing data comparing young and aged flies has revealed that there is a ~25% decrease in *Pdfr* expression in the older flies (Kuintzle et al., 2017). This supports the present study's data which indicates PDFR overexpression partially rescued the lengthened period in *Hip14* RNAi flies.

2.5.5 Potential Mechanisms for How *Hip14* Regulates Circadian Rhythms

As noted, we have demonstrated that upregulating PDF signaling can ameliorate circadian defects in *Hip14* RNAi flies. We also investigated whether *Hip14*'s function in synaptic transmission can mediate these defects. One of HIP14's palmitoylation targets is cysteine string protein (*Csp*) (Ohyama et al., 2007a). CSP displays mislocalization in synapses in Hip14 mutants, which results in neurotransmitter release deficiency (Ohyama et al., 2007a). We tested whether *Csp* is a downstream gene of *Hip14* in mediating circadian defects by combining *Hip14* RNAi with *Csp* mutants. The results showed even stronger PDF staining and more evident morphology

phenotypes (more branches and puncta) in the dorsal projections. This suggests synergetic genetic interaction between *Hip14* and *Csp* in the LNvs.

However, whether the behavioral phenotypes are linked to the morphology phenotypes observed in the dorsal projection remains unclear. *Csp* mutants are able to enhance the morphology phenotype, but not the behavioral phenotype. However, these behavioral experiments should be repeated, at a later age, to match the staining data and confirm the results.

Chapter 3: Circadian Clocks Function in Concert with Heat Shock Organizing Protein to Modulate Mutant Huntingtin Aggregation and Toxicity

Fangke Xu[1], Elzbieta Kula-Eversole[1]*, Marta Iwanaszko[2], Alan L. Hutchison[3], Aaron Dinner[4], and Ravi Allada[1]

Affiliations

[1]Department of Neurobiology, Northwestern University, Evanston, IL, USA

[2]Feinberg School of Medicine, Northwestern University, Chicago, IL USA

[3]Medical Scientist Training Program, University of Chicago, Chicago IL, USA

[4]James Franck Institute, University of Chicago, Chicago, IL USA

*Present Address: Department of Obstetrics, Gynecology and Reproductive Biology College of Human Medicine, Grand Rapids Research Center, Michigan State University, Grand Rapids, MI, USA

Correspondence: r-allada@northwestern.edu

3.1 Summary

Neurodegenerative diseases commonly involve the disruption of circadian rhythms. Studies indicate that mutant Huntingtin (mHtt), the cause of Huntington's Disease (HD), disrupts circadian rhythms often before motor symptoms are evident. Yet little is known about the molecular mechanisms by which mHtt impairs circadian rhythmicity and whether circadian clocks can modulate HD pathogenesis. To address this question, we used a *Drosophila* HD model. We found that both environmental and genetic perturbations of the circadian clock alter mHtt-mediated neurodegeneration. To identify potential genetic pathways that mediate these effects, we applied a novel behavioral platform to screen for clock-regulated HD suppressors, identifying a role for *Heat Shock Protein 70/90 Organizing Protein* (*Hop*). *Hop* knockdown paradoxically reduces mHtt aggregation and toxicity. These studies demonstrate a role for the circadian clock in a neurodegenerative disease model and reveal a clock-regulated molecular and cellular pathway that links clock function to neurodegenerative disease.

Keywords: circadian, Huntington's disease, heat shock, transcriptome, genetic screen

3.2 Introduction

Considerable evidence suggests that disrupted clocks or sleep are associated with and potentially alter neurodegenerative disease processes (Musiek and Holtzman, 2016). In diseases from Alzheimer's disease (Giubilei et al., 2001; Satlin et al., 1995; Stopa et al., 1999), Parkinson's disease (Bordet et al., 2003; Kudo et al., 2011a), Huntington's disease (Aziz et al., 2009; Kalliolia et al., 2014; Morton et al., 2005; Pallier et al., 2007; van Wamelen et al., 2013), chronic traumatic encephalopathy (CTE) (Asken et al., 2016), TBI (Mathias and Alvaro, 2012; Verma et al., 2007),

and frontotemporal dementia (Anderson et al., 2009), circadian and/or sleep disruption has been consistently observed as evidenced by altered phase or amplitude of sleep-wake, activity, and/or temperature rhythms; melatonin and cortisol hormonal rhythms; circadian pacemaker neuron and clock gene rhythms. In many cases, the circadian or sleep disruption precedes the appearance of the diagnostic symptoms of the disease, suggesting that they are impaired early in the disease process. For example, reduction in melatonin levels is observed in patients even in preclinical AD stages (Braak stages I–II; (Wu et al., 2003). These studies suggest that the circadian clock is both a target of and may regulate neurodegenerative disease. Yet definitive evidence that the circadian clock can impact neurodegeneration in human disease models has been lacking.

To address the mechanistic relationship between circadian clocks and neurodegenerative diseases, we are using Huntington's disease models. Polyglutamine (polyQ) expansion in Huntingtin (mHtt) leads to dysfunction/death of medium spiny neurons in the striatum and the characteristic Huntington's chorea (Milnerwood and Raymond, 2010). Both human and animal studies indicate that mHtt also impairs circadian rhythms. Circadian behavioral rhythms are disrupted in HD patients and mouse models (Kudo et al., 2011b; Kuljis et al., 2012; Loh et al., 2013; Morton et al., 2005; Pallier et al., 2007). In HD patients, behavioral arrhythmicity is accompanied by disrupted melatonin rhythms (Aziz et al., 2009; Kalliolia et al., 2014) and reduced numbers of VIP+ neurons in the master circadian pacemaker suprachiasmatic nucleus in HD patients (van Wamelen et al., 2013). In mouse models, SCN electrical activity can be disrupted in the presence of intact core molecular clock oscillations, indicating that clock output is disrupted (Kudo et al., 2011b). Molecular clocks are not only evident in the SCN but also in other brain regions, such as the striatum. In HD mouse models, disrupted molecular rhythms are observed in the SCN (Morton et al., 2005; Pallier et al., 2007) as well as in the striatum (Morton et al., 2005) and cortex (Fahrenkrug et al., 2007). In transgenic R6/2 mice,

treatment with a sedative drug improved sleep-wake rhythms and reversed the dysregulated expression of Per2 and markedly improved their cognitive performance (Pallier et al., 2007; Pallier and Morton, 2009). Disrupted circadian rhythms and motor symptoms in mouse HD models were improved by time-restricted feeding (Wang et al., 2018; Whittaker et al., 2018). However, it was not known if these rhythm-improving interventions were solely symptomatic or if they altered the neurodegenerative process itself. Taken together, mHtt can disrupt the core clock and/or clock output of clock pacemaker neurons such as those in the SCN and may therefore contribute to behavioral rhythm disruption in HD. In addition, mHtt also targets clocks in the disease-relevant striatum. How mHtt and molecular clocks interact in clock expressing neurons remains unclear.

To study how circadian disruption can modulate Huntington's disease, we are using the fruit fly *Drosophila*, a well-established model organism in the study of circadian rhythms and neurodegenerative disease. The fruit fly is an evolutionarily conserved model system to study circadian rhythms (Allada and Chung, 2010b; Tataroglu and Emery, 2015). In flies, the CLOCK (CLK)/CYCLE (CYC) transcription factor (reviewed in (Mohawk et al., 2012; Zheng and Sehgal, 2008)) activates *period (per)* and *timeless (tim)*. PER and TIM proteins are in turn modified by protein kinases, such as DOUBLETIME (DBT) and inhibit CLK-CYC function (Kim et al., 2007; Kloss et al., 1998). The conservation extends to humans where mutations in the orthologs of fly *per* and *Dbt* are responsible for the circadian disorder, advanced sleep phase syndrome (Fu et al., 2001; Xu et al., 2005), providing a compelling rationale for using the fly as a model for circadian rhythms and its interaction with Huntington's pathology.

Valid *Drosophila* Huntington's models have been generated by expression of human Htt with varying polyQ lengths. These fly models recapitulate many features of human HD. These include reduced lifespan (Lee et al., 2004b; Wolfgang et al., 2005), motor deficits (Chongtham

and Agrawal, 2016; Lee et al., 2004b), neurodegeneration (Agrawal et al., 2005; Steffan et al., 2001), cytoplasmic followed by nuclear accumulation of mHtt (Jackson et al., 1998), and disrupted circadian rhythms (Sheeba et al., 2010). mHtt effects also depend on CAG repeat length (Jackson et al., 1998). In addition, the underlying molecular mechanisms of mHtt pathogenesis are conserved, including mTor (Ravikumar et al., 2004), histone acetylation (Ferrante et al., 2003; Hockly et al., 2003; Steffan et al., 2001), SUMOylation/ubiquitination (Steffan et al., 2004), and axonal transport (Gunawardena et al., 2003; Smith et al., 2014). The striking similarities between human, mammalian and fly HD including at the level of genes and therapeutics indicates that the fly can make important contributions to understanding HD.

While circadian clock mutations can enhance neurodegeneration, especially under challenge, including in a disease model (Krishnan et al., 2012; Means et al., 2015; Musiek et al., 2013), Whether these mutations exert their effects via their role in clocks versus pleiotropic effects remains unclear. Moreover, a role for the clock in mHtt toxicity has not been demonstrated. Here we provide evidence that circadian clocks can modulate neurotoxic effects of polyQ-containing proteins, such as those in Huntington's disease, representing a potential therapeutic avenue to slow disease progression. In addition, we identify pathways that may mediate clock control of mHtt aggregation and toxicity including a role for heat shock pathways.

3.3 Material and Methods (STAR Method)

EXPERIMENTAL MODEL AND SUBJECT DETAILS

Adult male *Drosophila* melanogaster were used for most of the experiments (behavior, staining and qPCR) except for RNA-seq and the behavior for Abeta42 expressing flies. Fly stocks were maintained at room temperature. Crosses were set on the standard cornmeal-yeast-agar medium (81.4g cornmeal, 19.2g yeast, 11.1g soy flour, 6.42g agar, 42.8ml corn syrup, 42.8ml

molasses, 5.35ml propionic acid and 13.4ml ethanol and 1.43g methylparaben per 1L of food), incubated under 12:12 or 10:10 (for the misalignment experiment) LD cycles at 25°C. Flies were collected within 24 hours after eclosing during the L phase and aged on the regular food under the LD condition their parents were entrained until they were used for behavior or staining experiments.

Adult female Pdf>Abeta42 flies were used for behavior assays due to the UAS-Abeta42 transgene landed on the X chromosome. Crosses were set on the regular food, incubated under 12:12 LD cycles at 25°C. Females were collected within 24 hours after eclosing during the L phase and aged on the standard cornmeal-yeast-agar medium under 12:12 LD. Female control flies (Pdf-Gal4 X control strains) were acquired with the same procedure.

RNA-seq samples were acquired from adult female Pdf>mGFP flies. Flies were raised on standard cornmeal-yeast-agar medium at 25°C and collected within 5 days after eclosing. Flies were kept under 12:12LD on 1.5X Sucrose-Yeast (SY) fly food at 25°C (HC25), 0.5X SY fly food at 25°C (LC25) or 1.5X SY fly food at 18°C (HC18) for 5 days before sampled for dissection and FACS.

Flies used for behavioral analysis were kept on tubes containing sucrose-agar food (5% sucrose and 2% agar) for 5 12:12 LD cycles (or 6 10:10 LD cycles) followed by 7 DD cycles.

METHOD DETAILS

Whole Mount Immunostaining

Fly crosses were set on the standard cornmeal-yeast-agar medium under 12:12 or 10:10 (for the misalignment experiment) LD cycles at 25°C. Flies eclosing within 24 hours were collected and kept under the conditions they were raised until the ages indicated in each experiment. Adult brains were dissected in PBS (137mM NaCl, 2.7mM KCl, 10mM Na_2HPO_4 and 1.8mM KH_2PO_4) within 10 minutes. Then brains were fixed in 3.7% formalin solution (diluted from 37% formalin

solution, Sigma-Aldrich) for 30 minutes. Brains were washed with 0.3% PBSTx (PBS with 0.3% Triton-X) for 4 times before primary antibody incubation. Primary antibodies were diluted in 0.3% PBSTx with 5% normal goat serum and incubation was done at 4°C overnight. Brains were washed for 4 times with 0.3% PBSTx after primary antibody incubation. Secondary antibodies were diluted in 0.3% PBSTx with 5% normal goat serum and incubation was done at 4°C overnight. Primary antibody dilutions were done as the followings: mouse anti-PDF (1:800, DSHB), rabbit anti-PER (1:8000, from Rosbash Lab). Secondary antibody dilutions were done as the followings: anti-mouse Alexa594 (1:800, invitrogen), anti-mouse Alexa488 (1:800, invitrogen), anti-rabbit Alexa594 (1:800, invitrogen), anti-rabbit Alexa488 (1:800, invitrogen), anti-rabbit Alexa647 (1:800, invitrogen).

Fly Stocks

RNAi lines used for screening and other overexpression lines were acquired from Bloomington Stock Center unless indicated separately. UAS-HttQ0/128 were kindly provided by Dr. Littleton. UAS-HttQ25/46/72/103-eGFP were kindly provided by Dr. Perrimon. UAS-TDP43-WT was kindly provided by Dr. Wu.

FACS, RNA Extraction from LNvs, RNA-seq and qPCR

LNvs were labelled with Pdf>mGFP. Fly brains were dissected at certain time points and processed as previously described (Kula-Eversole et al., 2010; Nagoshi et al., 2010). More specifically, brains were dissected in dissecting (pH7.4 9.9mM HEPES-KOH, 137mM NaCl, 5.4mM KCl, 0.17mM NaH_2PO_4, 0.22mM KH_2PO_4, 3.3mM glucose and 43.8mM sucrose) and kept in SMactive media (4.18mM KH_2PO_4, 1.05mM $CaCl_2$, 0.7mM $MgSO_4 \bullet 7H_2O$, 116mM NaCl, 8mM $NaHCO_3$, 2mg/ml glucose, 2mg/ml trehalose 0.35mg/ml α-ketoglutaric acid, 0.06mg/ml fumaric acid, 0.6mg/ml malic acid, 0.06mg/ml succinic acid, 2mg/ml yeast extract with 20% non-heat-inactivated FBS, 2μg/ml insulin and 5mM pH6.8 Bis-Tris) on ice right after dissection. Both dissecting saline and SMactive media contain 20μM DNQX, 50μM APV and 0.1μM TTX as final

concentration. After finishing dissection of all the brains needed for one experiment, brains were washed with 500μl dissecting saline twice (spin down at 2000rpm for 1min between washes). 100μl Papain solution (50unit/ml) for each sample was activated at 37°C for 10min prior to use. Saline washed brains were incubated in at room for 30min in the Papain solution. Papain was deactivated by adding 500μl SMactive media to the brain sample and the brains were washed with 500μl SMactive media for 3 times. Cells were dissociated by triturating brains with self-made medium opening P1000 filter tip for around 30 times followed by triturating brains with self-made small opening P1000 filter tip for around another 30 times. Cells were filtered with nylon filters (SEFAR NITEX 03-100/32). GFP positive cells were isolated at Flow Cytometry Facility at Northwestern University. RNA from FACS sorted LNvs were extracted with PicoPure Knits. We synthesized 1st and 2nd strand cDNA from RNA first with Superscript III and DNA polymerase. Then we amplified the RNA by synthesizing more RNA from the cDNA template with T7 RNA polymerase. Amplified RNA was purified with RNeasy Mini Kit (Qiagen). After the second round of cDNA synthesis from amplified RNA, the cDNA was submitted to HGAC at university of Chicago for library preparation and sequencing. Sequencing was done in HGAC at university of Chicago with Illumina HiSeq 2000. All samples are done with single end reads of 50 base pairs.

LNv cDNAs tested with qPCR were prepared in the same way described above. RNA from whole head samples was purified by TRIzol following the manufacturer protocol. Genomic DNA was digested by RQ1 DNase (Promega). First strand cDNA was synthesized using SuperScript III First-Strand Synthesis System (invitrogen) and applied for qPCR using SYBR Green supermix (BIO RAD).

QUANTIFICATION AND STATISTICAL ANALYSIS

Confocal Imaging and Data Quantification

Fly brains after immunostaining were imaged by Nikon C2 confocal. Data processing and quantification were done with Nikon NIS Elements. For sLNv number quantification, PDF positive sLNv number for each genotype under each condition was counted blindly. Sample sizes indicated in the legends represent number of hemispheres used for each experiment combined from at least 2 replicates. Two tail t-test was performed between two genotypes/conditions need to be compared.

For PER or GFP intensity measurements, the intermediate stack of each cell was chosen for measuring the mean intensity. Three areas for each hemisphere was randomly chosen and measured for background measurements. Cells in the same hemisphere used the same background mean intensity. The final mean intensity for PER or GFP signal from HttQ25-eGFP or HttQ46-eGFP was calculated by mean intensity measured from the middle stack of a cell minus the background mean intensity and then divided by the background mean intensity. Sample sizes indicated in the legends represent number of LNvs used for each experiment. Two tail t-test was performed between two genotypes/conditions need to be compared.

For aggregation quantification, a threshold was applied to the channel used for imaging Htt aggregation (threshold was usually between 2500 to 3500, and the same threshold was used for control and experimental groups in a certain experiment). The percentage of cells containing aggregates passing the threshold was calculated. Sample sizes indicated in the legends represent number of LNvs used for each experiment. Z-statistic, and the corresponding p-value, was determined for statistically comparing percentages.

Locomotor Activity Recording and Circadian Data Analysis

Behavior data recording, processing, plotting and analysis were done mainly as previously described (Pfeiffenberger et al., 2010a, b). Fly locomotor activity was recorded from the Drosophila Activity Monitoring (DAM) data collection system and then extracted with DAM File Scan. Rhythmicity was measured by power - significance (P-S), parameters calculated by

ClockLab (using Chi-square periodogram). Flies with P-S below 10 were considered arrhythmic and thus eliminated from the average period calculation. Flies lacking rhythmic power are considered as completely arrhythmic and are assigned with P-S=0, but are included in the average rhythmicity calculation. Activity actograms were plotted with either Counting Macro or ClockLab. Morning and evening Index were calculated with normalized activity given by output from Counting Macro. Morning Index = sum of normalized activity 3hr before light on / sum of normalized activity 6hr before light on. Evening Index = sum of normalized activity 3hr before light off / sum of normalized activity 6hr before light off (Seluzicki et al., 2014a). The interval for summarizing the activities used for anticipation calculation is adjusted for per^S under 12:12 (ZT6-8/ZT4-8) and 10:10 (ZT7.5-10/ZT5-10). The time of evening peak onset is calculated by finding the time when the largest increase in activity happens (Seluzicki et al., 2014a). Data are represented as mean ± SD for onset time. Behavior tests for HttQ128 flies, with or without modifiers, were done with flies enclosed within 3 days by the 1st day of behavior run. Behavior test for HttQ103 flies, with or without modifiers, were done with day 4-6 old flies. All flies for behavior were entrained from the embryonic stage (after egg-laying) under 12:12 LD cycles (or 10:10 LD as indicated in the text). Sample sizes indicated in the legends represent number of flies used for each experiment combined from at least 2 independent runs. Two tail t-test was performed for P-S, anticipation index or activity peak onset time between two genotypes/conditions need to be compared.

RNA-seq and qPCR Data Analysis

Reads from each time point under each food/temperature condition were quantified against Flybase transcript assembly, release 6.14, using kallisto (Bray et al., 2016b). Gene level quantification was obtained using tximport library, both for TPMs and counts data. Our LNv data comprise of three food/temperature combination conditions, with 12 time points per each condition: 1.5X Sucrose-Yeast (SY) fly food and 25°C),0.5X SY fly food and 25°C and 1.5X SY

fly food and 18°C. Genes which do not pass the threshold of TPM >1 in at least 50% of samples were filtered out, leaving 7863 genes; conditions were concatenated to generate a 36 time points as an input data for Boot eJTK to determine cycling genes (Hutchison et al., 2018). We applied Benjamini-Hochberg (BH) correction method to Gamma p-values calculated by Boot eJTK. BH corrected p-value of less than 0.05 and fold change greater than 1.5 (between peak and trough) were used as a threshold for detection of cycling genes. For qPCR, relative RNA abundance was calculated based on delta CT values relative to the geometric average of CT values of Rp49 and Cam as internal controls (Vandesompele et al., 2002). The RNA abundance of a gene in the experimental sample is then normalized to the RNA abundance for the same gene in the corresponding control in each experiment for fold change calculations. Significance is determined by t-test setting control to 1 in each experiment.

3.4 Results

3.4.1 Expression of mHtt in PDF clock neurons suppresses circadian rhythmicity in a polyQ length-dependent manner

To address the clocks-HD interaction, we did not attempt to fully model all aspects of HD in a fruit fly. Rather we focused specifically on the role of the molecular clock in modulating mHtt in clock-containing neurons. This endophenotype is potentially highly relevant to HD as a subset of clock neurons in the suprachiasmatic nucleus are known to be lost in HD, suggesting that mHtt targets these neurons. In addition, striatal neurons also contain molecular clocks (see (Morton et al., 2005)) suggesting a potential cell autonomous mechanism by which clocks could impact striatal neurodegeneration in the pathognomonic target of HD.

We expressed human Htt genes in a subgroup of fly circadian neurons, PDF+ ventral lateral neurons (LNv), using *pdfGAL4*. We mainly used two sets of human *Htt* transgenes, the first set, HttQ128 and HttQ0 (the non-pathogenic control for HttQ128 lacking polyQ repeats), which

contains exon 1, 2, and part of 3 of the *Htt* gene (Romero et al., 2008), and the second set, *HttQ103-eGFP*, *HttQ72-eGFP*, *HttQ46-eGFP*, and *HttQ25-eGFP* (the last is the non-pathogenic control for *HttQ103/72/46*) contains the first exon of the *Htt* gene with varying polyQ lengths (Zhang et al., 2010b). The eGFP fusions facilitate tracking of polyQ aggregation (see below). PDF+ LNv can be further divided into large (lLNv) and small LNv (sLNv), the latter playing a crucial role in driving free-running rhythms under constant darkness conditions (Grima et al., 2004; Stoleru et al., 2005). Expression of HttQ128 in the PDF+ LNv induces arrhythmicity and loss of the sLNv subset, comparable to the loss of subsets of SCN neurons observed in humans (Sheeba et al., 2010; Sheeba et al., 2008). Consistent with prior studies, we observed polyQ length dependent impairment of circadian rhythmicity (Power-Significance; P-S; for HttQ128 and HttQ103, Table 3.1). These effects are accompanied by age-dependent loss of a subset of sLNv (Figure 3.1A and B). Not all toxic neurodegenerative genes induce these effects. Transgenic expression of Aβ42 induces retinal degeneration in flies(Burr et al., 2014). To determine if this transgene can alter rhythmicity, we drove expression in PDF neurons. However, it failed to reduce rhythmicity when expressed in PDF neurons, even after aging for several weeks (Figure 3.1C). Thus, we hypothesize that clock neurons (or at least a subset) are especially sensitive to mHtt consistent with HD neuropathology.

In addition to cell loss, disrupted molecular clocks may also underlie poor behavioral rhythmicity in mHtt flies. It has been previously shown that the presence of even a single sLNv is sufficient for behavioral rhythms (Helfrich-Forster, 1998) and thus additional changes may be needed to suppress rhythms. Disruptions of circadian clock oscillations have been observed in mammalian HD models. Using both the HttQ128 and HttQ103 models, we observed strong reductions in PER levels at typical peak times of day in both the remaining sLNvs as well as the lLNvs, which do not undergo apparent cell loss (Figure 3.1D-F). These data also indicate that we are inducing functional levels of mHtt in both sets of neurons even though we do not observe

	Period	P-S	n	R%
Pdf-Gal4/U-HttQ0#10-2	24.5±0.1	97±10	16	94%
Pdf-Gal4/U-HttQ128#35	X	0±0 ***	14	0%
Pdf-Gal4/+;U-HttQ25-eGFP/+	24.2±0.1	93±10	14	100%
Pdf-Gal4/+;U-HttQ46-eGFP/+	24.2±0.1	99±12	17	94%
Pdf-Gal4/+;U-HttQ72-eGFP/+	24.8±0.1	84±13	15	96%
Pdf-Gal4;U-HttQ103-eGFP/+	24.0±0.1	42±9***	16	75%

Table 3.1. Polyglutamine length dependent effects of Htt on circadian rhythmicity

(*p<0.05, **p<0.01, ***p<0.005 compared to non-pathogenic Htt control lines respectively)

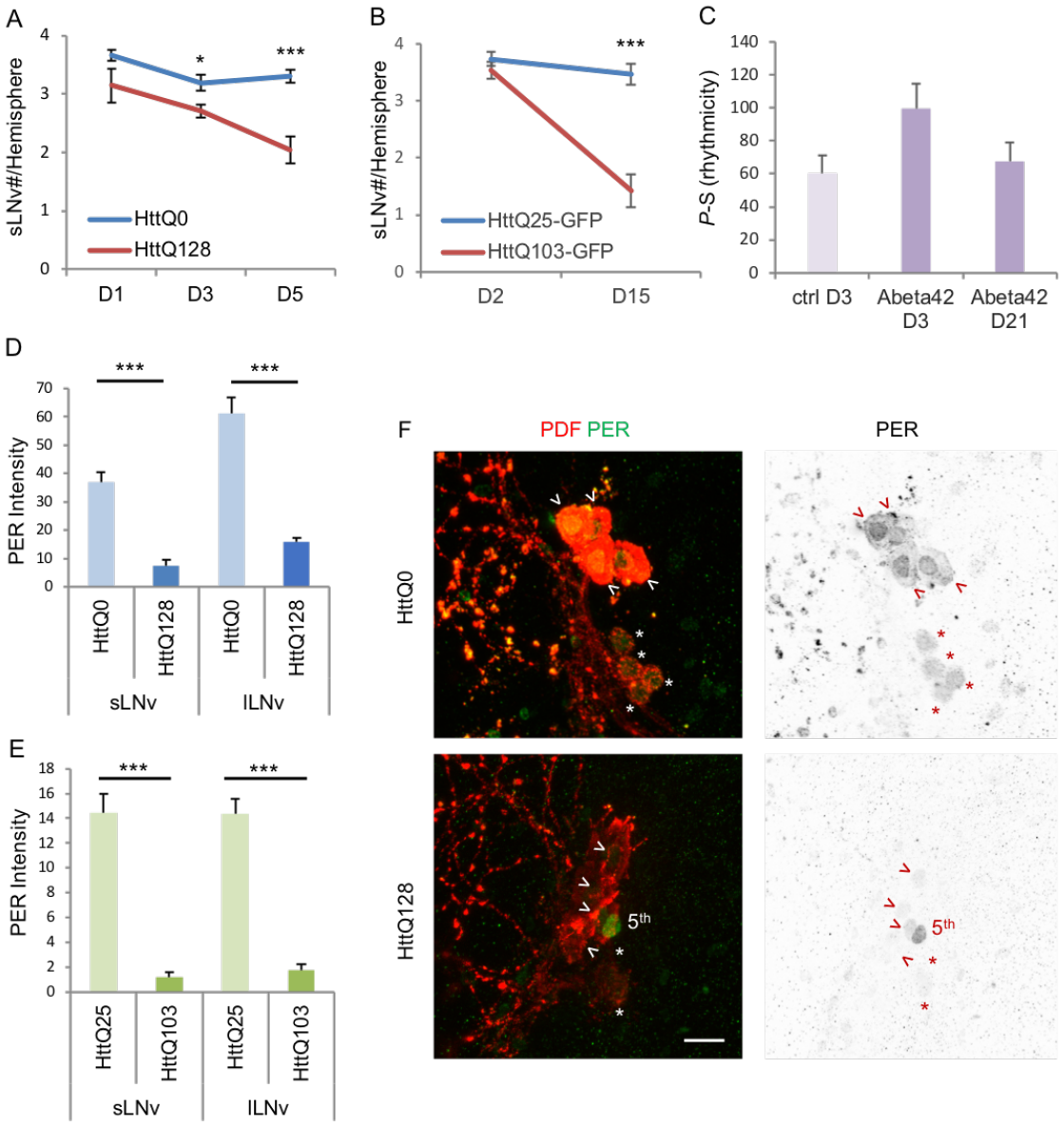

Figure 3.1. HttQ128 and HttQ103 reduce sLNv cell number and strongly suppress PER levels

A. sLNv cell number at different ages are shown for HttQ0 and HttQ128 expressing flies (n=8-23). B. sLNv cell number at different ages are shown for HttQ103 expressing flies (n=12-15). HttQ103 overexpression significantly decreases PDF positive sLNv number at D15 compared to HttQ25. C. Rhythmicity (P-S) is indicated for various genotypes including flies with(Abeta42) and without (ctrl) Abeta42 in PDF neurons at either the age of day 3 (D3) or day 21 (D21). (n=8-15). D,E. PER intensity at ZT0 in s- and l-LNv in Pdf>HttQ0 and Pdf>HttQ128 flies (D; n=6-23) and Pdf>HttQ25 and Pdf>HttQ103 flies at age day 15 (E; n=7-28) at ZT0 in sLNvs and lLNvs is quantified and shown (N=6-23). (*:p<0.05 **:p<0.01, ***:p<0.005 two-tail t-test) F. Representative images of LNvs (sLNv, lLNv, and 5th sLNv) expressing HttQ0 or HttQ128 are shown. Staining of PER is indicated in green while co-staining of PDF is indicated in red. Asterisks indicate sLNvs while arrowheads indicate lLNvs. The PDF- 5th sLNv is labelled with "5th" if it is evident in the image. Scale bar indicate 10μm.

lLNv cell loss. These potent clock disrupting effects of *mHtt* on molecular rhythms are consistent with fly and mammalian studies (Khaskheli et al., 2017; Morton et al., 2005; Pallier et al., 2007). These data establish a molecular pathway, the core circadian clock, to assay mHtt effects on pre-degenerative neuronal function in a genetic model system.

3.4.2 Heterozygous *Clk^{Jrk}* mutants suppress mHtt effects on sLNv cell number and mHtt aggregate formation

While effects of mHtt on the core clock have been previously observed, it is unclear if the clock can, in turn, impact HD pathogenesis. Genetic evidence suggests the clock may influence neuronal survival, but this has not been established in HD in flies or mammals. To test the role of the clock in HD pathogenesis, we tested the core clock mutant *Clk^{Jrk}*. *Clk^{Jrk}* contains a premature stop codon truncating the activation domain but retaining its dimerization domain resulting in a dominant negative form of this transcriptional activator (Allada et al., 1998). Homozygotes are arrhythmic with low *per* RNA levels while heterozygotes exhibit reduced levels with low amplitude oscillations (Allada et al., 1998). As *Clk^{Jrk}* homozygotes apparently lack detectable sLNv (Park and Hall, 1998), we tested heterozygotes. First in flies expressing HttQ0 we did not observe any reduction in the number of sLNv consistent with idea that *Clk^{Jrk}* heterozygotes do not display developmental phenotypes evident in homozygotes (Figure 3.2A). Surprisingly, we found that more sLNv were spared in HttQ128 expressing flies (Figure 3.2A). To further confirm that this is likely due to a circadian effect rather than a pleiotropic *Clk* function, we examined a second circadian clock mutant *per^{01}* as well as *per^{01}; Clk^{Jrk}*/+ double mutants. Interestingly, while *per^{01}* failed to suppress (or enhance) HttQ128 effects, *per^{01}* was able to suppress the neuroprotective effect of *Clk^{Jrk}*/+ (Figure 3.2A). The notion that *per^{01}* does not show the same phenotype as *Clk^{Jrk}*/+ (Figure 3.2A). The notion that *per^{01}* does not show the same phenotype as *Clk^{Jrk}* is not surprising as they “fix” the clock at opposite points in the cycle. The

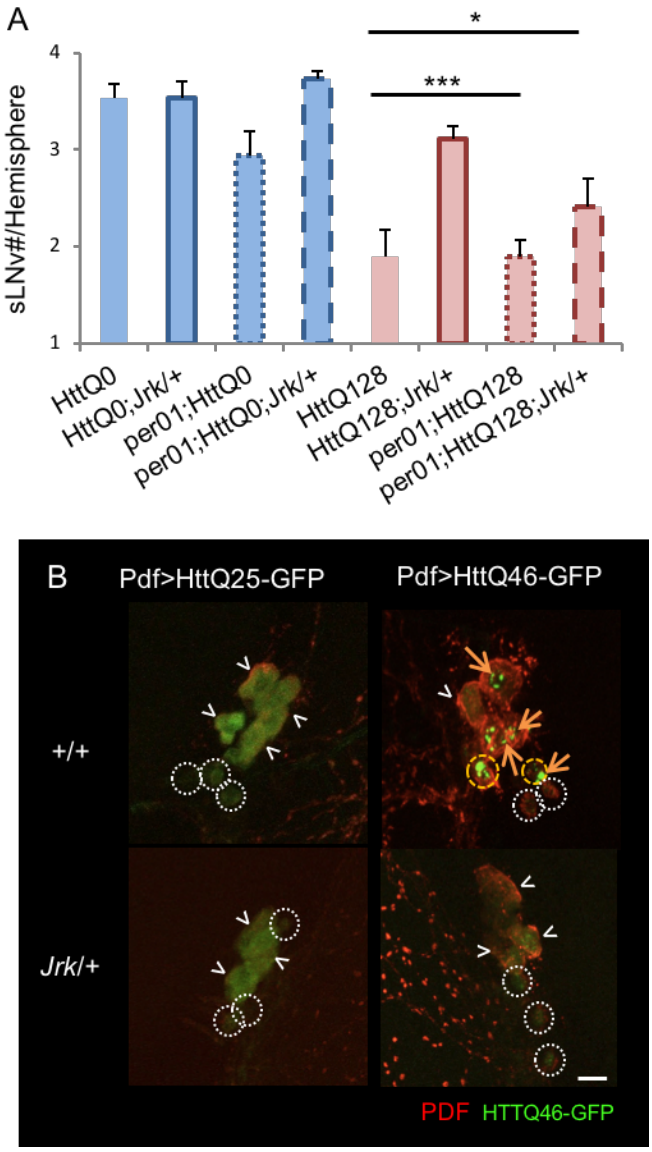

Figure 3.2. mHtt-induced sLNv Loss and Aggregate Formation in *Clk^{Jrk}/+* Flies

A. The number of sLNv present per brain hemisphere is indicated for various genotypes where HttQ0 and HttQ128 indicate fragments of Htt with (Q128) and without (Q0) polyglutamines. per^{01} and Jrk indicate *per^{01}* and *Clk^{Jrk}* mutants (n=17~29; *:p<0.05 **:p<0.01, ***:p<0.005) B. Representative images of LNvs (sLNv and lLNv) expressing HttQ25-eGFP and HttQ46-eGFP (in green) are shown for wild-type (+/+) and *Clk^{Jrk}/+* (Jrk/+). Co-staining for PDF is indicated in red. White arrowheads indicate lLNvs. White arrowheads indicate lLNvs. White dot circles label sLNvs without aggregates. Yellow dash circles label sLNvs with aggregates. Example aggregates are pointed out by orange arrows. Scale bar indicates 10μm.

lack of a *per*^{01} phenotype could be explained by a ceiling effect to how much the clock can enhance mHtt effects. Nonetheless, we hypothesize that abrogation of PER repressor activity enhances CLK activated transcription suppressing the *Clk*^{Jrk}/+ effect. Importantly, it highlights the importance of the PER negative feedback loop, a cornerstone of the circadian clock, in HttQ128 effects. Moreover, it indicates that low *per* is not responsible for *Clk* effects as *per*^{01} does not have any apparent phenotype but instead likely reflects other CLK-activated genes.

3.4.3 Misalignment between endogenous circadian periodicity and daily light-dark cycles can suppress mHtt effects on sLNv cell number and aggregate formation

One issue with the use of arrhythmic clock mutants is that one cannot easily distinguish between the role of a clock gene in the circadian clock from other pleiotropic effects of these genes. Circadian resonance experiments, where the timing of the endogenous clock is matched or mismatched with the cycles of daily environmental cycles (Yan et al., 1998), is the gold standard to definitively demonstrate functional roles of circadian timing. To test the role of circadian timing, we entrained *pdfGAL4/UASHttQ128* flies under 12:12 and 10:10 LD cycles from the time of egg laying, i.e., throughout development. Thus, the only difference between the two groups is in the daily timing of the light-dark cycle to which the flies entrain. Flies are capable of entraining to these altered light:dark cycles as evidenced by the coherence (low standard deviation) on the first day of constant darkness for the evening activity offset (Figure 3.S1). Surprisingly, we found that more sLNv were spared under 10:10 than under 12:12 conditions (Figure 3.3A). These effects were accompanied by a reduction in mHtt aggregates. Aggregates are quantified by identifying spots of high fluorescence intensity, reflecting the high concentrations of GFP-tagged proteins. Using the eGFP tagged HttQ72, we found a reduction in the % of sLNv that contain aggregates in 10:10 v. 12:12 conditions (Figure 3.3B and C).

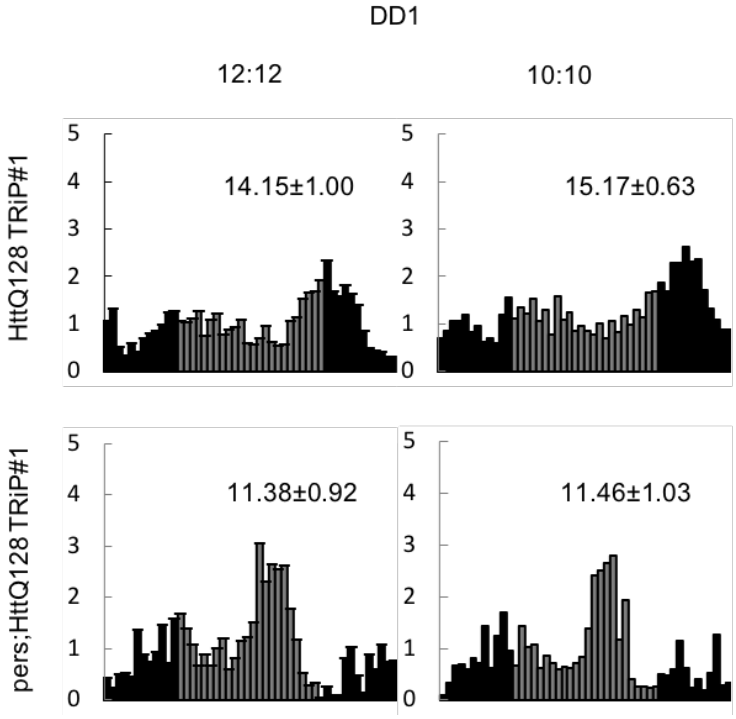

Figure 3.S1. HttQ128-Expressing Flies Exhibit Synchronous Free-Running Rhythms in Constant Darkness after 12:12 or 10:10 Light-Dark Cycle Entrainment

Averaged activity eductions for Pdf>HttQ128 flies in *per*$^{+}$ or *per*^{S} on the 1st day of DD after 5 days 12:12 LD entrainment (left) and the 1st day of DD after 6 cycles (5 days) 10:10 LD entrainment (right) are shown. The time of the onset of the evening peak is indicated +/- standard error of the mean calculated in hours after the subjective light on (see Methods) and labeled on each eduction graph. Related to Figure 3.

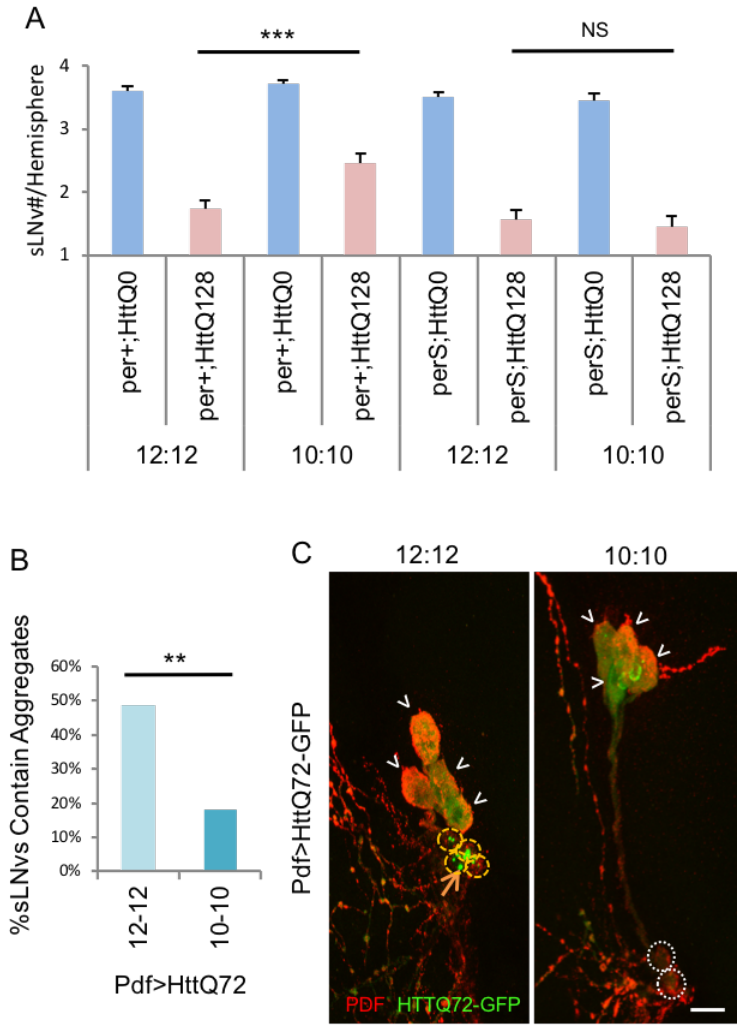

Figure 3.3. Exposure to 10L:10D Cycles Reduces mHtt-mediated sLNv Cell Loss and Aggregate Formation

A. The number of sLNv present per brain hemisphere at age day 5 is indicated for various genotypes and environmental cycles where HttQ0 and HttQ128 indicate fragments of Htt with (Q128) and without (Q0) polyglutamines. *per+* and *per^S* indicate wild-type and *per^S* mutants (n=36-62) B. Percentage of LNvs containing HttQ72-eGFP aggregates are indicated under 12 h light: 12 dark conditions (12-12) and 10 h light: 10 h dark conditions (10-10; n=37-39). C. Representative images of LNvs (sLNv and lLNv) expressing HttQ72-eGFP (in green) are shown under 12:12 and 10:10 conditions. Co-staining for PDF is indicated in red. White arrowheads indicate lLNvs. White dot circles label sLNvs without aggregates. Yellow dash circles label sLNvs with aggregates. Example aggregates are pointed out by orange arrows. Scale bar indicates 10μm. For all panels, *:p<0.05 **:p<0.01, ***:p<0.005. Scale bar indicates 10μm.

To determine if this effect was due to circadian clock timing, we examined *per*^{S} flies with an endogenous period of 19 h that more closely aligns with the 10:10 cycle. We found that the neuroprotective effect of 10:10 is no longer evident, indicating the effect is related to circadian timing (Figure 3.3A). Thus, by first altering the timing of light-dark cycles we can alter mHtt induced cell loss and then by altering the timing of the clock to more closely match these cycles we can reverse this effect. These studies provide compelling evidence that altering clock timing in relation to environmental cycles can modify mHtt-induced effects.

As wild-type and *per*^{S} flies are able to entrain to both 12:12 and 10:10 cycles, we more closely examined light-dark activity profiles in these flies including in the HttQ128 models. Wild type and HttQ128 flies display a robust evening anticipatory rise in locomotor activity in advance of lights-off under 12:12 conditions consistent with the notion that non-PDF neurons are critical for evening anticipation (Figure 3.S2). However, this peak is absent under 10:10 conditions, likely due to the delayed phase of entrainment. *per*^{S} flies on the other hand show a phase advance of the evening peak in LD but, unlike wild-type, retain robust evening anticipation in 10:10 cycles (Figure 3.S2). Thus, genetic/environmental conditions that retain evening anticipation exhibit normal mHtt effects, while in the case where evening anticipation is not evident during the light phase we observe a reduction in those effects. We are not claiming a functional link between evening anticipation and mHtt effects. However, it is possible that clock regulated genes may exhibit a similar pattern and the phase relationship between circadian gene expression and the timing of the light-dark cycle may be important for mHtt-induced neurodegeneration. Taken together, we have demonstrated through multiple lines of evidence that modulation of the circadian clock can alter the neurotoxic effects of mHtt, providing a molecular pathway impacting HD pathogenesis.

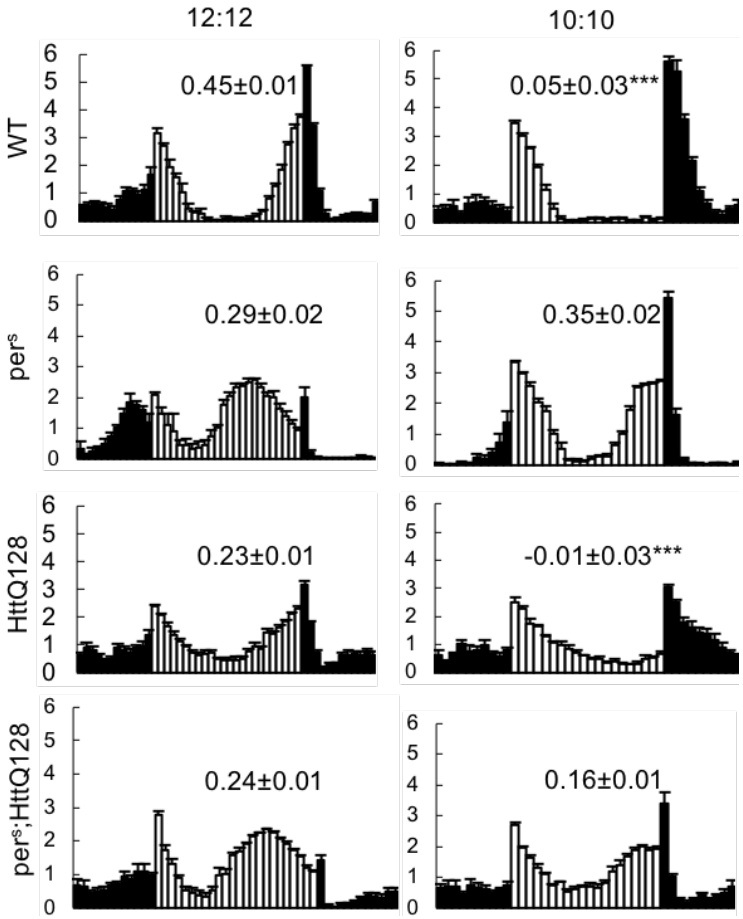

Figure 3.S2. Wild-Type Flies Expressing HttQ128 Do Not Exhibit Anticipation of Light-Dark Transitions in 10:10 Cycles

Averaged activity eductions for control (Wt) flies and Pdf>HttQ128 flies over 4 days of 12:12 or 5 cycles of 10:10 LD. Evening anticipation index for each genotype and condition is labeled on the graph. T-tests were performed for the flies with the same genotype between 12:12 and 10:10 to look for changes under 10:10 with *per+* (*p<0.05, **p<0.01, ***p<0.005). Related to Figure 3.

3.4.4 RNAi screen of LNv clock-regulated genes identified replicable suppressors of mHtt induced behavioral arrhythmicity

As both environmental (10:10 LD) and genetic (Clk^{Jrk}/+) manipulations of the circadian clock reduced mHtt-induced neuronal loss, we hypothesized that manipulations of clock-controlled genes may mediate these effects. To identify these mediators, we performed RNA sequencing from FACS sorted PDF+ LNvs at 2 h time resolution across 3 LD cycles. We labeled PDF+ neurons with GFP, dissected and dissociated brains and FACS selected GFP+ neurons as we previously described(Nagoshi et al., 2010). Libraries were generated (TruSeq Sample Preparation kit) and RNA-Seq was performed (HiSeq2000, Illumina). Sequence alignments and quantitation were performed using Kallisto (Bray et al., 2016a). While these experiments were performed using two different temperatures and diets, we performed rhythmic gene detection across the 3 days of data using the boot empirical JTK_CYCLE with asymmetry search method with Benjamini-Hochberg correction for false discovery (boot eJTK; gammaBH<0.05, fold change>1.5) (Hutchison et al., 2018). We reasoned that robust clock-controlled genes should be cycling irrespective of diet and temperature. Using this approach, we identify 1789 cycling genes, including the core clock genes, validating the overall approach (Figure 3.S3). We will more fully describe this data set elsewhere.

To identify clock-controlled genes (CCGs) that modulate mHtt toxicity, we performed an RNAi screen to knockdown CCGs and assayed HttQ128 effects on behavioral rhythmicity. We prioritized robustly cycling genes as well as those which have been previously implicated as mHtt modifiers in prior studies (Doumanis et al., 2009; Zhang et al., 2010b). As behavioral rhythmicity is a functional readout of intact LNvs, it is possible that modifiers could improve rhythmicity by suppressing HttQ effects on neuron loss as well as pre-degenerative neuron function. To our knowledge, a genetic screen enabling discovery of modifiers of mHtt pre-degenerative function has not previously been performed in animals. We hypothesize that such “early” modifiers may

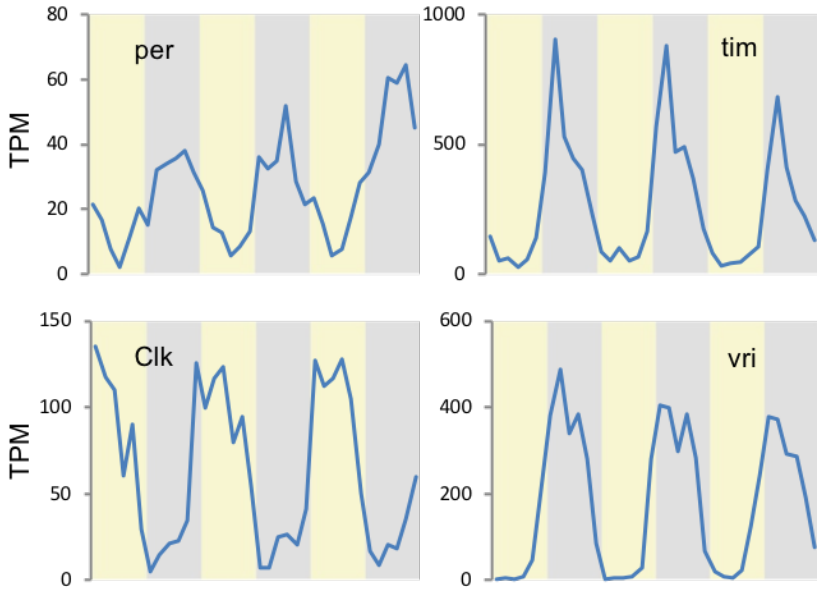

Figure 3.S3. Oscillating Transcript Levels for Core Clock Genes in PDF^{+} LNv Across 24h Light-Dark Cycles

Transcript levels in transcripts per million (TPM) for four core clock genes, *period* (*per*), *timeless* (*tim*), *Clock* (*Clk*) and *vrille* (*vri*) across three 24 hour light:dark cycles. Light and dark periods are indicated in yellow and gray, respectively. Each profile is in the following order: standard 1.5x sucrose-yeast (SY) food at 25°C, 1.5xSY at 18°C, and 0.5xSY at 25°C. Related to Figure 4.

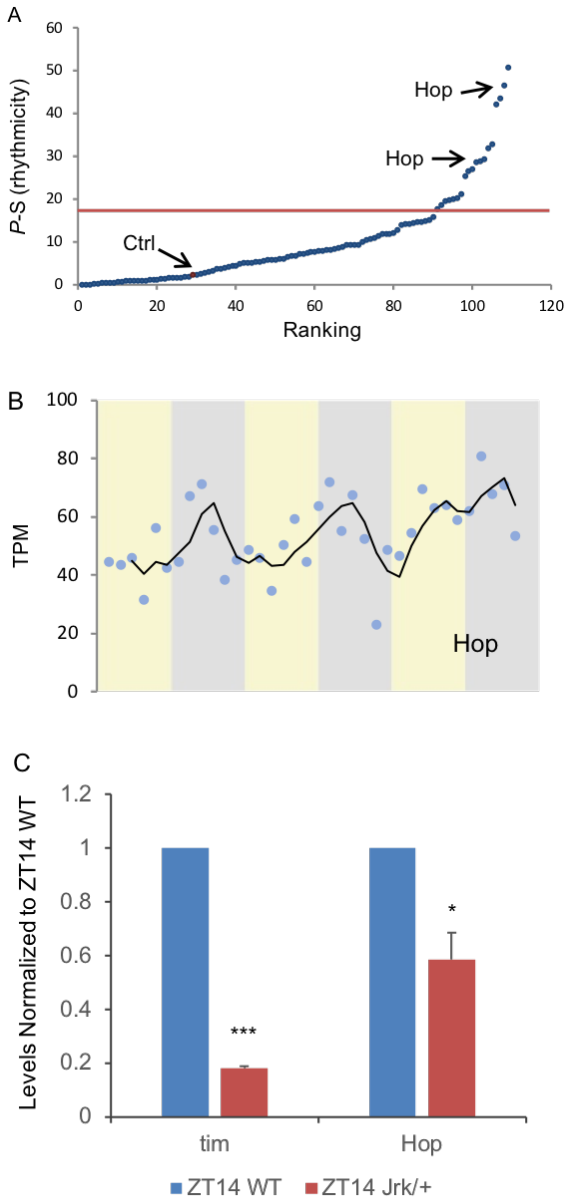

Figure 3.4. Identification of Hsp70/90 Organizing Protein (*Hop*) in a Screen for Cycling Genes That Suppress HttQ128-Induced Arrhythmicity

A. X-axis indicates ranking of screened RNAi lines based on their average rhythmicity (Power-Significance; P-S) values in pdf>HttQ128 flies. The red line indicates the cut-off for RNAi to be considered modifiers, and the red circle (Ctrl) indicates the average P-S of the control. Two independent *Hop* RNAi lines that are modifiers are indicated by black arrows. B. Transcript levels in transcripts per million (TPM) for *Hop* across three 24 hour light:dark cycles. Light and dark periods are indicated in yellow and gray, respectively. Trend line indicates a 3 h window moving average. Each profile is in the following order: standard 1.5x sucrose-yeast (SY) food at 25°C, 1.5xSY at 18°C, and 0.5xSY at 25°C. C. LNv transcript levels at ZT14 for *tim* and *Hop* from Clk^{Jrk}/+ (ZT14 Jrk/+) are normalized to wild-type (ZT14 WT). Average levels for 4 replicates are shown. * indicates $p<0.05$ by t-test.

highlight pathways with therapeutic potential before irreversible cell loss. We screened around 150 lines mainly from Bloomington TRiP collection and identified 16 primary hits that suppressed the effects of HttQ128 on behavioral rhythmicity (Figure 3.4A). Here we initially focus on *Hsp70/90 Organizing Protein* (*Hop*). Other modifiers will be described more fully elsewhere. *Hop*, also known as stress inducible protein STI1, functions as a co-chaperone for the major protein chaperones Hsp70 and 90 to facilitate protein folding (Baindur-Hudson et al., 2015). While the *Hop* transcript does not exhibit a rhythmic amplitude comparable to the core clock genes, it consistently peaks across all three days during the nighttime (Figure 3.4B), a time around which CLK-activated cycling gene expression, such as *per,* is peaking (Figure 3.S3). Using quantitative PCR from FACS sorted PDF+ LNv, we found reductions in both *Clk*-activated *tim* transcript and *Hop* transcript in Clk^{Jrk}/+ mutants consistent with the idea that *Clk* activates *Hop* (Figure 3.4C).

3.4.5 Impairment of the Hsp70/90 Organization Protein and Other Heat Shock Chaperone Components Suppresses mHtt Toxicity

Several studies have shown that elevated expression or activity of heat shock proteins, including *Hop* itself, reduces mHtt or polyQ toxicity and/or aggregation formation (Chan et al., 2000; Hay et al., 2004; Kuo et al., 2013; Wolfe et al., 2013) while reduction of heat shock pathway components enhances mHtt or polyQ toxicity (Brehme et al., 2014; Wolfe et al., 2013). Surprisingly, *Hop* RNAi knockdown using two independent RNAi reagents partially suppressed arrhythmicity caused by HttQ128 (Figure 3.5A). On the other hand, *Hop* RNAi in otherwise wild-type flies did not further improve their rhythms indicating the phenotype is mHtt-dependent (Figure 3.S4). To determine if these effects were specific to mHtt, we expressed a mutant form Tar Domain Protein 43 (A315T) that causes an inherited form of amyotrophic lateral sclerosis (Gitcho et al., 2008)(ALS). Expression in PDF neurons caused suppression of free running rhythmicity (Figure 3.5A). Previous studies had shown that overexpression of the fly homolog of glycogen

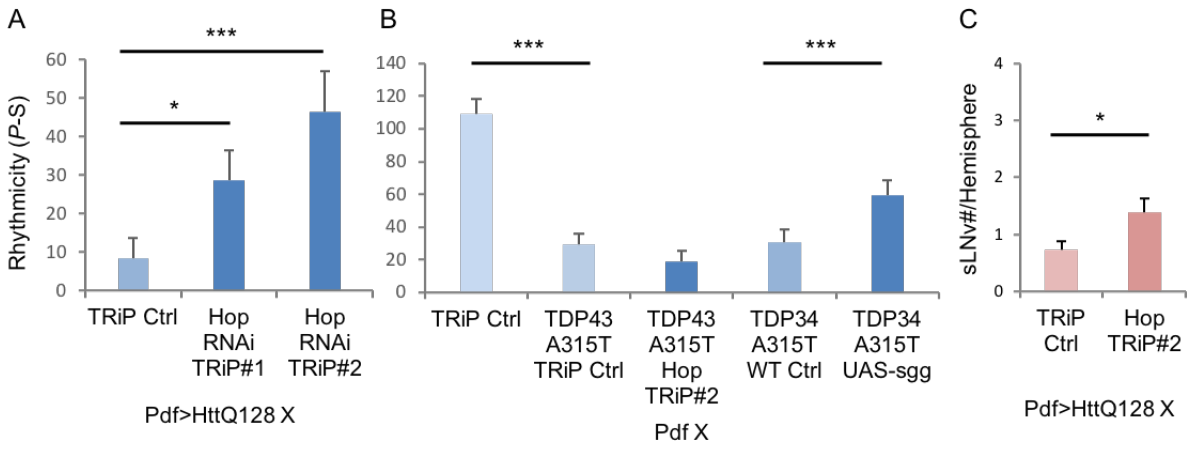

Figure 3.5. *Hop* RNAi Suppresses mHtt-mediated Arrhythmicity, Aggregate Formation and Cell Loss

A. Rhythmicity (P-S) is indicated for various genotypes including flies expressing HttQ128 in PDF neurons in a TRiP RNAi library control background (HttQ128 TRiP Ctrl) and expressing two independent *Hop* TRiP RNAi lines (HttQ128 Hop RNAi TRiP #1 and #2; n=17-19). B. Rhythmicity (P-S) is indicated for various genotypes including flies expressing TDP43A315T in PDF neurons in a TRiP RNAi library control background (TDP43A315T TRiP Ctrl) and expressing Hop RNAi lines (TDP43A315T Hop TRiP #2; n=11-22). C. The number of sLNv present per brain hemisphere is indicated for various genotypes where either *Hop* RNAi (TRiP) or TRiP control and HttQ128 expression are shown (n=18-19). (*:p<0.05 **p<0.01, ***:p<0.005)

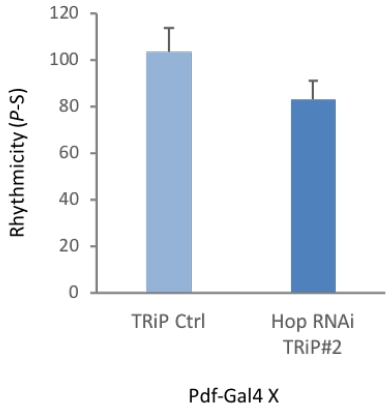

Figure 3.S4. Flies Expressing *Hop* RNAi Exhibit Robust Free-Running Rhythms

Rhythmicity (P-S) is indicated for flies expressing Hop RNAi (TRiP#2) in PDF neurons in a TRiP RNAi library control background (TRiP Ctrl) (n=19). Related to Figure 5.

synthase kinase 3, shaggy (*sgg*), could partially suppress TDP43A315T effects (Sreedharan et al., 2015) and in fact, we observed similar results (Figure 3.5B). However, a *Hop* RNAi line that was able to suppress arrhythmicity due to mHtt was unable to do so with TDP43A315T (Figure 3.6B), revealing the polyQ specificity of *Hop* effects. In addition, knockdown of *Hop* also partially restored rhythmicity in flies expressing HttQ103-eGFP expression (Figure 3.5C). Rescue of behavioral rhythmicity was accompanied by a very modest (<1 neuron/hemisphere) increase in PDF positive sLNv cell number (Figure 3.5D).

We then asked if *Hop* could affect mHtt levels or aggregation. In *Hop* RNAi flies, we examined HttQ72-eGFP and found a significantly reduced number of HttQ72-eGFP aggregates/sLNv neuron (Figure 3.6A,B). It is possible that *Hop* RNAi reduces the mHtt toxicity through diminishing the pdfGAL4 activity. As aggregation can independently affect mHtt levels, we examined the levels of non-pathogenic HttQ25-eGFP as a surrogate for assessing pdfGAL4 activity. We found that *Hop* knockdown actually increases HttQ25-eGFP levels (Figure 3.6C,D). Thus, our data suggest *Hop* suppression effects are not via *Hop* reduction of pdfGAL4 activity and are likely due to a direct effect on HttQ72 aggregation. Taken together these data suggest that clock control of the *Hop* driven protein chaperone cycle is a link between the clock and mHtt toxicity.

The finding that *Hop* reduction is neuroprotective could potentially be explained by proteotoxic stress induced by *Hop* loss resulting in induction of other chaperones. To test this hypothesis, we assessed the transcript levels of heat shock chaperones as well as *heat shock factor* (*Hsf*) after pan-cellular (Act5C-Gal4 mediated) *Hop* RNAi knockdown. *Hop* knockdown results in an up regulation of *Hsp70* transcript but not *Hsp40* or *Hsf* (Figure 3.S5). Of note, Hsp70 can suppress mHtt-induced neurodegeneration (Jana et al., 2000a; Warrick et al., 1999) (Ormsby et al., 2013; Wacker et al., 2009). Thus, Hsp70 induction could provide a mechanism for Hop knockdown mediate neuroprotection.

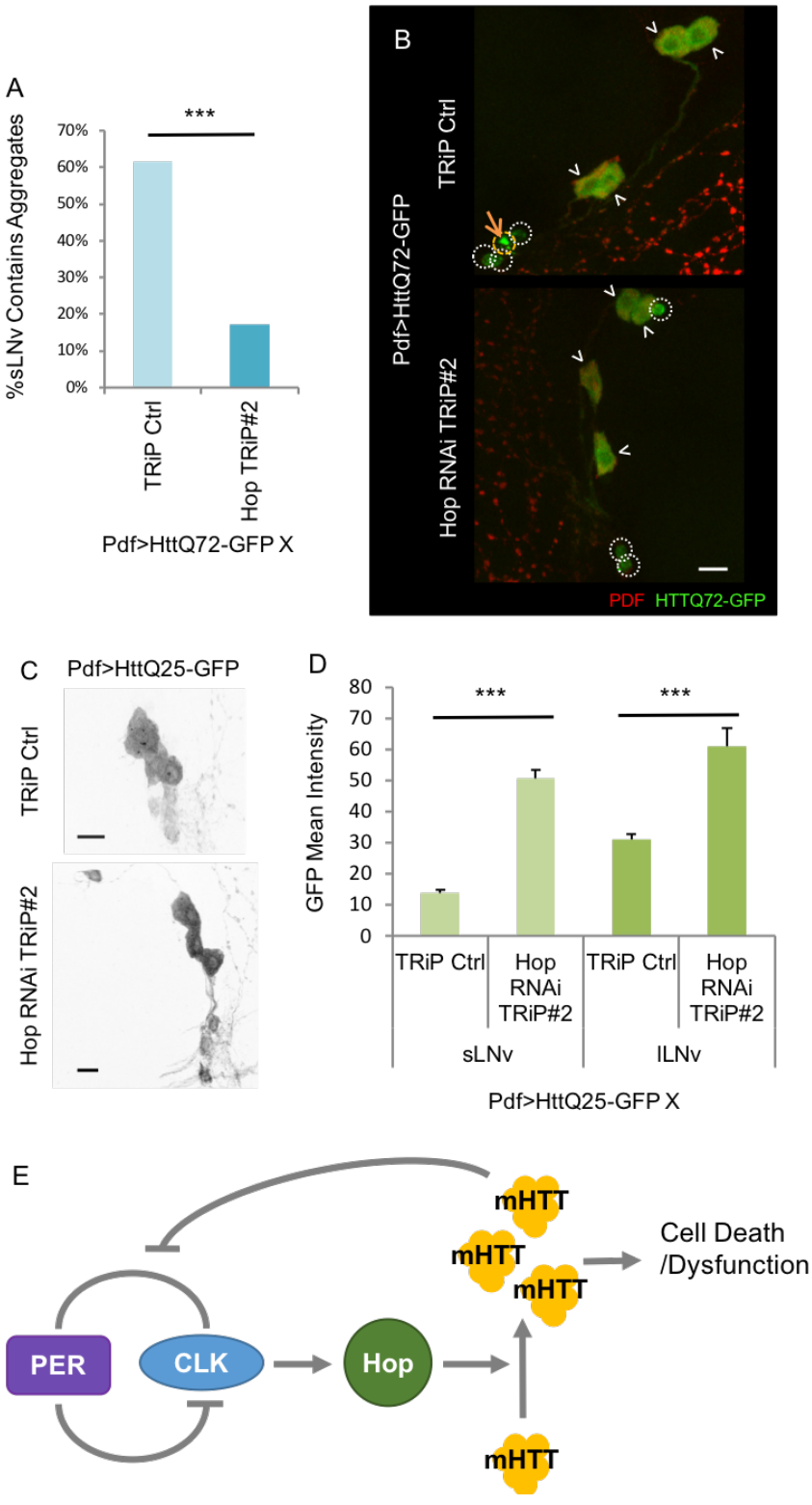
A
%sLNv Contains Aggregates
70%
60%
50%
40%
30%
20%
10%
0%
***
TRiP Ctrl
Hop TRiP#2
Pdf>HttQ72-GFP X
B
Pdf>HttQ72-GFP
TRiP Ctrl
Hop RNAi TRiP#2
PDF HTTQ72-GFP
C
Pdf>HttQ25-GFP
TRiP Ctrl
Hop RNAi TRiP#2
D
GFP Mean Intensity
80
70
60
50
40
30
20
10
0
***
***
TRiP Ctrl
Hop RNAi TRiP#2
TRiP Ctrl
Hop RNAi TRiP#2
sLNv
lLNv
Pdf>HttQ25-GFP X
E
mHTT
mHTT
mHTT
Cell Death
/Dysfunction
PER
CLK
Hop
mHTT

(continued)

Figure 3.6. *Hop* RNAi Suppresses mHtt Aggregate Formation and Increases pdfGAL4-driven HttQ25-eGFP Levels

A,B. Percentage of LNvs (labeled with PDF in red) at age day 7 containing HttQ72-eGFP aggregates (in green) or in a TRiP RNAi library control background (TRiP Ctrl) and expressing a Hop TRiP RNAi lines (RNAi TRiP #2; n=26-29; *p<0.05 **p<0.01, ***:p<0.005). White arrowheads indicate lLNvs. White dot circles label sLNvs without aggregates. Yellow dash circles label sLNvs with aggregates. Example aggregates are pointed out by orange arrows. Scale bar indicates 10μm. C. Representative images of LNvs (sLNv and lLNv) expressing HttQ25-eGFP are shown in TRiP RNAi library control background (TRiP Ctrl) and expressing a Hop TRiP RNAi lines (Hop RNAi TRiP #2). Asterisks indicate sLNvs. D. GFP Intensity in the sLNv and lLNv for TRiP Ctrl and Hop TRiP RNAi lines is quantified and shown. Scale bar indicates 10μm. (n=8-20; *:p<0.05 **:p<0.01, ***:p<0.005)

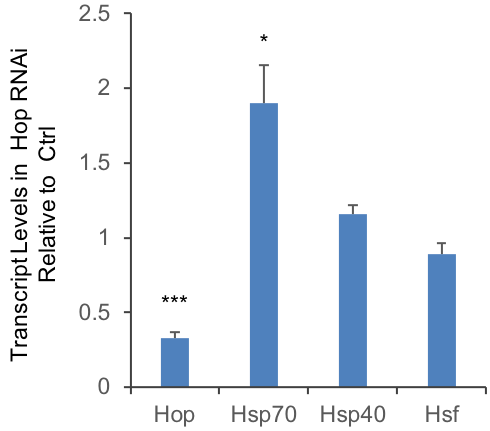

Figure 3.S5. *Hop* RNAi knockdown results in selective up regulation of Hsp70

Levels for *Hop,* and heat shock response related genes *(Hsp70, Hsp40* and *Hsf)* in from Act5C driven *Hop* RNAi flies normalized to Act5C TRiP control flies in each replicate. Averaged normalized levels for 3 replicates are shown with error bars indicating standard error of the mean.* indicated significance by t-test setting control to 1 in each experiment (*p<0.05, **p<0.01, ***p<0.005). Related to Figure 5 and 6.

3.5 Discussion

Considerable evidence suggests that disrupted clocks or sleep are associated with and potentially alter neurodegenerative disease processes(Musiek and Holtzman, 2016). Yet it has been difficult to establish causal relationships between disrupted clocks and neurodegenerative disease. Here we provide evidence that altering clock function can impact the toxicity of mHtt in clock neurons. In addition, we performed a genetic screen of clock-controlled genes to identify candidate pathways that may mediate clock effects. These studies establish a functional role for the clock in an ND disease model as well as identify putative molecular links between the clock and neurodegeneration.

This work demonstrated that altering clocks can modulate neurodegeneration in an animal model of disease, in this case, HD. We demonstrate that circadian clocks can modulate mHtt aggregation and cell death. First, partial abrogation of the core circadian transcription factor *Clk* is neuroprotective in mHtt models. Second, we show that that these effects are abrogated by loss of *per* highlighting the important role of *per* negative feedback. Third, we found that alteration in the daily timing of light-dark cycles (10:10) is neuroprotective. Finally, speeding up the clock to closely match these cycles eliminates these effects. While clock dependent neuropathological changes have been described in otherwise wild-type or neurodegeneration-prone animals (Kim et al., 2018; Krishnan et al., 2012; Means et al., 2015; Musiek et al., 2013), it remains unclear if these effects are via their functions in the clock or not. Moreover, we are unaware of clock-dependent changes in animal models of HD. Taken together, we have demonstrated that modulation of the circadian clock using multiple interventions can alter the neurotoxic effects of mHtt, providing a novel pathway impacting HD pathogenesis.

Clk^{Jrk}/+ effects are likely via their adult function in clocks not via their potential pleiotropic non-circadian developmental role of *Clk*. While *Clk*^{Jrk} homozygotes exhibit selective developmental loss of the sLNv, we actually observe an increase in sLNv cell number in mHtt-

expressing Clk^{Jrk}/+ flies. Moreover, we find that Clk^{Jrk}/+ flies, unlike their homozygous mutant counterparts, exhibit a wild-type number of sLNv and have a grossly normal morphology. The fact that the Clk^{Jrk}/+ effect can be partially rescued by per^{01}, which itself does not display any apparent developmental abnormality, provides further support Clk^{Jrk} effects on mHtt are not developmental but rather reflect the adult *per* feedback loop related function. As loss of *per* alone does not alter mHtt effects on cell number, our data are most consistent with hypothesis that reduction in another *Clk* activated gene could specifically mediate these effects. As a transcript that peaks in the night, at a time when many *Clk* target genes peak and is reduced in Clk^{Jrk}/+ mutants, *Hop* represents a candidate direct mediator of *Clk* effects.

While our results provide abundant evidence for a clock-HD link, our data also indicate that not all circadian disruptions are created equal with respect to mHtt effects. In particular, the absence of an effect on cell loss in the arrhythmic per^{01} mutant does not preclude a role for the circadian clock in mHtt toxicity. It is known that neither clock gene knockouts nor ablation of the SCN alter learning and memory (Ruby et al., 2008). These results alone may suggest that the SCN has no role in learning and memory. Yet SCN-dependent dysrhythmia can disrupt memory processing (Ruby et al., 2008). Similarly, there are many examples of clock-regulated phenomena that impact a physiological or pathological output where genetic disruption of one limb of the clock has a robust phenotype, but loss of the opposing limb has no detectable phenotype. For example, astrogliosis was also observed in other circadian clock mutants, namely double knockouts of Bmal1 partners Clock and Npas2 but not in Per1/Per2 double KO mice (Musiek et al.,2013). Mutations in the positive or negative limb in the clock “fix” the clock at different points of a 24 h cycle. Thus, it remains possible that the clock may oscillate between a transcriptional state that modifies mHtt and one that does not. We hypothesize that loss of *per* fixes the clock at the point that it does not modify mHtt. Consistent this hypothesis, when moved from this point in the cycle

in Clk^{Jrk}/+ mutants, we find that loss of *per* can enhance the toxicity of mHtt, providing compelling evidence for a functional role for the *per* feedback loop.

One surprise is that both our genetic and environmental perturbations to disrupt or alter clock function appear to be neuroprotective. This is evident both at the level of cell number and reduced number of aggregates. How could clock disruption be damaging in other contexts, even ones related to neuronal viability, but be protective in this case? First, our manipulations are comparatively subtle. Clk^{Jrk} heterozygotes retain some rhythmicity, albeit with reduced amplitude(Allada et al., 1998). Similarly, flies also are still able to entrain to 10:10 cycles although with an altered phase relative to the light dark cycle. In the case of *Clk/cyc* homozygotes, it is not possible to assess cell loss as these flies do not have apparent sLNv. One possibility is that our clock perturbations lead to *Hop* down regulation at the appropriate time of day leading to neuroprotection (Figure 3.6E). Understanding the molecular mechanisms by which the clock can impact neurodegeneration under these conditions will help to test this model.

To address the molecular mechanisms by which the clock impacts HD we applied a functional behavioral screen for modifiers of mHtt function that enabled the discovery of genes that are important for pre-degenerative mHtt-induced neuronal dysfunction. Unbiased genetic screens have been crucial in fly mHtt models of Huntington disease (Doumanis et al., 2009; Miller et al., 2010; Rincon-Limas et al., 2012; Zhang et al., 2010b). Genetic screens in *Drosophila* have largely focused on those impacting the mHtt dependent rough eye phenotype that may reflect developmental or cell death processes rather than earlier neural dysfunction. Retinal degeneration is not central for Htt dependent motor dysfunction or HD progression. Thus, our model more closely approximates a known target of mHtt (clock expressing neurons in the SCN and striatum) and can capture molecular pathways important for pre-cell death neural dysfunction. While we observed canonical cell loss, we also found robust reductions in the core clock protein PER reflecting a robust marker for pre-cell death mHtt toxicity. We propose that the discovery of

functional modifiers may provide effective therapeutic targets for intervention at an early stage before irreversible cell death has occurred.

One pathway through which mHtt can impair clock neuron function is via effects on the core clock. mHtt expression using the HttQ128 and HttQ103 models strongly suppresses PER levels in both the sLNv and the lLNv, consistent with effects observed in mammalian models. We do not yet know whether mHtt suppresses production of PER (e.g., its transcription) or enhances its degradation. Intriguingly, *Clk* contains a polyQ domain up to 33 amino acids long (Allada et al., 1998), suggesting that mHtt effects may act via sequestering this transcriptional activator. Given that low PER per se does not lead to enhanced mHtt effects on cell death, the simplest interpretation is that mHtt effects on PER do not mediate mHtt effects on cell death but may instead contribute to disrupted behavioral rhythms (Figure 3.6E).

Another paradoxical result is the finding that impairment of a heat shock chaperone pathway is neuroprotective with mHtt. In contrast to our results, overexpression of heat shock proteins (e.g. Hsp70/40/110) rescues polyQ induced degeneration (Chan et al., 2000; Hay et al., 2004; Kuo et al., 2013). Reduction of *Hop* in *C. elegans* or yeast enhances toxicity from polyQ proteins (Brehme et al., 2014; Wolfe et al., 2013). *Hop* reduction can also enhance Tau-induced degeneration in the eye (Ambegaokar and Jackson, 2011). Here we find that *Hop* knockdown using two independent RNAi lines partially suppresses mHtt-induced arrhythmicity, aggregates, and cell loss. Interestingly, *Hop* knockdown also can suppress Tau-mediated neurodegeneration in flies (Butzlaff et al., 2015) and SCA3Q78-mediated neurodegeneration (Vossfeldt et al., 2012). One possibility is that *Hop* knockdown may result in compensatory up regulation of other more efficacious chaperones with respect to mHtt. For example, inhibition of HSP90 leads to activation of Heat shock transcription factor 1(HSF1), thus, results in induction of other HS proteins such as Hsp70 (Fujikake et al., 2008; Kudryavtsev et al., 2017). Consistent with this model, we observed induction of *Hsp70* after *Hop* knockdown. Alternatively, *Hop* knockdown may

impact other pathways that in turn lead to effects on mHtt. For example, *Hop*, as well as other heat shock components, are involved in the loading of small RNAs to the RISC complex (Iwasaki et al., 2015).

Several features of our model suggest that the results described here will be broadly applicable. The underlying molecular mechanisms for both circadian clocks and HD are widely conserved between *Drosophila* and mammals. The expression of mHtt in clock expressing neurons can model the established neurodegeneration of clock-expressing neurons in the striatum and suprachiasmatic nucleus seen in HD patients. As such, this central clock neuron model is likely more valid than eye models that have been prominently used for genetic screening.

The finding that the clock can modulate mHtt toxicity also has potential pathologic and therapeutic implications. One implication is that the clock could modulate various features of mHtt aggregate formation, dissociation, and/or degradation. For example, aggregation formation may be up regulated at night due to the nightly up regulation of *Hop*. Notably, clock control of heat shock pathway components has also been observed in mammals (Reinke et al., 2008). If a similar scenario is evident in human HDs, then timed therapeutic interventions, termed chronotherapy, could be efficacious. Similarly, we demonstrated that environmental manipulations can alter mHtt toxicity. Altering the phase of molecular oscillations relative to the environmental cycle may also provide a promising new therapeutic strategy for this fatal disease. Given the prevalence of circadian disruption across neurodegenerative disease, it will be of great interest to see how broad the role of the clock is in other neurodegenerative disease models.

Chapter 4: Atx2 functions via CrebA to Mediate mHtt Toxicity in Circadian Clock Neurons

Fangke Xu[1], Elzbieta Kula-Eversole[1*], Marta Iwanaszko[2], Chunghun Lim[1**], Ravi Allada[1]

Affiliations

[1]Department of Neurobiology, Northwestern University, Evanston, IL, USA

[2]Feinberg School of Medicine, Northwestern University, Chicago, IL USA

*Present Address: Department of Obstetrics, Gynecology and Reproductive Biology College of Human Medicine, Grand Rapids Research Center, Michigan State University, Grand Rapids, MI, USA

**Present Address: School of Life Sciences, Ulsan National Institute of Science and Technology, Ulsan, South Korea

Correspondence: r-allada@northwestern.edu

4.1 Summary

Disruption of circadian rhythms at the behavior, physiological and molecular level is a prominent and often early feature of many neurodegenerative diseases including Huntington's disease (HD). In HD patients and animal models, striatal and hypothalamic neurons expressing molecular circadian clocks are targets of mutant Huntingtin (mHtt) pathogenicity. Yet how mHtt disrupts circadian rhythms remains unclear. In a genetic screen for modifiers of mHtt effects on circadian behavior in *Drosophila*, we discovered a role for the neurodegenerative disease gene *Ataxin2* (*Atx2*). Loss- and gain-of-function manipulations of *Atx2* suppress and enhance the impact of mHtt on circadian behavior as well as mHtt aggregation and demonstrate a role for *Atx2* in promoting mHtt aggregation as well as mHtt-mediated neuronal dysfunction and loss. RNAi knockdown of the Fragile X mental retardation gene, *Fmr1*, an *Atx2* partner, also suppresses mHtt effects. *Atx2* knockdown reduces the *cAMP response binding protein A* (*CrebA*) transcript. *CrebA* transcript level shows a prominent time-of-day regulation in clock neurons. Loss of *CrebA* also suppresses mHtt effects on behavior and cell loss. Our results indicate a prominent role of *Atx2* in mediating mHtt pathology, specifically via its regulation of *CrebA*, defining a novel molecular pathway in HD pathogenesis.

4.2 Introduction

Circadian disruption is prevalent in Huntington's disease (HD) patients and animal models. HD is caused by a triplet (CAG) expansion in the Huntingtin gene (*Htt*) resulting in expansion of a polyglutamine (polyQ) repeat (mHtt), mHtt aggregation, degeneration of striatal medium spiny neurons, and characteristic involuntary motor symptoms(Rosas et al., 2002; Vonsattel and DiFiglia, 1998). In addition, circadian behavioral rhythms are strongly disrupted in HD patients (Goodman and Barker, 2010; Morton et al., 2005; Wulff et al., 2010) and in animal models (Fisher

et al., 2013; Morton et al., 2005; Pallier et al., 2007; Sheeba et al., 2010). In fact, circadian and/or sleep changes often appear even before the characteristic motor symptoms (Cuturic et al., 2009; Diago et al., 2017; Goodman et al., 2011; Hunter et al., 2010; Kantor et al., 2013).

Impaired rhythmicity is typically accompanied by physiological, cellular, and molecular changes in circadian pacemaker neurons. Clock-driven rhythms in melatonin are altered In HD patients (Aziz et al., 2009; Kalliolia et al., 2014). In postmortem HD brains, the numbers of master circadian pacemaker neurons in the hypothalamic suprachiasmatic nucleus (SCN) are reduced, especially of the subset expressing the neuropeptide vasoactive intestinal peptide (VIP) (van Wamelen et al., 2013). Similarly, in flies, mHtt expression selectively reduces the number of a subset of clock neurons, the small ventral lateral neurons (sLNv), important for free running circadian behavior (Sheeba et al., 2010). The core molecular clock is also impacted in mouse models with disrupted *mPer2* or *mBmal1* mRNA oscillations in both the SCN (Morton et al., 2005; Pallier et al., 2007). The core circadian oscillator is evident outside of the SCN, including in the striatum, and striatal molecular oscillations are also altered suggesting that there are common mHtt mechanisms between the SCN and striatum.

To address the mechanisms by which mHtt impacts circadian behavior, we are employing the fruit fly, *Drosophila*. As in mammals, the circadian behavior is driven by a focused set of pacemaker neurons. Of special importance are those expressing the neuropeptide Pigment Dispersing Factor (PDF), subdivided into ~4 sLNv and ~4 large LNv per hemisphere(Helfrich-Forster, 1998; Park and Hall, 1998). PDF-expressing sLNvs are especially important for maintaining robust rhythmicity under constant darkness conditions (Lin et al., 2004; Renn et al., 1999b; Yoshii et al., 2009). Nevertheless, even a single sLNv is sufficient to maintain behavioral rhythmicity (Helfrich-Forster, 1998).

Within these clock neurons, a molecular negative feedback loop, largely conserved between invertebrates and vertebrates, is responsible for behavioral rhythms. In flies, the

CLOCK(CLK)/CYCLE(CYC) heterodimer directly activates the transcription of *period* (*per*) and *timeless* (*tim*) with peak mRNA expression occurring in the early night (Allada et al., 1998; Dubowy and Sehgal, 2017; Rutila et al., 1998). In turn, PER and TIM work in concert to repress CLK/CYC activation (Dubowy and Sehgal, 2017; Lee et al., 1999). Phosphorylation and ubiquitination result in PER/TIM degradation and initiation of a new transcriptional cycle every 24 hours (Chiu et al., 2011; Kloss et al., 1998; Ko et al., 2002; Luo et al., 2012; Price et al., 1998). CLK/CYC also directly activate transcription of *vrille* (*vri*) and *Pdp1ε* (Cyran et al., 2003), also peaking in the early night. VRI and PDP1 feedback to control rhythmic *Clk* expression(Cyran et al., 2003; Glossop et al., 2003). Translational control of *per* especially in the LNv is also critical for molecular and behavioral rhythms. Of note, this pathway involves the neurodegenerative disease gene *Ataxin2* (*Atx2*) and its partner *tyf* which interact with the polyA binding protein (PABP) to promote PER translation(Lim and Allada, 2013b; Lim et al., 2011b; Zhang et al., 2013). Of note *Atx2* can also repress translation via an alternative TYF-independent pathway to control rhythms in the LNv (Lee et al., 2017). This alternative pathway involves miRNA-mediated silencing (Lee et al., 2018) and may function with the *Drosophila* homolog of the Fragile Mental Retardation gene *Fmr1* (McCann et al., 2011; Sudhakaran et al., 2014).

Expressing human Htt with varying polyQ lengths in *Drosophila* recapitulates features of HD. These effects include polyQ length dependence (Zhang et al., 2010b), locomotor impairment (Ehrnhoefer et al., 2006; Lee et al., 2004b; Romero et al., 2008; Zhang et al., 2010b), cytoplasmic or nuclear aggregate formation(Lee et al., 2004b; Weiss et al., 2012), and neurodegeneration(Lee et al., 2004b). Molecular mechanisms discovered in fly HD models are conserved with those found in mammalian models, including mTor-induced autophagy (Ravikumar et al., 2004), histone acetylation (Ferrante et al., 2003; Hockly et al., 2003; Steffan et al., 2001), SUMOylation/ubiquitination(Steffan et al., 2004), and axonal transport(Gunawardena et al., 2003; Smith et al., 2014). mHtt also strongly disrupts sleep and/or circadian behavioral rhythms (Fisher

et al., 2013; Gonzales and Yin, 2010; Gonzales et al., 2016; Loh et al., 2013; Pallier et al., 2007; Prakash et al., 2017; Sheeba et al., 2010) as well as selective loss of circadian clock neurons(Sheeba et al., 2010). Despite the conservation of disrupted circadian rhythms in HD and HD models, the molecular mechanisms by which mHtt impacts circadian behavior remain unclear.

4.3 Material and Methods

Whole Mount Immunostaining

Fly crosses were set under 12:12 LD cycles at 25C. Flies eclosing within 24 hours were collected and kept under their respective conditions until the ages indicated in each experiment. Adult brains were dissected in PBS (137mM NaCl, 2.7mM KCl, 10mM Na_2HPO_4 and 1.8mM KH_2PO_4) within 10 minutes. Then brains were fixed in 3.7% formalin solution for 30 minutes. Brains were washed with 0.3% PBSTx 4 times before primary antibody incubation. Primary antibodies were diluted in 0.3% PBSTx with 5% normal goat serum and incubation was done at 4C overnight. Brains were washed for 4 times with 0.3% PBSTx after primary antibody incubation. Secondary antibodies were diluted in 0.3% PBSTx with 5% normal goat serum and incubation was done at 4C overnight. Primary antibody dilutions were done as the followings: mouse anti-PDF (1:800, DSHB), rabbit anti-GFP (1:1000, invitrogen). Secondary antibody dilutions were done as the followings: anti-mouse Alexa594 (1:800, invitrogen), anti-mouse Alexa488 (1:800, invitrogen), anti-rabbit Alexa594 (1:800, invitrogen), anti-rabbit Alexa488 (1:800, invitrogen), anti-rabbit Alexa647 (1:800, invitrogen)

Confocal Imaging and Data Quantification

Fly brains after immunostaining were imaged by Nikon C2 confocal. Data processing and quantification were done with Nikon NIS Elements. For PDF+ sLNv number quantification, male Pdf>HttQ128 flies with modifiers or corresponding controls were dissected at the age of day 10 (to match the age of the same genotypes of flies when they were in the middle of the DD period

during behavior test). For aggregation quantification, male Pdf>HttQ72-eGFP flies with modifiers or corresponding controls were dissected at the age of day 7 (since aggregation at this age is clearer for quantification). For aggregation visualization in the less toxic line, male Pdf>HttQ46-eGFP flies with modifiers or corresponding controls were dissected at the age of day 30 (or at the age of day 2 or 5 for HttQ46 with *Atx2* related transgenes). For GFP intensity measurements, the intermediate stack of each cell was chosen for measuring the mean intensity. Three areas for each hemisphere were randomly chosen and measured as background. The average of those three areas were calculated for background mean intensity. Cells in the same hemisphere were quantified against the same background mean intensity. The final mean intensity for GFP signal from nlsGFP or HttQ25-eGFP or HttQ46-eGFP for each cell was calculated by mean intensity measured from the middle stack of a cell minus the background mean intensity and then divided by the background mean intensity. For aggregate quantification, a threshold for intensity was applied to the channel used for imaging Htt aggregates (threshold was usually between 2500 to 3500, and the same threshold was used for control and experimental groups in a certain experiment). The number of aggregates over the threshold in each cell was counted and the percentage of cells that contained aggregates was calculated. Z-statistic, and the corresponding p-value, was determined for statistically comparing percentages.

Locomotor Activity Recording and Circadian Data Analysis

Behavior data recording, processing, plotting and analysis were done mainly as previously described (Pfeiffenberger et al., 2010a, b). Behavior for HttQ128 (and corresponding controls) were done with flies eclosed within 3 days prior to the loading day. Behavior for HttQ103-eGFP (and corresponding controls) were done with flies eclosed within 3 days, and aged for 5 days on average prior to the loading day. Fly locomotor activity was recorded from the Drosophila Activity Monitoring (DAM) data collection system and then extracted with DAM File Scan. Rhythmicity was measured by power - significance (P-S), parameters calculated by ClockLab (using Chi-

square periodogram) and t-test was performed between specific a genotype and its control. Activity actograms were plotted by ClockLab. Flies with P-S below 10 were considered arrhythmic and thus eliminated from the average period calculation. Flies lacking rhythmic power are considered as completely arrhythmic and are assigned with P-S=0, but are included in the average rhythmicity calculation. Morning and evening Index were calculated with normalized activity given by output from Counting Macro. All flies for behavior were entrained from the embryonic stage (after egg-laying) under 12:12 LD cycles.

Fly Stocks

RNAi lines used for screening and other overexpression lines were acquired from Bloomington Stock Center unless indicated separately. UAS-HttQ0/128 were kindly provided by Dr. Littleton. UAS-HttQ25/46/72/103-eGFP were kindly provided by Dr. Perrimon. UAS-TDP43-A315T was kindly provided by Dr. Wu. Coding sequence for generating ATX2ΔLsm lines were amplified with primers: ATX2dN-5N GATCGCGGCCGCATGGGTAACAAGCCCCGTGGC and ATX-PBC3Xb GATCTCTAGACTGTGGCTGATGCTGCTG. The sequence was subcloned into a modified pUAS-C5 vector with a C-terminal 3xFLAG tag to generate UAS-ATX2ΔLsm transgenic lines (see details in (Lim and Allada, 2013b)).

RNA Sequencing and Data Analysis

LNvs were labeled with Pdf>mGFP. Fly brains were dissected at certain time points and processed as previously described (Kula-Eversole et al., 2010; Nagoshi et al., 2010). RNA from FACS sorted LNvs were extracted with PicoPure Knits. We synthesized 1st and 2nd strand cDNA from RNA first with Superscript III and DNA polymerase. Then we amplified the RNA by synthesizing more RNA from the cDNA template with T7 RNA polymerase. After the second round of cDNA synthesis from amplified RNA, the cDNA was submitted to HGAC at the University of Chicago for library preparation and sequencing. Sequencing was done in HGAC at University of Chicago with Illumina HiSeq 2000. All samples are done with single-end reads of 50 base pairs.

Reads were quantified against Flybase transcript assembly, release 6.14, using Kallisto (Bray et al., 2016b). Gene-level quantification was obtained using tximport library, both for TPMs and counts data. Our LNv data comprise of three food/temperature combination conditions, with 12 time points per each condition: 1.5X Sucrose-Yeast (SY) fly food and 25°C),0.5X SY fly food and 25°C and 1.5X SY fly food and 18°C. Genes which do not pass the threshold of TPM >1 in at least 50% of samples were filtered out, leaving 7863 genes; conditions were concatenated to generate a dataset contains 36 time points as an input data for Boot eJTK to determine cycling genes (Hutchison et al., 2018). We applied the Benjamini-Hochberg (BH) correction method to Gamma p-values calculated by Boot eJTK. BH corrected p-value of less than 0.05 and fold change greater than 1.5 (between peak and trough) was used as a threshold for detection of cycling genes. Estimated counts acquired from Kallisto were used as input for DEseq2 for differential expression analysis. Two replicates of ZT0 *Atx2* RNAi LNv samples were compared to wild-type control LNv samples at ZT0 and ZT2 while two replicates of ZT12 *Atx2* RNAi LNv samples were compared to wild-type control LNv samples at ZT12 and ZT14. Similarly, two replicates of ZT4 tyf mutant LNv samples were compared to wild-type control LNv samples at ZT2 and ZT4 while two replicates of ZT16 tyf mutant samples were compared to wild-type control LNv samples at ZT14 and ZT16. All flies from those experiments were raised under regular food, under 25°C, 12:12 LD cycles and aged on 1.5X SY fly food, under 25°C, 12:12 LD cycles prior to dissections. The significance of differential expression of genes is determined by the adjusted p-value from DEseq2 (adjp<0.05).

4.4 Results

4.4.1 A genetic screen for mHtt modifiers results in the discovery of *Atx2* as a potent dose-dependent mediator of mHtt effects

To discover genes important for mHtt effects on circadian rhythms, we performed an RNAi screen to look for modifier effects of mHtt induced arrhythmicity by expressing HttQ128 in PDF+ LNv using *PdfGAL4* (*PdfGAL4/UAS-HttQ128*) (Lee et al., 2004b; Prakash et al., 2017). As our data suggest that the circadian clock might modify mHtt effects (Xu et al., 2019), we focused on clock-controlled genes in PDF+ LNv, identified using RNA-sequencing from FACS-sorted LNv (Figure 4.S1). We selected for RNAi screening those genes with the most robust cycling or genes previously implicated in neurodegenerative disease, including HD. Here we focus on the most robust and well-validated modifier of HttQ128, *Ataxin2* (*Atx2*). *Atx2* is an RNA-binding protein and a translational regulator most well-known for its role in spinocerebellar ataxia type 2 (Auburger et al., 2017; Lee et al., 2018; Pulst et al., 1996). *Atx2* displays a modest rhythm in the LNvs, consistent with clock control (Figure 4.S2; gammaBH=0.045). Validating a role for *Atx2*, we found that two independent *Atx2* RNAi lines (*Atx2* RNAi TRiP#2 (TRiP.HMS02726), and #1(TRiP.HMS01392)) suppress HttQ128 effects on behavioral rhythms (Figure 4.1A). Given that *Atx2* had also been previously shown to play a role in circadian behavior, we also examined *Atx2* RNAi effects in the absence of HttQ128 but did not find any significant effect on rhythms (Figure 4.1B). We hypothesize that these lines may be weaker than those previously published (see also below). To determine if these effects were unique to our HttQ128 model, we also tested a mHtt containing exon 1 with a polyQ of 103 (HttQ103)(Zhang et al., 2010b). We found that expression of HttQ103 in PDF clock neurons strongly reduced behavioral rhythmicity (Figure 4.1C). Importantly, RNAi mediated knockdown of *Atx2* also suppressed this arrhythmicity (Figure 4.1D). To determine if improved rhythms were due to reduced cell loss, we assessed mHtt induced sLNv cell loss in *Atx2* RNAi flies. While wild-type flies typically have 4 sLNv/hemisphere (Helfrich-Forster et al., 2007), HttQ128 expressing flies only exhibit about <1 sLNv/hemisphere by day 10 post-eclosion, a time when circadian behavior is significantly affected. We found that *Atx2* RNAi did not significantly affect HttQ128 mediated cell loss, suggesting that the improved rhythmicity is

principally due to an alteration in mHtt-induced neuronal dysfunction rather than neuronal loss (Figure 4.1E). To determine if *Atx2* affects mHtt induced aggregation, we employed a GFP tagged mHtt transgene, HttQ72(Zhang et al., 2010b). By day 7 post-eclosion, we observe aggregates (see Methods) in about ~30% of sLNv neurons. Strikingly, these aggregates are undetectable in HttQ72-GFP flies co-expressing *Atx2* RNAi (Figure 4.1F,G).

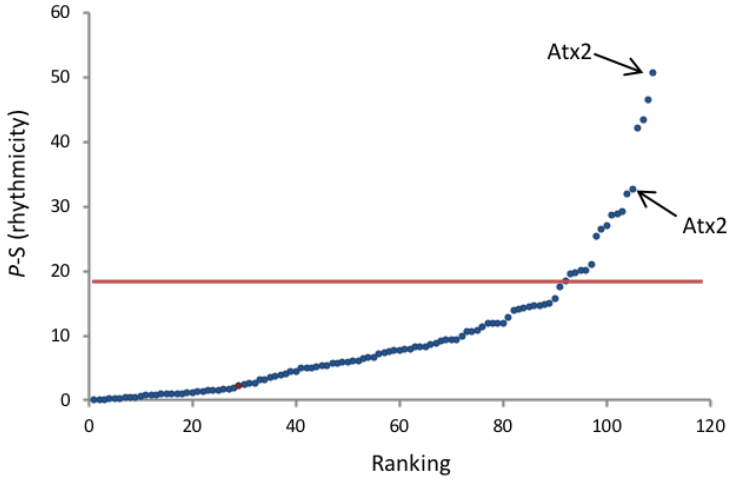

Figure 4.S1. RNAi Screening for mHtt Toxicity Suppressors with Circadian Behavior Identifies *Atx2* RNAi as A Suppressor

A. X-axis indicates ranking of screened RNAi lines based on their average rhythmicity (Power-Significance; P-S) values in Pdf>HttQ128 flies. The red line indicates the cut-off for RNAi to be considered modifiers, and the red circle (Ctrl) indicates the average P-S of the control. Two independent *Atx2* RNAi lines that are modifiers are indicated by black.

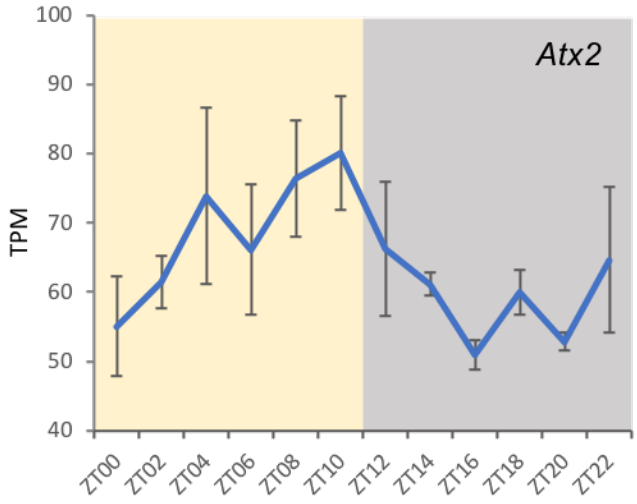

Figure 4.S2. *Atx2* Transcript Is Identified as Cycling in LNvs

Averaged transcript levels in transcripts per million (TPM) for *Atx2* across three 24 hour light:dark cycles. Light and dark periods are indicated in yellow and gray, respectively. Data for each time point is averaged from three conditions: standard 1.5x sucrose-yeast (SY) food at 25°C, 0.5xSY at 25°C,1.5xSY at 18°C.

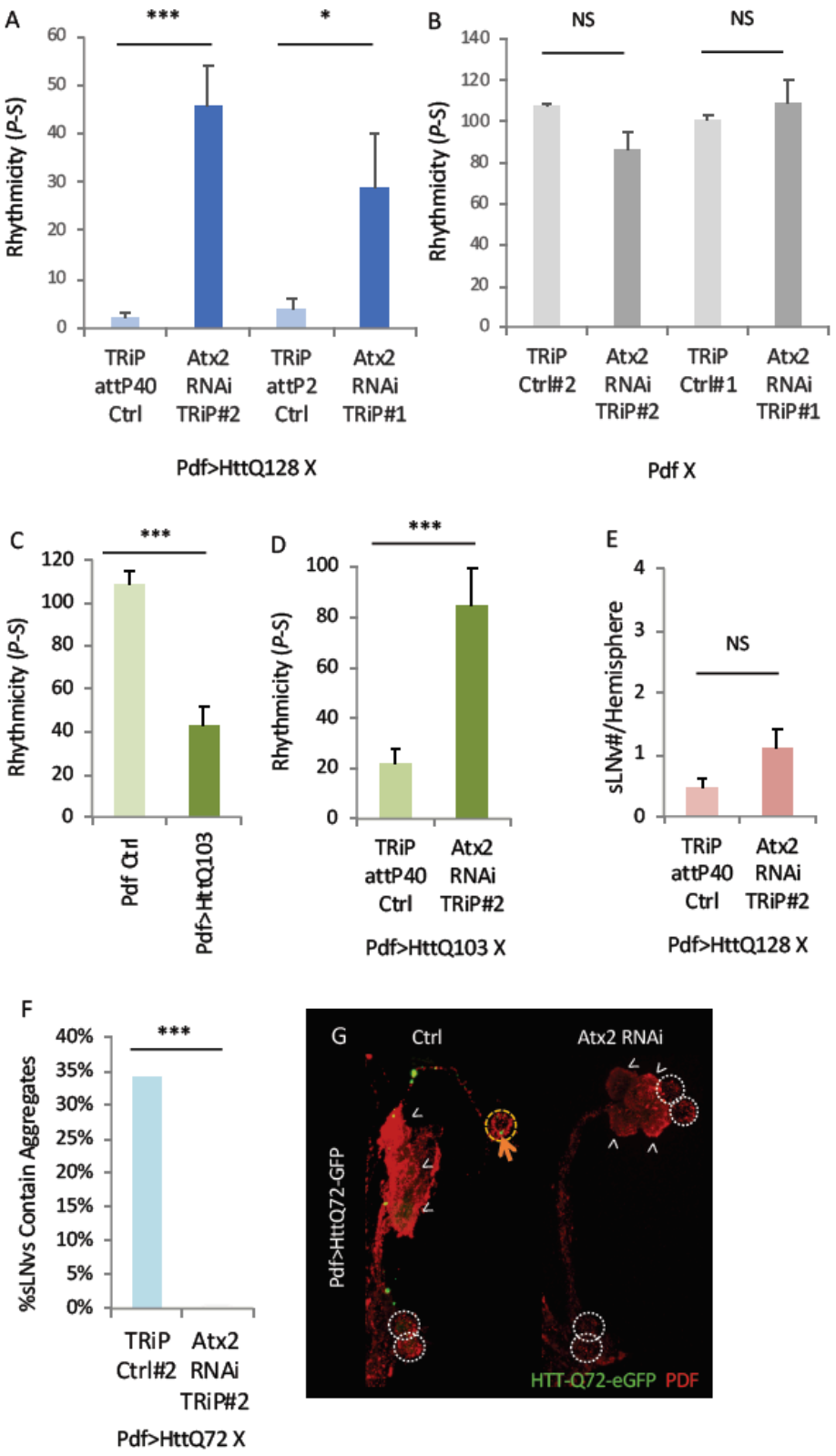
A
***
*
Rhythmicity (P-S)
60
50
40
30
20
10
0
TRiP attP40 Ctrl
Atx2 RNAi TRiP#2
TRiP attP2 Ctrl
Atx2 RNAi TRiP#1
Pdf>HttQ128 X
B
NS
NS
Rhythmicity (P-S)
140
120
100
80
60
40
20
0
TRiP Ctrl#2
Atx2 RNAi TRiP#2
TRiP Ctrl#1
Atx2 RNAi TRiP#1
Pdf X
C
***
Rhythmicity (P-S)
120
100
80
60
40
20
0
Pdf Ctrl
Pdf>HttQ103
D
***
Rhythmicity (P-S)
100
80
60
40
20
0
TRiP attP40 Ctrl
Atx2 RNAi TRiP#2
Pdf>HttQ103 X
E
NS
sLNv#/Hemisphere
4
3
2
1
0
TRiP attP40 Ctrl
Atx2 RNAi TRiP#2
Pdf>HttQ128 X
F
***
%sLNvs Contain Aggregates
40%
35%
30%
25%
20%
15%
10%
5%
0%
TRiP Ctrl#2
Atx2 RNAi TRiP#2
Pdf>HttQ72 X
G
Ctrl
Atx2 RNAi
Pdf>HttQ72-GFP
HTT-Q72-eGFP PDF

(continued)

Figure 4.1 RNAi Screening for mHtt Toxicity Suppressors with Circadian Behavior Identifies Atx2 RNAi as A Suppressor

A. Rhythmicity (P-S) is indicated for various genotypes including flies expressing HttQ128 in PDF neurons in a TRiP RNAi library control background (HttQ128 TRiP Ctrl) and expressing two independent *Atx2* TRiP RNAi lines (HttQ128 *Atx2* RNAi TRiP #2 and #1; n=11-32; *p<0.05 **p<0.01, ***:p<0.005, error bars represent standard error). B. Rhythmicity (P-S) is indicated for various genotypes including flies expressing two independent *Atx2* TRiP RNAi lines in PDF neurons (*Atx2* RNAi TRiP #2 and #1) or only PdfGAL4 in the TRiP RNAi library control background (TRiP attP40 ctrl and attP2 Ctrl; n=7-8; error bars represent standard error). C. Rhythmicity (P-S) is indicated for various genotypes including flies expressing HttQ103 in PDF neurons (Pdf>HttQ103) or only PdfGAL4 in the wild-type background (Pdf Ctrl; n=14-16; *p<0.05 **p<0.01, ***:p<0.005, error bars represent standard error) D. Rhythmicity (P-S) is indicated for various genotypes including flies expressing HttQ103 in PDF neurons in a TRiP RNAi library control background (HttQ103 TRiP attP40 Ctrl) and expressing *Atx2* TRiP RNAi#2 (HttQ103 *Atx2* RNAi TRiP #2; n=8-10;*:p<0.05 **p<0.01, ***:p<0.005, error bars represent standard error) E. The number of sLNv present per brain hemisphere at day 5 is indicated for various genotypes where either *Atx2* RNAi (Atx2 TRiP#2) or TRiP RNAi library control (TRiP attP40 Ctrl) and HttQ128 are expressed is shown (n=19-26; *p<0.05 **p<0.01, ***:p<0.005). F. Percentage of sLNvs at age day 7 containing HttQ72-eGFP aggregates in a TRiP RNAi library control background (TRiP attP40 Ctrl) and expressing an *Atx2* TRiP RNAi line (Atx2 RNAi TRiP #2) is quantified (n=27-41; *p<0.05 **p<0.01, ***:p<0.005, error bars represent standard error). G. Representative images of LNvs (sLNv and lLNv) for corresponding genotypes in F are shown. White arrowheads indicate lLNvs (regardless of aggregation formed or not). White dot circles label sLNvs without aggregates. Yellow dash circles label sLNvs with aggregates. Example aggregates are pointed out by orange arrows.

Atx2 RNAi knockdown with a different line (VDRC100423, KK108843) has been associated with a reduction in behavioral rhythmicity in the absence of mHtt (Lim and Allada, 2013a; Zhang et al., 2013). We wanted to determine if this line (KK) also modified mHtt. First, we confirmed that *Atx2* knockdown with this line suppressed rhythms as previously reported (Figure 4.S3A). Also as expected given the poor rhythms on their own, we failed to see an improvement of rhythms in mHtt expressing flies (Figure 4.S3B). Nonetheless, we tested this line for its effect on mHtt-induced sLNv loss and aggregation. In contrast to the other Atx2 lines tested (Figure 4.1D), we observed a modest increase in PDF+ sLNv cell number (Figure 4.S3C, p=0.0026). We also tested the effects of this line on mHtt induced aggregation, in this case, using HttQ46-GFP which exhibits significant aggregation in the sLNv by age day 30. Here we confirmed that *Atx2* knockdown reduced aggregation, further confirming a role for *Atx2* in this process. (Figure 4.S3D). Taken together, these results collectively confirm a role of *Atx2* knockdown in mediating mHtt effects.

To address whether *Atx2* effects on mHtt are dose-dependent, we tested the effect of *Atx2* overexpression (PdfGAL4/UAS-Atx2; Atx2 OX). Given that we expect *Atx2* overexpression would enhance mHtt effects, we used the HttQ103 model which retains more residual rhythmicity than Pdf>HttQ128. Here we found that *Atx2* OX significantly reduced rhythmicity in HttQ103 flies while having no significant effect in a wild-type background. (Figure 4.2A). To assess its effects on mHtt aggregation, we co-expressed *Atx2* with HttQ46-GFP in PDF neurons. We found that nuclear GFP signal was more aggregated and enhanced in *Atx2* OX flies in the lLNvs compared to the wild-type controls (Figure 4.2B, yellow arrows). In the sLNv, no aggregates are evident in wild-type flies but are observable in the *Atx2* OX flies (Figure 4.2B, orange arrows). Thus, down or up-regulating *Atx2* can suppress or enhance, respectively, mHtt effects.

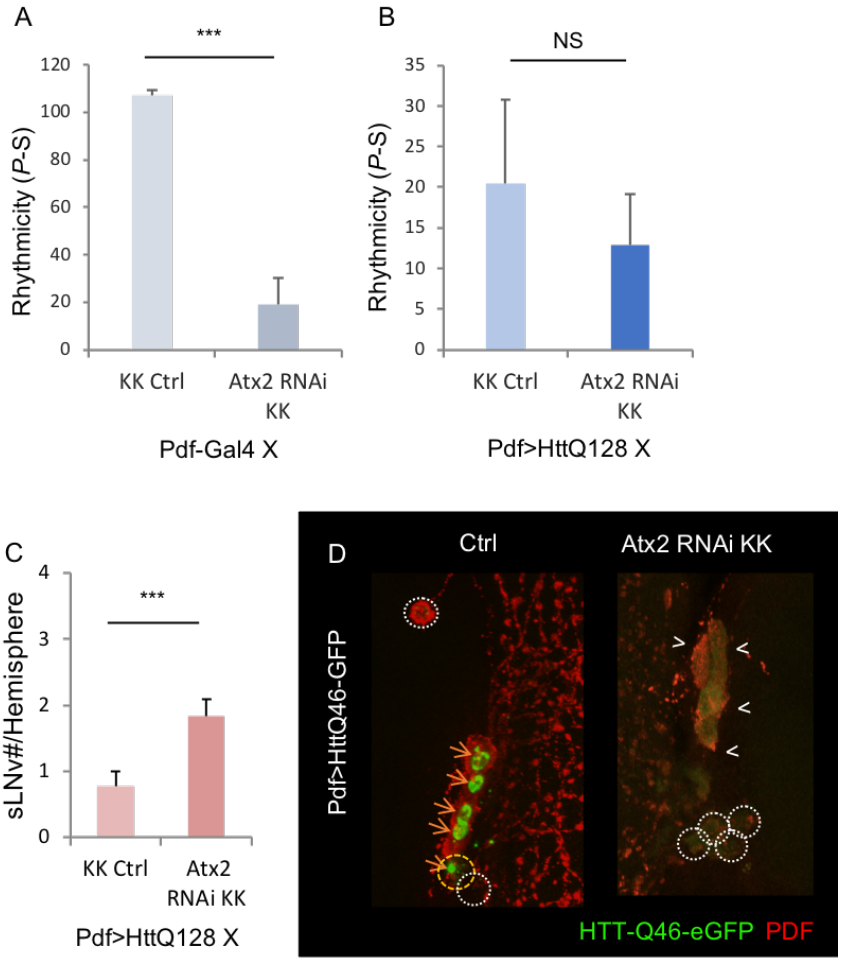

Figure 4.S3. Independent Atx2 RNAi Line Rescues PDF Positive sLNv Loss and Aggregation

A. Rhythmicity (P-S) is indicated for various genotypes including flies expressing an *Atx2* KK RNAi line (Atx2 RNAi KK) or PdfGAL4 only in the KK RNAi library control background (KK Ctrl; n=6-8). B. Rhythmicity (P-S) is indicated for various genotypes including flies expressing HttQ128 in PDF neurons in a KK RNAi library control background (HttQ128 TRiP Ctrl) and expressing an *Atx2* KK RNAi lines (HttQ128 *Atx2* RNAi KK; n=6-8, error bars represent SE). C. The number of sLNv present per brain hemisphere at day 5 is indicated for various genotypes where either *Atx2* RNAi (KK) or KK RNAi library control (KK Ctrl) and HttQ128 expression is shown (n=13-24; *p<0.05 **p<0.01, ***:p<0.005, error bars represent SE). D. Representative images of LNvs (sLNv and lLNv) expressing HttQ46-eGFP at day 30 are shown in the control background (Ctrl) and expressing an ATX2 overexpression line (UAS-Atx2). White dot circles label sLNvs without aggregates. Yellow dash circles label sLNvs with aggregates. Example aggregates are pointed out by orange arrows.

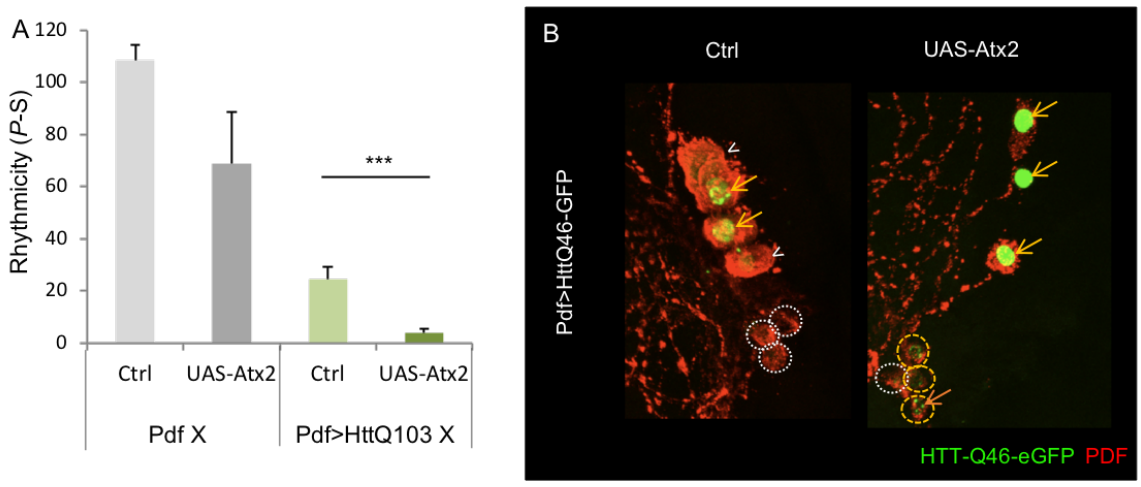

Figure 4.2. ATX2 Overexpression Enhances mHtt Toxicity

A. Rhythmicity (P-S) is indicated for various genotypes including flies expressing ATX2 in PDF neurons (UAS-Atx2) or only PdfGAL4 in the wild-type control background (Ctrl) as well as flies expressing HttQ103 in PDF neurons in a wild-type control background (HttQ103 Ctrl) and expressing *Atx2* TRiP RNAi#2 or *Atx2* overexpression (HttQ103 UAS-Atx2; n=8-26; *:p<0.05 **p<0.01, ***:p<0.005, error bars represent SE). B. Representative images of LNvs (sLNv and lLNv) expressing HttQ46-eGFP at day 30 are shown in the wild-type control background (Ctrl) or with ATX2 overexpression (UAS-Atx2). White arrowheads indicate lLNvs (regardless of aggregation formed or not). White dot circles label sLNvs without aggregates. Yellow dash circles label sLNvs with aggregates. Example aggregates are pointed out by orange arrows.

4.4.2 The PABP-binding Domain but Not the LSM Domain, nor *tyf* is Critical for *Atx2*'s Effects on mHtt

Atx2 functions via direct association with target RNAs and the polyA binding protein (PABP) (Satterfield and Pallanck, 2006; Yokoshi et al., 2014). These functions are accomplished via two conserved domains: the PAM2 domain, important for interactions with PABP and the Like Smith (Lsm) domain, which binds RNA (Tharun, 2009; Yokoshi et al., 2014). The Lsm domain is also important for interactions with the PER translational regulator TYF (Lim and Allada, 2013b). To elucidate the functions of these domains, we overexpressed Atx2 lacking the PAM2 domain (UAS-Atx2-ΔPAM) or the Lsm domain (UAS-Atx2-ΔLsm). Consistent with our prior report(Lim and Allada, 2013b), expression of two of the three independent transgenic insertions of Atx2-ΔPAM significantly reduced rhythmicity when expressed without mHtt (Figure 4.3A, left panel). Yet despite this reduced rhythmicity, all three lines significantly improve rhythmicity in HttQ128 expressing flies (Figure 4.3A, right panel). On the other hand, Atx2-ΔLsm failed to alter rhythms in a wild-type or HttQ128 expressing background (Figure 4.3A). Since HttQ128 rhythmicity is already very poor, we also overexpressed Atx2-ΔLsm in the more rhythmic Pdf>HttQ103 background and found enhancement of HttQ103 induced arrhythmicity (Figure 4.3B), similar to that observed with wild-type Atx2 overexpression (Figure 4.2A). To determine the basis of improved rhythms in Atx2-ΔPAM flies, we assessed PDF+ sLNv cell number and found significant increases in all three Atx2-ΔPAM lines (Figure 4.3C). These Atx2-dPAM lines also reduced HttQ46-GFP aggregates in the LNvs (Figure 4.3D). Taken together, the data suggest that the PAM2 domain but not the Lsm domain in Atx2 mediates its enhancement of mHtt toxicity.

ATX2 interacts with TYF to regulate the translation of PER in the LNv(Lim et al., 2011a). To determine if tyf mediates Atx2 effects on mHtt, we examined mHtt induced arrhythmicity, cell loss and aggregate in a loss-of-function tyf^{e} mutant. Because of the critical role of *tyf* in PER translation and the profound arrhythmicity of *tyf* mutants(Lim et al., 2011b), we did not assess

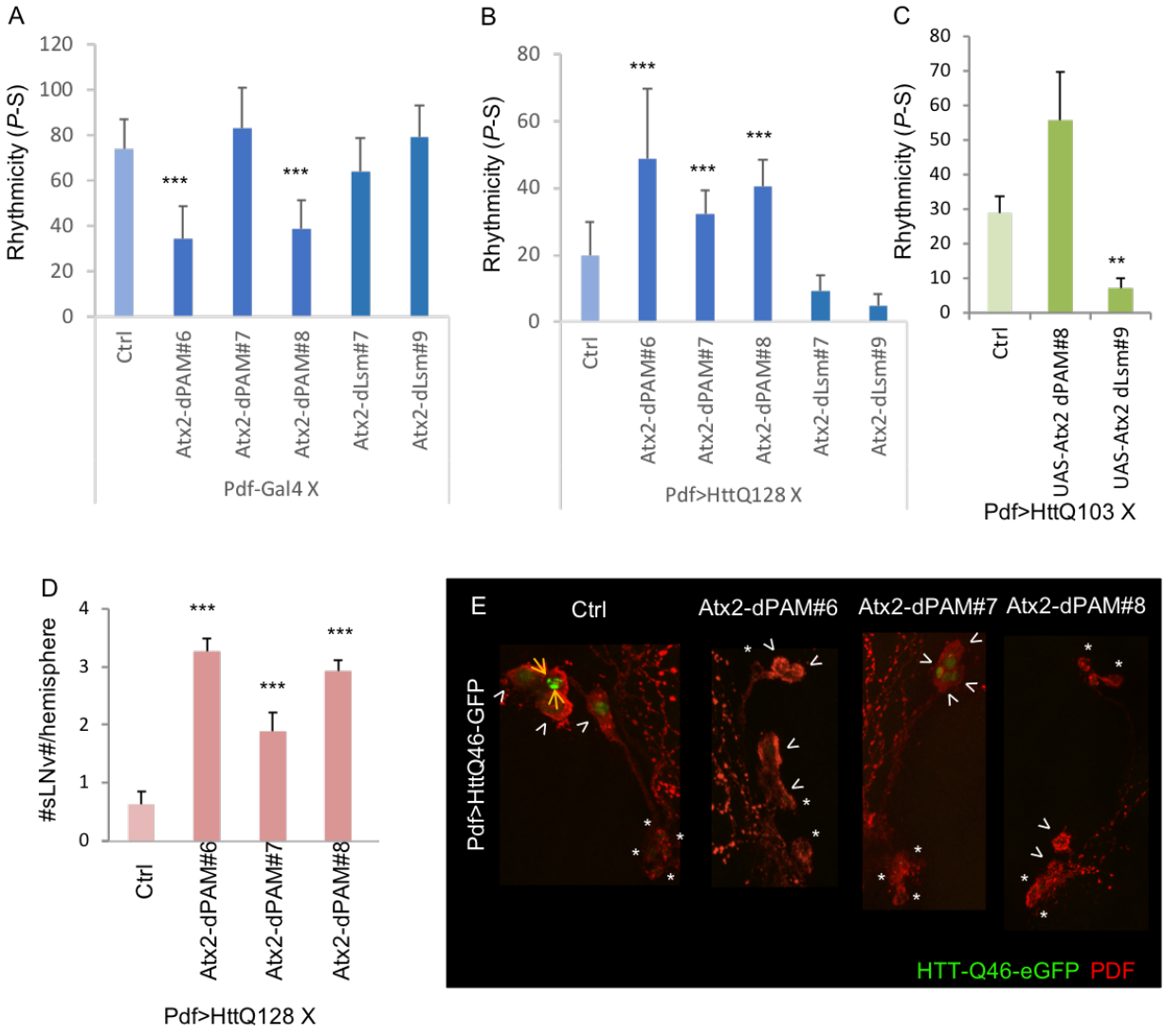
A
Rhythmicity (P-S)
120
100
80
60
40
20
0
***
***
Ctrl
Atx2-dPAM#6
Atx2-dPAM#7
Atx2-dPAM#8
Atx2-dLsm#7
Atx2-dLsm#9
Pdf-Gal4 X
B
Rhythmicity (P-S)
80
60
40
20
0
***
***
***
Ctrl
Atx2-dPAM#6
Atx2-dPAM#7
Atx2-dPAM#8
Atx2-dLsm#7
Atx2-dLsm#9
Pdf>HttQ128 X
C
Rhythmicity (P-S)
80
70
60
50
40
30
20
10
0
**
Ctrl
UAS-Atx2 dPAM#8
UAS-Atx2 dLsm#9
Pdf>HttQ103 X
D
#sLNv#/hemisphere
4
3
2
1
0
***
***
***
Ctrl
Atx2-dPAM#6
Atx2-dPAM#7
Atx2-dPAM#8
Pdf>HttQ128 X
E
Ctrl
Atx2-dPAM#6
Atx2-dPAM#7
Atx2-dPAM#8
Pdf>HttQ46-GFP
HTT-Q46-eGFP PDF

(continued)

Figure 4.3. ATX2 Lacking the PABP-binding (PAM2) Domain mHtt Toxicity while Atx2 Lacking the Lsm Domain Does Not

A. Rhythmicity (P-S) is indicated for various genotypes including flies expressing three independent ATX2 lacking PAM2 domain and two independent ATX2 lacking Lsm domain in PDF neurons (Atx2-dPAM#6/7/8 and Atx2-dLsm#7/9) or only PdfGAL4 in the wild-type control background (Ctrl; n=6-12; *:p<0.05 **p<0.01, ***:p<0.005, error bars represent SE) B. Rhythmicity (P-S) is indicated for various genotypes including flies expressing HttQ128 in PDF neurons in a TRiP RNAi library control background (Ctrl) and expressing three independent overexpression of ATX2 lacking PAM domain lines and two independent overexpression of Atx2 lacking Lsm domain lines (Atx2-dPAM#6/7/8 and Atx2-dLsm#7/9; n=14-22; *:p<0.05 **p<0.01, ***:p<0.005, error bars represent SE). C. Rhythmicity (P-S) is indicated for various genotypes including flies expressing HttQ103 in PDF neurons in a wild-type control background (HttQ103 Ctrl) and expressing Atx2-dPAM#8 or Atx2-dLsm#9 overexpression (HttQ103 UAS-Atx2-dPAM#8 and UAS-Atx2-dLsm#9; n=6-34; *:p<0.05 **p<0.01, ***:p<0.005, error bars represent SE). D. The number of sLNv present per brain hemisphere at day 10 is indicated for various genotypes where either ATX2 lacking PAM2 domain (Atx2-dPAM#6/7/8) or wild-type control (Ctrl) together with HttQ128 are expressed is shown (n=15-19; *p<0.05 **p<0.01, ***:p<0.005, error bars represent SE). E. Representative images of LNvs (sLNv and lLNv) expressing HttQ46-eGFP at day 30 are shown in the wild-type control background (Ctrl) or with ATX2-dPAM overexpression (Atx2-dPAM#6/7/8). White arrowheads indicate lLNvs (regardless of aggregation formed or not). White asterisks label sLNvs without aggregates. Yellow dash circles label sLNvs with aggregates. Example aggregates are pointed out by orange arrows.

their behavioral rhythms. However, we failed to observe any significant effect of *tyf* loss on sLNv cell number (Figure 4.S4A) nor the % of sLNv containing HttQ72 aggregates (Figure 4.S4B). Thus, these data suggest that *Atx2* effects are independent of its role in PER translation.

4.4.3 *Atx2* Affects PolyQ but not TDP43 Mediated Toxicity

Given that Atx2 has been implicated in other neurodegenerative diseases, we asked if the *Atx2* effects seen here are specific to mHtt or not. To test this, we examined two other neurodegenerative models that can reduce behavioral rhythms when expressed in PDF neurons. First, we found expression of another polyQ protein, ATXN3Q78, involved in Machado-Joseph disease (Ichikawa et al., 2001; Kawaguchi et al., 1994) and a mutant form of Tar Domain Protein 43 (TDP43-A315T), which is involved in a familial autosomal dominant form of amyotrophic lateral sclerosis (Gitcho et al., 2008; Neumann et al., 2006) in PDF neurons results in a robust reduction in overall rhythmicity, similar to previously observed (Kadener et al., 2006). Similar to what has been shown for mHtt, *Atx2* knockdown or Atx2-ΔPAM overexpression suppresses the arrhythmicity of ATXN3Q78 expression (Figure 4.4A). On the other hand, no suppression was observed in the case of TDP43-A315T-induced arrhythmicity, indicating that the *Atx2* effects are specific to polyQ toxicity (Figure 4.4B).

4.4.4 *Atx2* Effects Do Not Necessarily Function Via Reductions in mHtt Expression

The reduction in mHtt toxicity mediated by *Atx2* knockdown could due to lower mHtt levels either by reducing the activity of the PdfGAL4 driver or by a more direct effect on mHtt, for example, by reducing mHtt translation. The former is inconsistent with our finding that PdfGAL4 driven UAS-TDP43A315T effects on circadian behavior are unaffected by *Atx2* knockdown (Figure 4.4B). To address this question, we assessed changes in GFP fluorescence in the sLNv expressing HttQ25-GFP and HttQ46-GFP driven by PdfGAL4 during *Atx2* manipulations. As

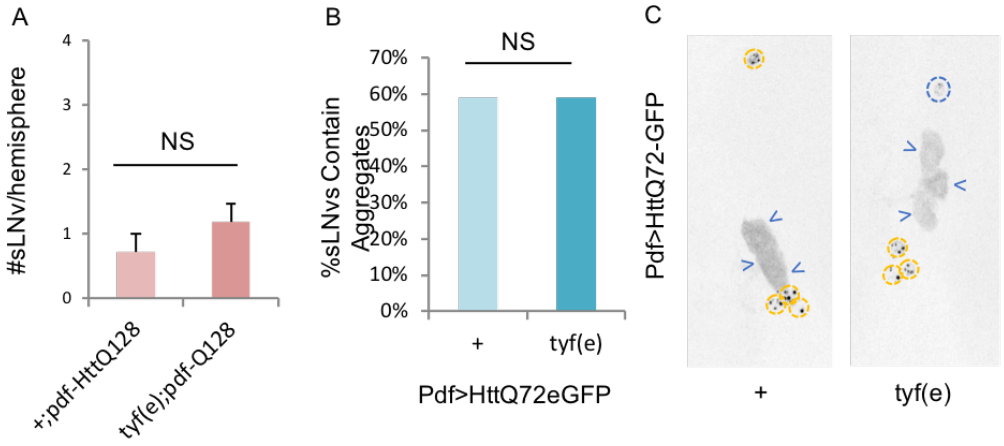

Figure 4.S4. *tyf* Mutant Does Not Affect mHtt sLNv Cell Loss nor Aggregation

A. The number of sLNv present per brain hemisphere is indicated for various genotypes at day 5 under wild-type control (+) or *tyf* mutant *(tyf(e)*) background with HttQ128 expression is shown (n=11-26). B. Percentage of sLNvs at age day 7 containing HttQ72-eGFP aggregates in a wild-type control (+) or *tyf* mutant *(tyf(e)*) background and expressing HttQ72 is quantified (n=39-49; *p<0.05 **p<0.01, ***:p<0.005). C. Representative images of LNvs (sLNv and lLNv) for corresponding genotypes in B are shown. Blue arrowheads indicate lLNvs. Blue dot circles label sLNvs without aggregates. Yellow dash circles label sLNvs with aggregates.

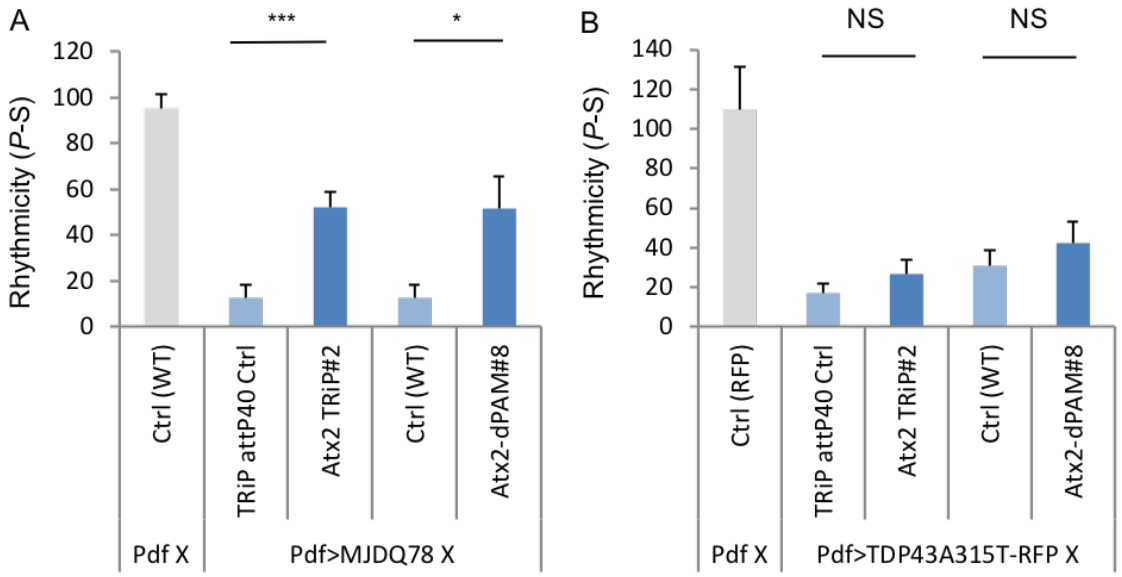

Figure 4.4. *Atx2* Reduction or ATX2 Lacking PAM Domain Rescues Behavior Rhythmicity Decrease in MJDQ78 But Not Mutant TDP43

A. Rhythmicity (P-S) is indicated for various genotypes including flies expressing only PdfGAL4 in the wild-type control background (Pdf X Ctrl(WT)) as well as flies expressing ATX3Q78 (MJDQ78) in PDF neurons in a TRiP RNAi library control background (MJDQ78 TRiP Ctrl#2) or wild-type control (Ctrl) and expressing *Atx2* RNAi lines (MJDQ78 Atx2 TRiP #2) or overexpression of ATX2 lacking PAM domain (MJDQ78 Atx2-dPAM#8; n=5-17; *p<0.05 **p<0.01, ***:p<0.005, error bars represent SE). B. Rhythmicity (P-S) is indicated for various genotypes including flies expressing only PdfGAL4 in the RFP expressing background (Pdf X Ctrl(RFP)) as well as flies expressing mutant TDP43 (TDP43A315T) in PDF neurons in a TRiP RNAi library control background (TDP43A315T TRiP Ctrl#2) or wild-type control (Ctrl) and expressing *Atx2* RNAi lines (TDP43A315T Atx2 TRiP #2) or overexpression of ATX2 lacking PAM domain (TDP43A315T Atx2-dPAM#8; n=9-15; NS:not significant, error bars represent SE).

aggregation can stabilize HttQ46-GFP, we addressed levels of mHtt in younger flies (day 2) prior to the appearance of aggregates. As ATX2 overexpression can trigger premature aggregation (Figure 4.5A,B), we also focused our analysis on those sLNvs which did not show aggregation. While we observed significant reductions in GFP expression with *Atx2* RNAi, levels of HttQ25 nor HttQ46 were not affected either by Atx2-ΔPAM nor *Atx2* overexpression. Thus, *Atx2* effects may operate via both changes in Htt levels but likely also act by other mechanisms.

4.4.5 The *Drosophila* Homolog of the Fragile X Mental Retardation Gene *Fmr1* and *Atx2* Partner Is Important for mHtt Effects on Circadian Rhythms and Clock Neurons

ATX2 also interacts with FMR1 and they may work together via a miRNA pathway to control protein translation (McCann et al., 2011; Sudhakaran et al., 2014). Specific RNAs bond by FMR1 are downregulated in *Fmr1* knockout mice, implying FMR1 could not only silence gene expression but also stabilize its targets (Zhang et al., 2018a). FMR1 is most well-known for its role in Fragile X syndrome also due to a triplet repeat expansion in the 5' untranslated region of the *FMR1* gene (Garcia-Arocena and Hagerman, 2010). Notably, those carrying premutations, i.e., those with intermediate length expansions, also exhibit a neurodegenerative syndrome resulting in ataxia potentially due to an alternative translation of the triplet repeat sequence (Kearse et al., 2016). To test whether loss of *Fmr1* can also modify Htt effects, we used RNAi knockdown. We found that *Fmr1* knockdown can improve rhythmicity in HttQ128 expressing flies (Figure 4.6A), while they have little or no effect when expressed in a wild-type background (Figure 4.6B). We confirmed the role of *Fmr1* with a second independent RNAi line (Figure 4.6A. *Fmr1* RNAi TRiP#1, (TRiP.HMS00248) and, *Fmr1* RNAi TRiP#2, (TRiP.GL00075)). To assess the impact on cell death and aggregation, we assayed PDF+ sLNv number and aggregation. We observed a modest increase in sLNv cell number with one line reaching statistical significance (Figure 4.6C, $p=0.0063$). Moreover, both lines reduce the percentage of sLNvs that contains

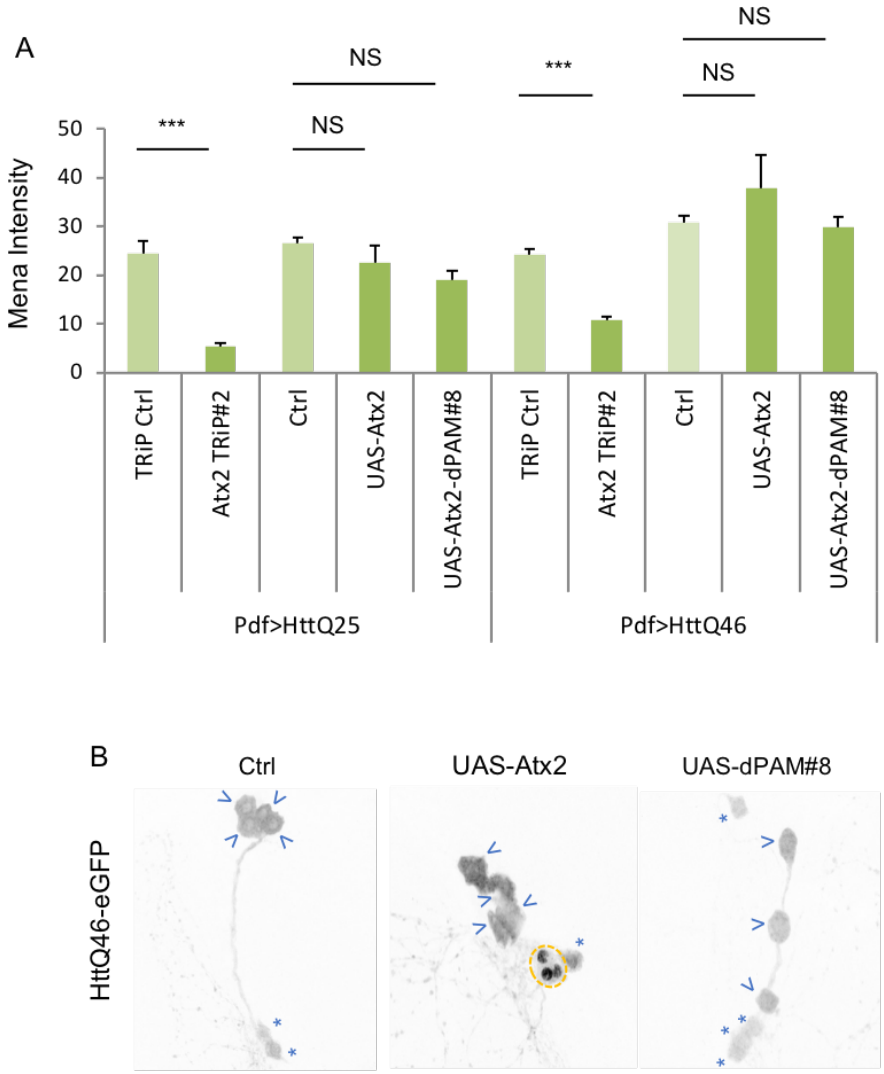

Figure 4.5. *Atx2* Knockdown Decreases Htt and mHtt Levels while Atx2 or Atx2-dPAM Overexpression Does Not Affect Htt or mHtt Levels Prior to Aggregation Formation

A. GFP Intensity in the sLNv for flies expressing HttQ25 or HttQ46 in a TRiP RNAi library control background (TRiP Ctrl#2) and expressing *Atx2* RNAi lines (Atx2 TRiP #2) at age day 5 is quantified and shown. GFP Intensity in the sLNv without aggregates formed for flies expressing HttQ25 or HttQ46 in a wild-type control background (Ctrl) and expressing UAS-Atx2 and UAS-dPAM at age day 2 is quantified and shown (n=5-38; *p<0.05 **p<0.01, ***:p<0.005, error bars represent SE). B. Representative images of LNvs (sLNv and lLNv) expressing HttQ46-eGFP at age day 2 are shown in wild-type control background (Ctrl) and overexpressing Atx2 or Atx2 lacking the PAM domain (UAS-dPAM). Blue arrowheads indicate lLNvs. Blue asterisks label sLNvs without aggregates. Yellow dash circles label sLNvs with nuclear accumulation/aggregation of HttQ46 (not used for GFP intensity quantification).

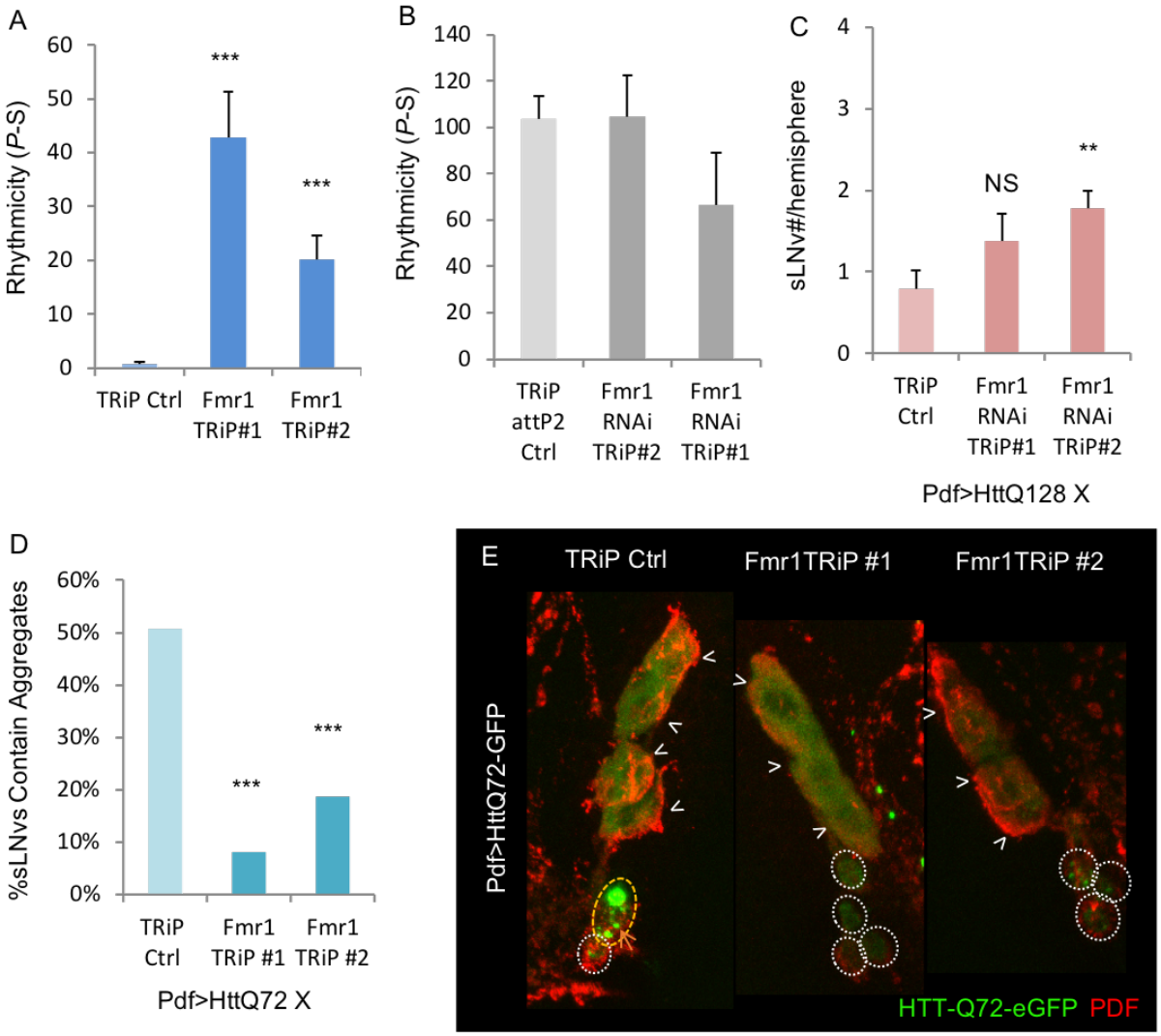

Figure 4.6. *Fmr1* Knockdown Suppresses mHtt Toxicity

A. Rhythmicity (P-S) is indicated for various genotypes including flies expressing HttQ128 in PDF neurons in a TRiP RNAi library control background (HttQ128 TRiP Ctrl) and expressing two independent *Fmr1* TRiP RNAi lines (HttQ128 Fmr1 RNAi TRiP #1 and #2; n=22-25; *p<0.05 **p<0.01, ***:p<0.005, error bars represent SE). B. Rhythmicity (P-S) is indicated for various genotypes including flies expressing two independent *Fmr1* TRiP RNAi lines in PDF neurons (Fmr1 RNAi TRiP #1 and #2) or only PdfGAL4 in the TRiP RNAi library control background (TRiP Ctrl; n=8-19). C. The number of sLNv present per brain hemisphere is indicated for various genotypes where either two independent *Fmr1* RNAi (*Fmr1* RNAi TRiP #1/2) or TRiP RNAi library control (TRiP Ctrl) control and HttQ128 are expressed is shown (n=9-14; *p<0.05 **p<0.01, ***:p<0.005, error bars represent SE). D. Percentage of LNvs (labeled with PDF in red) at age day 7 containing HttQ72-eGFP aggregates (in green) in a TRiP RNAi library control background (TRiP Ctrl) and expressing two independent *Fmr1* TRiP RNAi lines (*Fmr1* RNAi TRiP #1/2) is quantified (n=32-65; *p<0.05 **p<0.01, ***:p<0.005, error bars represent SE). E. Representative images of LNvs (sLNv and lLNv) for corresponding genotypes in D are shown. White arrowheads indicate lLNvs (regardless of aggregation formed or not). White dot circles label sLNvs without aggregates. Yellow dash circles label sLNvs with aggregates. Example aggregates are pointed out by orange arrows.

HttQ72 aggregates (Figure 4.6D,E). These data provide evidence that *Fmr1* may work together with *Atx2* by regulating other target gene expression to regulate mHtt toxicity since knock down of either of them leads to similar rescue effects. Since we found PAM domain (the interaction with PABP) is important for the rescue effects, which also suggests the role of *Atx2* in regulating other RNAs are critical. Taken together, these data indicate that genes whose mRNA stability is affected by ATX2 could participate in the rescue caused by *Atx2* knockdown.

4.4.6 *Atx2*, but not *tyf*, Regulates the Cycling Gene *CrebA*

To discover potential gene-specific targets of *Atx2* action, we conducted RNA sequencing from flow activated cell sorted PDF+ LNvs in which we co-expressed Atx2 RNAi (KK108843). While *Atx2* effects are thought to be primarily posttranscriptional, we reasoned that changes in RNA metabolism, including translation, could affect RNA half-life and, as a result, RNA levels (Parker, 2012; Roy and Jacobson, 2013). We assessed the effects of *Atx2* RNAi at dawn and dusk ZT0/2 and ZT12/14 (around light-on and lights-off in 12:12 LD cycles). In order to find *Atx2* regulated genes, we employed DEseq2 with an adjusted p-value threshold < 0.05. *Atx2* expression is robustly reduced by >75%, validating RNAi efficiency (Figure 4.7A). 960 differentially expressed genes were found at ZT0-2 with 1243 genes at ZT12-14 with 396 evident at both time points. As this *Atx2* RNAi line is known to disrupt PER expression and circadian rhythms (Lim et al., 2011b; Zhang et al., 2013), we expected to observe changes in core clock genes. We observed significant increases in *vri* at ZT0 and reductions in *tim* at ZT12 (Figure 4.7B,C). As ATX2's binding partner in PER translation initiation, TYF also strongly affects the core clock(Lim et al., 2011b). Genes that are misregulated in both *Atx2* RNAi and tyf mutant could be more likely due to their effect on the clock, such as *vri* and *tim* (Figure 4.7E,F). Since *Atx2* affects and tyf mutant does not affect mHtt toxicity, we reasoned that *Atx2* function in mHtt toxicity would be via genes that are selectively regulated by *Atx2* and not *tyf*. We similarly FACS sorted LNv

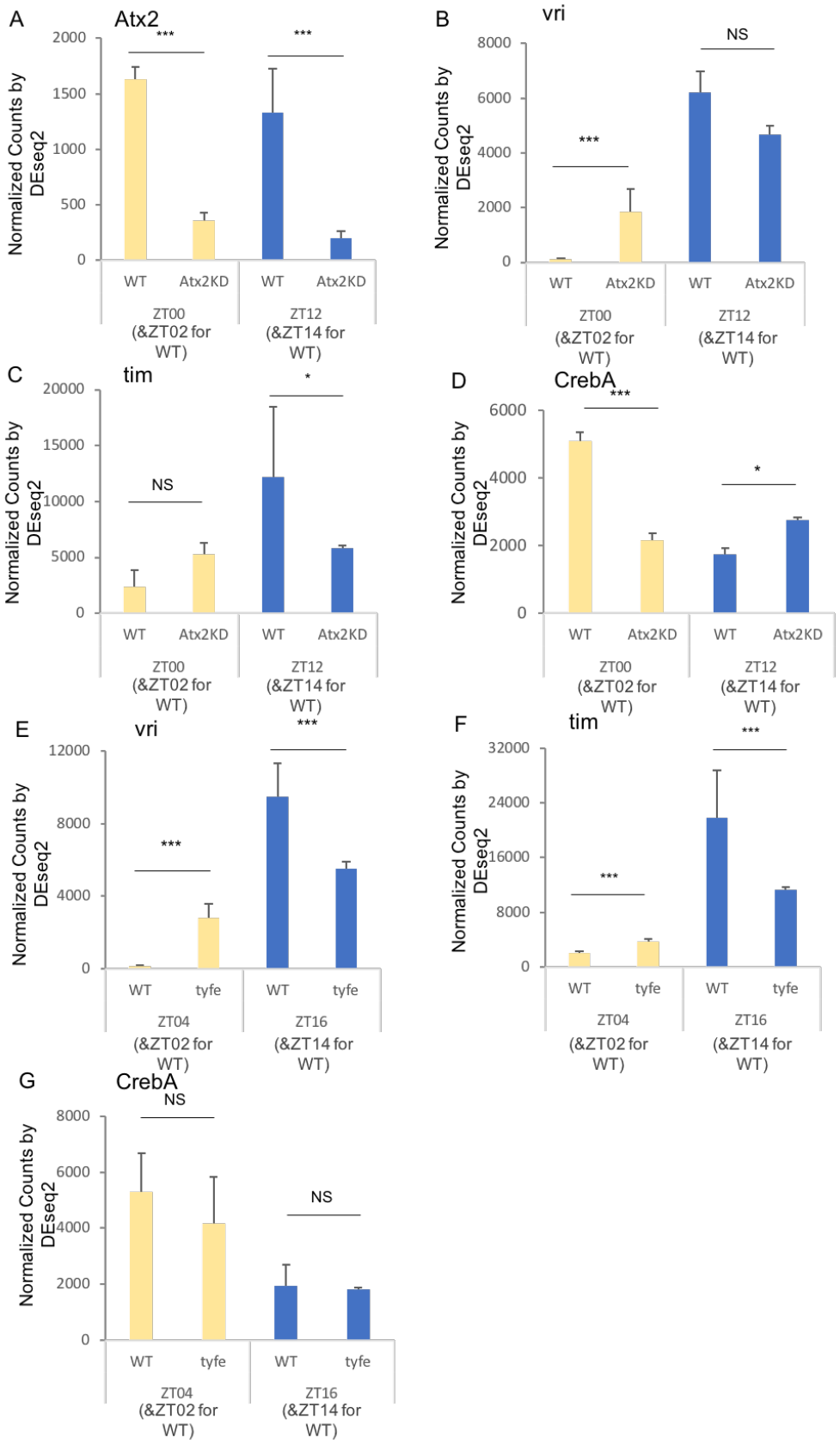
A
Atx2
Normalized Counts by DEseq2
2000
1500
1000
500
0
***
***
WT
Atx2KD
WT
Atx2KD
ZT00 (&ZT02 for WT)
ZT12 (&ZT14 for WT)
B
vri
Normalized Counts by DEseq2
8000
6000
4000
2000
0
***
NS
WT
Atx2KD
WT
Atx2KD
ZT00 (&ZT02 for WT)
ZT12 (&ZT14 for WT)
C
tim
Normalized Counts by DEseq2
20000
15000
10000
5000
0
NS
*
WT
Atx2KD
WT
Atx2KD
ZT00 (&ZT02 for WT)
ZT12 (&ZT14 for WT)
D
CrebA
Normalized Counts by DEseq2
6000
4000
2000
0
***
*
WT
Atx2KD
WT
Atx2KD
ZT00 (&ZT02 for WT)
ZT12 (&ZT14 for WT)
E
vri
Normalized Counts by DEseq2
12000
8000
4000
0
***
***
WT
tyfe
WT
tyfe
ZT04 (&ZT02 for WT)
ZT16 (&ZT14 for WT)
F
tim
Normalized Counts by DEseq2
32000
24000
16000
8000
0
***
***
WT
tyfe
WT
tyfe
ZT04 (&ZT02 for WT)
ZT16 (&ZT14 for WT)
G
CrebA
Normalized Counts by DEseq2
8000
6000
4000
2000
0
NS
NS
WT
tyfe
WT
tyfe
ZT04 (&ZT02 for WT)
ZT16 (&ZT14 for WT)

(continued)

Figure 4.7. Decreases in *Atx2* but Not *tyf* in LNvs Causes Aberrant Expression of *CrebA*

A-D. The expression level of various genes of interest (*Atx2, vri, tim, CrebA*) in flies expressing mGFP in the LNvs in the wild-type background (WT) or with the expression of *Atx2* RNAi KK (Atx2 KD) at two time points is shown in normalized counts calculated by DEseq2. E-G. The expression level of various genes of interest (*vri, tim, CrebA*) in flies expressing mGFP in the LNvs in the wild-type background (WT) or in the *tyf* mutant (tyf(e)) at two time points is shown in normalized counts calculated by DEseq2. Asterisks indicate the significance using the adjusted p-values calculated by DEseq2 (*p<0.05 **p<0.01, ***:p<0.005, error bars represent SE).

from wild-type and *tyf* mutants and found 429 genes were found differentially regulated at both time points (ZT4 and ZT16), 98 of which were also regulated by *Atx2* RNAi. Among the remaining 298 *Atx2*-dependent, *tyf*-independent genes, one was cyclic AMP response element-binding protein A (*CrebA*; Figure 4.7D). *CrebA* also showed a significant difference (~3x) between ZT0/2 and ZT12/14 consistent with an underlying oscillation, one which was previously observed with a similar phase at the protein level in the LNv (Mizrak et al., 2012). We find that *Atx2* RNAi significantly reduces *CrebA* levels at ZT0 and mildly elevated *CrebA* at ZT12 while there was not a significant effect in *tyf* mutants (Figure 4.7G). Thus, our data suggest that *Atx2* dependent regulation of cycling *CrebA* may be critical for mHtt toxicity.

4.4.7 *CrebA* Knockdown Suppresses mHtt Effects on Behavior, Cell Loss, and Aggregation

To determine if *CrebA* affects mHtt, we assayed its effect on mHtt-mediated arrhythmicity. *CrebA* overexpression affects circadian period length (Mizrak et al., 2012). As expected, we found a few *CrebA* RNAi lines also decrease the rhythmicity even without the mHtt expression (data not shown). We identified one RNAi line (*CrebA* RNAi TRiP#2 (TRiP.JF02189)) that does not reduce rhythmicity on its own (Figure 4.8A). However, this line rescues the arrhythmicity caused by HttQ128 (Figure 4.8B). To confirm that the phenotype was due to *CrebA*, we used a transgenic rescue. We found that *CrebA* expression “rescued” the HttQ128-induced arrhythmicity, while it did not reduce rhythms on its own (Figure 4.8C). Knocking down *CrebA* also rescues arrhythmicity caused by HttQ103 (Figure 4.8D), confirming *CrebA* as a modifier for mHtt induced arrhythmicity.

To understand how *CrebA* regulates mHtt toxicity, we assayed effects on sLNv cell number and mHtt aggregation. *CrebA* knockdown increased sLNv cell number from <1 to ~2 (Figure 4.9A, p=0.00064). *CrebA* RNAi also essentially eliminated HttQ72-GFP aggregates in the sLNv (Figure 4.9B,C). To determine if the reduction of mHtt toxicity and aggregation was via

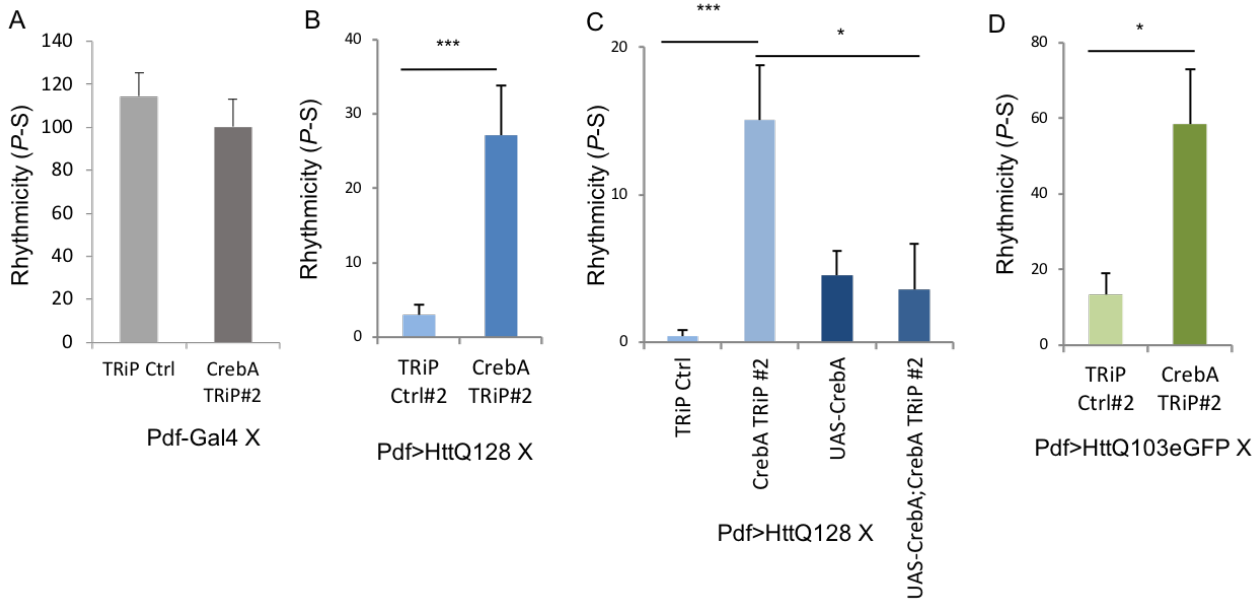

Figure 4.8. *CrebA* Knockdown Suppresses mHtt Induced Arrhythmicity in Two Different mHtt Models

A. Rhythmicity (P-S) is indicated for various genotypes including flies expressing *CrebA* TRiP RNAi lines in PDF neurons (CrebA TRiP #2) or only PdfGAL4 in the TRiP RNAi library control background (TRiP Ctrl; n=7-8, error bars represent SE). B. Rhythmicity (P-S) is indicated for various genotypes including flies expressing HttQ128 in PDF neurons in a TRiP RNAi library control background (HttQ128 TRiP Ctrl) and expressing a *CrebA* TRiP RNAi line (HttQ128 CrebA TRiP#2; n=20 ; *p<0.05 **p<0.01, ***:p<0.005, error bars represent SE). C. Rhythmicity (P-S) is indicated for various genotypes including flies expressing HttQ128 in PDF neurons in a TRiP RNAi library control background (HttQ128 TRiP Ctrl) and expressing a *CrebA* TRiP RNAi line (HttQ128 CrebA RNAi TRiP#2) or a CrebA overexpression line (Htt Q128 UAS-CrebA) or the combination of RNAi and overexpression (HttQ128 UAS-CrebA;CrebA RNAi TRiP#2; n=10-22 ; *p<0.05 **p<0.01, ***:p<0.005, error bars represent SE). D. Rhythmicity (P-S) is indicated for various genotypes including flies expressing HttQ103 in PDF neurons in a TRiP RNAi library control background (HttQ103 TRiP Ctrl) and expressing a *CrebA* TRiP RNAi line (HttQ103 CrebA RNAi TRiP#2; n=7 ; *p<0.05 **p<0.01, ***:p<0.005, error bars represent SE).

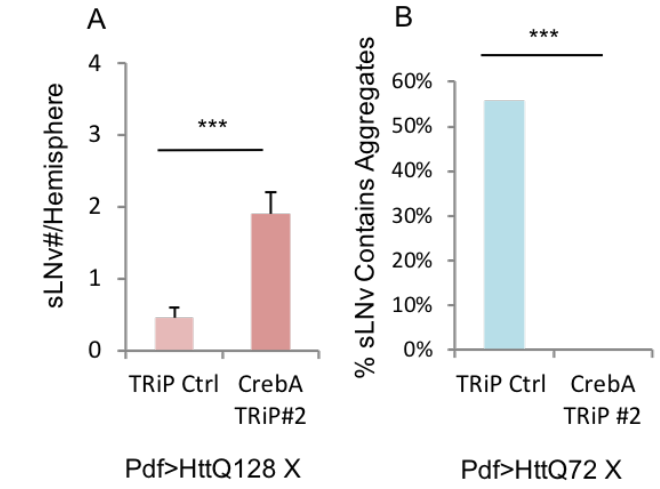
A
sLNv#/Hemisphere
4
3
2
1
0
***
TRiP Ctrl
CrebA TRiP#2
Pdf>HttQ128 X
B
% sLNv Contains Aggregates
60%
50%
40%
30%
20%
10%
0%
***
TRiP Ctrl
CrebA TRiP #2
Pdf>HttQ72 X

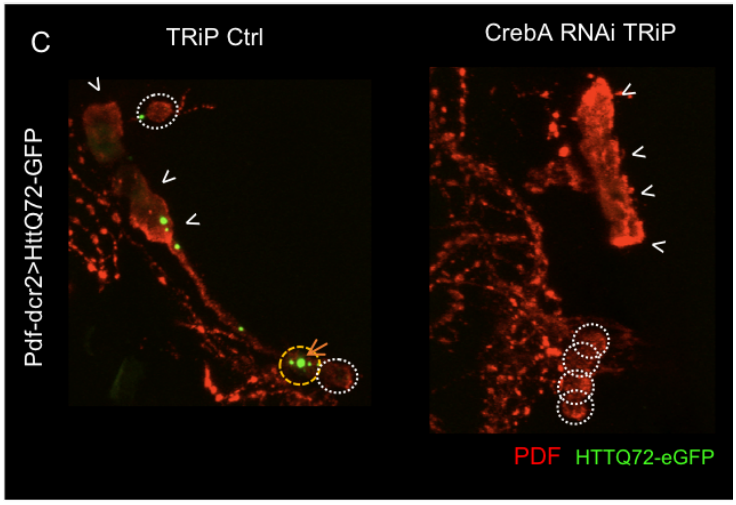
C
TRiP Ctrl
CrebA RNAi TRiP
Pdf-dcr2>HttQ72-GFP
PDF
HTTQ72-eGFP

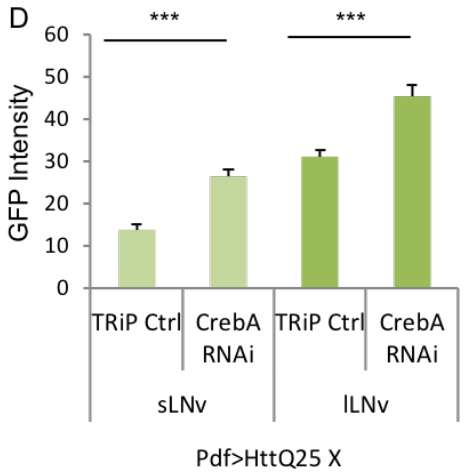
D
GFP Intensity
60
50
40
30
20
10
0
***
***
TRiP Ctrl
CrebA RNAi
TRiP Ctrl
CrebA RNAi
sLNv
lLNv
Pdf>HttQ25 X

(continued)

Figure 4.9. *CrebA* Knockdown Suppresses mHtt Induced Cell Loss and Aggregation Despite Elevated Htt Levels

A. The number of sLNv present per brain hemisphere at age day 5 is indicated for various genotypes where either *CrebA* RNAi (CrebA TRiP#2) or TRiP RNAi library control (TRiP Ctrl) and HttQ128 are expressed is shown (n=20-26; *p<0.05 **p<0.01, ***:p<0.005, error bars represent SE). B. Percentage of sLNvs at age day 7 containing HttQ72-eGFP aggregates in a TRiP RNAi library control background (TRiP Ctrl) and expressing a *CrebA* TRiP RNAi lines (CrebA TRiP #2) is quantified (n=43-44; *p<0.05 **p<0.01, ***:p<0.005, error bars represent SE). C. Representative images of LNvs (sLNv and lLNv) for corresponding genotypes in B are shown. White arrowheads indicate lLNvs (regardless of aggregation formed or not). White dot circles label sLNvs without aggregates. Yellow dash circles label sLNvs with aggregates. Example aggregates are pointed out by orange arrows. D. GFP Intensity in the sLNv or lLNv for flies expressing HttQ25 in a TRiP RNAi library control background (TRiP Ctrl) and expressing CrebA RNAi is quantified and shown (n=8-20 ; *p<0.05 **p<0.01, ***:p<0.005, error bars represent SE).

a reduction in levels, we assessed the effects of *CrebA* RNAi on non-aggregation prone HttQ25-GFP driven by *PdfGAL4*. In fact, we find that *CrebA* RNAi modestly increases HttQ25-GFP levels (Figure 4.9D). Thus, changes in mHtt aggregation are not likely due to a reduction in mHtt levels. Taken together, these data provide evidence for a role of *CrebA* as a mediator of *Atx2* effects on mHtt toxicity.

4.5 Discussion

Using a behavioral platform for identifying modifiers of mHtt toxicity, we have identified a novel molecular pathway in which *Atx2* activates CrebA expression to promote mHtt aggregation and toxicity. *Atx2* effects are bidirectional, where loss-of-function using RNAi knockdown or a ΔPAM dominant negative mutant reduce mHtt effects while overexpression increases mHtt effects. Loss of *Fmr1*, a partner of *Atx2*, showed similar phenotypes suggesting ATX2 functions with FMR1 in miRNA-mediated translational control. Transcriptome analysis of *Atx2* regulated gene expression demonstrated a role in increasing *CrebA* transcript levels. Indeed, *CrebA* knockdown also reduces mHtt toxicity, demonstrating a novel molecular pathway by which *Atx2* controls mHtt toxicity.

Using multiple independent reagents, we demonstrate a potent role for Atx2 in mediating mHtt toxicity on clock neurons. To reduce *Atx2* function, we applied both RNAi-mediated knockdown and a dominant negative form of *Atx2* that is missing the PABP binding PAM2 domain crucial for its translation activation function (Lim et al., 2011b). We observed suppression of mHtt-induced arrhythmicity with two independent RNAi lines and three independent Atx2ΔPAM transgenics. Among the lines that we screened, *Atx2* RNAi was the most potent modifier of mHtt induced arrhythmicity arguing for a crucial role. The effect on aggregation is consistent with those identified for *Atx2* RNAi as part of a large scale RNAi screen in an in vitro tissue culture cell model, although these results were not validated in vivo(Zhang et al., 2010). These effects are

bidirectional, i.e., ATX2 overexpression can enhance mHtt-induced arrhythmicity. Bidirectional effects extend to effects on mHtt aggregation where *Atx2* loss- and gain-of function reduce and increase aggregation, respectively. The potency and dose sensitivity of *Atx2* effects on mHtt toxicity suggest a key role for this RNA-binding protein.

In addition to behavioral and molecular effects, we also demonstrated that Atx2 can suppress both mHtt effects on pre-degenerative neuronal dysfunction as well as cell death. We find suppression of mHtt-induced arrhythmicity is often accompanied by increases in the number of sLNv (Figure 4.3BD/6BC/8B&9A) responsible for free-running rhythmicity, indicating that loss of *Atx2* function can reduce mHtt induced neuronal loss. However, we also find that *Atx2* RNAi can suppress mHtt effects on rhythmicity without changing sLNv cell number. Thus, these effects are likely via suppression of mHtt-induced dysfunction of the remaining viable neurons rather than changes in cell death. This finding highlights a role for *Atx2* in mHtt-induced neural dysfunction but also the potential of our behavioral screening platform to identify functional pre-degenerative changes. Given that sleep-wake changes often occur even prior to the advent of full HD symptoms (Arnulf et al., 2008; Goodman et al., 2011; Hunter et al., 2010), it is possible that these changes could also reflect potentially reversible neuronal dysfunction. We propose identifying molecular pathways, such as *Atx2*, important for mHtt effects prior to cell death may be especially useful to slow or even prevent the onset of HD.

Our results indicate that *Atx2* effects are not via their established role in translation of the core clock component PER but likely function through a translational repression pathway involving FMR1. First, we find that *Atx2* manipulations that have no effect on behavioral rhythmicity can still suppress mHtt induced arrhythmicity and aggregation (Figure 4.1A). Loss of the partner of *Atx2*, *tyf*, involved in PER translation robustly suppresses rhythmicity and PER levels but has no effect on mHtt aggregation nor cell death (Lim et al., 2011a; Zhang et al., 2013) (Figure 4.S4). Loss of per also fails to alter mHtt induced cell death (Xu et al., 2019) . In addition to its role in

PER translation, *Atx2* also plays a role in miRNA-mediated translational repression (Sudhakaran et al., 2014). Here we tested the function of an established partner of ATX2 in this pathway, FMR1. We found that *Fmr1* knockdown suppresses mHtt-induced arrhythmicity, aggregation and cell death (Figure 4.7B,C,D). These data suggest that *Atx2* and *Fmr1* may act in concert to enhance mHtt toxicity. Our data suggest that *Atx2* may work via multiple modes, one of which is possibly through regulating mHtt levels. Using RNAi we observed reductions in the expression of both HttQ25-GFP and HttQ46-GFP in the sLNv(Figure 4.5A), suggesting a potential role in regulating Htt translation. On the other hand, we did not observe changes using either *Atx2* overexpression of expression of the dominant negative Atx2ΔPAM, indicating that *Atx2* can exert effects independent of regulating mHtt levels.

To discover potential targets of *Atx2*, we assessed the transcriptome in the LNv using RNAi knockdown and discovered that *Atx2* effects may be mediated by activating expression of the transcription factor *CrebA*. After *Atx2* RNAi knockdown, we find that CrebA transcript levels are substantially reduced at their peak time. Yet these same changes are not observed in a *tyf* mutant which similarly impairs the core clock, suggesting a tyf and core clock independent mechanism which parallels the divergent effects of *Atx2* and *tyf* on mHtt toxicity. Interestingly, the mammalian homologs of *CrebA*, Creb3L1 or Creb3L2 are up-regulated in HD iPS cells or mouse models, respectively (Consortium, 2012; Giles et al., 2012), suggesting that CREBs could be facilitating the HD pathology. Consistent with this model, we find that *CrebA* knockdown can suppress effects of mHtt on circadian behavior, cell death, and aggregation. The behavioral effects are rescued by a wild-type transgene, providing independent evidence for an in vivo function. While we cannot rule out a function of the other *Atx2*-dependent, *tyf*-independent genes identified in our transcriptomic analysis, these data demonstrate clearly a role for one of those targets, *CrebA*, in mediating mHtt effects in vivo.

How might *Atx2* regulate *CrebA*? An AUUUU motif is enriched in 3'UTRs of genes bound and stabilized by ATXN2 (Yokoshi et al., 2014). Notably, we find multiple AUUUU elements are located in the fly CrebA 3'UTR. In fact, when we looked more broadly, we found a U rich motif is significantly enriched in the 3' UTRs of *Atx2* regulated genes in our dataset (data not shown). Although whether Fmr1 would have a similar effect on *CrebA* transcript level need to be further determined, we hypothesize that ATX2 stabilizes *CrebA* transcripts in the PDF neurons at least in the morning.

In addition to a role for *Atx2/CrebA* in mHtt induced arrhythmicity, both *Atx2* and *CrebA* transcripts themselves display time-of-day variation in levels. While *Atx2* oscillations are modest, those for *CrebA* are much more robust (~3-fold), consistent with other studies that examine *CrebA* at the protein level (Mizrak et al., 2012). Moreover, *Atx2* appears to be important for *CrebA* oscillations. Thus *Atx2* and especially *CrebA* may represent conduits through which the circadian clock can impact mHtt pathogenesis.

These data on *Atx2* effects on mHtt add to other data linking *Atx2* to multiple neurodegenerative diseases, suggesting that *Atx2* may be a "master regulator" of neurodegeneration. The gene name Ataxin2 stems from its role in spinocerebellar ataxia 2 (SCA2) (Pulst et al., 1996) caused by an inherited polyQ expansion within the gene itself. This results in loss of cerebellar Purkinje neurons and ataxia(Lastres-Becker et al., 2008). Notably disrupted REM sleep has been observed even in those who are presymptomatic, potentially due to pons degeneration(Boesch et al., 2006; Rodriguez-Labrada et al., 2011; Tuin et al., 2006). Atx2 is also pivotal for polyQ mediated neurodegeneration involving other spinocerebellar ataxia genes, Atxn1 and Atxn3. Atx2 overexpression enhances the toxicity of ATXN3Q78 and ATXN1Q82 while the reduced Atx2 function can suppress ATXN1Q82 toxicity as assayed by fly retinal degeneration (Al-Ramahi et al., 2007; Lessing and Bonini, 2008). *Atx2* also plays a key role in mediating the toxicity of other proteins involved in ALS, including TDP43, Fused in Sarcoma (FUS), and

C9ORF72 (Becker et al., 2017; Elden et al., 2010; Lattante et al., 2014; Nihei et al., 2012; Van Blitterswijk et al., 2014). Individuals with intermediate length polyQ expansions (Q27-32) of ATXN2 exhibited an elevated risk of developing ALS (Elden et al., 2010). Atx2 can bidirectionally modify the toxicity of the ALS gene TDP43 (Elden et al., 2010). Overexpression of human Atx2 with intermediate length polyQ expansion enhances C9ORf72 induced neuronal toxicity in mammalian neuronal culture (Ciura et al., 2016) and enhances TDP43 induced retinal degeneration(Kim et al., 2014). Atxn2 KO alleviates TDP43 toxicity in survival rate and locomotor tests in mice model while Atxn2 KD reduces the recruitment of TDP43 to stress granules in the human cells (Becker et al., 2017). *Atx2* also regulates retinal degeneration due to FUS as well as the poly-glycine-arginine repeats derived from the ALS genes C9ORF72 (Bakthavachalu et al., 2018). Given the multiple roles of ATX2 in a range of neurodegenerative diseases, we hypothesize that it may be a key therapeutic node for their prevention and treatment (van den Heuvel et al., 2014).

Chapter 5: Summary and Discussion

5.1 Summary

In this thesis, we have applied large-scale *Drosophila* genetics to understand the bidirectional relationship between circadian clocks and neurodegenerative disease. We have demonstrated that the expression of several human ND genes in the circadian neurons in the fly leads to circadian defects. Those genes include mutant *HTT* and *ATXN3*, wild-type or mutant *TDP43* and *FUS*, human *PSEN2* or fly mutant *Psn*, GGGGCC repeat from *C9ORF72*, and the RAN translation arginine-rich poly-dipeptide product. In addition, knocking down fly *Hip14* also causes circadian defects. Most of the arrhythmicity observed in flies expressing those toxic ND genes are accompanied by the loss of PDF and the degeneration of sLNvs or both lLNvs and sLNvs.

The finding that circadian clock modulation can impact mHtt toxicity implies that the rhythmic expression of clock-controlled genes is important. Yet our RNAi experiments do not distinguish between changes in levels versus changes in timing as important mediators of mHtt toxicity. While previous data mainly focused on whether ND would affect circadian rhythms, we hypothesized clock perturbation would affect ND pathogenesis in return. Using mHtt expression in the PDF neurons as a model, our environmental perturbation data showed that although 10:10 LD rescues mHtt toxicity in flies with wild-type *per*, it fails to rescue flies with the per^{s} mutation. This suggests that the rescue from 10:10 is not only due to environmental cues but also because of the interaction between environmental disruption and the internal clock. When we introduced a genetic perturbation to the *Clk* gene with Clk^{Jrk} and tested its effect on mHtt toxicity, our data showed that other than the rescue from Clk^{Jrk}, per^{01} was able to partially suppress the rescue effect from *Clk*. This is likely due to PER's inhibitory function on CLK activity and therefore justifies the role the core clock is playing in rescuing mHtt toxicity.

Leveraging the power of our high-throughput behavioral model, we discovered multiple clock-controlled pathways that appear to modify mHtt toxicity, including those involved in transcription, translation, and chaperone pathways. Based on our evidence that the clock could regulate mHtt toxicity, we then asked what genes/pathways are mediating the effect of the clock on mHtt toxicity. We screened for cycling genes that could rescue mHtt induced arrhythmicity using behavioral assays, followed by testing the candidates found from the behavioral assays in sLNv degeneration and aggregation rescue. Genes participating in protein homeostasis, RNA metabolism regulation, and possibly other pathways were identified. This potentially links circadian clocks to mHtt toxicity. We identified *Hop*, a potential direct target of CLK, as an enhancer of mHtt toxicity. We also found that *Atx2*, working via its target *CrebA*, mediates mHtt toxicity.

However, there are a few questions that we planned to investigate but have been unable to answer due to current limitations. In this chapter, we will address questions we want to further understand, and the potential broader implications based on our current data.

5.2 Could the Manipulation of the Cycling Pattern but not Level of The Modifiers be Sufficient to Affect mHtt Toxicity?

We have identified several clock-controlled genes whose function is important for mHtt toxicity, as evidenced by RNAi screening. Yet it remains unclear if it is their rhythmic expression or their absolute levels that are important for mHtt modification. In fact, this is a general issue in the circadian clocks field where tools to dissect the role of timing in circadian gene expression have not been applied to address this question. Genes that exhibit rhythmic expression are likely to be controlled by the clock. Our strategy was to screen cycling genes in order to help us identify candidates that link the clock and the mHtt pathogenesis. Follow-up studies on these candidates revealed the pathways in which they are involved in, but major questions still remain. One issue

is that we mainly tested knocking down the cycling genes and occasionally overexpression. However, whether the cycling feature of the RNAs is important for their effects on mHtt toxicity is not clear but definitely worth further investigation. For example, synchronization of cycling genes in the same pathway that regulates mHtt pathogenesis could be important to ensure that all the key factors reach a certain concentration and work at the same time. If one of the genes in the pathway exhibit an opposite phase, even when the rest of the genes are still expressed at regular phase and level, the anti-phase gene would become the rate-limiting factor. Thus, the consequences of this situation resemble the knockdown of a certain gene and may lead to a dysfunctional pathway. To test the hypothesis that altering the phases but not the overall expression level of the cycling genes might result in similar effects as manipulation of the level only, ideally, we would like to exchange the promoter of the gene of interest to a promoter of another gene that peaks at the opposite phase (e.g. by utilizing CRISPR). However, one difficulty is that this new promoter needs to be able to maintain a similar expression level to the original promoter. Even though almost 2000 cycling genes were identified in our LNv dataset, when we actually searched for genes whose promoter might be suitable to replace our modifiers' promoters, we could only find very few ideal candidates that fulfill all of the ideal criteria.

5.3 Does mHTT Exhibit Time-dependent Toxicity?

Demonstrating that the timing of the circadian clock can modulate mHtt toxicity suggests that the circadian clock might directly impact, i.e., time, features of mHtt toxicity, including aggregation. The other question we are not able to address in our current study is whether or not mHtt exhibits a different severity of toxicity depending on the time of the day. For example, if the modifiers which modulate mHTT's propensity to form aggregates are cycling, we could hypothesize that mHtt is more prone to aggregation at a certain time of the day, or that aggregation dynamics might vary throughout the day.

To address this question, we assayed the rate of HTT-GFP aggregation at different times of day using fluorescence recovery after photobleaching (FRAP) experiments. The recovery time after FRAP is commonly used to access the dynamics of the aggregation (Chai et al., 2002). However, FRAP has not yet been published in the neurons residing in the whole brain. We had technical issues such as stabilizing the brains in the culture medium for long-term signal recording during our attempts. If other good live imaging techniques can be applied to recording aggregates in the whole brain explants directly, we could possibly even track the aggregation for days after entrainment. It would be exciting to explore whether mHTT has any time-dependent properties during the pathogenesis. One prediction of our work is that aggregation might be happening at a specific time of day which could, in turn, inform the daily timing of therapeutic interventions (see below).

5.4 How Can Clock "Disruptions" Be Beneficial?

One of our most surprising results is that the misalignment and disruption of the circadian clock were neuroprotective. There are several potential reasons that disruption of clock leads to different, or even opposite consequences. First, a summary of other studies mentioned previously: many phenotypes are observed in one circadian mutant but not the other. Thus, whether the disruption of the clock is harmful or beneficial could depend on whether targets controlled by a certain circadian gene are enhancers or suppressors for the pathogenesis elicited by a certain ND gene or stress. For instance, clock disruption enhances the chemotherapy efficacy for oncogenesis results from loss of *p53*, because a pro-apoptotic gene, *p73* is upregulated in the absence of both *Cry1* and *Cry2* (Lee and Sancar, 2011). In our case, since modifiers (e.g. *Hop*) controlled by CLK works as an enhancer for mHtt toxicity, down-regulation of the clock (Clk^{Jrk} heterozygous mutant) mitigates mHtt pathogenesis.

Secondly, the genes controlled by the clock vary between different tissues (Panda et al., 2002). Even among all of the circadian neurons, the cycling genes are diverse between subgroups of neurons (Abruzzi et al., 2017; Nagoshi et al., 2010). Therefore, the consequences of disruptions in the circadian rhythms could also be tissue/neuron-specific. This may explain the discrepancy between previous data, for example, the *per*^{01} mutant accelerating the vacuolization in the whole brain induced by oxidative stress (Krishnan et al., 2012) and our data. Genes regulating degeneration caused by oxidative stress would be different from genes mediating aggregation-related neuronal toxicity. Even for genes similarly involved in both pathways, those controlled by the clock, particularly in the LNvs, could not be under circadian control in other neurons in the brain. Depending on the primary neuron/tissue affected in different diseases, the consequences may be distinct for each case.

Thirdly, both our clock disruption conditions (*Clk*^{Jrk} heterozygous mutant and 10:10 LD cycle) do not completely obliterate the clock function. CLK target genes are still cycling but at a lower amplitude in the *Clk*^{Jrk} heterozygous mutant (Allada et al., 1998). Flies are still entrained under 10:10 LD (as shown in Chapter 2) but with lower PER expression (data not shown). This argues that deleterious effects from the more severe clock disruptions (clock gene KO or double KO mutant) may vitiate critical pathways while the “milder” disruptions might be substantial to maintain those ways but affect other modifiers.

5.5 Cell-type Dependent Selective Susceptibility of ND Genes Is Reflected in *Drosophila*

We screened through an unprecedented number of neurodegenerative disease models and discovered that only some of those exhibit significant effects on circadian rhythmicity. The finding that most of the genes do not induce phenotypes suggests that PDF neurons are specifically sensitive to specific toxic molecules, especially those that have previously been implicated in ALS.

Among the ND genes showing circadian phenotypes, we found ones that cause degeneration of similar neuron types in humans, displaying a similar toxicity to circadian neurons. Medium spiny neurons are primarily affected in HD, while Purkinje neurons are the main targets of degeneration in SCA3 (Ilieva et al., 2009; Jackson, 2014). Notably, both types are GABAergic neurons that receive glutamate signals (Jackson, 2014). We found that both disease-associated genes, mHtt and mATXN3, degenerate at least sLNvs. Loss of PDF signal progresses in a similar time course as other markers labeling the LNvs (e.g. PdfGAL4 driven mGFP). Both TDP43 and FUS, which cause motor neuron degeneration in humans, lead to aggressive loss of both lLNvs and sLNvs. In addition, the onset of the PDF signal decrease occurs much earlier than the loss of other makers (e.g. RFP tag from TDP43 and FUS), which distinguishes from the case of mHtt. By contrast, α-synucleins, which cause dopamine neuron degeneration, did not affect LNvs (Feany and Bender, 2000; Jackson, 2014). In addition, all of the modifiers that rescued ATXN3Q78 induced arrhythmicity were able to suppress mHtt toxicity, while none of them have effects on TDP43 induced arrhythmicity (data shown in Appendix 2). This observation further indicates that the ND genes, which degenerate similar types of neuron in human, may elicit toxicity via similar mechanisms/molecular pathways in the fly circadian neurons.

Taken together, testing ND genes in fly circadian neurons might recapitulate the feature of selective vulnerability of various brain regions and reserve the similarity in pathogenesis among different NDs.

5.6 Findings in Fly Circadian Neurons Can be Translated to Mammals

One concern of studying ND in the *Drosophila* model is whether discoveries in the fly can be translated to humans. We favor the idea that results from PDF neurons will extend to SCN neurons and even to the striatal neurons that are responsible for the diagnostic symptoms in HD. As reviewed in Chapter 1, the core molecular clock is highly conserved between fly and mammal

(Hardin, 2011; Mohawk et al., 2012). In addition, fly PDF neurons and mammalian SCN neurons share similar electrophysiology properties and both respond to GABA signaling (Chung et al., 2009; Flourakis et al., 2015; Ono et al., 2018; Parisky et al., 2009), suggesting that they probably react in an analogous way to environmental cues. SCN neurons exhibit molecular defects, but the primarily affected neurons are in the striatum for HD (Jackson, 2014). Although the striatum is not a center for generating circadian rhythms, core clock genes still exist and display a cycling expression pattern in that region (Iijima et al., 2002; Schnell et al., 2014), suggesting that the findings in circadian neurons may be applicable to striatum neurons as well.

5.7 *Atx2* As A Converging Point for Different NDs

The finding that *Atx2* is a robust modifier of mHtt toxicity suggests that it may be a key node in mediating a range of neurodegenerative diseases, including those involved in polyQ and ALS. Other than the fact that *Atx2* itself is an ND gene in SCA2 (Pulst et al., 1996), our data on *Atx2* supplies further evidence of its role in mediating multiple neurodegenerative diseases. Previous studies have shown that *Atx2* is also pivotal for polyQ mediated neurodegeneration involving other spinocerebellar ataxia genes, *Atxn1* and *Atxn3*. *Atx2* overexpression enhances the toxicity of ATXN3Q78 and ATXN1Q82 (retinal degeneration) while reducing *Atx2* function can suppress ATXN1Q82 toxicity in the fly (Al-Ramahi et al., 2007; Lessing and Bonini, 2008). ATXN2 also mediates retinal degeneration due to overexpression of TDP43, FUS, and the poly-glycine-arginine dipeptides (product from C9ORF72) through different domains (Bakthavachalu et al., 2018; Kim et al., 2014). Patients with intermediate-length polyQ expansions (Q27-32) of ATXN2 exhibit an elevated risk of developing ALS (Elden et al., 2010). Atxn2 KO alleviates TDP43 toxicity on survival rate and locomotor tests in the mouse model, while *Atxn2* KD reduces the recruitment of TDP43 to stress granules in human cells (Becker et al., 2017). Although *Atx2* has been found

to be an enhancer for mHtt aggregation in fly S2 cell screening (Zhang et al., 2010b), it has not been tested for its effect on mHtt toxicity *in vivo.* Here, we are the first to identify *Atx2* as an enhancer for mHtt toxicity. These data suggest that *Atx2* acts as a converging point that regulates multiple NDs. We will be discussing the possible pathways through which *Atx2* might work to mediate multiple NDs in parallel.

5.7.1 Stress Granules

One pathway through which *Atx2* might exert effects on multiple NDs is via its role in stress granules, a subcellular structure implicated in neuronal viability. Under stress, mRNA translation is arrested and transcripts localize to a cytoplasmic membraneless organelle termed stress granules (SG) (Anderson and Kedersha, 2008). The translation is restored upon stress release (Anderson and Kedersha, 2008). SGs are associated with multiple NDs including AD, ALS, and FTD (Ga et al., 2018). Markers for SGs, such as TIA-1 and G3BP, co-localize with tau and mHTT aggregates, while TDP43 and FUS are recruited to SGs (Bosco et al., 2010; Colombrita et al., 2009; Furukawa et al., 2009; Liu-Yesucevitz et al., 2010; Vanderweyde et al., 2012; Waelter et al., 2001; Wolozin, 2012). Mutations in valosin-containing protein (VCP, a gene involved in SG clearance) and TIA-1 are associated with familial ALS and/or FTD, further implying the relationship between SG and NDs (Buchan et al., 2013; Doi et al., 2010; Johnson et al., 2011; Mackenzie et al., 2017).

SGs consist of proteins that could initiate mHtt aggregation. Most of the components that make up SGs are RNA-binding proteins harboring prion-like domains (Anderson and Kedersha, 2008; Li et al., 2013). The prion-like domains make the RNA-binding proteins susceptible to form aggregates (Li et al., 2013; Maziuk et al., 2017). Therefore, a plausible mechanism of how SGs are related to multiple NDs is that aggregations initiated by different proteins facilitate each other to form aggregates together. Indeed, ND/SG proteins that are able to induce aggregation on their

own have been found in other aggregations. HTT inclusions in HD patients are also positive for TDP43 and FUS (Doi et al., 2008; Schwab et al., 2008a), while FUS is also found in inclusions in SCA1/2/3 patient brains(Doi et al., 2010). TIA-1 and mHTT could cross-seed the fibrillation of each other (Furukawa et al., 2009).

Based on the evidence above, we propose that ATX2, an SG component and an RNA-binding protein that contains the prion-like domain (Bakthavachalu et al., 2018; Lastres-Becker et al., 2016; Nonhoff et al., 2007; Ralser et al., 2005), maybe the link between SGs and neurodegenerative diseases, including HD. Our data, showing that ATX2 lacking PAM2 domain suppresses mHtt toxicity, further implicates the connection between SG and HD, since deletion of the PAM2 domain in ATXN2 partially affects its recruitment to stress granules (Nihei et al., 2012). To specifically test whether *Atx2* mediates mHtt toxicity through SG formation, we first confirmed that ATX2 co-localizes with mHTT aggregates in the cytoplasm in LNvs (data not shown). However, we failed to induce SGs in fly brains using difference stresses, including heat shock and arsenite treatment. Therefore, we were not able to access whether SG formation accelerated mHtt toxicity in a more direct way. Although knocking down other SG components also suppress mHtt toxicity (data are shown in appendix 2), we cannot rule out that it may be due to broader effects from translation regulation, as these SG components are involved in translation machinery (Anderson and Kedersha, 2008).

5.7.2 Translation/RNA Metabolism Regulation

As an RNA binding protein, ATXN2 plays a key role in regulating gene expression through multiple mechanisms, including translation activation and microRNA dependent gene silencing (Lee et al., 2017; Lim and Allada, 2013a; Sudhakaran et al., 2014; Zhang et al., 2013). In addition to potentially mediating the interaction between SG and ND aggregations, genes regulated by *Atx2* may also contribute to multiple NDs, especially those that share common pathogenesis pathways.

One common consequence of the accumulation of toxic ND proteins is the impairment of protein homeostasis and the naturally triggered reduction in protein synthesis (Brignull et al., 2007; Hetz et al., 2015). The absence of *Atxn2* attenuates the global protein synthesis rate, which may be further protective for the cells from the damaged protein homeostasis (Fittschen et al., 2015). Genes participating in protein metabolisms and protein folding are enriched in RNAs directly bound by ATXN2 (Yokoshi et al., 2014), suggesting those may be the converging pathways that targets of ATXN2 work through to modulate pathogenesis of diverse NDs. Our result that *CrebA,* as a target of *Atx2,* is facilitating the mHtt toxicity supports the view that not only could *Atx2* directly affect the toxicity of ND genes but also its targets may contribute to the regulation of pathogenesis.

5.8 Circadian Defects as Preclinical Hallmarks for ND Pathogenesis: Identify Time Frame for Early Interventions to Prevent More Severe Disease Pathogenesis?

Sleep and circadian disruptions have been identified in preclinical patients for HD, PD, and AD, indicating those phenotypes manifest themselves prior to more severe neuronal dysfunction/death (Postuma et al., 2012; Trenkwalder, 1998; Wu et al., 2003; Wu et al., 2006) (Cuturic et al., 2009; Diago et al., 2017; Goodman et al., 2011). Therefore, circadian/sleep abnormalities might be used as hallmarks to identify an early therapeutic window. By establishing ND models in circadian neurons in *Drosophila*, we asked whether circadian/sleep phenotypes are also evident before the neuronal loss. In our HD model, in addition to the severe decrease of PER in arrhythmic flies expressing mHtt, we observed a significant reduction in PER and CLK in the behavioral rhythmic flies without sLNv degeneration (young HttQ103 expressing flies), which suggests that partial impairment of the molecular clock occurs prior to neurodegeneration. Additional evidence confirming that behavioral phenotypes occur before neuronal loss stems from our observations of the presence of PDF neuron cell bodies in arrhythmic flies. In the TDP43 and FUS expressing flies, PDF signal decrease, rather than the presence of the cell body, is more

correlated with behavioral defects (data shown in Chapter 2). Thus, modifiers found through behavioral screening might implicate pathways that mediate the early stage disease pathogenesis and prevent the manifestation of later hallmarks, such as nuclear aggregation (Menalled et al., 2003). In fact, almost all of our modifiers that rescue arrhythmicity are able to suppress the mHtt aggregation (data shown in Chapter 2,3, and Appendix 2). Modifiers identified through the behavior assay provide candidates for therapeutic targeting at an early stage.

5.9 The potential of Chronotherapy as A Novel Treatment for NDs

As discussed above, our current model has several limitations, including the fact that we are studying a particular subgroup of neurons and that we are currently not able to test the effect of the phase of the cycling genes. However, our study sheds some insight on how circadian rhythms might influence the therapeutic approaches for HD. Our finding that the timing of the circadian clock is important in mHtt toxicity suggests that there may be specific times of day in which the mHtt toxicity is occurring and thus specific times of day which interventions that block toxicity are especially effective, a strategy referred to as chronotherapy. Notably, most of the drug targets for commonly used medications are under clock control (Zhang et al., 2014).

One therapeutic strategy for treating NDs is to reduce aggregation. An antibody that recognizes the first 17 amino acids in the N-term fragment of Htt (scFv-C4) has been used to decrease mHtt aggregation, level, and toxicity in the mouse, cell model, and flies (Lecerf et al., 2001; Snyder-Keller et al., 2010; Wolfgang et al., 2005). Antibodies that recognize Aβ have also been developed and tested (Fuller et al., 2015). Neuroinflammation is one of the side effects of using antibodies as well as other chemicals as treatments for NDs (Fuller et al., 2015; Schwartz, 2017; Wild and Tabrizi, 2014). Antibodies are usually constitutively expressed in the models described above. We hypothesized previously that if mHtt aggregation peaks at a certain time of the day, treatment targeting this period would be the most effective. Antibodies expressed under

a promoter that synchronizes the peak expression in phase with the mHtt toxicity peak can work at the same efficacy but at a lower level overall, thus resulting in less severe side effects. Moreover, it is known that inflammatory responses are regulated by circadian rhythms (Fonken et al., 2015). For example, hippocampal microglia rhythmically express immune genes (Fonken et al., 2015). Antibodies expressed in the opposite phase as peak immune gene expression could minimize the side effect.

Drugs that act on mHtt modifiers but not on mHtt directly could still exhibit time-of-day dependent efficacy if the specific genes/pathways they are targeting are under clock control. It has been reported that chemicals that activate autophagy through inhibiting mTOR pathway rescue mHtt toxicity in multiple animal models (Ravikumar et al., 2004; Renna et al., 2010), and the mTOR pathway is under clock control in some tissues (Zhang et al., 2014). Another example is that the up-regulation of co-chaperones has a positive therapeutic effect on mHtt and that heat shock factor (HSF) expression and its target genes involved in the stress response can be induced by light pulse (Bates et al., 2015; Ono et al., 2018). This suggests that circadian timing or light cues may affect treatment if those genes/pathways are selected as drug targets.

References

Abruzzi, K.C., Zadina, A., Luo, W.F., Wiyanto, E., Rahman, R., Guo, F., Shafer, O., and Rosbash, M. (2017). RNA-seq analysis of Drosophila clock and non-clock neurons reveals neuron-specific cycling and novel candidate neuropeptides. PLoS Genet *13*.

Agrawal, N., Pallos, J., Slepko, N., Apostol, B.L., Bodai, L., Chang, L.W., Chiang, A.S., Thompson, L.M., and Marsh, J.L. (2005). Identification of combinatorial drug regimens for treatment of Huntington's disease using Drosophila. Proc Natl Acad Sci U S A *102*, 3777-3781.

Akashi, M., Tsuchiya, Y., Yoshino, T., and Nishida, E. (2002). Control of intracellular dynamics of mammalian period proteins by casein kinase I epsilon (CKI epsilon) and CKI delta in cultured cells. Mol Cell Biol *22*, 1693-1703.

Al-Ramahi, I., Perez, A.M., Lim, J., Zhang, M.H., Sorensen, R., de Haro, M., Branco, J., Pulst, S.M., Zoghbi, H.Y., and Botas, J. (2007). DAtaxin-2 mediates expanded Ataxin-1-induced neurodegeneration in a Drosophila model of SCA1. PLoS Genet *3*, 2551-2564.

Allada, R., and Chung, B.Y. (2010a). Circadian Organization of Behavior and Physiology in Drosophila. Annu Rev Physiol *72*, 605-624.

Allada, R., and Chung, B.Y. (2010b). Circadian organization of behavior and physiology in Drosophila. Annu Rev Physiol *72*, 605-624.

Allada, R., White, N.E., So, W.V., Hall, J.C., and Rosbash, M. (1998). A mutant Drosophila homolog of mammalian Clock disrupts circadian rhythms and transcription of period and timeless. Cell *93*, 791-804.

Ambegaokar, S.S., and Jackson, G.R. (2011). Functional genomic screen and network analysis reveal novel modifiers of tauopathy dissociated from tau phosphorylation. Hum Mol Genet *20*, 4947-4977.

Anderson, K.N., Hatfield, C., Kipps, C., Hastings, M., and Hodges, J.R. (2009). Disrupted sleep and circadian patterns in frontotemporal dementia. Eur J Neurol *16*, 317-323.

Anderson, P., and Kedersha, N. (2008). Stress granules: The Tao of RNA triage. Trends Biochem Sci *33*, 141-150.

Andrew, S.E., Goldberg, Y.P., Kremer, B., Telenius, H., Theilmann, J., Adam, S., Starr, E., Squitieri, F., Lin, B., Kalchman, M.A.*, et al.* (1993). The Relationship between Trinucleotide (Cag) Repeat Length and Clinical-Features of Huntington Disease. Am J Hum Genet *53*, 1118-1118.

Antoch, M.P., Gorbacheva, V.Y., Vykhovanets, O., Toshkov, I.A., Kondratov, R.V., Kondratova, A.A., Lee, C., and Nikitin, A.Y. (2008). Disruption of the circadian clock due to the Clock mutation has discrete effects on aging and carcinogenesis. Cell Cycle *7*, 1197-1204.

Arai, T., Hasegawa, M., Akiyama, H., Ikeda, K., Nonaka, T., Mori, H., Mann, D., Tsuchiya, K., Yoshida, M., Hashizume, Y.*, et al.* (2006). TDP-43 is a component of ubiquitin-positive tau-negative inclusions in frontotemporal lobar degeneration and amyotrophic lateral sclerosis. Biochem Biophys Res Commun *351*, 602-611.

Arble, D.M., Bass, J., Laposky, A.D., Vitaterna, M.H., and Turek, F.W. (2009). Circadian Timing of Food Intake Contributes to Weight Gain. Obesity *17*, 2100-2102.

Arnulf, I., Nielsen, J., Lohmann, E., Schieffer, J., Wild, E., Jennum, P., Konofal, E., Walker, M., Oudiette, D., Tabrizi, S.*, et al.* (2008). Rapid eye movement sleep disturbances in Huntington disease. Arch Neurol-Chicago *65*, 482-488.

Arrasate, M., Mitra, S., Schweitzer, E.S., Segal, M.R., and Finkbeiner, S. (2004). Inclusion body formation reduces levels of mutant huntingtin and the risk of neuronal death. Nature *431*, 805-810.

Ash, P.E.A., Vanderweyde, T.E., Youmans, K.L., Apicco, D.J., and Wolozin, B. (2014). Pathological stress granules in Alzheimer's disease. Brain Res *1584*, 52-58.

Ashley, C.T., Jr., and Warren, S.T. (1995). Trinucleotide repeat expansion and human disease. Annu Rev Genet *29*, 703-728.

Ashmore, L.J., and Sehgal, A. (2003). A fly's eye view of circadian entrainment. J Biol Rhythms *18*, 206-216.

Asken, B.M., Sullan, M.J., Snyder, A.R., Houck, Z.M., Bryant, V.E., Hizel, L.P., McLaren, M.E., Dede, D.E., Jaffee, M.S., DeKosky, S.T.*, et al.* (2016). Factors Influencing Clinical Correlates of Chronic Traumatic Encephalopathy (CTE): a Review. Neuropsychol Rev *26*, 340-363.

Aso, Y., Grubel, K., Busch, S., Friedrich, A.B., Siwanowicz, I., and Tanimoto, H. (2009). The Mushroom Body of Adult Drosophila Characterized by GAL4 Drivers. J Neurogenet *23*, 156-U129.

Atwal, R.S., Xia, J., Pinchev, D., Taylor, J., Epand, R.M., and Truant, R. (2007). Huntingtin has a membrane association signal that can modulate huntingtin aggregation, nuclear entry and toxicity. Hum Mol Genet *16*, 2600-2615.

Auburger, G., Sen, N.E., Meierhofer, D., Basak, A.N., and Gitler, A.D. (2017). Efficient Prevention of Neurodegenerative Diseases by Depletion of Starvation Response Factor Ataxin-2. Trends Neurosci *40*, 507-516.

Auluck, P.K., Chan, H.Y., Trojanowski, J.Q., Lee, V.M., and Bonini, N.M. (2002). Chaperone suppression of alpha-synuclein toxicity in a Drosophila model for Parkinson's disease. Science *295*, 865-868.

Aziz, N.A., Pijl, H., Frolich, M., Schroder-van der Elst, J.P., van der Bent, C., Roelfsema, F., and Roos, R.A.C. (2009). Delayed onset of the diurnal melatonin rise in patients with Huntington's disease. J Neurol *256*, 1961-1965.

Bae, B.I., Xu, H., Igarashi, S., Fujimuro, M., Agrawal, N., Taya, Y., Hayward, S.D., Moran, T.H., Montell, C., Ross, C.A.*, et al.* (2005). p53 mediates cellular dysfunction and behavioral abnormalities in Huntington's disease. Neuron *47*, 29-41.

Baindur-Hudson, S., Edkins, A.L., and Blatch, G.L. (2015). Hsp70/Hsp90 organising protein (hop): beyond interactions with chaperones and prion proteins. Subcell Biochem *78*, 69-90.

Bakthavachalu, B., Huelsmeier, J., Sudhakaran, I.P., Hillebrand, J., Singh, A., Petrauskas, A., Thiagarajan, D., Sankaranarayanan, M., Mizoue, L., Anderson, E.N.*, et al.* (2018). RNP-Granule Assembly via Ataxin-2 Disordered Domains Is Required for Long-Term Memory and Neurodegeneration. Neuron *98*, 754-+.

Baldo, B., Weiss, A., Parker, C.N., Bibel, M., Paganetti, P., and Kaupmann, K. (2012). A Screen for Enhancers of Clearance Identifies Huntingtin as a Heat Shock Protein 90 (Hsp90) Client Protein. Journal of Biological Chemistry *287*, 1406-1414.

Banez-Coronel, M., Ayhan, F., Tarabochia, A.D., Zu, T., Perez, B.A., Tusi, S.K., Pletnikova, O., Borchelt, D.R., Ross, C.A., Margolis, R.L.*, et al.* (2015). RAN Translation in Huntington Disease. Neuron *88*, 667-677.

Bardai, F.H., Verma, P., Smith, C., Rawat, V., Wang, L.L., and D'Mello, S.R. (2013). Disassociation of Histone Deacetylase-3 from Normal Huntingtin Underlies Mutant Huntingtin Neurotoxicity. Journal of Neuroscience *33*, 11833-11838.

Barmada, S.J., Skibinski, G., Korb, E., Rao, E.J., Wu, J.Y., and Finkbeiner, S. (2010). Cytoplasmic Mislocalization of TDP-43 Is Toxic to Neurons and Enhanced by a Mutation Associated with Familial Amyotrophic Lateral Sclerosis. Journal of Neuroscience *30*, 639-649.

Bates, G.P., Dorsey, R., Gusella, J.F., Hayden, M.R., Kay, C., Leavitt, B.R., Nance, M., Ross, C.A., Scahill, R.I., Wetzel, R.*, et al.* (2015). Huntington disease. Nat Rev Dis Primers *1*.

Becher, M.W., Kotzuk, J.A., Sharp, A.H., Davies, S.W., Bates, G.P., Price, D.L., and Ross, C.A. (1998). Intranuclear neuronal inclusions in Huntington's disease and dentatorubral and pallidoluysian atrophy: Correlation between the density of inclusions and IT15 CAG triplet repeat length. Neurobiol Dis *4*, 387-397.

Becker, L.A., Huang, B., Bieri, G., Ma, R., Knowles, D.A., Jafar-Nejad, P., Messing, J., Kim, H.J., Soriano, A., Auburger, G.*, et al.* (2017). Therapeutic reduction of ataxin-2 extends lifespan and reduces pathology in TDP-43 mice. Nature *544*, 367-+.

Benedetti, F., Dallaspezia, S., Colombo, C., Pirovano, A., Marino, E., and Smeraldi, E. (2008). A length polymorphism in the circadian clock gene Per3 influences age at onset of bipolar disorder. Neurosci Lett *445*, 184-187.

Benilova, I., Karran, E., and De Strooper, B. (2012). The toxic Abeta oligomer and Alzheimer's disease: an emperor in need of clothes. Nat Neurosci *15*, 349-357.

Benn, C.L., Landles, C., Li, H., Strand, A.D., Woodman, B., Sathasivam, K., Li, S.H., Ghazi-Noori, S., Hockly, E., Faruque, S.M.N.N.*, et al.* (2005). Contribution of nuclear and extranuclear polyQ to neurological phenotypes in mouse models of Huntington's disease. Hum Mol Genet *14*, 3065-3078.

Bersuker, K., Hipp, M.S., Calamini, B., Morimoto, R.I., and Kopito, R.R. (2013). Heat Shock Response Activation Exacerbates Inclusion Body Formation in a Cellular Model of Huntington Disease. Journal of Biological Chemistry *288*, 23633-23638.

Bier, E. (2005). Drosophila, the golden bug, emerges as a tool for human genetics. Nat Rev Genet *6*, 9-23.

Bilen, J., and Bonini, N.M. (2005a). Drosophila as a model for human neurodegenerative disease. Annu Rev Genet *39*, 153-171.

Bilen, J., and Bonini, N.M. (2005b). Drosophila as a model for human neurodegenerative disease. Annu Rev Genet *39*, 153-171.

Bloom, G.S. (2014). Amyloid-beta and Tau The Trigger and Bullet in Alzheimer Disease Pathogenesis. Jama Neurol *71*, 505-508.

Bordet, R., Devos, D., Brique, S., Touitou, Y., Guieu, J.D., Libersa, C., and Destee, A. (2003). Study of circadian melatonin secretion pattern at different stages of Parkinson's disease. Clin Neuropharmacol *26*, 65-72.

Bosco, D.A., Lemay, N., Ko, H.K., Zhou, H.R., Burke, C., Kwiatkowski, T.J., Sapp, P., McKenna-Yasek, D., Brown, R.H., and Hayward, L.J. (2010). Mutant FUS proteins that cause amyotrophic lateral sclerosis incorporate into stress granules. Hum Mol Genet *19*, 4160-4175.

Botta, R., Doniparthi, S., Sasidharan, A., Yadav, R., Pal, P., Jain, S., and Kutty, B.M. (2016). Assessment of sleep spindle density among genetically positive spinocerebellar ataxias type 1, 2 and 3 patients: A comparative study. Movement Disord *31*, S98-S98.

Bray, N.L., Pimentel, H., Melsted, P., and Pachter, L. (2016a). Near-optimal probabilistic RNA-seq quantification. Nat Biotechnol *34*, 525-527.

Bray, N.L., Pimentel, H., Melsted, P., and Pachter, L. (2016b). Near-optimal probabilistic RNA-seq quantification (vol 34, pg 525, 2016). Nat Biotechnol *34*, 888-888.

Breen, D.P., Vuono, R., Nawarathna, U., Fisher, K., Shneerson, J.M., Reddy, A.B., and Barker, R.A. (2014). Sleep and Circadian Rhythm Regulation in Early Parkinson Disease. Jama Neurol *71*, 589-595.

Brehme, M., Voisine, C., Rolland, T., Wachi, S., Soper, J.H., Zhu, Y.T., Orton, K., Villella, A., Garza, D., Vidal, M.*, et al.* (2014). A Chaperome Subnetwork Safeguards Proteostasis in Aging and Neurodegenerative Disease. Cell Rep *9*, 1135-1150.

Brignull, H.R., Morley, J.F., and Morimoto, R.I. (2007). The stress of misfolded proteins: C-elegans models for neurodegenerative disease and aging. Molecular Aspects of the Stress Response: Chaperones, Membranes and Networks *594*, 167-189.

Brustovetsky, N. (2016). Mutant Huntingtin and Elusive Defects in Oxidative Metabolism and Mitochondrial Calcium Handling. Mol Neurobiol *53*, 2944-2953.

Buchan, J.R., Kolaitis, R.M., Taylor, J.P., and Parker, R. (2013). Eukaryotic Stress Granules Are Cleared by Autophagy and Cdc48/VCP Function. Cell *153*, 1461-1474.

Burr, A.A., Tsou, W.L., Ristic, G., and Todi, S.V. (2014). Using Membrane-Targeted Green Fluorescent Protein To Monitor Neurotoxic Protein-Dependent Degeneration of Drosophila Eyes. J Neurosci Res *92*, 1100-1109.

Busino, L., Bassermann, F., Maiolica, A., Lee, C., Nolan, P.M., Godinho, S.I.H., Draetta, G.F., and Pagano, M. (2007). SCFFbxl3 controls the oscillation of the circadian clock by directing the degradation of cryptochrome proteins. Science *316*, 900-904.

Butland, S.L., Sanders, S.S., Schmidt, M.E., Riechers, S.P., Lin, D.T.S., Martin, D.D.O., Vaid, K., Graham, R.K., Singaraja, R.R., Wanker, E.E.*, et al.* (2014). The palmitoyl acyltransferase HIP14 shares a high proportion of interactors with huntingtin: implications for a role in the pathogenesis of Huntington's disease. Hum Mol Genet *23*, 4142-4160.

Butzlaff, M., Hannan, S.B., Karsten, P., Lenz, S., Ng, J., Vossfeldt, H., Prussing, K., Pflanz, R., Schulz, J.B., Rasse, T.*, et al.* (2015). Impaired retrograde transport by the Dynein/Dynactin complex contributes to Tau-induced toxicity. Hum Mol Genet *24*, 3623-3637.

Cai, Y., Liu, S., Sothern, R.B., Xu, S., and Chan, P. (2010). Expression of clock genes Per1 and Bmal1 in total leukocytes in health and Parkinson's disease. Eur J Neurol *17*, 550-554.

Carmine-Simmen, K., Proctor, T., Tschape, J., Poeck, B., Triphan, T., Strauss, R., and Kretzschmar, D. (2009). Neurotoxic effects induced by the Drosophila amyloid-beta peptide suggest a conserved toxic function. Neurobiol Dis *33*, 274-281.

Caviston, J.P., and Holzbaur, E.L.F. (2009). Huntingtin as an essential integrator of intracellular vesicular trafficking. Trends Cell Biol *19*, 147-155.

Caviston, J.P., Ross, J.L., Antony, S.M., Tokito, M., and Holzbaur, E.L. (2007). Huntingtin facilitates dynein/dynactin-mediated vesicle transport. Proc Natl Acad Sci U S A *104*, 10045-10050.

Ceriani, M.F., Darlington, T.K., Staknis, D., Mas, P., Petti, A.A., Weitz, C.J., and Kay, S.A. (1999). Light-dependent sequestration of TIMELESS by CRYPTOCHROME. Science *285*, 553-556.

Cermakian, N., Lamont, E.W., Boudreau, P., and Boivin, D.B. (2011). Circadian Clock Gene Expression in Brain Regions of Alzheimer's Disease Patients and Control Subjects. J Biol Rhythms *26*, 160-170.

Chai, Y.H., Shao, J.Q., Miller, V.M., Williams, A., and Paulson, H.L. (2002). Live-cell imaging reveals divergent intracellular dynamics of polyglutamine disease proteins and supports a sequestration model of pathogenesis. Proc Natl Acad Sci U S A *99*, 9310-9315.

Chan, H.Y.E., Warrick, J.M., Gray-Board, G.L., Paulson, H.L., and Bonini, N.M. (2000). Mechanisms of chaperone suppression of polyglutamine disease: selectivity, synergy and medullation of protein solubility in Drosophila. Hum Mol Genet *9*, 2811-2820.

Chen, K.F., Possidente, B., Lomas, D.A., and Crowther, D.C. (2014). The central molecular clock is robust in the face of behavioural arrhythmia in a Drosophila model of Alzheimer's disease. Dis Model Mech *7*, 445-458.

Chen, S., Sayana, P., Zhang, X.J., and Le, W.D. (2013). Genetics of amyotrophic lateral sclerosis: an update. Mol Neurodegener *8*.

Chen, Y.B., Yang, M.X., Deng, J.W., Chen, X.P., Ye, Y., Zhu, L., Liu, J.H., Ye, H.H., Shen, Y., Li, Y.*, et al.* (2011). Expression of human FUS protein in Drosophila leads to progressive neurodegeneration. Protein Cell *2*, 477-486.

Chi, N.F., Shiao, G.M., Ku, H.L., and Soong, B.W. (2013). Sleep disruption in spinocerebellar ataxia type 3: A genetic and polysomnographic study. J Chin Med Assoc *76*, 25-30.

Chiang, H.C., Wang, L., Xie, Z.L., Yau, A., and Zhong, Y. (2010). PI3 kinase signaling is involved in A beta-induced memory loss in Drosophila. Proc Natl Acad Sci U S A *107*, 7060-7065.

Chiu, J.C., Ko, H.W., and Edery, I. (2011). NEMO/NLK Phosphorylates PERIOD to Initiate a Time-Delay Phosphorylation Circuit that Sets Circadian Clock Speed. Cell *145*, 357-370.

Chongtham, A., and Agrawal, N. (2016). Curcumin modulates cell death and is protective in Huntington's disease model. Sci Rep-Uk *6*.

Chung, B.Y., Kilman, V.L., Keath, J.R., Pitman, J.L., and Allada, R. (2009). The GABA(A) Receptor RDL Acts in Peptidergic PDF Neurons to Promote Sleep in Drosophila. Current Biology *19*, 386-390.

Clark, I.E., Dodson, M.W., Jiang, C.G., Cao, J.H., Huh, J.R., Seol, J.H., Yoo, S.J., Hay, B.A., and Guo, M. (2006). Drosophila pink1 is required for mitochondrial function and interacts genetically with parkin. Nature *441*, 1162-1166.

Collins, B., Kane, E.A., Reeves, D.C., Akabas, M.H., and Blau, J. (2012). Balance of Activity between LN(v)s and Glutamatergic Dorsal Clock Neurons Promotes Robust Circadian Rhythms in Drosophila (vol 74, pg 706, 2012). Neuron *74*, 1138-1138.

Colombrita, C., Zennaro, E., Fallini, C., Weber, M., Sommacal, A., Buratti, E., Silani, V., and Ratti, A. (2009). TDP-43 is recruited to stress granules in conditions of oxidative insult. J Neurochem *111*, 1051-1061.

Courtet, P., and Olie, E. (2012). Circadian dimension and severity of depression. Eur Neuropsychopharmacol *22 Suppl 3*, S476-481.

Crowther, D.C., Kinghorn, K.J., Miranda, E., Page, R., Curry, J.A., Duthie, F.A.I., Gubb, D.C., and Lomas, D.A. (2005). Intraneuronal A beta, non-amyloid aggregates and neurodegeneration in a Drosophila model of Alzheimer's disease. Neuroscience *132*, 123-135.

Cuturic, M., Abramson, R.K., Vallini, D., Frank, E.M., and Shamsnia, M. (2009). Sleep Patterns in Patients With Huntington's Disease and Their Unaffected First-Degree Relatives: A Brief Report. Behav Sleep Med *7*, 245-254.

Cyran, S.A., Buchsbaum, A.M., Reddy, K.L., Lin, M.C., Glossop, N.R., Hardin, P.E., Young, M.W., Storti, R.V., and Blau, J. (2003). vrille, Pdp1, and dClock form a second feedback loop in the Drosophila circadian clock. Cell *112*, 329-341.

Davies, S.W., Turmaine, M., Cozens, B.A., DiFiglia, M., Sharp, A.H., Ross, C.A., Scherzinger, E., Wanker, E.E., Mangiarini, L., and Bates, G.P. (1997). Formation of neuronal intranuclear inclusions underlies the neurological dysfunction in mice transgenic for the HD mutation. Cell *90*, 537-548.

Davis, S., Mirick, D., and Stevens, R. (2002). Re: Night shift work, light at night, and risk of breast cancer - Responses. J Natl Cancer I *94*, 533-533.

De Mario, A., Scarlatti, C., Costiniti, V., Primerano, S., Lopreiato, R., Cali, T., Brini, M., Giacomello, M., and Carafoli, E. (2016). Calcium Handling by Endoplasmic Reticulum and Mitochondria in a Cell Model of Huntington's Disease. PLoS Curr *8*.

de Mezer, M., Wojciechowska, M., Napierala, M., Sobczak, K., and Krzyzosiak, W.J. (2011). Mutant CAG repeats of Huntingtin transcript fold into hairpins, form nuclear foci and are targets for RNA interference. Nucleic Acids Res *39*, 3852-3863.

DeJesus-Hernandez, M., Mackenzie, I.R., Boeve, B.F., Boxer, A.L., Baker, M., Rutherford, N.J., Nicholson, A.M., Finch, N.A., Flynn, H., Adamson, J.*, et al.* (2011). Expanded GGGGCC Hexanucleotide Repeat in Noncoding Region of C9ORF72 Causes Chromosome 9p-Linked FTD and ALS. Neuron *72*, 245-256.

Diago, E.B., Perez, J.P., Lasaosa, S.S., Alebesque, A.V., Horta, S.M., Kulisevsky, J., and del Val, J.L. (2017). Circadian rhythm and autonomic dysfunction in presymptomatic and early Huntington's disease. Parkinsonism Relat D *44*, 95-100.

DiFiglia, M., Sapp, E., Chase, K.O., Davies, S.W., Bates, G.P., Vonsattel, J.P., and Aronin, N. (1997). Aggregation of huntingtin in neuronal intranuclear inclusions and dystrophic neurites in brain. Science *277*, 1990-1993.

Dodson, M.W., and Guo, M. (2007). Pink1, Parkin, DJ-1 and mitochondrial dysfunction in Parkinson's disease. Curr Opin Neurobiol *17*, 331-337.

Doi, H., Koyano, S., Suzuki, Y., Nukina, N., and Kuroiwa, Y. (2010). The RNA-binding protein FUS/TLS is a common aggregate-interacting protein in polyglutamine diseases. Neurosci Res *66*, 131-133.

Doi, H., Okamura, K., Bauer, P.O., Furukawa, Y., Shimizu, H., Kurosawa, M., Machida, Y., Miyazaki, H., Mitsui, K., Kuroiwa, Y.*, et al.* (2008). RNA-binding protein TLS is a major nuclear aggregate-interacting protein in huntingtin exon 1 with expanded polyglutamine-expressing cells. Journal of Biological Chemistry *283*, 6489-6500.

Doumanis, J., Wada, K., Kino, Y., Moore, A.W., and Nukina, N. (2009). RNAi screening in Drosophila cells identifies new modifiers of mutant huntingtin aggregation. PLoS One *4*, e7275.

Dubowy, C., and Sehgal, A. (2017). Circadian Rhythms and Sleep in Drosophila melanogaster. Genetics *205*, 1373-1397.

Dudek, M., Gossan, N., Yang, N., Im, H.J., Ruckshanthi, J.P.D., Yoshitane, H., Li, X., Jin, D., Wang, P., Boudiffa, M.*, et al.* (2016). The chondrocyte clock gene Bmal1 controls cartilage homeostasis and integrity. J Clin Invest *126*, 365-376.

Durr, A. (2010). Autosomal dominant cerebellar ataxias: polyglutamine expansions and beyond. Lancet Neurol *9*, 885-894.

Ehrnhoefer, D.E., Duennwald, M., Markovic, P., Wacker, J.L., Engemann, S., Roark, M., Legleiter, J., Marsh, J.L., Thompson, L.M., Lindquist, S.*, et al.* (2006). Green tea (-)-epigallocatechin-gallate modulates early events in huntingtin misfolding and reduces toxicity in Huntington's disease models. Hum Mol Genet *15*, 2743-2751.

Elden, A.C., Kim, H.J., Hart, M.P., Chen-Plotkin, A.S., Johnson, B.S., Fang, X.D., Armakola, M., Geser, F., Greene, R., Lu, M.M., *et al.* (2010). Ataxin-2 intermediate-length polyglutamine expansions are associated with increased risk for ALS. Nature *466*, 1069-U1077.

Emery, P., So, W.V., Kaneko, M., Hall, J.C., and Rosbash, M. (1998). CRY, a Drosophila clock and light-regulated cryptochrome, is a major contributor to circadian rhythm resetting and photosensitivity. Cell *95*, 669-679.

Emery, P., Stanewsky, R., Helfrich-Forster, C., Emery-Le, M., Hall, J.C., and Rosbash, M. (2000). Drosophila CRY is a deep brain circadian photoreceptor. Neuron *26*, 493-504.

Fahrenkrug, J., Popovic, N., Georg, B., Brundin, P., and Hannibal, J. (2007). Decreased VIP and VPAC2 receptor expression in the biological clock of the R6/2 Huntington's disease mouse. J Mol Neurosci *31*, 139-148.

Fan, H.C., Ho, L.I., Chi, C.S., Chen, S.J., Peng, G.S., Chan, T.M., Lin, S.Z., and Harn, H.J. (2014). Polyglutamine (PolyQ) Diseases: Genetics to Treatments. Cell Transplant *23*, 441-458.

Fang, Y.S., Sathyanarayanan, S., and Sehgal, A. (2007). Post-translational regulation of the Drosophila circadian clock requires protein phosphatase 1 (PP1). Genes Dev *21*, 1506-1518.

Feany, M.B., and Bender, W.W. (2000). A Drosophila model of Parkinson's disease. Nature *404*, 394-398.

Fernandez, M.P., Berni, J., and Ceriani, M.F. (2008). Circadian remodeling of neuronal circuits involved in rhythmic behavior. PLoS Biol *6*, 518-524.

Fernandez-Hernandez, I., Scheenaard, E., Pollarolo, G., and Gonzalez, C. (2016). The translational relevance of Drosophila in drug discovery. Embo Rep *17*, 471-472.

Ferrante, R.J., Kubilus, J.K., Lee, J., Ryu, H., Beesen, A., Zucker, B., Smith, K., Kowall, N.W., Ratan, R.R., Luthi-Carter, R., *et al.* (2003). Histone deacetylase inhibition by sodium butyrate chemotherapy ameliorates the neurodegenerative phenotype in Huntington's disease mice. Journal of Neuroscience *23*, 9418-9427.

Ferreira, J.J., Desboeuf, K., Galitzky, M., Thalamas, C., Brefel-Courbon, C., Fabre, N., Senard, J.M., Montastruc, J.L., Sampaio, C., and Rascol, O. (2006). Sleep disruption, daytime somnolence and 'sleep attacks' in Parkinson's disease: a clinical survey in PD patients and age-matched healthy volunteers. Eur J Neurol *13*, 209-214.

Finelli, A., Kelkar, A., Song, H.J., Yang, H.D., and Konsolaki, M. (2004). A model for studying Alzheimer's A beta 42-induced toxicity in Drosophila melanogaster. Mol Cell Neurosci *26*, 365-375.

Fisher, S.P., Black, S.W., Schwartz, M.D., Wilk, A.J., Chen, T.M., Lincoln, W.U., Liu, H.W., Kilduff, T.S., and Morairty, S.R. (2013). Longitudinal analysis of the electroencephalogram and sleep phenotype in the R6/2 mouse model of Huntington's disease. Brain *136*, 2159-2172.

Fittschen, M., Lastres-Becker, I., Halbach, M.V., Damrath, E., Gispert, S., Azizov, M., Walter, M., Muller, S., and Auburger, G. (2015). Genetic ablation of ataxin-2 increases several global translation factors in their transcript abundance but decreases translation rate. Neurogenetics *16*, 181-192.

Flourakis, M., Kula-Eversole, E., Hutchison, A.L., Han, T.H., Aranda, K., Moose, D.L., White, K.P., Dinner, A.R., Lear, B.C., Ren, D.J., *et al.* (2015). A Conserved Bicycle Model for Circadian Clock Control of Membrane Excitability. Cell *162*, 836-848.

Fonken, L.K., Finy, M.S., Walton, J.C., Weil, Z.M., Workman, J.L., Ross, J., and Nelson, R.J. (2009). Influence of light at night on murine anxiety- and depressive-like responses. Behav Brain Res *205*, 349-354.

Fonken, L.K., Frank, M.G., Kitt, M.M., Barrientos, R.M., Watkins, L.R., and Maier, S.F. (2015). Microglia inflammatory responses are controlled by an intrinsic circadian clock. Brain Behavior and Immunity *45*, 171-179.

Fossgreen, A., Bruckner, B., Czech, C., Masters, C.L., Beyreuther, K., and Paro, R. (1998). Transgenic Drosophila expressing human amyloid precursor protein show gamma-secretase activity and a blistered-wing phenotype. Proc Natl Acad Sci U S A *95*, 13703-13708.

Fox, R.M., Hanlon, C.D., and Andrew, D.J. (2010). The CrebA/Creb3-like transcription factors are major and direct regulators of secretory capacity. Journal of Cell Biology *191*, 479-492.

Fu, Y., Jones, C.R., Toh, K., Virshup, D., and Ptacek, L.J. (2001). An hPer2 phosphorylation site mutation in familial Advanced Sleep-Phase Syndrome. Am J Hum Genet *69*, 597-597.

Fujikake, N., Nagai, Y., Popiel, H.A., Okamoto, Y., Yamaguchi, M., and Toda, T. (2008). Heat shock transcription factor 1-activating compounds suppress polyglutamine-induced neurodegeneration through induction of multiple molecular chaperones. Journal of Biological Chemistry *283*, 26188-26197.

Fuller, J.P., Stavenhagen, J.B., Christensen, S., Kartberg, F., Glennie, M.J., and Teeling, J.L. (2015). Comparing the efficacy and neuroinflammatory potential of three anti-abeta antibodies. Acta Neuropathol *130*, 699-711.

Furukawa, Y., Kaneko, K., Matsumoto, G., Kurosawa, M., and Nukina, N. (2009). Cross-Seeding Fibrillation of Q/N-Rich Proteins Offers New Pathomechanism of Polyglutamine Diseases. Journal of Neuroscience *29*, 5153-5162.

Ga, L., Cookson, M.R., Petrucelli, L., and La Spade, A.R. (2018). Converging pathways in neurodegeneration, from genetics to mechanisms. Nat Neurosci *21*, 1300-1309.

Gafni, J., Hermel, E., Young, J.E., Wellington, C.L., Hayden, M.R., and Ellerby, L.M. (2004). Inhibition of calpain cleavage of huntingtin reduces toxicity - Accumulation of calpain/caspase fragments in the nucleus. Journal of Biological Chemistry *279*, 20211-20220.

Garcia-Arocena, D., and Hagerman, P.J. (2010). Advances in understanding the molecular basis of FXTAS. Hum Mol Genet *19*, R83-R89.

Gekakis, N., Staknis, D., Nguyen, H.B., Davis, F.C., Wilsbacher, L.D., King, D.P., Takahashi, J.S., and Weitz, C.J. (1998). Role of the CLOCK protein in the mammalian circadian mechanism. Science *280*, 1564-1569.

Giacobini, E., and Gold, G. (2013). Alzheimer disease therapy-moving from amyloid-beta to tau. Nat Rev Neurol *9*, 677-686.

Gitcho, M.A., Baloh, R.H., Chakraverty, S., Mayo, K., Norton, J.B., Levitch, D., Hatanpaa, K.J., White, C.L., Bigio, E.H., Caselli, R.*, et al.* (2008). TDP-43 A315T mutation in familial motor neuron disease. Ann Neurol *63*, 535-538.

Giubilei, F., Patacchioli, F.R., Antonini, G., Monti, M.S., Tisei, P., Bastianello, S., Monnazzi, P., and Angelucci, L. (2001). Altered circadian cortisol secretion in Alzheimer's disease: Clinical and neuroradiological aspects. J Neurosci Res *66*, 262-265.

Glossop, N.R., Houl, J.H., Zheng, H., Ng, F.S., Dudek, S.M., and Hardin, P.E. (2003). VRILLE feeds back to control circadian transcription of Clock in the Drosophila circadian oscillator. Neuron *37*, 249-261.

Godin, J.D., Colombo, K., Molina-Calavita, M., Keryer, G., Zala, D., Charrin, B.C., Dietrich, P., Volvert, M.L., Guillemot, F., Dragatsis, I.*, et al.* (2010). Huntingtin is required for mitotic spindle orientation and mammalian neurogenesis. Neuron *67*, 392-406.

Gonnissen, H.K., Rutters, F., Mazuy, C., Martens, E.A., Adam, T.C., and Westerterp-Plantenga, M.S. (2012). Effect of a phase advance and phase delay of the 24-h cycle on energy metabolism, appetite, and related hormones. Am J Clin Nutr *96*, 689-697.

Gonzales, E., and Yin, J. (2010). Drosophila Models of Huntington's Disease exhibit sleep abnormalities. PLoS Curr *2*.

Gonzales, E.D., Tanenhaus, A.K., Zhang, J.B., Chaffee, R.P., and Yin, J.C.P. (2016). Early-onset sleep defects in Drosophila models of Huntington's disease reflect alterations of PKA/CREB signaling. Hum Mol Genet *25*, 837-852.

Goodman, A.O.G., and Barker, R.A. (2010). How vital is sleep in Huntington's disease? J Neurol *257*, 882-897.

Goodman, A.O.G., Rogers, L., Pilsworth, S., McAllister, C.J., Shneerson, J.M., Morton, A.J., and Barker, R.A. (2011). Asymptomatic Sleep Abnormalities Are a Common Early Feature in Patients with Huntington's Disease. Curr Neurol Neurosci *11*, 211-217.

Greeve, I., Kretzschmar, D., Tschape, J.A., Beyn, A., Brellinger, C., Schweizer, M., Nitsch, R.M., and Reifegerste, R. (2004). Age-dependent neurodegeneration and Alzheimer-amyloid plaque formation in transgenic Drosophila. Journal of Neuroscience *24*, 3899-3906.

Griffin, E.A., Staknis, D., and Weitz, C.J. (1999). Light-independent role of CRY1 and CRY2 in the mammalian circadian clock. Science *286*, 768-771.

Grima, B., Chelot, E., Xia, R.H., and Rouyer, F. (2004). Morning and evening peaks of activity rely on different clock neurons of the Drosophila brain. Nature *431*, 869-873.

Guillaumond, F., Dardente, H., Giguere, V., and Cermakian, N. (2005). Differential control of Bmal1 circadian transcription by REV-ERB and ROR nuclear receptors. J Biol Rhythms *20*, 391-403.

Gunawardena, S., Her, L.S., Brusch, R.G., Laymon, R.A., Niesman, I.R., Gordesky-Gold, B., Sintasath, L., Bonini, N.M., and Goldstein, L.S. (2003). Disruption of axonal transport by loss of huntingtin or expression of pathogenic polyQ proteins in Drosophila. Neuron *40*, 25-40.

Hamblencoyle, M., Konopka, R.J., Zwiebel, L.J., Colot, H.V., Dowse, H.B., Rosbash, M., and Hall, J.C. (1989). A New Mutation at the Period Locus of Drosophila-Melanogaster with Some Novel Effects on Circadian-Rhythms. J Neurogenet *5*, 229-256.

Hanford, N., and Figueiro, M. (2013). Light Therapy and Alzheimer's Disease and Related Dementia: Past, Present, and Future. J Alzheimers Dis *33*, 913-922.

Hardiman, O. (2011). Management of respiratory symptoms in ALS. J Neurol *258*, 359-365.

Hardin, P.E. (2011). Molecular genetic analysis of circadian timekeeping in Drosophila. Adv Genet *74*, 141-173.

Harper, D.G., Volicer, L., Stopa, E.G., McKee, A.C., Nitta, M., and Satlin, A. (2005). Disturbance of endogenous circadian rhythm in aging and Alzheimer disease. Am J Geriat Psychiat *13*, 359-368.

Hay, D.G., Sathasivam, K., Tobaben, S., Stahl, B., Marber, M., Mestril, R., Mahal, A., Smith, D.L., Woodman, B., and Bates, G.P. (2004). Progressive decrease in chaperone protein levels in a mouse model of Huntington's disease and induction of stress proteins as a therapeutic approach. Hum Mol Genet *13*, 1389-1405.

He, W.T., Xue, W., Gao, Y.G., Hong, J.Y., Yue, H.W., Jiang, L.L., and Hu, H.Y. (2017). HSP90 recognizes the N-terminus of huntingtin involved in regulation of huntingtin aggregation by USP19. Sci Rep-Uk *7*.

He, W.T., Zheng, X.M., Zhang, Y.H., Gao, Y.G., Song, A.X., van der Goot, F.G., and Hu, H.Y. (2016). Cytoplasmic Ubiquitin-Specific Protease 19 (USP19) Modulates Aggregation of Polyglutamine-Expanded Ataxin-3 and Huntingtin through the HSP90 Chaperone. PLoS One *11*.

Helfrich-Forster, C. (1998). Robust circadian rhythmicity of Drosophila melanogaster requires the presence of lateral neurons: a brain-behavioral study of disconnected mutants. J Comp Physiol A *182*, 435-453.

Helfrich-Forster, C., Shafer, O.T., Wulbeck, C., Grieshaber, E., Rieger, D., and Taghert, P. (2007). Development and morphology of the clock-gene-expressing lateral neurons of Drosophila melanogaster. Journal of Comparative Neurology *500*, 47-70.

Hetz, C., Chevet, E., and Oakes, S.A. (2015). Proteostasis control by the unfolded protein response (vol 17, pg 829, 2015). Nat Cell Biol *17*, 1088-1088.

Hilditch-Maguire, P., Trettel, F., Passani, L.A., Auerbach, A., Persichetti, F., and MacDonald, M.E. (2000). Huntingtin: an iron-regulated protein essential for normal nuclear and perinuclear organelles. Hum Mol Genet *9*, 2789-2797.

Hockly, E., Richon, V.M., Woodman, B., Smith, D.L., Zhou, X.B., Rosa, E., Sathasivam, K., Ghazi-Noori, S., Mahal, A., Lowden, P.A.S*., et al.* (2003). Suberoylanilide hydroxamic acid, a histone deacetylase inhibitor, ameliorates motor deficits in a mouse model of Huntington's disease. Proc Natl Acad Sci U S A *100*, 2041-2046.

Hsu, R.J., Hsiao, K.M., Lin, M.J., Li, C.Y., Wang, L.C., Chen, L.K., and Pan, H.C. (2011). Long Tract of Untranslated CAG Repeats Is Deleterious in Transgenic Mice. PLoS One *6*.

Huang, K., Sanders, S.S., Kang, R., Carroll, J.B., Sutton, L., Wan, J., Singaraja, R., Young, F.B., Liu, L., El-Husseini, A.*, et al.* (2011). Wild-type HTT modulates the enzymatic activity of the neuronal palmitoyl transferase HIP14. Hum Mol Genet *20*, 3356-3365.

Huang, K., Yanai, A., Kang, R., Arstikaitis, P., Singaraja, R.R., Metzler, M., Mullard, A., Haigh, B., Gauthier-Campbell, C., Gutekunst, C.A.*, et al.* (2004). Huntingtin-interacting protein HIP14 is a palmitoyl transferase involved in palmitoylation and trafficking of multiple neuronal proteins. Neuron *44*, 977-986.

Huang, Z.L., Liu, Q., Peng, Y., Dai, J.Y., Xie, Y.N., Chen, W.N., Long, S.M., Pei, Z., Su, H.X., and Yao, X.L. (2018). Circadian Rhythm Dysfunction Accelerates Disease Progression in a Mouse Model With Amyotrophic Lateral Sclerosis. Front Neurol *9*.

Huber, A.L., Papp, S.J., Chan, A.B., Henriksson, E., Jordan, S.D., Kriebs, A., Nguyen, M., Wallace, M., Li, Z.Z., Metallo, C.M.*, et al.* (2016). CRY2 and FBXL3 Cooperatively Degrade c-MYC. Mol Cell *64*, 774-789.

Hunter, A., Bordelon, Y., Cook, I., and Leuchter, A. (2010). QEEG Measures in Huntington's Disease: A Pilot Study. PLoS Curr *2*, RRN1192.

Hutchison, A.L., Allada, R., and Dinner, A.R. (2018). Bootstrapping and Empirical Bayes Methods Improve Rhythm Detection in Sparsely Sampled Data. J Biol Rhythms *33*, 339-349.

Hyun, S., Lee, Y., Hong, S.T., Bang, S., Paik, D., Kang, J.K., Shin, J., Lee, J., Jeon, K., Hwang, S.*, et al.* (2005). Drosophila GPCR Han is a receptor for the circadian clock neuropeptide PDF. Neuron *48*, 267-278.

Ichikawa, Y., Goto, J., Hattori, M., Toyoda, A., Ishii, K., Jeong, S.Y., Hashida, H., Masuda, N., Ogata, K., Kasai, F.*, et al.* (2001). The genomic structure and expression of MJD, the Machado-Joseph disease gene. J Hum Genet *46*, 413-422.

Iijima, K., Liu, H.P., Chiang, A.S., Hearn, S.A., Konsolaki, M., and Zhong, Y. (2004). Dissecting the pathological effects of human A beta 40 and A beta 42 in Drosophila: A potential model for Alzheimer's disease. Neurobiol Aging *25*, S17-S17.

Iijima, M., Nikaido, T., Akiyama, M., Moriya, T., and Shibata, S. (2002). Methamphetamine-induced, suprachiasmatic nucleus-independent circadian rhythms of activity and mPer gene expression in the striatum of the mouse. European Journal of Neuroscience *16*, 921-929.

Ilieva, H., Polymenidou, M., and Cleveland, D.W. (2009). Non-cell autonomous toxicity in neurodegenerative disorders: ALS and beyond. Journal of Cell Biology *187*, 761-772.

Imarisio, S., Carmichael, J., Korolchuk, V., Chen, C.W., Saiki, S., Rose, C., Krishna, G., Davies, J.E., Ttofi, E., Underwood, B.R.*, et al.* (2008). Huntington's disease: from pathology and genetics to potential therapies. Biochemical Journal *412*, 191-209.

Iwasaki, S., Sasaki, H.M., Sakaguchi, Y., Suzuki, T., Tadakuma, H., and Tomari, Y. (2015). Defining fundamental steps in the assembly of the Drosophila RNAi enzyme complex. Nature *521*, 533-U274.

Jackson, G.R., Salecker, I., Dong, X.Z., Yao, X., Arnheim, N., Faber, P.W., MacDonald, M.E., and Zipursky, S.L. (1998). Polyglutamine-expanded human huntingtin transgenes induce degeneration of Drosophila photoreceptor neurons. Neuron *21*, 633-642.

Jackson, G.R., Wiedau-Pazos, M., Sang, T.K., Wagle, N., Brown, C.A., Massachi, S., and Geschwind, D.H. (2002). Human wild-type tau interacts with wingless pathway components and produces neurofibrillary pathology in Drosophila. Neuron *34*, 509-519.

Jackson, W.S. (2014). Selective vulnerability to neurodegenerative disease: the curious case of Prion Protein. Dis Model Mech *7*, 21-29.

Jana, N.R., Tanaka, M., Wang, G., and Nukina, N. (2000a). Polyglutamine length-dependent interaction of Hsp40 and Hsp70 family chaperones with truncated N-terminal huntingtin: their role in suppression of aggregation and cellular toxicity. Hum Mol Genet *9*, 2009-2018.

Jana, N.R., Tanaka, M., Wang, G.H., and Nukina, N. (2000b). Polyglutamine length-dependent interaction of Hsp40 and Hsp70 family chaperones with truncated N-terminal huntingtin: their role in suppression of aggregation and cellular toxicity. Hum Mol Genet *9*, 2009-2018.

Jang, A.R., Moravcevic, K., Saez, L., Young, M.W., and Sehgal, A. (2015). Drosophila TIM Binds Importin alpha 1, and Acts as an Adapter to Transport PER to the Nucleus. PLoS Genet *11*.

Jankovic, J. (2008). Parkinson's disease: clinical features and diagnosis. J Neurol Neurosur Ps *79*, 368-376.

Johnson, J.O., Mandrioli, J., Benatar, M., Abramzon, Y., Van Deerlin, V.M., Trojanowski, J.Q., Gibbs, J.R., Brunetti, M., Gronka, S., Wuu, J.*, et al.* (2011). Exome Sequencing Reveals VCP Mutations as a Cause of Familial ALS (vol 68, pg 857, 2010). Neuron *69*, 397-397.

Joiner, W.J., Crocker, A., White, B.H., and Sehgal, A. (2006). Sleep in Drosophila is regulated by adult mushroom bodies. Nature *441*, 757-760.

Jonas, E.A. (2014). Impaired import: how huntingtin harms. Nat Neurosci *17*, 747-749.

Juenemann, K., Weisse, C., Reichmann, D., Kaether, C., Calkhoven, C.F., and Schilling, G. (2011). Modulation of Mutant Huntingtin N-Terminal Cleavage and Its Effect on Aggregation and Cell Death. Neurotox Res *20*, 120-133.

Kadener, S., Stoleru, D., McDonald, M., Nawathean, P., and Rosbash, M. (2007). Clockwork Orange is a transcriptional repressor and a new Drosophila circadian pacemaker component. Genes Dev *21*, 1675-1686.

Kadener, S., Villella, A., Kula, E., Palm, K., Pyza, E., Botas, J., Hall, J.C., and Rosbash, M. (2006). Neurotoxic protein expression reveals connections between the circadian clock and mating behavior in Drosophila. Proc Natl Acad Sci U S A *103*, 13537-13542.

Kalliolia, E., Silajdzic, E., Nambron, R., Hill, N.R., Doshi, A., Frost, C., Watt, H., Hindmarsh, P., Bjorkqvist, M., and Warner, T.T. (2014). Plasma Melatonin Is Reduced in Huntington's Disease. Movement Disord *29*, 1511-1515.

Kaltenbach, L.S., Romero, E., Becklin, R.R., Chettier, R., Bell, R., Phansalkar, A., Strand, A., Torcassi, C., Savage, J., Hurlburt, A.*, et al.* (2007). Huntingtin interacting proteins are genetic modifiers of neurodegeneration. PLoS Genet *3*, e82.

Kaneko, M., and Hall, J.C. (2000). Neuroanatomy of cells expressing clock genes in Drosophila: Transgenic manipulation of the period and timeless genes to mark the perikarya of circadian pacemaker neurons and their projections. Journal of Comparative Neurology *422*, 66-94.

Kaneko, M., Helfrich-Forster, C., and Hall, J.C. (1997a). Spatial and temporal expression of the period and timeless genes in the developing nervous system of Drosophila: newly identified pacemaker candidates and novel features of clock gene product cycling. J Neurosci *17*, 6745-6760.

Kaneko, M., HelfrichForster, C., and Hall, J.C. (1997b). Spatial and temporal expression of the period and timeless genes in the developing nervous system of Drosophila: Newly identified pacemaker candidates and novel features of clock gene product cycling. Journal of Neuroscience *17*, 6745-6760.

Kantor, S., Szabo, L., Varga, J., Cuesta, M., and Morton, A.J. (2013). Progressive sleep and electroencephalogram changes in mice carrying the Huntington's disease mutation. Brain *136*, 2147-2158.

Kawaguchi, Y., Okamoto, T., Taniwaki, M., Aizawa, M., Inoue, M., Katayama, S., Kawakami, H., Nakamura, S., Nishimura, M., Akiguchi, I.*, et al.* (1994). Cag Expansions in a Novel Gene for Machado-Joseph Disease at Chromosome 14q32.1. Nat Genet *8*, 221-228.

Kearse, M.G., Green, K.M., Krans, A., Rodriguez, C.M., Linsalata, A.E., Goldstrohm, A.C., and Todd, P.K. (2016). CGG Repeat-Associated Non-AUG Translation Utilizes a Cap-Dependent Scanning Mechanism of Initiation to Produce Toxic Proteins. Mol Cell *62*, 314-322.

Khaskheli, M.N., Baloch, S., Sheeba, A., Baloch, S., Khan, F., and Ansari, M.R. (2017). Acute renal morbidities with obstetrical emergencies: An important women health issue. Pak J Med Sci *33*, 594-598.

Kim, E.Y., and Edery, I. (2006). Balance between DBT/CKI epsilon kinase and protein phosphatase activities regulate phosphorylation and stability of Drosophila CLOCK protein. Proc Natl Acad Sci U S A *103*, 6178-6183.

Kim, E.Y., Ko, H.W., Yu, W.J., Hardin, P.E., and Edery, I. (2007). A DOUBLETIME kinase binding domain on the Drosophila PERIOD protein is essential for its hyperphosphorylation, transcriptional repression, and circadian clock function. Mol Cell Biol *27*, 5014-5028.

Kim, H.J., Raphael, A.R., LaDow, E.S., McGurk, L., Weber, R.A., Trojanowski, J.Q., Lee, V.M., Finkbeiner, S., Gitler, A.D., and Bonini, N.M. (2014). Therapeutic modulation of eIF2alpha phosphorylation rescues TDP-43 toxicity in amyotrophic lateral sclerosis disease models. Nat Genet *46*, 152-160.

Kim, M., Subramanian, M., Cho, Y.H., Kim, G.H., Lee, E., and Park, J.J. (2018). Short-term exposure to dim light at night disrupts rhythmic behaviors and causes neurodegeneration in fly models of tauopathy and Alzheimer's disease. Biochem Biophys Res Commun *495*, 1722-1729.

Kloss, B., Price, J.L., Saez, L., Blau, J., Rothenfluh, A., Wesley, C.S., and Young, M.W. (1998). The Drosophila clock gene double-time encodes a protein closely related to human casein kinase I epsilon. Cell *94*, 97-107.

Kloss, B., Rothenfluh, A., Young, M.W., and Saez, L. (2001). Phosphorylation of PERIOD is influenced by cycling physical associations of DOUBLE-TIME, PERIOD, and TIMELESS in the Drosophila clock. Neuron *30*, 699-706.

Ko, H.W., Jiang, J., and Edery, I. (2002). Role for Slimb in the degradation of Drosophila Period protein phosphorylated by Doubletime. Nature *420*, 673-678.

Kojima, S., Shingle, D.L., and Green, C.B. (2011). Post-transcriptional control of circadian rhythms. J Cell Sci *124*, 311-320.

Kondratov, R.V., Kondratova, A.A., Gorbacheva, V.Y., Vykhovanets, O.V., and Antoch, M.P. (2006). Early aging and age-related pathologies in mice deficient in BMAL1, the core component of the circadian clock. Genes Dev *20*, 1868-1873.

Konopka, R.J., and Benzer, S. (1971). Clock Mutants of Drosophila-Melanogaster. Proc Natl Acad Sci U S A *68*, 2112-&.

Koshy, B.T., and Zoghbi, H.Y. (1997). The CAG/polyglutamine tract diseases: Gene products and molecular pathogenesis. Brain Pathol *7*, 927-942.

Kota, K.P., Wagner, S.R., Huerta, E., Underwood, J.M., and Nickerson, J.A. (2008). Binding of ATP to UAP56 is necessary for mRNA export. J Cell Sci *121*, 1526-1537.

Krashes, M.J., Keene, A.C., Leung, B., Armstrong, J.D., and Waddell, S. (2007). Sequential use of mushroom body neuron subsets during Drosophila odor memory processing. Neuron *53*, 103-115.

Krishnan, N., Rakshit, K., Chow, E.S., Wentzell, J.S., Kretzschmar, D., and Giebultowicz, J.M. (2012). Loss of circadian clock accelerates aging in neurodegeneration-prone mutants. Neurobiol Dis *45*, 1129-1135.

Kryndushkin, D., Pripuzova, N., Burnett, B.G., and Shewmaker, F. (2013). Non-targeted Identification of Prions and Amyloid-forming Proteins from Yeast and Mammalian Cells. Journal of Biological Chemistry *288*, 27100-27111.

Kudo, T., Loh, D.H., Truong, D., Wu, Y.F., and Colwell, C.S. (2011a). Circadian dysfunction in a mouse model of Parkinson's disease. Exp Neurol *232*, 66-75.

Kudo, T., Schroeder, A., Loh, D.H., Kuljis, D., Jordan, M.C., Roos, K.P., and Colwell, C.S. (2011b). Dysfunctions in circadian behavior and physiology in mouse models of Huntington's disease. Exp Neurol *228*, 80-90.

Kudryavtsev, V.A., Khokhlova, A.V., Mosina, V.A., Selivanova, E.I., and Kabakov, A.E. (2017). Induction of Hsp70 in tumor cells treated with inhibitors of the Hsp90 activity: A predictive marker and promising target for radiosensitization. PLoS One *12*.

Kuintzle, R.C., Chow, E.S., Westby, T.N., Gvakharia, B.O., Giebultowicz, J.M., and Hendrix, D.A. (2017). Circadian deep sequencing reveals stress-response genes that adopt robust rhythmic expression during aging. Nat Commun *8*.

Kula, E., Levitan, E.S., Pyza, E., and Rosbash, M. (2006). PDF cycling in the dorsal protocerebrum of the Drosophila brain is not necessary for circadian clock function. J Biol Rhythms *21*, 104-117.

Kula-Eversole, E., Nagoshi, E., Shang, Y.H., Rodriguez, J., Allada, R., and Rosbash, M. (2010). Surprising gene expression patterns within and between PDF-containing circadian neurons in Drosophila. Proc Natl Acad Sci U S A *107*, 13497-13502.

Kuljis, D., Schroeder, A.M., Kudo, T., Loh, D.H., Willison, D.L., and Colwell, C.S. (2012). Sleep and circadian dysfunction in neurodegenerative disorders: insights from a mouse model of Huntington's disease. Minerva Pneumol *51*, 93-106.

Kumar-Singh, S., Theuns, J., Van Broeck, B., Pirici, D., Vennekens, K., Corsmit, E., Cruts, M., Dermaut, B., Wang, R., and Van Broeckhoven, C. (2006). Mean age-of-onset of familial Alzheimer disease caused by presenilin mutations correlates with both increased A beta 42 and decreased A beta 40. Hum Mutat *27*, 686-695.

Kuo, Y., Ren, S., Lao, U., Edgar, B.A., and Wang, T. (2013). Suppression of polyglutamine protein toxicity by co-expression of a heat-shock protein 40 and a heat-shock protein 110. Cell Death Dis *4*.

Kwiatkowski, T.J., and Vanderburg, C.R. (2009). Mutations in the FUS/TLS gene on chromosome 16 cause familial amyotrophic lateral sclerosis (vol 323, pg 1205, 2009). Science *324*, 465-465.

Kwok, R.S., Li, Y.H., Lei, A.J., Edery, I., and Chiu, J.C. (2015). The Catalytic and Non-catalytic Functions of the Brahma Chromatin-Remodeling Protein Collaborate to Fine-Tune Circadian Transcription in Drosophila. PLoS Genet *11*.

Labbadia, J., and Morimoto, R.I. (2013). Huntington's disease: underlying molecular mechanisms and emerging concepts. Trends Biochem Sci *38*, 378-385.

Lastres-Becker, I., Nonis, D., Eich, F., Klinkenberg, M., Gorospe, M., Kotter, P., Klein, F.A.C., Kedersha, N., and Auburger, G. (2016). Mammalian ataxin-2 modulates translation control at the pre-initiation complex via PI3K/mTOR and is induced by starvation. Bba-Mol Basis Dis *1862*, 1558-1569.

Lawlor, K.T., O'Keefe, L.V., Samaraweera, S.E., van Eyk, C.L., McLeod, C.J., Maloney, C.A., Dang, T.H.Y., Suter, C.M., and Richards, R.I. (2011). Double-stranded RNA is pathogenic in Drosophila models of expanded repeat neurodegenerative diseases. Hum Mol Genet *20*, 3757-3768.

Lecerf, J.M., Shirley, T.L., Zhu, Q., Kazantsev, A., Amersdorfer, P., Housman, D.E., Messer, A., and Huston, J.S. (2001). Human single-chain Fv intrabodies counteract in situ huntingtin aggregation in cellular models of Huntington's disease. Proc Natl Acad Sci U S A *98*, 4764-4769.

Lee, C., Bae, K., and Edery, I. (1999). PER and TIM inhibit the DNA binding activity of a Drosophila CLOCK-CYC/dBMAL1 heterodimer without disrupting formation of the heterodimer: a basis for circadian transcription. Mol Cell Biol *19*, 5316-5325.

Lee, C., Etchegaray, J.P., Cagampang, F.R.A., Loudon, A.S.I., and Reppert, S.M. (2001). Posttranslational mechanisms regulate the mammalian circadian clock. Cell *107*, 855-867.

Lee, J., Kim, M., Itoh, T.Q., and Lim, C. (2018). Ataxin-2: A versatile posttranscriptional regulator and its implication in neural function. Wires Rna *9*.

Lee, J., Yoo, E., Lee, H., Park, K., Hur, J.H., and Lim, C. (2017). LSM12 and ME31B/DDX6 Define Distinct Modes of Posttranscriptional Regulation by ATAXIN-2 Protein Complex in Drosophila Circadian Pacemaker Neurons. Mol Cell *66*, 129-+.

Lee, J.H., and Sancar, A. (2011). Circadian clock disruption improves the efficacy of chemotherapy through p73-mediated apoptosis. Proc Natl Acad Sci U S A *108*, 10668-10672.

Lee, J.M., Ramos, E.M., Lee, J.H., Gillis, T., Mysore, J.S., Hayden, M.R., Warby, S.C., Morrison, P., Nance, M., Ross, C.A.*, et al.* (2012). CAG repeat expansion in Huntington disease determines age at onset in a fully dominant fashion. Neurology *78*, 690-695.

Lee, W.C., Yoshihara, M., and Littleton, J.T. (2004a). Cytoplasmic aggregates trap polyglutamine-containing proteins and block axonal transport in a Drosophila model of Huntington's disease. Proc Natl Acad Sci U S A *101*, 3224-3229.

Lee, W.C.M., Yoshihara, M., and Littleton, J.T. (2004b). Cytoplasmic aggregates trap polyglutamine-containing proteins and block axonal transport in a Drosophila model of Huntington's disease. Proc Natl Acad Sci U S A *101*, 3224-3229.

LeGates, T.A., Altimus, C.M., Wang, H., Lee, H.K., Yang, S., Zhao, H., Kirkwood, A., Weber, E.T., and Hattar, S. (2012). Aberrant light directly impairs mood and learning through melanopsin-expressing neurons. Nature *491*, 594-598.

Lessing, D., and Bonini, N.M. (2008). Polyglutamine genes interact to modulate the severity and progression of neurodegeneration in Drosophila. PLoS Biol *6*, 266-274.

Li, L., Liu, H., Dong, P., Li, D., Legant, W.R., Grimm, J.B., Lavis, L.D., Betzig, E., Tijan, R., and Liu, Z. (2016). Real-time imaging of Huntingtin aggregates diverting target search and gene transcription. Elife *5*.

Li, L.B., Yu, Z.M., Teng, X.Y., and Bonini, N.M. (2008). RNA toxicity is a component of ataxin-3 degeneration in Drosophila. Nature *453*, 1107-U1109.

Li, W.T., Kwok, C.C.H., Chan, D.C.W., Wang, F., and Tse, L.A. (2018). Weak circadian rhythm increases neutropenia risk among breast cancer patients undergoing adjuvant chemotherapy. Breast Cancer Res Tr *168*, 483-493.

Li, Y., Ray, P., Rao, E.J., Shi, C., Guo, W.R., Chen, X.P., Woodruff, E.A., Fushimi, K., and Wu, J.Y. (2010). A Drosophila model for TDP-43 proteinopathy. Proc Natl Acad Sci U S A *107*, 3169-3174.

Li, Y.R., King, O.D., Shorter, J., and Gitler, A.D. (2013). Stress granules as crucibles of ALS pathogenesis. Journal of Cell Biology *201*, 361-372.

Lim, C., and Allada, R. (2013a). ATAXIN-2 activates PERIOD translation to sustain circadian rhythms in Drosophila. Science *340*, 875-879.

Lim, C., and Allada, R. (2013b). ATAXIN-2 Activates PERIOD Translation to Sustain Circadian Rhythms in Drosophila. Science *340*, 875-879.

Lim, C., Chung, B.Y., Pitman, J.L., McGill, J.J., Pradhan, S., Lee, J., Keegan, K.P., Choe, J., and Allada, R. (2007). Clockwork orange encodes a transcriptional repressor important for circadian-clock amplitude in Drosophila. Curr Biol *17*, 1082-1089.

Lim, C., Lee, J., Choi, C., Kilman, V.L., Kim, J., Park, S.M., Jang, S.K., Allada, R., and Choe, J. (2011a). The novel gene twenty-four defines a critical translational step in the Drosophila clock. Nature *470*, 399-403.

Lim, C., Lee, J., Choi, C., Kilman, V.L., Kim, J., Park, S.M., Jang, S.K., Allada, R., and Choe, J. (2011b). The novel gene twenty-four defines a critical translational step in the Drosophila clock. Nature *470*, 399-U152.

Lim, J., and Yue, Z.Y. (2015). Neuronal Aggregates: Formation, Clearance, and Spreading. Dev Cell *32*, 491-501.

Lin, H.F. (2012). Capturing the Cloud: UAP56 in Nuage Assembly and Function. Cell *151*, 699-701.

Lin, J.M., Kilman, V.L., Keegan, K., Paddock, B., Emery-Le, M., Rosbash, M., and Allada, R. (2002). A role for casein kinase 2alpha in the Drosophila circadian clock. Nature *420*, 816-820.

Lin, Y., Stormo, G.D., and Taghert, P.H. (2004). The neuropeptide pigment-dispersing factor coordinates pacemaker interactions in the Drosophila circadian system. Journal of Neuroscience *24*, 7951-7957.

Lipton, J.O., Yuan, E.D., Boyle, L.M., Ebrahimi-Fakhari, D., Kwiatkowski, E., Nathan, A., Guttler, T., Davis, F., Asara, J.M., and Sahin, M. (2015). The Circadian Protein BMAL1 Regulates Translation in Response to S6K1-Mediated Phosphorylation. Cell *161*, 1138-1151.

Liu-Yesucevitz, L., Bilgutay, A., Zhang, Y.J., Vanderwyde, T., Citro, A., Mehta, T., Zaarur, N., McKee, A., Bowser, R., Sherman, M.*, et al.* (2010). Tar DNA Binding Protein-43 (TDP-43) Associates with Stress Granules: Analysis of Cultured Cells and Pathological Brain Tissue. PLoS One *5*.

Lo Coco, D., Mattaliano, P., Spataro, R., Mattaliano, A., and La Bella, V. (2011). Sleep-wake disturbances in patients with amyotrophic lateral sclerosis. J Neurol Neurosur Ps *82*, 839-842.

Lo Coco, D., Piccoli, F., and La Bella, V. (2010). Restless Legs Syndrome in Patients with Amyotrophic Lateral Sclerosis. Movement Disord *25*, 2658-2661.

Loh, D.H., Kudo, T., Truong, D., Wu, Y.F., and Colwell, C.S. (2013). The Q175 Mouse Model of Huntington's Disease Shows Gene Dosage- and Age-Related Decline in Circadian Rhythms of Activity and Sleep. PLoS One *8*.

Long, D.M., Blake, M.R., Dutta, S., Holbrook, S.D., Kotwica-Rolinska, J., Kretzschmar, D., and Giebultowicz, J.M. (2014). Relationships between the Circadian System and Alzheimer's Disease-Like Symptoms in Drosophila. PLoS One *9*.

Lowrey, P.L., Shimomura, K., Antoch, M.P., Yamazaki, S., Zemenides, P.D., Ralph, M.R., Menaker, M., and Takahashi, J.S. (2000). Positional syntenic cloning and functional characterization of the mammalian circadian mutation tau. Science *288*, 483-491.

Lu, B., and Palacino, J. (2013). A novel human embryonic stem cell-derived Huntington's disease neuronal model exhibits mutant huntingtin (mHTT) aggregates and soluble mHTT-dependent neurodegeneration. Faseb J *27*, 1820-1829.

Lunkes, A., Lindenberg, K.S., Ben-Haiem, L., Weber, C., Devys, D., Landwehrmeyer, G.B., Mandel, J.L., and Trottier, Y. (2002). Proteases acting on mutant Huntingtin generate cleaved products that differentially build up cytoplasmic and nuclear inclusions. Mol Cell *10*, 259-269.

Luo, M.J., Zhou, Z.L., Magni, K., Christoforides, C., Rappsilber, J., Mann, M., and Reed, R. (2001). Pre-mRNA splicing and mRNA export linked by direct interactions between UAP56 and Aly. Nature *413*, 644-647.

Luo, W.F., Li, Y., Tang, C.H.A., Abruzzi, K.C., Rodriguez, J., Pescatore, S., and Rosbash, M. (2012). CLOCK deubiquitylation by USP8 inhibits CLK/CYC transcription in Drosophila. Genes Dev *26*, 2536-2549.

Mackenzie, I.R., Nicholson, A.M., Sarkar, M., Messing, J., Purice, M.D., Pottier, C., Annu, K., Baker, M., Perkerson, R.B., Kurti, A*., et al.* (2017). TIA1 Mutations in Amyotrophic Lateral Sclerosis and Frontotemporal Dementia Promote Phase Separation and Alter Stress Granule Dynamics. Neuron *95*, 808-+.

Mackenzie, I.R.A., Rademakers, R., and Neumann, M. (2010). TDP-43 and FUS in amyotrophic lateral sclerosis and frontotemporal dementia. Lancet Neurol *9*, 995-1007.

Malpel, S., Klarsfeld, A., and Rouyer, F. (2002). Larval optic nerve and adult extra-retinal photoreceptors sequentially associate with clock neurons during Drosophila brain development. Development *129*, 1443-1453.

Manczak, M., and Reddy, H. (2015). Mitochondrial division inhibitor 1 protects against mutant huntingtin-induced abnormal mitochondrial dynamics and neuronal damage in Huntington's disease. Hum Mol Genet *24*, 7308-7325.

Mangiarini, L., Sathasivam, K., Seller, M., Cozens, B., Harper, A., Hetherington, C., Lawton, M., Trottier, Y., Lehrach, H., Davies, S.W*., et al.* (1996). Exon 1 of the HD gene with an expanded CAG repeat is sufficient to cause a progressive neurological phenotype in transgenic mice. Cell *87*, 493-506.

Martin, D.D.O., Ladha, S., Ehrnhoefer, D.E., and Hayden, M.R. (2015). Autophagy in Huntington disease and huntingtin in autophagy. Trends Neurosci *38*, 26-35.

Martindale, D., Hackam, A., Wieczorek, A., Ellerby, L., Wellington, C., McCutcheon, K., Singaraja, R., Kazemi-Esfarjani, P., Devon, R., Kim, S.U*., et al.* (1998). Length of huntingtin and its polyglutamine tract influences localization and frequency of intracellular aggregates. Nat Genet *18*, 150-154.

Martinek, S., Inonog, S., Manoukian, A.S., and Young, M.W. (2001). A role for the segment polarity gene shaggy/GSK-3 in the Drosophila circadian clock. Cell *105*, 769-779.

Mathias, J.L., and Alvaro, P.K. (2012). Prevalence of sleep disturbances, disorders, and problems following traumatic brain injury: A meta-analysis. Sleep Med *13*, 898-905.

Matsui, H., Nishinaka, K., Oda, M., Hara, N., Komatsu, K., Kubori, T., and Udaka, F. (2006). Excessive daytime sleepiness in Parkinson disease: A SPECT study. Sleep *29*, 917-920.

Matsumoto, A., Ukai-Tadenuma, M., Yamada, R.G., Houl, J., Uno, K.D., Kasukawa, T., Dauwalder, B., Itoh, T.Q., Takahashi, K., Ueda, R.*, et al.* (2007). A functional genomics strategy reveals clockwork orange as a transcriptional regulator in the Drosophila circadian clock. Genes Dev *21*, 1687-1700.

Maziuk, B., Ballance, H.I., and Wolozin, B. (2017). Dysregulation of RNA Binding Protein Aggregation in Neurodegenerative Disorders. Front Mol Neurosci *10*.

McCann, C., Holohan, E.E., Das, S., Dervan, A., Larkin, A., Lee, J.A., Rodrigues, V., Parker, R., and Ramaswami, M. (2011). The Ataxin-2 protein is required for microRNA function and synapse-specific long-term olfactory habituation. Proc Natl Acad Sci U S A *108*, E655-E662.

Means, J.C., Venkatesan, A., Gerdes, B., Fan, J.Y., Bjes, E.S., and Price, J.L. (2015). Drosophila Spaghetti and Doubletime Link the Circadian Clock and Light to Caspases, Apoptosis and Tauopathy. PLoS Genet *11*.

Meignin, C., and Davis, I. (2008). UAP56 RNA helicase is required for axis specification and cytoplasmic mRNA localization in Drosophila. Dev Biol *315*, 89-98.

Menalled, L.B., Sison, J.D., Dragatsis, I., Zeitlin, S., and Chesselet, M.F. (2003). Time course of early motor and neuropathological anomalies in a knock-in mouse model of Huntington's disease with 140 CAG repeats. Journal of Comparative Neurology *465*, 11-26.

Merrilees, J., Hubbard, E., Mastick, J., Miller, B.L., and Dowling, G.A. (2009). Rest-activity and behavioral disruption in a patient with frontotemporal dementia. Neurocase *15*, 515-526.

Merrilees, J., Hubbard, E., Mastick, J., Miller, B.L., and Dowling, G.A. (2014). Sleep in Persons With Frontotemporal Dementia and Their Family Caregivers. Nurs Res *63*, 129-136.

Metzger, S., Saukko, M., Che, H.V., Tong, L.A., Puder, Y., Riess, O., and Nguyen, H.P. (2010). Age at onset in Huntington's disease is modified by the autophagy pathway: implication of the V471A polymorphism in Atg7. Hum Genet *128*, 453-459.

Mielcarek, M., Benn, C.L., Franklin, S.A., Smith, D.L., Woodman, B., Marks, P.A., and Bates, G.P. (2011). SAHA Decreases HDAC 2 and 4 Levels In Vivo and Improves Molecular Phenotypes in the R6/2 Mouse Model of Huntington's Disease. PLoS One *6*.

Miller, J., Arrasate, M., Shaby, B.A., Mitra, S., Masliah, E., and Finkbeiner, S. (2010). Quantitative Relationships between Huntingtin Levels, Polyglutamine Length, Inclusion Body Formation, and Neuronal Death Provide Novel Insight into Huntington's Disease Molecular Pathogenesis. Journal of Neuroscience *30*, 10541-10550.

Milnerwood, A.J., and Raymond, L.A. (2010). Early synaptic pathophysiology in neurodegeneration: insights from Huntington's disease. Trends Neurosci *33*, 513-523.

Mitchell, P.J., and Tjian, R. (1989). Transcriptional Regulation in Mammalian-Cells by Sequence-Specific DNA-Binding Proteins. Science *245*, 371-378.

Mizielinska, S., Gronke, S., Niccoli, T., Ridler, C.E., Clayton, E.L., Devoy, A., Moens, T., Norona, F.E., Woollacott, I.O.C., Pietrzyk, J.*, et al.* (2014). C9orf72 repeat expansions cause neurodegeneration in Drosophila through arginine-rich proteins. Science *345*, 1192-1194.

Mizrak, D., Ruben, M., Myers, G.N., Rhrissorrakrai, K., Gunsalus, K.C., and Blau, J. (2012). Electrical Activity Can Impose Time of Day on the Circadian Transcriptome of Pacemaker Neurons. Current Biology *22*, 1871-1880.

Mohawk, J.A., Green, C.B., and Takahashi, J.S. (2012). Central and Peripheral Circadian Clocks in Mammals. Annual Review of Neuroscience, Vol 35 *35*, 445-462.

Morton, A.J. (2013). Circadian and sleep disorder in Huntington's disease. Exp Neurol *243*, 34-44.

Morton, A.J., Wood, N.I., Hastings, M.H., Hurelbrink, C., Barker, R.A., and Maywood, E.S. (2005). Disintegration of the sleep-wake cycle and circadian timing in Huntington's disease (vol 25, pg 157, 2005). Journal of Neuroscience *25*, 3994-3994.

Muraro, N.I., and Ceriani, M.F. (2015). Acetylcholine from Visual Circuits Modulates the Activity of Arousal Neurons in Drosophila. Journal of Neuroscience *35*, 16315-16327.

Muraro, N.I., Pirez, N., and Ceriani, M.F. (2013). The Circadian System: Plasticity at Many Levels. Neuroscience *247*, 280-293.

Musiek, E.S. (2015). Circadian clock disruption in neurodegenerative diseases: cause and effect? Front Pharmacol *6*.

Musiek, E.S., and Holtzman, D.M. (2016). Mechanisms linking circadian clocks, sleep, and neurodegeneration. Science *354*, 1004-1008.

Musiek, E.S., Lim, M.M., Yang, G.R., Bauer, A.Q., Oi, L., Lee, Y., Roh, J.H., Ortiz-Gonzalez, X., Dearborn, J.T., Culver, J.P.*, et al.* (2013). Circadian clock proteins regulate neuronal redox homeostasis and neurodegeneration. J Clin Invest *123*, 5389-5400.

Nagoshi, E., Sugino, K., Kula, E., Okazaki, E., Tachibana, T., Nelson, S., and Rosbash, M. (2010). Dissecting differential gene expression within the circadian neuronal circuit of Drosophila. Nat Neurosci *13*, 60-U220.

Nalavade, R., Griesche, N., Ryan, D.P., Hildebrand, S., and Krauss, S. (2013). Mechanisms of RNA-induced toxicity in CAG repeat disorders. Cell Death Dis *4*.

Neumann, M., Sampathu, D.M., Kwong, L.K., Truax, A.C., Micsenyi, M.C., Chou, T.T., Bruce, J., Schuck, T., Grossman, M., Clark, C.M.*, et al.* (2006). Ubiquitinated TDP-43 in frontotemporal lobar degeneration and amyotrophic lateral sclerosis. Science *314*, 130-133.

Nihei, Y., Ito, D., and Suzuki, N. (2012). Roles of Ataxin-2 in Pathological Cascades Mediated by TAR DNA-binding Protein 43 (TDP-43) and Fused in Sarcoma (FUS). Journal of Biological Chemistry *287*, 41310-41323.

Nitabach, M.N., and Taghert, P.H. (2008). Organization of the Drosophila circadian control circuit. Current Biology *18*, R84-R93.

Nollen, E.A.A., Garcia, S.M., van Haaften, G., Kim, S., Chavez, A., Morimoto, R.I., and Plasterk, R.H.A. (2004). Genome-wide RNA interference screen identifies previously undescribed regulators of polyglutamine aggregation. Proc Natl Acad Sci U S A *101*, 6403-6408.

Nonhoff, U., Ralser, M., Welzel, F., Piccini, I., Balzereit, D., Yaspo, M.L., Lehrach, H., and Krobitsch, S. (2007). Ataxin-2 interacts with the DEAD/H-box RNA helicase DDX6 and interferes with P-bodies and stress granules. Mol Biol Cell *18*, 1385-1396.

Ohyama, T., Verstreken, P., Ly, C.V., Rosenmund, T., Rajan, A., Tien, A.C., Haueter, C., Schulze, K.L., and Bellen, H.J. (2007a). Huntingtin-interacting protein 14, a palmitoyl transferase required for exocytosis and targeting of CSP to synaptic vesicles. Journal of Cell Biology *179*, 1481-1496.

Ohyama, T., Verstreken, P., Ly, C.V., Rosenmund, T., Rajan, A., Tien, A.C., Haueter, C., Schulze, K.L., and Bellen, H.J. (2007b). Huntingtin-interacting protein 14, a palmitoyl transferase required for exocytosis and targeting of CSP to synaptic vesicles. J Cell Biol *179*, 1481-1496.

Ono, D., Honma, K., Yanagawa, Y., Yamanaka, A., and Honma, S. (2018). Role of GABA in the regulation of the central circadian clock of the suprachiasmatic nucleus. J Physiol Sci *68*, 333-343.

Ormsby, A.R., Ramdzan, Y.M., Mok, Y.F., Jovanoski, K.D., and Hatters, D.M. (2013). A Platform to View Huntingtin Exon 1 Aggregation Flux in the Cell Reveals Divergent Influences from Chaperones hsp40 and hsp70. Journal of Biological Chemistry *288*, 37192-37203.

Paez-Colasante, X., Figueroa-Romero, C., Sakowski, S.A., Goutman, S.A., and Feldman, E.L. (2015). Amyotrophic lateral sclerosis: mechanisms and therapeutics in the epigenomic era. Nat Rev Neurol *11*, 266-279.

Pal, A., Severin, F., Lommer, B., Shevchenko, A., and Zerial, M. (2006). Huntingtin-HAP40 complex is a novel Rab5 effector that regulates early endosome motility and is up-regulated in Huntington's disease. Journal of Cell Biology *172*, 605-618.

Pallier, P.N., Maywood, E.S., Zheng, Z.G., Chesham, J.E., Inyushkin, A.N., Dyball, R., Hastings, M.H., and Morton, A.J. (2007). Pharmacological imposition of sleep slows cognitive decline and reverses dysregulation of circadian gene expression in a transgenic mouse model of huntington's disease. Journal of Neuroscience *27*, 7869-7878.

Pallier, P.N., and Morton, A.J. (2009). Management of sleep/wake cycles improves cognitive function in a transgenic mouse model of Huntington's disease. Brain Res *1279*, 90-98.

Pallos, J., Bodai, L., Lukacsovich, T., Purcell, J.M., Steffan, J.S., Thompson, L.M., and Marsh, J.L. (2008). Inhibition of specific HDACs and sirtuins suppresses pathogenesis in a Drosophila model of Huntington's disease. Hum Mol Genet *17*, 3767-3775.

Panda, S., Antoch, M.P., Miller, B.H., Su, A.I., Schook, A.B., Straume, M., Schultz, P.G., Kay, S.A., Takahashi, J.S., and Hogenesch, J.B. (2002). Coordinated transcription of key pathways in the mouse by the circadian clock. Cell *109*, 307-320.

Pandey, U.B., Nie, Z.P., Batlevi, Y., McCray, B.A., Ritson, G.P., Nedelsky, N.B., Schwartz, S.L., DiProspero, N.A., Knight, M.A., Schuldiner, O.*, et al.* (2007). HDAC6 rescues neurodegeneration and provides an essential link between autophagy and the UPS. Nature *447*, 859-863.

Panov, A.V., Gutekunst, C.A., Leavitt, B.R., Hayden, M.R., Burke, J.R., Strittmatter, W.J., and Greenamyre, J.T. (2002). Early mitochondrial calcium defects in Huntington's disease are a direct effect of polyglutamines. Nat Neurosci *5*, 731-736.

Parisky, K.M., Agosto, J., Pulver, S.R., Shang, Y.H., Kuklin, E., Hodge, J.J.L., Kang, K., Liu, X., Garrity, P.A., Rosbash, M.*, et al.* (2009). PDF Cells Are a GABA-Responsive Wake-Promoting Component of the Drosophila Sleep Circuit (vol 60, pg 672, 2008). Neuron *61*, 152-152.

Park, J., Lee, S.B., Lee, S., Kim, Y., Song, S., Kim, S., Bae, E., Kim, J., Shong, M.H., Kim, J.M.*, et al.* (2006). Mitochondrial dysfunction in Drosophila PINK1 mutants is complemented by parkin. Nature *441*, 1157-1161.

Park, J.H., and Hall, J.C. (1998). Isolation and chronobiological analysis of a neuropeptide pigment-dispersing factor gene in Drosophila melanogaster. J Biol Rhythms *13*, 219-228.

Paulson, H.L., Perez, M.K., Trottier, Y., Trojanowski, J.Q., Subramony, S.H., Das, S.S., Vig, P., Mandel, J.L., Fischbeck, K.H., and Pittman, R.N. (1997). Intranuclear inclusions of expanded polyglutamine protein in spinocerebellar ataxia type 3. Neuron *19*, 333-344.

Pedroso, J.L., Braga-Neto, P., Felicio, A.C., Aquino, C.C.H., do Prado, L.B.F., do Prado, G.F., and Barsottini, O.G.P. (2011). Sleep disorders in cerebellar ataxias. Arq Neuro-Psiquiat *69*, 253-257.

Perrin, V., Regulier, E., Abbas-Terki, T., Hassig, R., Brouillet, E., Aebischer, P., Luthi-Carter, R., and Deglon, N. (2007). Neuroprotection by Hsp104 and Hsp27 in lentiviral-based rat models of Huntington's disease. Mol Ther *15*, 903-911.

Pfeffer, M., Gispert, S., Auburger, G., Wicht, H., and Korf, H.W. (2017). Impact of Ataxin-2 knock out on circadian locomotor behavior and PER immunoreaction in the SCN of mice. Chronobiol Int *34*, 129-137.

Pfeiffenberger, C., Lear, B.C., Keegan, K.P., and Allada, R. (2010a). Locomotor activity level monitoring using the Drosophila Activity Monitoring (DAM) System. Cold Spring Harb Protoc *2010*, pdb prot5518.

Pfeiffenberger, C., Lear, B.C., Keegan, K.P., and Allada, R. (2010b). Processing circadian data collected from the Drosophila Activity Monitoring (DAM) System. Cold Spring Harb Protoc *2010*, pdb prot5519.

Pfeiffenberger, C., Lear, B.C., Keegan, K.P., and Allada, R. (2010c). Processing sleep data created with the Drosophila Activity Monitoring (DAM) System. Cold Spring Harb Protoc *2010*, pdb prot5520.

Picot, M., Cusumano, P., Klarsfeld, A., Ueda, R., and Rouyer, F. (2007). Light activates output from evening neurons and inhibits output from morning neurons in the Drosophila circadian clock. PLoS Biol *5*, 2513-2521.

Pitman, J.L., McGill, J.J., Keegan, K.P., and Allada, R. (2006). A dynamic role for the mushroom bodies in promoting sleep in Drosophila. Nature *441*, 753-756.

Porter, B., Macfarlane, R., and Walker, R. (2008). The frequency and nature of sleep disorders in a community-based population of patients with Parkinson's disease. Eur J Neurol *15*, 46-50.

Postuma, R.B., Gagnon, J.F., and Montplaisir, J.Y. (2012). REM sleep behavior disorder: From dreams to neurodegeneration. Neurobiol Dis *46*, 553-558.

Prakash, P., Nambiar, A., and Sheeba, V. (2017). Oscillating PDF in termini of circadian pacemaker neurons and synchronous molecular clocks in downstream neurons are not sufficient for sustenance of activity rhythms in constant darkness. PLoS One *12*, e0175073.

Price, J.L., Blau, J., Rothenfluh, A., Abodeely, M., Kloss, B., and Young, M.W. (1998). Double-time is a novel Drosophila clock gene that regulates PERIOD protein accumulation. Cell *94*, 83-95.

Pulst, S.M., Nechiporuk, A., Nechiporuk, T., Gispert, S., Chen, X.N., LopesCendes, I., Pearlman, S., Starkman, S., OrozcoDiaz, G., Lunkes, A.*, et al.* (1996). Moderate expansion of a normally biallelic trinucleotide repeat in spinocerebellar ataxia type 2. Nat Genet *14*, 269-276.

Ralser, M., Albrecht, M., Nonhoff, U., Lengauer, T., Lehrach, H., and Krobitsch, S. (2005). An integrative approach to gain insights into the cellular function of human ataxin-2. J Mol Biol *346*, 203-214.

Ravikumar, B., Vacher, C., Berger, Z., Davies, J.E., Luo, S.Q., Oroz, L.G., Scaravilli, F., Easton, D.F., Duden, R., O'Kane, C.J.*, et al.* (2004). Inhibition of mTOR induces autophagy and reduces toxicity of polyglutamine expansions in fly and mouse models of Huntington disease. Nat Genet *36*, 585-595.

Refinetti, R., and Menaker, M. (1992). The Circadian-Rhythm of Body-Temperature of Normal and Tau-Mutant Golden-Hamsters. J Therm Biol *17*, 129-133.

Reinke, H., Saini, C., Fleury-Olela, F., Dibner, C., Benjamin, I.J., and Schibler, U. (2008). Differential display of DNA-binding proteins reveals heat-shock factor 1 as a circadian transcription factor. Genes Dev *22*, 331-345.

Reiter, L.T., Potocki, L., Chien, S., Gribskov, M., and Bier, E. (2001). A systematic analysis of human disease-associated gene sequences in Drosophila melanogaster. Genome Res *11*, 1114-1125.

Renn, S.C., Park, J.H., Rosbash, M., Hall, J.C., and Taghert, P.H. (1999a). A pdf neuropeptide gene mutation and ablation of PDF neurons each cause severe abnormalities of behavioral circadian rhythms in Drosophila. Cell *99*, 791-802.

Renn, S.C.P., Park, J.H., Rosbash, M., Hall, J.C., and Taghert, P.H. (1999b). A pdf neuropeptide gene mutation and ablation of PDF neurons each cause severe abnormalities of behavioral circadian rhythms in Drosophila. Cell *99*, 791-802.

Renna, M., Jimenez-Sanchez, M., Sarkar, S., and Rubinsztein, D.C. (2010). Chemical Inducers of Autophagy That Enhance the Clearance of Mutant Proteins in Neurodegenerative Diseases. Journal of Biological Chemistry *285*, 11061-11067.

Reppert, S.M., and Weaver, D.R. (2002). Coordination of circadian timing in mammals. Nature *418*, 935-941.

Riazanskaia, N., Lukiw, W.J., Grigorenko, A., Korovaitseva, G., Dvoryanchikov, G., Moliaka, Y., Nicolaou, M., Farrer, L., Bazan, N.G., and Rogaev, E. (2002). Regulatory region variability in the human presenilin-2 (PSEN2) gene: potential contribution to the gene activity and risk for AD. Mol Psychiatr *7*, 891-898.

Rincon-Limas, D.E., Jensen, K., and Fernandez-Funez, P. (2012). Drosophila Models of Proteinopathies: the Little Fly that Could. Curr Pharm Design *18*, 1108-1122.

Roh, J.H., Huang, Y., Bero, A.W., Kasten, T., Stewart, F.R., Bateman, R.J., and Holtzman, D.M. (2012). Disruption of the sleep-wake cycle and diurnal fluctuation of beta-amyloid in mice with Alzheimer's disease pathology. Sci Transl Med *4*, 150ra122.

Romero, E., Cha, G.H., Verstreken, P., Ly, C.V., Hughes, R.E., Bellen, H.J., and Botas, J. (2008). Suppression of neurodegeneration and increased neurotransmission caused by expanded full-length huntingtin accumulating in the cytoplasm. Neuron *57*, 27-40.

Roos, R.A.C. (2010). Huntington's disease: a clinical review. Orphanet J Rare Dis *5*.

Rosas, H.D., Liu, A.K., Hersch, S., Glessner, M., Ferrante, R.J., Salat, D.H., van der Kouwe, A., Jenkins, B.G., Dale, A.M., and Fischl, B. (2002). Regional and progressive thinning of the cortical ribbon in Huntington's disease. Neurology *58*, 695-701.

Ross, C.A., and Poirier, M.A. (2004). Protein aggregation and neurodegenerative disease. Nat Med *10*, S10-S17.

Ross, C.A., and Tabrizi, S.J. (2011). Huntington's disease: from molecular pathogenesis to clinical treatment. Lancet Neurol *10*, 83-98.

Ruby, N.F., Hwang, C.E., Wessells, C., Fernandez, F., Zhang, P., Sapolsky, R., and Heller, H.C. (2008). Hippocampal-dependent learning requires a functional circadian system. Proc Natl Acad Sci U S A *105*, 15593-15598.

Rutila, J.E., Suri, V., Le, M., So, W.V., Rosbash, M., and Hall, J.C. (1998). CYCLE is a second bHLH-PAS clock protein essential for circadian rhythmicity and transcription of Drosophila period and timeless. Cell *93*, 805-814.

Rutten, S., Vriend, C., van den Heuvel, O.A., Smit, J.H., Berendse, H.W., and van der Werf, Y.D. (2012). Bright Light Therapy in Parkinson's Disease: An Overview of the Background and Evidence. Parkinsons Dis-Us.

Sahl, S.J., Weiss, L.E., Duim, W.C., Frydman, J., and Moerner, W.E. (2012). Cellular Inclusion Bodies of Mutant Huntingtin Exon 1 Obscure Small Fibrillar Aggregate Species. Sci Rep-Uk *2*.

Sanders, S.S., and Hayden, M.R. (2015). Aberrant palmitoylation in Huntington disease. Biochem Soc Trans *43*, 205-210.

Sanders, S.S., Mui, K.K.N., Sutton, L.M., and Hayden, M.R. (2014). Identification of Binding Sites in Huntingtin for the Huntingtin Interacting Proteins HIP14 and HIP14L. PLoS One *9*.

Sarkar, S., Krishna, G., Imarisio, S., Saiki, S., O'Kane, C.J., and Rubinsztein, D.C. (2008). A rational mechanism for combination treatment of Huntington's disease using lithium and rapamycin. Hum Mol Genet *17*, 170-178.

Sarkar, S., Ravikumar, B., Floto, R.A., and Rubinsztein, D.C. (2009). Rapamycin and mTOR-independent autophagy inducers ameliorate toxicity of polyglutamine-expanded huntingtin and related proteinopathies. Cell Death Differ *16*, 46-56.

Sarov-Blat, L., So, W.V., Liu, L., and Rosbash, M. (2000). The Drosophila takeout gene is a novel molecular link between circadian rhythms and feeding behavior. Cell *101*, 647-656.

Sathyanarayanan, S., Zheng, X.Z., Xiao, R., and Sehgal, A. (2004). Posttranslational regulation of Drosophila PERIOD protein by protein phosphatase 2A. Cell *116*, 603-615.

Satlin, A., Volicer, L., Stopa, E.G., and Harper, D. (1995). Circadian locomotor activity and core-body temperature rhythms in Alzheimer's disease. Neurobiol Aging *16*, 765-771.

Satterfield, T.F., and Pallanck, L.J. (2006). Ataxin-2 and its Drosophila homolog, ATX2, physically assemble with polyribosomes. Hum Mol Genet *15*, 2523-2532.

Saudou, F., Finkbeiner, S., Devys, D., and Greenberg, M.E. (1998). Huntingtin acts in the nucleus to induce apoptosis but death does not correlate with the formation of intranuclear inclusions. Cell *95*, 55-66.

Schaefer, M.H., Wanker, E.E., and Andrade-Navarro, M.A. (2012). Evolution and function of CAG/polyglutamine repeats in protein-protein interaction networks. Nucleic Acids Res *40*, 4273-4287.

Schnell, A., Albrecht, U., and Sandrelli, F. (2014). Rhythm and Mood: Relationships Between the Circadian Clock and Mood-Related Behavior. Behav Neurosci *128*, 326-343.

Schwab, C., Arai, T., Hasegawa, M., Yu, S., and McGeer, P.L. (2008a). Colocalization of Transactivation-Responsive DNA-Binding Protein 43 and Huntingtin in Inclusions of Huntington Disease. J Neuropath Exp Neur *67*, 1159-1165.

Schwab, C., Arai, T., Hasegawa, M., Yu, S., and McGeer, P.L. (2008b). Colocalization of transactivation-responsive DNA-binding protein 43 and huntingtin in inclusions of Huntington disease. J Neuropathol Exp Neurol *67*, 1159-1165.

Schwartz, M. (2017). Can immunotherapy treat neurodegeneration? Science *357*, 254-255.

Seelaar, H., Kamphorst, W., Rosso, S.M., Azmani, A., Masdjedi, R., de Koning, I., Maat-Kievit, J.A., Anar, B., Kaat, L.D., Breedveld, G.J.*, et al.* (2008). Distinct genetic forms of frontotemporal dementia. Neurology *71*, 1220-1226.

Selkoe, D.J. (2001). Alzheimer's disease: Genes, proteins, and therapy. Physiol Rev *81*, 741-766.

Seluzicki, A., Flourakis, M., Kula-Eversole, E., Zhang, L., Kilman, V., and Allada, R. (2014a). Dual PDF signaling pathways reset clocks via TIMELESS and acutely excite target neurons to control circadian behavior. PLoS Biol *12*, e1001810.

Seluzicki, A., Flourakis, M., Kula-Eversole, E., Zhang, L.Y., Kilman, V., and Allada, R. (2014b). Dual PDF Signaling Pathways Reset Clocks Via TIMELESS and Acutely Excite Target Neurons to Control Circadian Behavior. PLoS Biol *12*.

Shafer, O.T., Helfrich-Forster, C., Renn, S.C.P., and Taghert, P.H. (2006). Reevaluation of Drosophila melanogaster's neuronal circadian pacemakers reveals new neuronal classes. Journal of Comparative Neurology *498*, 180-193.

Shafer, O.T., and Taghert, P.H. (2009). RNA-Interference Knockdown of Drosophila Pigment Dispersing Factor in Neuronal Subsets: The Anatomical Basis of a Neuropeptide's Circadian Functions. PLoS One *4*.

Shearman, L.P., Sriram, S., Weaver, D.R., Maywood, E.S., Chaves, I., Zheng, B.H., Kume, K., Lee, C.C., van der Horst, G.T.J., Hastings, M.H.*, et al.* (2000). Interacting molecular loops in the mammalian circadian clock. Science *288*, 1013-1019.

Sheeba, V., Fogle, K.J., and Holmes, T.C. (2010). Persistence of Morning Anticipation Behavior and High Amplitude Morning Startle Response Following Functional Loss of Small Ventral Lateral Neurons in Drosophila. PLoS One *5*.

Sheeba, V., Fogle, K.J., Kaneko, M., Rashid, S., Chou, Y.T., Sharma, V.K., and Holmes, T.C. (2008). Large Ventral Lateral Neurons Modulate Arousal and Sleep in Drosophila. Current Biology *18*, 1537-1545.

Shimohata, T., Onodera, O., and Tsuji, S. (2001). Expanded polyglutamine stretches lead to aberrant transcriptional regulation in polyglutamine diseases. Hum Cell *14*, 17-25.

Sinadinos, C., Burbidge-King, T., Soh, D., Thompson, L.M., Marsh, J.L., Wyttenbach, A., and Mudher, A.K. (2009). Live axonal transport disruption by mutant huntingtin fragments in Drosophila motor neuron axons. Neurobiol Dis *34*, 389-395.

Singaraja, R.R., Hadano, S., Metzler, M., Givan, S., Wellington, C.L., Warby, S., Yanai, A., Gutekunst, C.A., Leavitt, B.R., Yi, H.*, et al.* (2002). HIP14, a novel ankyrin domain-containing protein, links huntingtin to intracellular trafficking and endocytosis. Hum Mol Genet *11*, 2815-2828.

Singaraja, R.R., Huang, K., Sanders, S.S., Milnerwood, A.J., Hines, R., Lerch, J.P., Franciosi, S., Drisdel, R.C., Vaid, K., Young, F.B.*, et al.* (2011). Altered palmitoylation and neuropathological deficits in mice lacking HIP14. Hum Mol Genet *20*, 3899-3909.

Singaraja, R.R., Milnerwood, A., Huang, K., El-Husseini, A., Raymond, L., and Hayden, M. (2008). Loss of Huntingtin interacting protein HIP14 in vivo recapitulates features of Huntington's disease. J Neurol Neurosur Ps *79*, A1-A1.

Sitaraman, D., Aso, Y., Jin, X., Chen, N., Felix, M., Rubin, G.M., and Nitabach, M.N. (2015). Propagation of Homeostatic Sleep Signals by Segregated Synaptic Microcircuits of the Drosophila Mushroom Body. Current Biology *25*, 2915-2927.

Sittler, A., Lurz, R., Lueder, G., Priller, J., Lehrach, H., Hayer-Hartl, M., Hartl, U., and Wanker, E.E. (2002). Geldanamycin activates a heat shock response and inhibits huntingtin aggregation in a cell culture model of Huntington's disease. Eur J Hum Genet *10*, 270-270.

Sivachenko, A., Li, Y., Abruzzi, K.C., and Rosbash, M. (2013). The Transcription Factor Mef2 Links the Drosophila Core Clock to Fas2, Neuronal Morphology, and Circadian Behavior. Neuron *79*, 281-292.

Smith, G.A., Rocha, E.M., McLean, J.R., Hayes, M.A., Izen, S.C., Isacson, O., and Hallett, P.J. (2014). Progressive axonal transport and synaptic protein changes correlate with behavioral and neuropathological abnormalities in the heterozygous Q175 KI mouse model of Huntington's disease. Hum Mol Genet *23*, 4510-4527.

Smolensky, M.H., Hermida, R.C., and Portaluppi, F. (2017). Circadian mechanisms of 24-hour blood pressure regulation and patterning. Sleep Med Rev *33*, 4-16.

Smotrys, J.E., and Linder, M.E. (2004). Palmitoylation of intracellular signaling proteins: Regulation and function. Annu Rev Biochem *73*, 559-587.

Snyder-Keller, A., McLear, J.A., Hathorn, T., and Messer, A. (2010). Early or Late-Stage Anti-N-Terminal Huntingtin Intrabody Gene Therapy Reduces Pathological Features in B6.HDR6/1 Mice. J Neuropath Exp Neur *69*, 1078-1085.

Sobczak, K., de Mezer, M., Michlewski, G., Krol, J., and Krzyzosiak, W.J. (2003). RNA structure of trinucleotide repeats associated with human neurological diseases. Nucleic Acids Res *31*, 5469-5482.

Song, W.J., Chen, J., Petrilli, A., Liot, G., Klinglmayr, E., Zhou, Y., Poquiz, P., Tjong, J., Pouladi, M.A., Hayden, M.R*., et al.* (2011). Mutant huntingtin binds the mitochondrial fission GTPase dynamin-related protein-1 and increases its enzymatic activity. Nat Med *17*, 377-U181.

Spillantini, M.G., Schmidt, M.L., Lee, V.M.Y., Trojanowski, J.Q., Jakes, R., and Goedert, M. (1997). alpha-synuclein in Lewy bodies. Nature *388*, 839-840.

Sreedharan, J., Neukomm, L.J., Brown, R.H., and Freeman, M.R. (2015). Age-Dependent TDP-43-Mediated Motor Neuron Degeneration Requires GSK3, hat-trick, and xmas-2. Current Biology *25*, 2130-2136.

Stanewsky, R., Kaneko, M., Emery, P., Beretta, B., Wager-Smith, K., Kay, S.A., Rosbash, M., and Hall, J.C. (1998). The cry(b) mutation identifies cryptochrome as a circadian photoreceptor in Drosophila. Cell *95*, 681-692.

Steffan, J.S., Agrawal, N., Pallos, J., Rockabrand, E., Trotman, L.C., Slepko, N., Illes, K., Lukacsovich, T., Zhu, Y.Z., Cattaneo, E*., et al.* (2004). SUMO modification of Huntingtin and Huntington's disease pathology. Science *304*, 100-104.

Steffan, J.S., Bodai, L., Pallos, J., Poelman, M., McCampbell, A., Apostol, B.L., Kazantsev, A., Schmidt, E., Zhu, Y.Z., Greenwald, M*., et al.* (2001). Histone deacetylase inhibitors arrest polyglutamine-dependent neurodegeneration in Drosophila. Nature *413*, 739-743.

Steffan, J.S., Kazantsev, A., Spasic-Boskovic, O., Greenwald, M., Zhu, Y.Z., Gohler, H., Wanker, E.E., Bates, G.P., Housman, D.E., and Thompson, L.M. (2000). The Huntington's disease protein interacts with p53 and CREB-binding protein and represses transcription. Proc Natl Acad Sci U S A *97*, 6763-6768.

Stephenson, R.M., N.H. (2013). Drosophila melanogaster: a fly through its history and current use. Jornal of Royal College of Physician of Edinburrgh *43*.

Stevens, R.G. (2005). Circadian disruption and breast cancer from melatonin to clock genes. Epidemiology *16*, 254-258.

Stevens, R.G., and Rea, M.S. (2001). Light in the built environment: potential role of circadian disruption in endocrine disruption and breast cancer. Cancer Cause Control *12*, 279-287.

Stevens, S., Comella, C.L., and Stepanski, E.J. (2004). Daytime sleepiness and alertness in patients with Parkinson disease. Sleep *27*, 967-972.

Stokkan, K.A., Yamazaki, S., Tei, H., Sakaki, Y., and Menaker, M. (2001). Entrainment of the circadian clock in the liver by feeding. Science *291*, 490-493.

Stoleru, D., Peng, Y., Agosto, J., and Rosbash, M. (2004). Coupled oscillators control morning and evening locomotor behaviour of Drosophila. Nature *431*, 862-868.

Stoleru, D., Peng, Y., Nawathean, P., and Rosbash, M. (2005). A resetting signal between Drosophila pacemakers synchronizes morning and evening activity. Nature *438*, 238-242.

Stopa, E.G., Volicer, L., Kuo-Leblanc, V., Harper, D., Lathi, D., Tate, B., and Satlin, A. (1999). Pathologic evaluation of the human suprachiasmatic nucleus in severe dementia. J Neuropath Exp Neur *58*, 29-39.

Stowers, R.S., and Isacoff, E.Y. (2007). Drosophila huntingtin-interacting protein 14 is a presynaptic protein required for photoreceptor synaptic transmission and expression of the palmitoylated proteins synaptosome-associated protein 25 and cysteine string protein. Journal of Neuroscience *27*, 12874-12883.

Sudhakaran, I.P., Hillebrand, J., Dervan, A., Das, S., Holohan, E.E., Hulsmeier, J., Sarov, M., Parker, R., VijayRaghavan, K., and Ramaswami, M. (2014). FMRP and Ataxin-2 function together in long-term olfactory habituation and neuronal translational control. Proc Natl Acad Sci U S A *111*, E99-E108.

Tabuchi, M., Lone, S.R., Liu, S., Liu, Q.L., Zhang, J.L., Spira, A.P., and Wu, M.N. (2015). Sleep Interacts with A beta to Modulate Intrinsic Neuronal Excitability. Current Biology *25*, 702-712.

Takahashi, J.S., Hong, H.K., Ko, C.H., and McDearmon, E.L. (2008). The genetics of mammalian circadian order and disorder: implications for physiology and disease. Nat Rev Genet *9*, 764-775.

Tanaka, N.K., Tanimoto, H., and Ito, K. (2008). Neuronal assemblies of the Drosophila mushroom body. Journal of Comparative Neurology *508*, 711-755.

Tataroglu, O., and Emery, P. (2015). The molecular ticks of the Drosophila circadian clock. Curr Opin Insect Sci *7*, 51-57.

Tharun, S. (2009). Roles of Eukaryotic Lsm Proteins in the Regulation of Mrna Function. Int Rev Cel Mol Bio *272*, 149-+.

Todd, P.K., and Paulson, H.L. (2010). RNA-Mediated Neurodegeneration in Repeat Expansion Disorders. Ann Neurol *67*, 291-300.

Tomioka, K., and Matsumoto, A. (2010). A comparative view of insect circadian clock systems. Cell Mol Life Sci *67*, 1397-1406.

Tranah, G.J., Blackwell, T., Stone, K.L., Ancoli-Israel, S., Paudel, M.L., Ensrud, K.E., Cauley, J.A., Redline, S., Hillier, T.A., Cummings, S.R.*, et al.* (2011). Circadian activity rhythms and risk of incident dementia and mild cognitive impairment in older women. Ann Neurol *70*, 722-732.

Trenkwalder, C. (1998). Sleep dysfunction in Parkinson's disease. Clin Neurosci *5*, 107-114.

Truant, R., Atwal, R.S., Desmond, C., Munsie, L., and Tran, T. (2008). Huntington's disease: revisiting the aggregation hypothesis in polyglutamine neurodegenerative diseases. Febs J *275*, 4252-4262.

Tsunemi, T., Ashe, T.D., Morrison, B.E., Soriano, K.R., Au, J., Roque, R.A., Lazarowski, E.R., Damian, V.A., Masliah, E., and La Spada, A.R. (2012). PGC-1alpha rescues Huntington's disease proteotoxicity by preventing oxidative stress and promoting TFEB function. Sci Transl Med *4*, 142ra197.

Turek, F.W., Joshu, C., Kohsaka, A., Lin, E., Ivanova, G., McDearmon, E., Laposky, A., Losee-Olson, S., Easton, A., Jensen, D.R.*, et al.* (2005). Obesity and metabolic syndrome in circadian Clock mutant mice. Science *308*, 1043-1045.

Ueda, M., Li, S.O., Itoh, M., Wang, M.X., Hayakawa, M., Islam, S., Tana, Nakagawa, K., Chen, H.Y., and Nakagawa, T. (2016). Expanded polyglutamine embedded in the endoplasmic reticulum causes membrane distortion and coincides with Bax insertion. Biochem Biophys Res Commun *474*, 259-263.

Ugur, B., Chen, K.C., and Bellen, H.J. (2016). Drosophila tools and assays for the study of human diseases. Dis Model Mech *9*, 235-244.

Umezaki, Y., Yoshii, T., Kawaguchi, T., Helfrich-Forster, C., and Tomioka, K. (2012). Pigment-Dispersing Factor Is Involved in Age-Dependent Rhythm Changes in Drosophila melanogaster. J Biol Rhythms *27*, 423-432.

van Duijn, E., Kingma, E.M., and van der Mast, R.C. (2007). Psychopathology in verified Huntington's disease gene carriers. J Neuropsych Clin N *19*, 441-448.

van Roon-Mom, W.M.C., Hogg, V.M., Tippett, L.J., and Faull, R.L.M. (2006). Aggregate distribution in frontal and motor cortex in Huntington's disease brain. Neuroreport *17*, 667-670.

van Wamelen, D.J., Aziz, N.A., Anink, J.J., van Steenhoven, R., Angeloni, D., Fraschini, F., Jockers, R., Roos, R.A., and Swaab, D.F. (2013). Suprachiasmatic nucleus neuropeptide expression in patients with Huntington's Disease. Sleep *36*, 117-125.

Vanderweyde, T., Yu, H., Varnum, M., Liu-Yesucevitz, L., Citro, A., Ikezu, T., Duff, K., and Wolozin, B. (2012). Contrasting Pathology of the Stress Granule Proteins TIA-1 and G3BP in Tauopathies. Journal of Neuroscience *32*, 8270-8283.

Vandesompele, J., De Preter, K., Pattyn, F., Poppe, B., Van Roy, N., De Paepe, A., and Speleman, F. (2002). Accurate normalization of real-time quantitative RT-PCR data by geometric averaging of multiple internal control genes. Genome Biol *3*.

Verbaan, D., van Rooden, S.M., Visser, M., Marinus, J., and van Hilten, J.J. (2007). Nighttime sleep problems and daytime sleepiness in Parkinson's disease. Movement Disord *22*, S242-S242.

Verma, A., Anand, V., and Verma, N.P. (2007). Sleep Disorders in Chronic Traumatic Brain Injury. Journal of Clinical Sleep Medicine *3*, 357-362.

Videnovic, A., Noble, C., Reid, K.J., Peng, J., Turek, F.W., Marconi, A., Rademaker, A.W., Simuni, T., Zadikoff, C., and Zee, P.C. (2014). Circadian Melatonin Rhythm and Excessive Daytime Sleepiness in Parkinson Disease. Jama Neurol *71*, 463-469.

Vonsattel, J.P., Myers, R.H., Stevens, T.J., Ferrante, R.J., Bird, E.D., and Richardson, E.P., Jr. (1985). Neuropathological classification of Huntington's disease. J Neuropathol Exp Neurol *44*, 559-577.

Vonsattel, J.P.G., and DiFiglia, M. (1998). Huntington disease. J Neuropath Exp Neur *57*, 369-384.

Vossfeldt, H., Butzlaff, M., Prussing, K., Charthaigh, R.A.N., Karsten, P., Lankes, A., Hamm, S., Simons, M., Adryan, B., Schulz, J.B.*, et al.* (2012). Large-Scale Screen for Modifiers of Ataxin-3-Derived Polyglutamine-Induced Toxicity in Drosophila. PLoS One *7*.

Wacker, J.L., Huang, S.Y., Steele, A.D., Aron, R., Lotz, G.P., Nguyen, Q., Giorgini, F., Roberson, E.D., Lindquist, S., Masliah, E.*, et al.* (2009). Loss of Hsp70 Exacerbates Pathogenesis But Not Levels of Fibrillar Aggregates in a Mouse Model of Huntington's Disease. Journal of Neuroscience *29*, 9104-9114.

Waelter, S., Boeddrich, A., Lurz, R., Scherzinger, E., Lueder, G., Lehrach, H., and Wanker, E.E. (2001). Accumulation of mutant huntingtin fragments in aggresome-like inclusion bodies as a result of insufficient protein degradation. Mol Biol Cell *12*, 1393-1407.

Wang, H.B., Loh, D.H., Whittaker, D.S., Cutler, T., Howland, D., and Colwell, C.S. (2018). Time-Restricted Feeding Improves Circadian Dysfunction as well as Motor Symptoms in the Q175 Mouse Model of Huntington's Disease. Eneuro *5*.

Wangler, M.F., Hu, Y.H., and Shulman, J.M. (2017). Drosophila and genome-wide association studies: a review and resource for the functional dissection of human complex traits. Dis Model Mech *10*, 77-88.

Warrick, J.M., Chan, H.Y.E., Gray-Board, G.L., Chai, Y.H., Paulson, H.L., and Bonini, N.M. (1999). Suppression of polyglutamine-mediated neurodegeneration in Drosophila by the molecular chaperone HSP70. Nat Genet *23*, 425-428.

Warrick, J.M., Paulson, H.L., Gray-Board, G.L., Bui, Q.T., Fischbeck, K.H., Pittman, R.N., and Bonini, N.M. (1998). Expanded polyglutamine protein forms nuclear inclusions and causes neural degeneration in Drosophila. Cell *93*, 939-949.

Watson, M.R., Lagow, R.D., Xu, K.X., Zhang, B., and Bonini, N.M. (2008). A Drosophila model for amyotrophic lateral sclerosis reveals motor neuron damage by human SOD1. Journal of Biological Chemistry *283*, 24972-24981.

Waza, M., Adachi, H., Katsuno, M., Minamiyama, M., Sang, C., Tanaka, F., Inukai, A., Doyu, M., and Sobue, G. (2005). 17-AAG, an Hsp90 inhibitor, ameliorates polyglutamine-mediated motor neuron degeneration. Nat Med *11*, 1088-1095.

Weiss, K.R., Kimura, Y., Lee, W.C.M., and Littleton, J.T. (2012). Huntingtin Aggregation Kinetics and Their Pathological Role in a Drosophila Huntington's Disease Model. Genetics *190*, 581-U488.

Whittaker, D.S., Loh, D.H., Wang, H.B., Tahara, Y., Kuljis, D., Cutler, T., Ghiani, C.A., Shibata, S., Block, G.D., and Colwell, C.S. (2018). Circadian-based Treatment Strategy Effective in the BACHD Mouse Model of Huntington's Disease. J Biol Rhythms *33*, 535-554.

Whitwell, J.L., Weigand, S.D., Boeve, B.F., Senjem, M.L., Gunter, J.L., DeJesus-Hernandez, M., Rutherford, N.J., Baker, M., Knopman, D.S., Wszolek, Z.K.*, et al.* (2012). Neuroimaging signatures of frontotemporal dementia genetics: C9ORF72, tau, progranulin and sporadics. Brain *135*, 794-806.

Wild, E.J., and Tabrizi, S.J. (2014). Targets for Future Clinical Trials in Huntington's Disease: What's in the Pipeline? Movement Disord *29*, 1434-1445.

Williams, A.J., and Paulson, H.L. (2008). Polyglutamine neurodegeneration: protein misfolding revisited. Trends Neurosci *31*, 521-528.

Wittmann, C.W., Wszolek, M.F., Shulman, J.M., Salvaterra, P.M., Lewis, J., Hutton, M., and Feany, M.B. (2001). Tauopathy in Drosophila: Neurodegeneration without neurofibrillary tangles. Science *293*, 711-714.

Wolfe, K.J., Ren, H.Y., Trepte, P., and Cyr, D.M. (2013). The Hsp70/90 cochaperone, Sti1, suppresses proteotoxicity by regulating spatial quality control of amyloid-like proteins. Mol Biol Cell *24*, 3588-3602.

Wolfgang, W.J., Miller, T.W., Webster, J.M., Huston, J.S., Thompson, L.M., Marsh, J.L., and Messer, A. (2005). Suppression of Huntington's disease pathology in Drosophila by human single-chain Fv antibodies. Proc Natl Acad Sci U S A *102*, 11563-11568.

Wolozin, B. (2012). Regulated protein aggregation: stress granules and neurodegeneration. Mol Neurodegener *7*.

Wong, Y.C., and Holzbaur, E.L.F. (2014). The Regulation of Autophagosome Dynamics by Huntingtin and HAP1 Is Disrupted by Expression of Mutant Huntingtin, Leading to Defective Cargo Degradation. Journal of Neuroscience *34*, 1293-1305.

Wood-Kaczmar, A., Gandhi, S., and Wood, N.W. (2006). Understanding the molecular causes of Parkinson's disease. Trends Mol Med *12*, 521-528.

Wu, Y.H., Feenstra, M.G.P., Zhou, J.N., Liu, R.Y., Torano, J.S., Van Kan, H.J.M., Fischer, D.F., Ravid, R., and Swaab, D.F. (2003). Molecular changes underlying reduced pineal melatonin levels in Alzheimer disease: Alterations in preclinical and clinical stages. J Clin Endocr Metab *88*, 5898-5906.

Wu, Y.H., Fischer, D.F., Kalsbeek, A., Garidou-Boof, M.L., van der Vliet, J., van Heijningen, C., Liu, R.Y., Zhou, J.N., and Swaab, D.F. (2006). Pineal clock gene oscillation is disturbed in Alzheimer's disease, due to functional disconnection from the "master clock". Faseb Journal *20*, 1874-+.

Wulff, K., Gatti, S., Wettstein, J.G., and Foster, R.G. (2010). Sleep and circadian rhythm disruption in psychiatric and neurodegenerative disease PERSPECTIVES. Nat Rev Neurosci *11*, 589-+.

Wyttenbach, A., Swartz, J., Kita, H., Thykjaer, T., Carmichael, J., Bradley, J., Brown, R., Maxwell, M., Schapira, A., Orntoft, T.F*., et al.* (2001). Polyglutamine expansions cause decreased CRE-mediated transcription and early gene expression changes prior to cell death in an inducible cell model of Huntington's disease. Hum Mol Genet *10*, 1829-1845.

Xu, F., Kula-Eversole, E., Iwanaszko, M., Hutchison, A.L., Dinner, A., and Allada, R. (2019). Circadian Clocks Function in Concert with Heat Shock Organizing Protein to Modulate Mutant Huntingtin Aggregation and Toxicity. Cell Rep *27*, 59-70 e54.

Xu, Y., Padiath, Q.S., Shapiro, R.E., Jones, C.R., Wu, S.C., Saigoh, N., Saigoh, K., Ptacek, L.J., and Fu, Y.H. (2005). Functional consequences of a CKIdelta mutation causing familial advanced sleep phase syndrome. Nature *434*, 640-644.

Yamamoto, S., Jaiswal, M., Charng, W.L., Gambin, T., Karaca, E., Mirzaa, G., Wiszniewski, W., Sandoval, H., Haelterman, N.A., Xiong, B.*, et al.* (2014). A Drosophila Genetic Resource of Mutants to Study Mechanisms Underlying Human Genetic Diseases. Cell *159*, 200-214.

Yan, O.Y., Andersson, C.R., Kondo, T., Golden, S.S., and Johnson, C.H. (1998). Resonating circadian clocks enhance fitness in cyanobacteria. Proc Natl Acad Sci U S A *95*, 8660-8664.

Yanai, A., Huang, K., Kang, R.J., Singaraja, R.R., Arstikaitis, P., Gan, L., Orban, P.C., Mullard, A., Cowan, C.M., Raymond, L.A.*, et al.* (2006). Palmitoylation of huntingtin by HIP14 is essential for its trafficking and function. Nat Neurosci *9*, 824-831.

Yang, Y.F., Gehrke, S., Imai, Y., Huang, Z.N., Ouyang, Y., Wang, J.W., Yang, L.C., Beal, M.F., Vogel, H., and Lu, B.W. (2006). Mitochondrial pathology and muscle and dopaminergic neuron degeneration caused inactivation of Drosophila Pink1 is rescued by by Parkin. Proc Natl Acad Sci U S A *103*, 10793-10798.

Yano, H., Baranov, S.V., Baranova, O.V., Kim, J., Pan, Y.C., Yablonska, S., Carlisle, D.L., Ferrante, R.J., Kim, A.H., and Friedlander, R.M. (2014). Inhibition of mitochondrial protein import by mutant huntingtin. Nat Neurosci *17*, 822-831.

Yokoshi, M., Li, Q., Yamamoto, M., Okada, H., Suzuki, Y., and Kawahara, Y. (2014). Direct Binding of Ataxin-2 to Distinct Elements in 3 ' UTRs Promotes mRNA Stability and Protein Expression. Mol Cell *55*, 186-198.

Yoshii, T., Todo, T., Wulbeck, C., Stanewsky, R., and Helfrich-Forster, C. (2008). Cryptochrome is present in the compound eyes and a subset of Drosophila's clock neurons. Journal of Comparative Neurology *508*, 952-966.

Yoshii, T., Wulbeck, C., Sehadova, H., Veleri, S., Bichler, D., Stanewsky, R., and Helfrich-Forster, C. (2009). The Neuropeptide Pigment-Dispersing Factor Adjusts Period and Phase of Drosophila's Clock. Journal of Neuroscience *29*, 2597-2610.

Yu, W.J., Houl, J.H., and Hardin, P.E. (2011). NEMO Kinase Contributes to Core Period Determination by Slowing the Pace of the Drosophila Circadian Oscillator. Current Biology *21*, 756-761.

Zala, D., Hinckelmann, M.V., and Saudou, F. (2013). Huntingtin's function in axonal transport is conserved in Drosophila melanogaster. PLoS One *8*, e60162.

Zhang, F., Kang, Y., Wang, M., Li, Y., Xu, T., Yang, W., Song, H., Wu, H., Shu, Q., and Jin, P. (2018a). Fragile X mental retardation protein modulates the stability of its m6A-marked messenger RNA targets. Hum Mol Genet *27*, 3936-3950.

Zhang, F., Wang, J., Xu, J., Zhang, Z., Koppetsch, B.S., Schultz, N., Vreven, T., Meignin, C., Davis, I., Zamore, P.D.*, et al.* (2012). UAP56 Couples piRNA Clusters to the Perinuclear Transposon Silencing Machinery. Cell *151*, 871-884.

Zhang, K., Daigle, J.G., Cunningham, K.M., Coyne, A.N., Ruan, K., Grima, J.C., Bowen, K.E., Wadhwa, H., Yang, P.G., Rigo, F.*, et al.* (2018b). Stress Granule Assembly Disrupts Nucleocytoplasmic Transport. Cell *173*, 958-+.

Zhang, L., Chung, B.Y., Lear, B.C., Kilman, V.L., Liu, Y., Mahesh, G., Meissner, R.A., Hardin, P.E., and Allada, R. (2010a). DN1(p) circadian neurons coordinate acute light and PDF inputs to produce robust daily behavior in Drosophila. Curr Biol *20*, 591-599.

Zhang, R., Lahens, N.F., Ballance, H.I., Hughes, M.E., and Hogenesch, J.B. (2014). A circadian gene expression atlas in mammals: Implications for biology and medicine. Proc Natl Acad Sci U S A *111*, 16219-16224.

Zhang, S., Binari, R., Zhou, R., and Perrimon, N. (2010b). A Genomewide RNA Interference Screen for Modifiers of Aggregates Formation by Mutant Huntingtin in Drosophila. Genetics *184*, 1165-U1491.

Zhang, T., Jiang, X., Xu, M., Wang, H., Sang, X., Qin, M., Bao, P., Wang, R., Zhang, C., Lu, H.*, et al.* (2018c). Sleep and circadian abnormalities precede cognitive deficits in R521C FUS knockin rats. Neurobiol Aging *72*, 159-170.

Zhang, Y., Ling, J.L., Yuan, C.Y., Dubruille, R., and Emery, P. (2013). A Role for Drosophila ATX2 in Activation of PER Translation and Circadian Behavior. Science *340*, 879-882.

Zhang, Y., Liu, Y.X., Bilodeau-Wentworth, D., Hardin, P.E., and Emery, P. (2010c). Light and Temperature Control the Contribution of Specific DN1 Neurons to Drosophila Circadian Behavior. Current Biology *20*, 600-605.

Zhao, J., Kilman, V.L., Keegan, K.P., Peng, Y., Emery, P., Rosbash, M., and Allada, R. (2003). Drosophila clock can generate ectopic circadian clocks. Cell *113*, 755-766.

Zhao, R., Shen, J.P., Green, M.R., MacMorris, M., and Blumenthal, T. (2004). Crystal structure of UAP56, a DExD/H-Box protein involved in pre-mRNA splicing and mRNA export. Structure *12*, 1373-1381.

Zheng, B.H., Albrecht, U., Kaasik, K., Sage, M., Lu, W.Q., Vaishnav, S., Li, Q., Sun, Z.S., Eichele, G., Bradley, A.*, et al.* (2001). Nonredundant roles of the mPer1 and mPer2 genes in the mammalian circadian clock. Cell *105*, 683-694.

Zheng, B.H., Larkin, D.W., Albrecht, U., Sun, Z.S., Sage, M., Eichele, G., Lee, C.C., and Bradley, A. (1999). The mPer2 gene encodes a functional component of the mammalian circadian clock. Nature *400*, 169-173.

Zheng, X., Koh, K., Sowcik, M., Smith, C.J., Chen, D., Wu, M.N., and Sehgal, A. (2009). An isoform-specific mutant reveals a role of PDP1 epsilon in the circadian oscillator. J Neurosci *29*, 10920-10927.

Zheng, X.Z., and Sehgal, A. (2008). Probing the relative importance of molecular oscillations in the circadian clock. Genetics *178*, 1147-1155.

Zhou, J.N., Hofman, M.A., and Swaab, D.F. (1995). Vip Neurons in the Human Scn in Relation to Sex, Age, and Alzheimers-Disease. Neurobiol Aging *16*, 571-576.

Zourlidou, A., Gidalevitz, T., Kristiansen, M., Landles, C., Woodman, B., Wells, D.J., Latchman, D.S., de Belleroche, J., Tabrizi, S.J., Morimoto, R.I.*, et al.* (2007). Hsp27 overexpression in the R6/2 mouse model of Huntington's disease: chronic neurodegeneration does not induce Hsp27 activation. Hum Mol Genet *16*, 1078-1090.

Zuccato, C., Ciammola, A., Rigamonti, D., Leavitt, B.R., Goffredo, D., Conti, L., MacDonald, M.E., Friedlander, R.M., Silani, V., Hayden, M.R.*, et al.* (2001). Loss of huntingtin-mediated BDNF gene transcription in Huntington's disease. Science *293*, 493-498.

Zuccato, C., Tartari, M., Crotti, A., Goffredo, D., Valenza, M., Conti, L., Cataudella, T., Leavitt, B.R., Hayden, M.R., Timmusk, T.*, et al.* (2003). Huntingtin interacts with REST/NRSF to modulate the transcription of NRSE-controlled neuronal genes. Nat Genet *35*, 76-83.

Appendix 1 Full dataset including ND genes have been screened with Pdf-Gal4 or 247-Gal4

Population based (using mean from all the genes tested) Z-score was calculated for each gene at each age.
Age delta=D21-D3 (for either period or P-S)

Z-score	p-value
2.57	0.01
1.96	0.05
1.65	0.1

(males, 12:12, 25)					Circadian										Sleep-LD			
Gal4	Transgene			age	period	Z score	Age delta	Z score		P-S	Z score	Age delta	Z score		minutes	Z score	Age delta	Z score
pdf-Gal4	ALS																	
	SOD1 (human)	P{UAS-hSOD1}16.2	33606	D3	24	-0.2194644				116.065	0.05655266				752.035706	-1.0551018		
				D21														
	SOD1 (human)	P{UAS-hSOD1.A4V}9.1	33607	D3	24	-0.2194644				85.2635	-1.0602898				975.535706	1.05407016		
				D21														
	SOD1 (human)	P{UAS-hSOD1.G85R} (4 copies)	33608	D3	24	-0.2194644				132.529	0.65351418				944.75	0.76354512		
				D21														
	Sod	P{UAS-Sod.IR}F103	24493	D3	24	-0.2194644	0.33333333	-0.527966		121.824	0.26537773	25.7092083	-0.8619776		724.875	-1.3114177	65.7321167	-0.326101116
				D21	24.3333333	-0.4336776				96.1152	0.87743711				659.142883	-1.7823563		
	Sod	P{UAS-Sod.IR}4	24491	D3	23.9375	-0.5218117	0.5625	0.14544926		111.029	-0.1260538	59.9151429	0.31888626		769.84375	-0.8870471	220.6600952	1.759150783
				D21	24.5	-0.0763061				51.1139	-0.6381691				549.183655	-2.7176248		
	Sod	P{TRiP.JF03321}attP2	29389	D3	24.25	0.98992456	0.15	-1.0666983		117.87	0.12198172	75.051375	0.84142217		949.166687	0.80522545	12.77081299	-1.038933363
				D21	24.1	-0.9339977				42.8183	-0.9175581				961.9375	0.79309176		
	Sod	P{TRiP.HMS01291}attP2	34616	D3	24	-0.2194644				91.722	-0.8261099				808.964294	-0.5178661		
				D21														
	Sod	P{TRiP.HMS00698}attP2	32909	D3	24	-0.2194644	0.6	0.25564449		29.907	-3.0674714	29.4346667	-0.7333666		875.21875	0.10737795	116.2391357	0.353697707
				D21	24.6	0.1381168				59.3417	-0.3610634				758.979614	-0.9331856		
	Sod	P{TRiP.GL01016}attP40	36804	D3	24	-0.2194644	0.75	0.6964254		118.795	0.15553506	78.5761429	0.96310489		1092.89282	2.16157057	191.6607056	1.368833728
				D21	24.75	0.45975116				60.6954	-0.3154698				901.232117	0.27675642		
	hFUS			D3														
				D21														
	Vap-33-1	P{UAS-Vap-33-1.P}3	26693	D3	23.6428571	-1.9471629				101.283	-0.4794539				799.1875	-0.6101298		
				D21														
	hTDP-43			D3	24	1.00840336	0.2	0.6964254		39.2202	-2.7297836	19.5005367	-1.0763145		1071.53125	1.95998117	4.34375	-1.152357351
				D21	23.8	-1.5772665				19.7196	-1.6955002				1075.875	1.76219786		
	CG7158 (hAlsin)	P{TRiP.HM05019}attP2	28533	D3	24	-0.2194644	0.25	-0.7728443		90.0483	-0.8867974	50.6542857	-0.0008188		992.833313	1.21730788	48.41668701	-0.559158004
				D21	24.25	-0.6123634				39.394	-1.032884				1041.25	1.46769167		
	AD																	
	Abeta42	P{UAS-APP.Abeta42.B}m26a	33769	D3	24.1875	0.68757732	0.3125	-0.5891856		143.783	1.06158412	39.552375	-0.1931297		817.875	-0.4337756	148.4821167	0.787671853
				D21	24.5	-0.0763061				104.231	1.15076311				669.392883	-1.6951739		
	Abeta42	P{UAS-APP.Abeta42.B}m26a	33770	D3	24	-0.2194644	0.125	-1.1401617		149.265	1.26034338	98.19055	1.64023722		882.25	0.17373193	25.53570557	-0.867124393
				D21	24.125	-0.880392				51.0742	-0.6395047				856.714294	-0.1018941		
	Abeta42	P{UAS-Abeta1-42.G}3	32037	D3	23.9285714	-0.5650041	0.82142857	0.90632107		85.2696	-1.0600677	57.8647917	0.24810364		810.928589	-0.499329	3.589294434	-1.162511939
				D21	24.75	0.45975116				27.4048	-1.436669				807.339294	-0.5218578		
	Abeta42	P{UAS-Abeta1-42.G}1	32038	D3	24	-0.2736981	-0.625	0.40415417		101.198	-0.0752204	33.4904167	-0.2565832		779.34375	-0.7973955		
				D21	24.625	0.27366761				67.7078	0.05399061							
	Abeta42 - Arctic	P{UAS-APP.Abeta42.E693G.VTR}8	33774	D3	24.0625	0.08288283	0.4375	-0.2218682		160.288	1.66002385	41.856825	-0.3045265		901.96875	0.359818	105.1294556	0.204167054
				D21	24.5	-0.0763061				118.431	1.62900882				796.839294	-0.6111665		
	Abeta42 - Arctic	P{UAS-APP.Abeta42.E693G.VTR}4	33773	D3	23.9375	-0.5218117	0.1625	-1.0299665		111.128	-0.1224486	28.8695952	-0.7528741		785.65625	-0.7378243	106.9419556	0.228562384
				D21	24.1	-0.9339977				82.2588	0.41076748				678.714294	-1.6158898		
	par-1	P{TRiP.HMS00405}attP2	32410	D3	24.25	0.98992456	0.35	-0.4789904		156.856	1.53559139	117.31475	2.30044653		893.65625	0.28137284	186.625	1.301055689
				D21	24.6	0.1381168				39.5411	-1.0279289				1080.28125	1.79967563		
	par-1	P{TRiP.GL00253}attP2	35342	D3	24.1875	0.68757732	0.72916667	0.63520583		139.272	0.89799886	37.1684048	-0.466381		810.40625	-0.5042583	84.7366333	-0.070309975
				D21	24.9166667	0.81712268				115.433	1.52803983				895.142883	0.22496388		
	tau (human)	P{UAS-MAPT.VTR}12D	33819	D3	24.2142857	0.81715471	0.61904762	0.31161667		100.671	-0.50164	54.1148095	0.11864603		849.321411	-0.1370155	99.34521484	0.126314112
				D21	24.8333333	0.63843692				106.012	1.21074288				749.976196	-1.009765		
	tau (human)	P{UAS-MAPT.B}31o	33820	D3	24.1875	0.68757732				99.7636	-0.5345271				908.1875	0.41850441		
				D21														
	tau (human)	P{UAS-MAPT.A}59A	181	D3	23.9375	-0.5218117	1.28571429	2.27064295		136.929	0.81306819	2.54003571	-1.6618282		915.28125	0.4854482	113.117981	0.311688549
				D21	25.2857143	1.60844532				139.469	2.33756728				802.163269	-0.565883		
	APP	P{UAS-APP.695.Exel}5	33795	D3	24.1428571	0.471615	0.60714286	0.27663405		133.163	0.67650704	7.79225	-1.4805103		891.34375	0.25954975	56.12945557	-0.455348057
				D21	24.75	0.45975116				125.371	1.86274049				835.214294	-0.2847644		
	APP	P{UAS-APP.695.Exel}3	33796	D3	24	-0.2194644	0.6875	0.51276669		131.518	0.61686586	11.3983929	-1.3560183		795.53125	-0.6446339	26.64733887	-0.852162373
				D21	24.6875	0.32573684				120.12	1.68589123				822.178589	-0.3956408		
	APLP1	P{UAS-APLP1.M}1	30538	D3											770.571411	-0.8801801	5.232177734	-1.140399564
				D21	24.8125	0.59376548				69.8978	-0.0055434				775.803589	-0.7900877		
	APLP2	P{UAS-APLP2.M}1	30122	D3	23.875	-0.8241589	1	1.43106026		98.2588	-0.5890926	52.49315	0.06266279		1009.03125	1.37016799	59.50067139	-0.409973204
				D21	24.875	0.7277798				45.7656	-0.8182938				949.530579	0.68756352		

	Appl	P{UAS-Appl.T}2	38403	D3															
				D21	24.7857143	0.53633077	0.75	0.6964254		75.165	0.17185316				753.303589	-0.9814636			
	BACE1	P{UAS-BACE1.VTR}A	33804	D3	24.75	0.45975116				81.506	-1.1965337	14.385125	-1.2529098		872.34375	0.08024654	99.41516113	0.127255554	
				D21	24.75	0.45975116				74.9815	0.16567303				772.928589	-0.8145413			
	BACE1	P{UAS-BACE1.L}2	29877	D3	23.75	-1.4288534	1.0625	1.61471897		113.013	-0.0541207	31.3479821	-0.6673148		851.84375	-0.1132122	110.3259277	0.27410893	
				D21	24.8125	0.59376548				81.6649	0.39076347				741.517822	-1.0817085			
	Psn	P{UAS-Psn.541.Exel}3	8310	D3															
				D21															
	Psn	P{UAS-Psn.541.Exel}2	8309	D3	24.0714286	0.1260753	0.64285714	0.38158189		104.633	-0.3579766	16.3523214	-1.1849978		850.142883	-0.1292633	42.20410156	-0.642776249	
				D21	24.7142857	0.38317155				88.2804	0.61356973				807.938782	-0.5167588			
	Psn	P{UAS-Psn.541.Exel}1	8308	D3	24	-0.2194644				124.183	0.35088595								
				D21															
	Psn	P{UAS-Psn.527.Exel}3	8306	D3	24	-0.2194644	0.25	-0.7728443		125.659	0.40440451	58.797225	0.28029328		824.535706	-0.3709185	114.7398071	0.333517505	
				D21	24.25	-0.6123634				66.8614	-0.1078051				709.795898	-1.3515223			
	Psn	P{UAS-Psn.527.Exel}2	8305	D3	24	-0.2194644				158.762	1.60469557				788.5	-0.7109878			
				D21															
	Psn	P{UAS-Psn.527.Exel}1	8304	D3															
				D21															
	Psn - D279A (D257A)	P{GMR-Psn.527.D279A}3	8332	D3															
				D21															
	Psn - D279A (D257A)	P{GMR-Psn.527.D279A}2	8333	D3	24.125	0.38523008													
				D21															
	Psn - D447A (D385A)	P{UAS-Psn.527.D447A}3	8323	D3															
				D21															
	Psn - D447A (D385A)	P{UAS-Psn.527.D447A}2	8322	D3															
				D21															
	Psn - D447A (D385A)	P{UAS-Psn.527.D447A}1	8321	D3															
				D21															
	Psn - M255V (M239V)	P{UAS-Psn.541.M255V}3	8313	D3	24	-0.2194644													
				D21															
	Psn - M255V (M239V)	P{UAS-Psn.541.M255V}2	8312	D3															
				D21															
	Psn - M255V (M239V)	P{UAS-Psn.541.M255V}1	8311	D3															
				D21															
	Psn - N157I (N141I)	P{UAS-Psn.541.N157I.Exel}3	8584	D3	24.1666667	0.58679491	0.4047619	-0.3180704		128.644	0.51265631	60.7232679	0.47167233		716.392883	-1.3914635	167.6785278	1.046045797	
				D21	24.5714286	0.07685311				67.9209	-0.0721235				884.071411	0.13079443			
	Psn - N157I (N141I)	P{UAS-Psn.541.N157I.Exel}1	8307	D3															
				D21											992	1.20944389			
	Psn - exon9 mutant	P{UAS-Psn.527.deltaE9}3	8337	D3	24.0625	0.08288283				127.752	0.48029045	71.737625	0.72702426						
				D21						56.0139	-0.4731406				723.6875	-1.3226241			
	Psn - exon9 mutant	P{UAS-Psn.527.deltaE9}2	8338	D3	24.125	0.38523008				134.446	0.72302239	58.0106071	0.25313751						
				D21						76.4353	0.21463411				701.0625	863.840364			
	APP - Swedish	P{UAS-APP.770.K670N.M671L.VTR	33793	D3	24.3333333	1.39305422													
				D21						92.7968	-0.7871403				939.4375	0.713411			
	APP and BACE1	P{UAS-BACE1.Exel}7b, P{UAS-APP.	33797	D3	24.125	0.38523008	0.775	0.76988889		140.211	0.93204365	96.4013	1.59202311						
				D21	24.9	0.78138552				43.8092	-0.8841837				831.142883	-0.3085665			
	APP and tau	P{UAS-APP.695.Exel}3, P{UAS-MAI	33802	D3	24.2857143	1.16269442				89.3666	-0.9115139	61.3878036	0.36972573						
				D21						74.5486	0.15109417				900.84375	0.34920136			
	APP, BACE1 and tau	P{UAS-MAPT.VTR}54, P{UAS-APP.(	33799	D3	24.0625	0.08288283				124.559	0.364533	24.799625	-0.656391						
				D21						99.7594	1.00017097				895.21875	0.29611817			
	APP, BACE1 and tau	P{UAS-APP.695.Exel}3, P{UAS-BAC	33800	D3	24.125	0.38523008	0.375	-0.4055269		135.936	0.7770693	49.7633036	0.12751084						
				D21	24.5	-0.0763061				86.1731	0.54259753				914.03125	0.47365194			
	Fe65 (aka APBB1)	P{UAS-HsapAPBB1-HA}3	29882	D3	23.9285714	-0.5650041	0.6547619	0.4165645		107.837	-0.241784	59.0421071	0.28874715						
				D21	24.5833333	0.10237965				48.7951	-0.7162614				820.5625	-0.4084137			
	Fe65 (aka APBB1)	P{UAS-HsapAPBB1-HA}2	29881	D3	23.9375	-0.5218117	0.20535714	-0.9040291		153.002	1.39584849	85.2290179	1.19277672		820.5625	-0.4084137	68.6875	-0.286323158	
				D21	24.1428571	-0.8421022				67.7729	-0.077108				889.25	0.17484141			
	ERAB (aka HSD17B10)	P{UAS-HSD17B10.Exel}1	33806	D3	24.6875	3.10635526				108.028	-0.2348676				710.1875	-1.4500238			
				D21															
	PSEN1	P{UAS-PSEN1.VTR}11	33811	D3	24.0625	0.08288283				115.972	0.05316631				888.15625	0.22946928			
				D21															
	PSEN1	P{UAS-PSEN1.VTR}1	33812	D3	24	-0.2194644	0.3125	-0.5891856		119.589	0.18430672	44.98825	-0.0224339		730.9375	-1.2542058	205.6875	1.557627256	
				D21	24.3125	-0.4783491				74.6003	0.15283285				936.625	0.57779391			

	PSEN1 - M146V	P{UAS-PSEN1.M146V.Exel}4	33813	D3	23.9375	-0.5218117	0.3125	-0.5891856		81.9996	-1.1786372	57.9743036	0.38535018		1042.53125	1.68630786	339.65625	3.360778585
				D21	24.25	-0.6123634				139.974	2.35456142				702.875	-1.4103886		
	PSEN1 - P267S	P{UAS-PSEN1.P267S.Exel}1	33814	D3														
				D21														
	PSEN2	P{UAS-PSEN2.Exel}7b	33817	D3	23.75	-1.4288534	0.55	0.10871751		51.8969	-2.2701371	19.5387143	-0.8215926		906.4375	0.40198964	0.6875	-1.201568618
				D21	24.3	-0.5051519				32.3581	-1.2698457				907.125	0.3268789		
	PSEN2 - M239V	P{UAS-PSEN2.M239V.Exel}2b	33815	D3	24.125	0.38523008				90.0083	-0.8882491				676.90625	-1.7640993		
				D21														
	PSEN2 - N141I	P{UAS-PSEN2.N141I.Exel}8b	33816	D3	24	-0.2194644	0.42857143	0.32622538		112.98	-0.0553166	44.0844464	-0.0508149		819.25	-0.4207998	69.6875	-0.272863666
				D21	24.4285714	-0.2294653				68.8954	-0.0393007				888.9375	0.17218341		
	SCA1/2/3																	
	Atx-1	P{UAS-Atx-1.T}MBR	39741	D3														
				D21														
	ATXN1	P{UAS-HsapATX1.82Q}F7	39740	D3	PerSLIH													
				D21														
	ATXN1	P{UAS-HsapATX1.2Q}F5	39738	D3														
				D21														
	MJD (human)	P{UAS-SCA3.fl-Q27.myc}46.2	33609	D3	23.9375	-0.5218117				108.019	-0.2352075	68.241375	0.60632604		944.53125	0.76148078	115.5516357	0.344444306
				D21	AR					39.7773	-1.0199764				828.979614	-0.337794		
	MJD (human)	P{UAS-HsapMJD.tr-Q27}N18.3d	8149	D3	24.0714286	0.1260753				66.4526	-1.7423568	65.812625	0.63148678		1051.90625	1.77477983	27.74682617	-0.837363832
				D21	AR					0.64	-2.338086				1079.65308	1.79433264		
	MJD (human)	P{UAS-SCA3.fl-Q84.myc}7.2	33610	D3	Very few progeny													
				D21														
	MJD (human)	P{UAS-HsapMJD.tr-Q78}c37.3	8141		24.625	2.80400802				63.3469	-1.8549688				861.178589	-0.0251192	119.3839111	0.396024786
															980.5625	0.95150844		
	MJD (human)	P{UAS-HsapMJD.tr-Q78}c211.2	8150	D3	23.9375	-0.5218117	0.6875	0.51276669		81.506	-0.641341	75.5394	2.79534459		888.84375	0.23595723	6.353942871	-1.125301176
				D21	23.25	-2.7565925				5.9666	-2.1586906				882.489807	0.11734195		
	PD																	
	alpha-synuclein (human)	P{UAS-HsapSNCA.F}5B	8146	D3	24	-0.2194644	0.625	0.32910797		110.835	-0.1331017	25.195875	-0.879699		906.625	0.40375908	157.3125	0.906524327
				D21	24.625	0.19172252				85.6388	0.52460023				1063.9375	1.66066233		
	alpha-synuclein (human)	P{UAS-HsapSNCA.A53T}15.3	8148	D3	24	-0.2194644	0.42857143	-0.2481051		115.183	0.02454875	44.145375	-0.2255207		1005.59375	1.33772826	15.09375	-1.007667811
				D21	24.4285714	-0.2294653				71.0371	0.03282981				1020.6875	1.2927954		
	alpha-synuclein (human)	P{UAS-HsapSNCA.A30P}40.1	8147	D3	23.625	-2.0335479	0.875	1.06374283		139.998	0.92434764	61.1919643	0.36296493		859.4375	-0.0415499	81.36608887	-0.115675791
				D21	24.5	-0.0763061				78.8063	0.29448859				940.803589	0.61333529		
	parkin	P{TRiP.JF01200}attP2	31259	D3	23.875	-0.8241589				165.643	1.85420992				872.9375	0.08584977		
				D21														
	parkin	P{TRiP.HMS01800}attP2	38333	D3	24.125	0.38523008				124.068	0.34673428				826.9375	-0.3482527		
				D21														
	parkin	P{TRiP.HMS01651}attP40	37509	D3	23.8571429	-0.9105438	0.39285714	-0.353053		104.757	-0.3534714	18.9875	-1.0940257		977.571411	1.07328114	44.45983887	-0.612415171
				D21	24.25	-0.6123634				99.8075	1.00179178				1022.03125	1.30422479		
	Pink1	P{TRiP.JF01672}attP2	31170	D3	23.9285714	-0.5650041	0.50892857	-0.0119725		91.7089	-0.8265858	34.615375	-0.5545172		973.5	1.03485919	26.5	-0.854145479
				D21	24.4375	-0.2103204				57.0935	-0.4367797				1000	1.11683592		
	Pink1	P{TRiP.JF01203}attP2	31262	D3	24.1428571	0.471615	0.14285714	-1.0876878		106.74	-0.281574	30.620875	-0.6924161		778.642883	-0.8040096	115.5133667	0.343929224
				D21	24	-1.1484207				76.119	0.20398307				894.15625	0.21657198		
	Pink1	P{TRiP.HMS01707}attP40	38262	D3	24.125	0.38523008	0.0625	-1.3238205		127.605	0.47496942	19.672875	-1.0703651		911.6875	0.45153395	28.90625	-0.821758577
				D21	24.1875	-0.7463777				85.0841	0.50592092				940.59375	0.61155049		
	DJ-1alpha	P{TRiP.JF01201}attP2	31260	D3	24.1428571	0.471615	0.54166667	0.08422969		107.843	-0.2415619	55.039375	0.15056406		755.4375	-1.022999	165.8125	1.02093001
				D21	24.6666667	0.2810654				52.804	-0.5812465				921.25	0.44702041		
	DJ-1alpha	P{TRiP.HMS01797}attP2	38330	D3														
				D21														
	dj-1beta	P{TRiP.JF01202}attP2	31261	D3	24.1428571	0.471615	0.45833333	-0.1606486		106.74	-0.281574	76.119	0.20398307		783.9375	-0.7540442	50.02679443	-0.537486776
				D21	24.3333333	-0.4336776				30.6209	-0.6924161				733.910706	-1.1464115		
	dj-1beta	P{TRiP.HMS01847}attP40	38378	D3						153.389	1.40990086				949.5625	0.80896074		
				D21														
	HtrA2	P{TRiP.HM05030}attP2	28544	D3	24	-0.2194644	0.33333333	-0.527966		46.5306	-2.4647123	9.695625	-1.4148016		899.625	0.3377	77.67858887	-0.165307668
				D21	24.3333333	-0.4336776				56.2263	-0.465988				821.946411	-0.3976156		
	HD																	
	HTT (human)	P{UAS-HTT.16Q.FL}F24	33810	D3	24.4375	1.89696629	0.375	-0.4055269		89.4114	-0.9098903	13.8314	-1.0008119		1038	1.6435464	1.21875	-1.194418263
				D21	24.8125	0.98488665				75.58	0.18583001				1036.78125	1.4296823		

	HTT (human)	P{UAS-HTT.128Q.FL}f27b	33808	D3	24.0625	0.08288283	0.38	-0.3908342		166.34	1.87947804	91.96	1.45255875		728	-1.281927	118	0.377398045
				D21	24.97	0.98478174				74.38	0.14541502				846	-0.1930255		
	Hip14	P{TRiP.JF01167}attP2	31591	D3	24.59	2.63469356	0.28571429	-0.6678965		122.01	0.27209021	69.348125	-0.0240543		866.5	0.02509901	95.2678833	0.071435301
				D21	24	-1.1484207				52.6614	0.06847029				961.767883	0.79164907		
	Hip14	P{TRiP.HMS01422}attP2	35012	D3	24.75	3.40870251	2.08333333	4.61447798		160.713	1.67545213	140.149125	2.9657791		993.21875	1.22094525	166.0146484	1.023650825
				D21	26.8333333	4.9268951				20.564	-1.6670625				827.204102	-0.3528958		
	HttQ0#10-2			D3	24.5	2.19931354				99	-0.5622155				1047	1.7284795		
				D21														
	HttQ128#3-5			D3	AR					0.4	-4.1373712				965	0.9546446		
				D21														
	HttQ25GFP			D3	24.25	0.98992456	0	0.6964254		51.1	-2.2990305	10.52	-1.1047955		773	-0.8572615	34	-0.753199289
				D21	24.25	-0.6123634				61.62	-0.284331				807	-0.5247437		
	HttQ103GFP			D3	24.88	4.03758477	0.17	0.6964254		89.06	-0.9226318	24.28	-0.6727082		882	0.17137268	4	-1.156984051
				D21	24.71	0.373982				64.78	-0.1779049				886	0.14719823		
	FXS																	
	Fmr1	P{TRiP.JF02634}attP2	27484	D3	24	-0.2194644	0.58333333	0.20666883		92.3455	-0.8035023	30.668	-0.4721141		788.59375	-0.7101031	21.96875	-0.915133803
				D21	24.5833333	0.10237965				61.6775	-0.2823945				766.625	-0.868157		
	Fmr1	P{TRiP.HMS00248}attP2	34944	D3	23.4285714	-2.9837821	0.28571429	-0.6678965		103.571	-0.3964644	26.9137857	-0.5900028		949.1875	0.80542186	57.15179443	-0.441587895
				D21	23.7142857	-1.7610575				76.6575	0.2221193				892.035706	0.19853549		
	Fmr1	P{TRiP.GL00075}attP2	35200	D3	24	-0.2194644	0.41666667	-0.2830877		78.2644	-1.3140705	13.2507619	-1.019045		588.875	-2.5948512	349.6964111	3.495914054
				D21	24.4166667	-0.2549919				65.0137	-0.1700352				938.571411	0.5943493		

(males, 12:12, 25C)					Circadian	Sleep-LD			
Gal4	Transgene		BL#	age	period	minutes	Z score	Age delta	Z score
247-Gal4	ALS								
	SOD1 (human)	P{UAS-hSOD1}16.2	33606	D3					
				D21		917	-0.45		
	SOD1 (human)	P{UAS-hSOD1.A4V}9.1	33607	D3		1000	0.49		
				D21					
	SOD1 (human)	P{UAS-hSOD1.G85R} (4 copies)	33608	D3					
				D21					
	Sod	P{UAS-Sod.IR}F103	24493	D3		765	-2.16	233.72619	2.44843418
				D21		998	0.49		
	Sod	P{UAS-Sod.IR}4	24491	D3		931	-0.29	203.8125	1.97955433
				D21		727	-2.64		
	Sod	P{TRiP.JF03321}attP2	29389	D3		888	-0.77	15.9330357	-0.965348
				D21		904	-0.60		
	Sod	P{TRiP.HMS01291}attP2	34616	D3		873	-0.93		
				D21					
	Sod	P{TRiP.HMS00698}attP2	32909	D3		Few progeny			
				D21					
	Sod	P{TRiP.GL01016}attP40	36804	D3		1070	1.28		
				D21					
	hFUS			D3					
				D21					
	Vap-33-1	P{UAS-Vap-33-1.P}3	26693	D3		Very few progeny (especially males)			
				D21					
	hTDP-43			D3		Lethal			
				D21					
	CG7158 (hAlsin)	P{TRiP.HM05019}attP2	28533	D3		1038	0.92	10.6428571	-1.0482685
				D21		1048	1.07		
	AD								
	Abeta42	P{UAS-APP.Abeta42.B}m26a	33769	D3		828	-1.45	215.614583	2.16454518
				D21		1043	1.01		
	Abeta42	P{UAS-APP.Abeta42.B}m26a	33770	D3		1019	0.71	10.2544643	-1.0543563
				D21		1029	0.85		
	Abeta42	P{UAS-Abeta1-42.G}3	32037	D3		959	0.03	120.6875	0.67661787
				D21		1080	1.43		
	Abeta42	P{UAS-Abeta1-42.G}1	32038	D3		1133	1.99		
				D21					
	Abeta42 - Arctic	P{UAS-APP.Abeta42.E693G.VTR}8	33774	D3		890	-0.75	37.28125	-0.630727
				D21		852	-1.20		
	Abeta42 - Arctic	P{UAS-APP.Abeta42.E693G.VTR}4	33773	D3		890	-0.75	37.28125	-0.630727
				D21		852	-1.20		
	par-1	P{TRiP.HMS00405}attP2	32410	D3		865	-1.02		
				D21					
	par-1	P{TRiP.GL00253}attP2	35342	D3		842	-1.28		
				D21					
	tau (human)	P{UAS-MAPT.VTR}12D	33819	D3		990	0.38	27.84375	-0.7786544
				D21		962	0.07		
	tau (human)	P{UAS-MAPT.B}31o	33820	D3					
				D21					
	tau (human)	P{UAS-MAPT.A}59A	181	D3					
				D21					
	APP	P{UAS-APP.695.Exel}5	33795	D3		955	-0.01	12.7589286	-1.0151003
				D21		968	0.14		
	APP	P{UAS-APP.695.Exel}3	33796	D3		1017	0.68		
				D21					
	APLP1	P{UAS-APLP1.M}1	30538	D3		930	-0.30	113.678571	0.56675696
				D21		1043	1.01		
	APLP2	P{UAS-APLP2.M}1	30122	D3		1015	0.66	110.263393	0.513226
				D21		1125	1.95		
	Appl	P{UAS-Appl.T}2	38403	D3		1087	1.47	124.03125	0.72902923
				D21		963	0.08		
	BACE1	P{UAS-BACE1.VTR}A	33804	D3		976	0.23	14.15625	-0.9931981
				D21		962	0.07		
	BACE1	P{UAS-BACE1.L}2	29877	D3					

				D21		967	0.13		
	Psn	P{UAS-Psn.541.Exel}3	8310	D3					
				D21					
	Psn	P{UAS-Psn.541.Exel}2	8309	D3					
				D21		955	-0.02		
	Psn	P{UAS-Psn.541.Exel}1	8308	D3		1167	2.38		
				D21					
	Psn	P{UAS-Psn.527.Exel}3	8306	D3					
				D21		922	-0.39		
	Psn	P{UAS-Psn.527.Exel}2	8305	D3		1011	0.62	181.21875	1.62541032
				D21		830	-1.45		
	Psn	P{UAS-Psn.527.Exel}1	8304	D3					
				D21		724	-2.68		
	Psn - D279A (D257A)	P{GMR-Psn.527.D279A}3	8332	D3					
				D21					
	Psn - D279A (D257A)	P{GMR-Psn.527.D279A}2	8333	D3					
				D21					
	Psn - D447A (D385A)	P{UAS-Psn.527.D447A}3	8323	D3					
				D21		977	0.24		
	Psn - D447A (D385A)	P{UAS-Psn.527.D447A}2	8322	D3					
				D21		806	-1.73		
	Psn - D447A (D385A)	P{UAS-Psn.527.D447A}1	8321	D3					
				D21					
	Psn - M255V (M239V)	P{UAS-Psn.541.M255V}3	8313	D3		1022	0.74		
				D21					
	Psn - M255V (M239V)	P{UAS-Psn.541.M255V}2	8312	D3					
				D21					
	Psn - M255V (M239V)	P{UAS-Psn.541.M255V}1	8311	D3					
				D21					
	Psn - N157I (N141I)	P{UAS-Psn.541.N157I.Exel}3	8584	D3		1012	0.63	37.3571429	-0.6295374
				D21		975	0.22		
	Psn - N157I (N141I)	P{UAS-Psn.541.N157I.Exel}1	8307	D3					
				D21					
	Psn - exon9 mutant	P{UAS-Psn.527.deltaE9}3	8337	D3		1012	0.62	101.15625	0.37047679
				D21		910	-0.53		
	Psn - exon9 mutant	P{UAS-Psn.527.deltaE9}2	8338	D3					
				D21		800	-1.81		
	APP - Swedish	P{UAS-APP.770.K670N.M671L.VTR}3	33793	D3		931	-0.28	28.25	-0.7722867
				D21		903	-0.61		
	APP and BACE1	P{UAS-BACE1.Exel}7b, P{UAS-APP.695.Exel}1	33797	D3					
				D21		984	0.32		
	APP and tau	P{UAS-APP.695.Exel}3, P{UAS-MAPT.VTR}31K	33802	D3		1017	0.68		
				D21					
	APP, BACE1 and tau	P{UAS-MAPT.VTR}54, P{UAS-APP.695.Exel}3, P{UAS-BACE1.Exel}9a	33799	D3		1006	0.56	123.3125	0.71776323
				D21		1129	2.00		
	APP, BACE1 and tau	P{UAS-APP.695.Exel}3, P{UAS-BACE1.Exel}9a, P{UAS-MAPT.VTR}31	33800	D3		831	-1.40	125.473214	0.75163118
				D21		957	0.01		
	Fe65 (aka APBB1)	P{UAS-HsapAPBB1-HA}3	29882	D3		964	0.09	63.09375	15.2735373
				D21		1027	0.82		
	Fe65 (aka APBB1)	P{UAS-HsapAPBB1-HA}2	29881	D3		931	-0.29	36.5	-0.6429727
				D21		894	-0.71		
	ERAB (aka HSD17B10)	P{UAS-HSD17B10.Exel}1	33806	D3		786	-1.92	127.125	0.77752197
				D21		913	-0.50		
	PSEN1	P{UAS-PSEN1.VTR}11	33811	D3		938	-0.21	71.1071429	-0.1005256
				D21		1009	0.61		
	PSEN1	P{UAS-PSEN1.VTR}1	33812	D3		1026	0.78	21.5625	-0.8771094
				D21		1004	0.56		
	PSEN1 - M146V	P{UAS-PSEN1.M146V.Exel}4	33813	D3					
				D21		905	-0.59		
	PSEN1 - P267S	P{UAS-PSEN1.P267S.Exel}1	33814	D3					
				D21					
	PSEN2	P{UAS-PSEN2.Exel}7b	33817	D3		Lethal			
				D21					
	PSEN2 - M239V	P{UAS-PSEN2.M239V.Exel}2b	33815	D3		963	0.08	58.28125	-0.3015641
				D21		1021	0.76		
	PSEN2 - N141I	P{UAS-PSEN2.N141I.Exel}8b	33816	D3					
				D21		1016	0.69		

	SCA1/2/3								
	Atx-1	P{UAS-Atx-1.T}MBR	39741	D3					
				D21					
	ATXN1	P{UAS-HsapATX1.82Q}F7	39740	D3		Lethal			
				D21					
	ATXN1	P{UAS-HsapATX1.2Q}F5	39738	D3		Lethal			
				D21					
	MJD (human)	P{UAS-SCA3.fl-Q27.myc}46.2	33609	D3		898	-0.66	3.90625	-1.1538609
				D21		894	-0.72		
	MJD (human)	P{UAS-HsapMJD.tr-Q27}N18.3d	8149	D3		954	-0.02	43.9375	-0.5263941
				D21		910	-0.53		
	MJD (human)	P{UAS-SCA3.fl-Q84.myc}7.2	33610	D3		Lethal			
				D21					
	MJD (human)	P{UAS-HsapMJD.tr-Q78}c37.3	8141			882	-0.83	101.9375	0.38272243
						984	0.33		
	MJD (human)	P{UAS-HsapMJD.tr-Q78}c211.2	8150	D3		848	-1.22		
				D21					
	PD								
	alpha-synuclein (human)	P{UAS-HsapSNCA.F}5B	8146	D3		964	0.08	10.7678571	-1.0463092
				D21		953	-0.04		
	alpha-synuclein (human)	P{UAS-HsapSNCA.A53T}15.3	8148	D3		990	0.38	13.9017857	-0.9971866
				D21		976	0.23		
	alpha-synuclein (human)	P{UAS-HsapSNCA.A30P}40.1	8147	D3					
				D21					
	parkin	P{TRiP.JF01200}attP2	31259	D3		767	-2.13	119.446429	0.65716479
				D21		887	-0.80		
	parkin	P{TRiP.HMS01800}attP2	38333	D3		869	-0.98	46.1428571	-0.4918264
				D21		823	-1.54		
	parkin	P{TRiP.HMS01651}attP40	37509	D3		1043	0.97	40.7053571	-0.5770561
				D21		1002	0.53		
	Pink1	P{TRiP.JF01672}attP2	31170	D3		844	-1.27	192.875	1.80811532
				D21		1037	0.93		
	Pink1	P{TRiP.JF01203}attP2	31262	D3		913	-0.49	16.09375	-0.9628289
				D21		929	-0.31		
	Pink1	P{TRiP.HMS01707}attP40	38262	D3		1034	0.87	52.7678571	-0.3879834
				D21		981	0.29		
	DJ-1alpha	P{TRiP.JF01201}attP2	31260	D3		942	-0.16	24.3928571	-0.8327451
				D21		918	-0.44		
	DJ-1alpha	P{TRiP.HMS01797}attP2	38330	D3		855	-1.13	78.53125	0.01584295
				D21		934	-0.25		
	dj-1beta	P{TRiP.JF01202}attP2	31261	D3		875	-0.91	3.82589286	-1.1551205
				D21		879	-0.89		
	dj-1beta	P{TRiP.HMS01847}attP40	38378	D3		1140	2.07	153.375	1.18897559
				D21		987	0.36		
	HtrA2	P{TRiP.HM05030}attP2	28544	D3		999	0.48	108.15625	0.48019775
				D21		890	-0.76		
	HD								
	HTT (human)	P{UAS-HTT.16Q.FL}F24	33810	D3		929	-0.31	68.4375	-0.1423708
				D21		997	0.48		
	HTT (human)	P{UAS-HTT.128Q.FL}f27b	33808	D3		800	-1.76	156.808036	1.24278645
				D21		956	0.00		
	Hip14	P{TRiP.JF01167}attP2	31591	D3		931	-0.28	9.30357143	-1.069261
				D21		940	-0.18		
	Hip14	P{TRiP.HMS01422}attP2	35012	D3		1028	0.81	19.34375	-0.911887
				D21		1048	1.06		
	FXS								
	Fmr1	P{TRiP.JF02634}attP2	27484	D3		885	-0.80	53.1875	-0.3814057
				D21		938	-0.21		
	Fmr1	P{TRiP.HMS00248}attP2	34944	D3		1008	0.58	6.65625	-1.1107562
				D21		1014	0.68		
	Fmr1	P{TRiP.GL00075}attP2	35200	D3		933	-0.26	27.75	-0.7801239
				D21		905	-0.58		

Appendix 2 Other RNAi Modifiers for mHtt Toxicity

In addition to the mHtt modifiers described in Chapter 3 and 4, we identified additional modifiers from our screen but have not independently verified their phenotypes with independent genetic reagents. Those modifiers include *tsu* (RNA binding protein), *Svil* (actin binding), *drl* (tyrosine kinase receptor), *GABA-B-R3* (GABA receptor), and *Bap60* (chromatin modification complex component) (listed in Table A2.1). For the top modifiers of interest, we also tested genes in the same pathway. Some of these related genes were identified as modifiers as well, which we will briefly summarize in the following sections. In addition, some genes were initially tested because they were identified as cycling using an older version of the cycling gene detection algorithm, but the genes appear to be noncycling in a newer version of the analysis. *Hel25E* is an example that scored as a modifier but no longer is considered to be a cycling gene We will also report data for this gene in the following sections.

RNAi Knockdown of Hel25E Suppresses mHtt Toxicity

Hel25E (Helicase at 25E) encodes an RNA helicase initially identified as a cycling gene and was initially tested and found to suppress HttQ128 induced arrhythmicity. Although Hel25E knockdown generates a mild reduction of rhythmicity on its own (see details in Appendix 3), we were still able to observe rescue in HttQ128 expressing flies. Two independent RNAi lines suppress arrhythmicity in caused by HttQ128 (TRiP BL33666 and NIG R4). Since knockdown of Hel25E affects PDF positive sLNv presence as well, it might be difficult to see rescue in sLNv degeneration due to HttQ128. Nevertheless, one of the lines was able to rescue the PDF-positive sLNvs (Table A2.1). We did not test Hel25E RNAi for its effect on aggregation due to the absence of sLNvs. We also tested whether HEL25E overexpression would enhance the aggregation formed by HttQ46, but no significant effect was observed (data not shown).

Reduction in Some Heat Shock Gene Function Suppresses mHtt Toxicity

Given the role of *Hop*, a key player in the heat shock chaperone pathway, in enhancing mHtt toxicity (see Chapter 3), we also tested other components in this pathway. Using this approach we identified additional genes that when knocked down or reduced could suppress mHtt toxicity. Since HOP is a scaffold protein that binds to HSP70 and 90, we hypothesized that Hsp70 or 90 could also affect Htt toxicity. Many HS proteins including HSP70, HSP27, HSP40, HSP110, have been reported as protectors against Htt toxicity (Perrin et al., 2007; Warrick et al., 1999; Zhang et al., 2010b). We find that RNAi knock-down of *Heat shock protein cognate 4 (Hsc70-4)* rescues arrhythmicity in HttQ128 flies (Table A2.1). *Hsc70-4* RNAi also decreases the aggregation in HttQ72 expressing flies (data not shown). By the time HttQ46 forms strong nucleus aggregations in lLNvs, only very small and sporadic cytoplasmic aggregates were seen with *Hsc70-4* RNAi. Interestingly, *Hsc70-4* knockdown with Pdf-Gal4 causes sLNv degeneration and arrhythmicity on its own. Loss of sLNv is first observed around D5, and flies are arrhythmic only after a short period of aging (data not shown). Thus, we were not able to quantify HttQ72 aggregation in sLNvs with *Hsc70-4* RNAi and the line failed to rescue HttQ103 induced arrhythmicity highly due to the circadian defects on its own. As additional reagents, we tested two dominant negative versions of HSC70-4 (D206S and K71S). We did not observe rescue of mHtt rhythmicity phenotypes by overexpressing both dominant negative HSC70-4. However, the expression of two dominant negative mutant HSC70-4 (D206S and K71S) leads to completely arrhythmicity or lengthened period respectively (1hr increase comparing to wild-type HSC70-4). This might mask the rescue effect from dominant negative HSC70-4 overexpression on mHtt if there is any. Moreover, we found a mild rescue with one *DnaJ-1 (Hsp40)* RNAi line and one dominant negative *Hsc70Cb* overexpressing line (Hsc70Cb.K68S) (Table A2.2).

RNAi Knockdown of Some Nucleocytoplasmic Transport Machinery Genes Suppresses mHtt Toxicity

Atx2, one of our major mHtt modifiers (see Chapter 4), is known to play an important role in regulating nucleocytoplasmic transport. Thus, we examined the function of other genes involved in this transport pathway. Since we found that ATX2 overexpression accelerates nuclear aggregation, one hypothesis is that ATX2 mediates nuclear translocation of mHTT. We asked whether genes involved in nucleocytoplasmic transport participate in regulating mHtt toxicity. One important gene in this process is *Ran*. *Ran* encodes a GTPase that shuttles between the cytoplasm and nucleus (Jang et al., 2015). A recent study has shown that ATXN2 overexpression alters the normal distribution of RAN in human cell culture (Zhang et al., 2018b). We find that knocking down *Ran* significantly rescues arrhythmicity in HttQ128 expressing flies (Table A2.3). Ran knockdown or dominant negative overexpression affect sLNv development, which causes difficulty in investigating its effects on PDF positive sLNv number and aggregation formation (Jang et al., 2015). We also tested other nucleocytoplasmic transport genes verified functional in the LNvs (Jang et al., 2015). Knockdown of *CG10478* (*αKap4*), which encodes a subunit of importin, promotes a moderate rescue of rhythmicity in HttQ128 flies (Table A2.3). *αKap4* RNAi also completely block the aggregates formed by HttQ72 (data not shown). In order to further verify if *αKap4* could modify Atx2's effect, we then combined *αKap4* RNAi with ATX2 overexpression to test whether knockdown of *αKap4* could block the accelerated aggregation in HttQ46 expressing flies caused by Atx2. We found *αKap4* RNAi delay the enhanced aggregation of HttQ46 duo to ATX2 overexpression (data not shown). Taken together, nucleocytoplasmic transport blocking reduces nuclear accumulation of mHtt and mHtt toxicity.

Knockdown of Some Translation Machinery/Stress Granule Related Genes Rescues mHtt Toxicity

In addition to their role in modifying mHtt (see Chapter 4), *Atx2* and *Fmr1* are also important in stress granules (SG), a subcellular structure thought to be important for stress-regulated translation. Under certain stress conditions such as oxidative stress, mRNAs re-localize to SG where their translation is arrested. Once the stress is relieved, transcripts will be released and translation will be resumed. The altered distribution of components participating in nucleocytoplasmic transport due to ATX2 overexpression can be induced by SG formation (Zhang et al., 2018b). Notably, there is substantial evidence suggesting SG plays an important role in NDs including HD. SG markers TIA-1 and eIF3 have been found in TDP43 inclusions in ALS patient brain tissues (Liu-Yesucevitz et al., 2010), indicating a strong link between SG and TDP43/FUS pathology. SG marker TIA-1 is found in tau pathology as well (Ash et al., 2014). A prior study that TDP43 colocalizes with mHtt aggregates in neurons from HD patients provides the possibility that other SG markers might also be found in mHtt aggregates (Schwab et al., 2008b). In fact, TIA-1 as well as the yeast homolog of ATX2, also co-localize with mHtt, adding more evidence that SG could be linked to HD (Kryndushkin et al., 2013; Waelter et al., 2001). As a site to regulate gene expression, many SG proteins are regular translation machinery components as well. We hypothesized that the other genes playing a role in translation/SG formation also affect mHtt toxicity. Consistent with this, we found that RNAi knockdown of *PABP, eIF3-S9,* and *eIF2alpha* suppress arrhythmicity in HttQ128 expressing flies (Table A2.4). However, RNAi to *Rox8* (homolog for mammalian *TIA-1*) has no effect (data not shown).

Potential Targets of CrebA Alter the Circadian Arrhythmicity Caused by mHtt

Given the role of the CrebA transcription factor as a mHtt modifier (see Chapter 4), we tested potential transcriptional targets. One-third of CrebA target genes are known to be involved in secretory pathways (Fox et al., 2010). We find that knocking down of one of those secretory pathway genes, *SsRβ* (*Signal sequence receptor β*), rescues arrhythmicity due to HttQ128 (Table S2.1). *SsRβ is* also down-regulated in the LNvs when CrebA is knocked down, indicating that its

transcription might be CrebA-dependent (data not shown). Several CrebA targets are components of the COPI or COPII transport complexes. Knocking down many of those genes in PDF neurons leads to a loss of sLNvs during development and flies have similar behavior phenotypes as Pdf mutants (data not shown, tested by Xu and Dr. Lee). Therefore, we were not able to test RNAi lines of those genes for potential rescuing of the arrhythmicity due to HttQ128 expression. Instead, we tested overexpression of some COPII complex components with the HttQ103 model for potential enhancement of arrhythmicity. Overexpression of two of the genes, *epsilon* and *deltaCOP*, accelerates the arrhythmicity in the HttQ103 expressing flies (data not shown). However, overexpression of these genes does not enhance aggregation formation in HttQ46 flies, at least at the age tested (data not shown).

Knockdown of Bap60 Suppresses mHtt Toxicity

Bap60 (Brahma associated protein 60kD) is a component of the *Brahma* Chromatin-Remodeling complex, which represses *per* and *tim* expression (Kwok et al., 2015). *Bap60* is weakly cycling in LNvs, suggesting it is potentially controlled by the clock (Table A2.1). One *Bap60* RNAi strain (TRIP#2) rescues the arrhythmicity in HttQ128 expressing flies, while a second RNAi line (TRIP #1) shows a non-significant trend towards increased rhythmicity. Since the Brahma complex regulates chromatin modification under circadian control (Kwok et al., 2015), it could be a good candidate to link the circadian clock and mHtt pathogenesis. We tested both *Bap60* RNAi lines for sLNv number rescue in HttQ128 expressing flies and aggregation in HttQ72 expressing flies. We observed significant rescue with the TRIP #1 RNAi line but not TRIP #2 (Table A2.1). However, RNAi knockdown of other components in the *Brahma* complex (*osa, mor, and brm,* (Metzger et al., 2010)) failed to rescue Htt rhythmicity defects (data not shown).

Specificity of mHtt Toxicity Modifiers in non-polyQ Neurodegeneration Models

To determine whether modifiers of mHtt were specific to mHtt, we tested the modifiers in non-polyQ disease models, specifically using the overexpression of the familial ALS mutant

TDP43A315T (Gitcho et al., 2008). To validate this ND model in the fly circadian system, we tested it with overexpression of e SHAGGY (SGG), which reduces TDP43 toxicity in motor neurons (Sreedharan et al., 2015). We found that SGG overexpression partially suppresses the arrhythmicity in TDP43A315T expressing flies. However, none of the modifier candidates tested suppress arrhythmicity caused by TDP43A315T (Table S2.5), consistent with the idea that the modifiers are specific to polyQ diseases and that they are not generally reducing the activity of the PdfGAL4 driver.

	GammaBH	Q128 P-S	Q103 P-S	sLNv#	HttQ72 aggregation#
TRiP attP40 Ctrl		2±1	22±6	0.46±0.14	0.61±0.16
Atx2 RNAi TRiP#2	4.5E-2◇	51±14 ***	85±15 ***	1.11±0.3	0.00±0.00***
Atx2 RNAi TRiP#1		44±22 ***	NT	NT	NT
TRiP attP2 Ctrl		6±2	13±6	0.72±0.11	1.17±0.14
Hop RNAi TRiP#2	5.0E-3◇	47±10 ***	66±10 ***	1.39±0.24 *	0.28±0.13 ***
Hop RNAi TRiP#1		28±8 *	NT	NT	NT
Hsc70-4 RNAi	0.15	42±7 ***	2±1	1.23±0.30	(blocked HttQ46 aggregation in lLNvs)
CrebA RNAi	6.8E-5◇	33±10 ***	59±14 *	1.9±0.3 **	0.00±0.00 ***
tsu RNAi	4.5E-2◇	27±9 *	26±7	0.91±0.17	NT
Svil RNAi	5.1E-7◇	26±13 *	46±9 *	NT	NT
drl RNAi	1.2E-5◇	20±8	52±7 *	NT	NT
Bap60 RNAi TRiP#2	3.9E-2◇	31±5 *	NT	1.42±0.26 *	0.06±0.04 ***
Bap60 RNAi TRiP#1		27±5	NT	0.87±0.22	0.90±0.37
Hel25E RNAi TRiP#1	3.9E-2◇	47±9***	40±9***	1.24±0.28*	NA (decreased sLNv)
GABA-B-R3 RNAi TRiP#1	7.2E-7◇	21±5***	27±5***	NT	NT
NIG Ctrl		20±5	NT	NT	NT
SsRβ NIG R1		59±13***	NT	NT	NT

Table A2.1. Summary of Top Modifiers Identified through Behavioral Screening with Pdf>HttQ128 and Follow-up Studies.

Abilities to rescue HttQ128 and HttQ103 induced arrhythmicity, PDF positive sLNv number, and reduced HttQ72 aggregation number of top modifier candidates we found through screening are listed (N=7~68). ◇ :Cycling based on our cut off for boot eJTK calculated data (GammaBH<0.05, FC>2) NT: Not tested NA: Not applicable (due to the reagent affects PDF positive sLNv number by itself) *:p<0.05 **:p<0.01, ***:p<0.005

Pdf>HttQ128 X	Period	P-S	n	R%
TRiP Ctrl#1	23.0±0.3	3±2	21	14%
Dna-J1 TRiP#1	25.0±0.1	26±6***	22	59%
TRiP Ctrl#1	23.2±0.2	3±1	28	18%
Hsc70Cb TRiP#1	23.5	2±2	12	8%
UAS-Hsc70Cb	23.8±0.3	6±3	16	13%
UAS-Hsc70Cb.K68S	23.1±0.1	33±7***	17	82%
Ctrl	24.1±0.1	13±6	13	31%
Hsc70-3	24.3±0.3	13±5	15	33%
Hsc70-3 D231S	23.1±0.3	11±4	19	37%
Hsc70-3 K97S	23.8±0.2	28±8	16	69%
Ctrl	24.4±0.2	15±7	15	33%
Hsc70-4	24.1±0.2	14±4	16	50%
Hsc70-4 D206S	22.0	1±1	18	6%
Hsc70-4 K71S	24.2±0.3	18±5	22	45%

Table A2.2. Knock-down of *DnaJ-1* (Drosophila *Hsp40*) Suppressed HttQ128 Toxicity Among Heat Shock Related Genes.

Pdf>HttQ128 X	Period	P-S	n	R%
TRiP Ctrl	X	0±0	20	0%
Rcc1(RanGEF) TRiP	23.0±0.5	13±8	11	18%
Nup153 TRiP	23.3±0.2	7±3	19	16%
Ran TRiP	24.4±0.2	33±8***	8	75%
U-dcr2 TRiP Ctrl	23.0±0.2	3±1	21	19%
U-dcr2 RanGAP TRiP	24.6±1.6	14±6	23	35%
U-dcr2 αKap4 TRiP	23.8±0.2	19±5*	16	44%
U-dcr2 αKap1 TRiP	23.3±0.2	5±2	18	17%
U-dcr2 αKap3 TRiP	23.3±0.2	2±1	19	11%

Table A2.3. Knock-down of *αKap4* Suppressed HttQ128 Toxicity Among Nucleocytoplamic Transport Related Genes.

Pdf>HttQ128 X	Period	P-S	n	R%
TRiP attP2 Ctrl	23.2±0.1	4±1	41	17%
eIF2alpha RNAi TRiP	23.6±0.0	20±7*	17	53%
eIF3-S9 RNAi TRiP	24.7±0.0	41±10***	12	67%
TRiP attP40	23.5	3±1	24	13%
PABP RNAi TRiP	23.8±0.0	29±10*	13	62%

Table A2.4. Knocking down of Other SG Related Genes Rescues HTtQ128 Induced Arrhythmicity

Pdf-G4;TDP43A315T X	Period	P-S	n	R%
TRiP attP40 Ctrl	23.5±0.2	11±4	19	21%
Atx2 RNAi (TRiP attP40)	23.1±0.1	27±7	15	60%
Ctrl	23.4±0.1	31±8	15	73%
UAS-sgg	23.3±0.1	59±10*	16	100%
UAS-Atx2-dPAM#8	23.3±0.3	42±11	9	78%
TRiP attP2 Ctrl	23.1±0.1	29±7	14	64%
CrebA RNAi (TRiP attP2)	23.0±0.2	27±7	22	55%
Hop RNAi (TRiP attP2)	24.1±0.8	19±6	22	50%
Fmr1 RNAi (TRiP attP2)	22.8±0.2	18±4	8	63%
Hel25E RNAi (TRiP attP2)	24.4±1.4	30±10	8	75%

Table A2.5. RNAi Lines for Modifiers Used for Mutant Htt Toxicity Test Do Not Show Rescue for TDP43A315T Induced Arrhythmicity

Behavioral data for flies with pdfGAL4 crossed with RNAi for each Htt modifier candidate are shown. Flies within 5 days of eclosion were used. Most RNAi lines that we found rescue Htt toxicity do not affect circadian rhythms on their own.

Reference

Ash, P. E. A., Vanderweyde, T. E., Youmans, K. L., Apicco, D. J., & Wolozin, B. (2014). Pathological stress granules in Alzheimer's disease. *Brain research, 1584*, 52-58. doi:10.1016/j.brainres.2014.05.052

Fox, R. M., Hanlon, C. D., & Andrew, D. J. (2010). The CrebA/Creb3-like transcription factors are major and direct regulators of secretory capacity. *Journal of Cell Biology, 191*(3), 479-492. doi:10.1083/jcb.201004062

Gitcho, M. A., Baloh, R. H., Chakraverty, S., Mayo, K., Norton, J. B., Levitch, D., . . . Cairns, N. J. (2008). TDP-43 A315T mutation in familial motor neuron disease. *Annals of Neurology, 63*(4), 535-538. doi:10.1002/ana.21344

Jang, A. R., Moravcevic, K., Saez, L., Young, M. W., & Sehgal, A. (2015). Drosophila TIM Binds Importin alpha 1, and Acts as an Adapter to Transport PER to the Nucleus. *PLoS genetics, 11*(2). doi:ARTN e1004974
10.1371/journal.pgen.1004974

Kryndushkin, D., Pripuzova, N., Burnett, B. G., & Shewmaker, F. (2013). Non-targeted Identification of Prions and Amyloid-forming Proteins from Yeast and Mammalian Cells. *Journal of Biological Chemistry, 288*(38), 27100-27111. doi:10.1074/jbc.M113.485359

Kwok, R. S., Li, Y. H., Lei, A. J., Edery, I., & Chiu, J. C. (2015). The Catalytic and Non-catalytic Functions of the Brahma Chromatin-Remodeling Protein Collaborate to Fine-Tune Circadian Transcription in Drosophila. *PLoS genetics, 11*(7). doi:ARTN e1005307
10.1371/journal.pgen.1005307

Liu-Yesucevitz, L., Bilgutay, A., Zhang, Y. J., Vanderwyde, T., Citro, A., Mehta, T., . . . Wolozin, B. (2010). Tar DNA Binding Protein-43 (TDP-43) Associates with Stress Granules: Analysis of Cultured Cells and Pathological Brain Tissue. *PloS one, 5*(10). doi:ARTN e13250
10.1371/journal.pone.0013250

Metzger, S., Saukko, M., Che, H. V., Tong, L. A., Puder, Y., Riess, O., & Nguyen, H. P. (2010). Age at onset in Huntington's disease is modified by the autophagy pathway: implication of the V471A polymorphism in Atg7. *Human Genetics, 128*(4), 453-459. doi:10.1007/s00439-010-0873-9

Perrin, V., Regulier, E., Abbas-Terki, T., Hassig, R., Brouillet, E., Aebischer, P., . . . Deglon, N. (2007). Neuroprotection by Hsp104 and Hsp27 in lentiviral-based rat models of Huntington's disease. *Molecular Therapy, 15*(5), 903-911. doi:10.1038/mt.sj.6300141

Schwab, C., Arai, T., Hasegawa, M., Yu, S., & McGeer, P. L. (2008). Colocalization of transactivation-responsive DNA-binding protein 43 and huntingtin in inclusions of Huntington disease. *J Neuropathol Exp Neurol, 67*(12), 1159-1165. doi:10.1097/NEN.0b013e31818e8951

Sreedharan, J., Neukomm, L. J., Brown, R. H., & Freeman, M. R. (2015). Age-Dependent TDP-43-Mediated Motor Neuron Degeneration Requires GSK3, hat-trick, and xmas-2. *Current Biology, 25*(16), 2130-2136. doi:10.1016/j.cub.2015.06.045

Waelter, S., Boeddrich, A., Lurz, R., Scherzinger, E., Lueder, G., Lehrach, H., & Wanker, E. E. (2001). Accumulation of mutant huntingtin fragments in aggresome-like inclusion bodies as a result of insufficient protein degradation. *Molecular Biology of the Cell, 12*(5), 1393-1407. doi:DOI 10.1091/mbc.12.5.1393

Warrick, J. M., Chan, H. Y. E., Gray-Board, G. L., Chai, Y. H., Paulson, H. L., & Bonini, N. M. (1999). Suppression of polyglutamine-mediated neurodegeneration in Drosophila by the molecular chaperone HSP70. *Nature genetics, 23*(4), 425-428.

Zhang, K., Daigle, J. G., Cunningham, K. M., Coyne, A. N., Ruan, K., Grima, J. C., . . . Lloyd, T. E. (2018). Stress Granule Assembly Disrupts Nucleocytoplasmic Transport. *Cell, 173*(4), 958-+. doi:10.1016/j.cell.2018.03.025

Zhang, S., Binari, R., Zhou, R., & Perrimon, N. (2010). A Genomewide RNA Interference Screen for Modifiers of Aggregates Formation by Mutant Huntingtin in Drosophila. *Genetics, 184*(4), 1165-U1491. doi:Doi 10.1534/Genetics.109.112516

Appendix 3 A Role for RNA Helicase Hel25E in Circadian Rhythms

As part of our screen for mHtt circadian rhythm modifiers, we discovered a role for *Hel25E* in regulating period length independent of mHtt. While the core mechanism controlling circadian rhythms is relatively well studied, there are still many regulatory steps that remain unknown. Regulation of the circadian clock is not restricted to transcriptional steps, as many studies have identified important roles for components involved in the post-transcriptional modification, translation, and post-translational modification. Moreover, there are still many questions on how output pathways are regulated by the core clock to drive circadian rhythms. Screening strategies have continued to be successful at identifying novel genes involved in the circadian system. In parallel to the mHtt toxicity screening (in Chapter 2), RNAi lines of the cycling genes were tested with PdfGAL4 and screened for behavioral phenotypes. To maximize the ability to detect phenotypes, timGAL4 was also used for the screening due to its stronger and broader expression in both PDF and non-PDF clock neurons. DCR2 overexpression was also included together with some of the RNAi lines, as DCR2 often enhances long-hairpin RNAi phenotypes in *Drosophila* by processing the dsRNA. Several genes with rhythmicity and/or period phenotypes have been identified in this screen. Here we will focus on one of them, *Hel25E,* which has a robust phenotype that has been verified using independent reagents.

Hel25E Knockdown Leads to Circadian Defects

Helicase at 25E (*Hel25E*, also known as *UAP56*) is an RNA helicase involved in splicing, localization and export(Kota et al., 2008; Luo et al., 2001; Meignin and Davis, 2008; Zhao et al., 2004). More recent studies have shown that it interacts with piRNA complex (a cluster of transposon fragments and RNA binding proteins processing the transposons (Zhang et al., 2012)) to mediate transposon-dependent gene silencing (Lin, 2012; Zhang et al., 2012). RNA binding proteins involved in translation have previously been found to play a role in the circadian clock

(Lee et al., 2017; Lim and Allada, 2013a; Zhang et al., 2013), but circadian functions of other types of RNA binding proteins have not been demonstrated.

Hel25E knockdown in PDF neurons significantly lengthens period, a phenotype that can at least be partially rescued by co-expression of wild-type *Hel25E*. PdfGAL4 Hel25E RNAi flies display a 1.5hr increase in the period (25.5 hr) compared to the control flies, and the period is rescued to 24.7 hr when wild-type fly HEL25E (UAS-UAP56) is overexpressed together with RNAi (Table A3.1). TimGAL4 has a much broader expression pattern than PdfGAL4, driving expression in most or all circadian neurons together with some other neurons and glial cells (Kaneko and Hall, 2000) (Zhao et al., 2003). The extension in period becomes more severe with knocks down *Hel25E* with timGAL4. The period in timGAL4;Hel25E RNAi flies is 27.7 hr while rescuing with HEL25E overexpression reverses the period back to 24.1 hr (Table A3.1). , We also observe a significant reduction in the rhythmicity in the timGAL4;Hel25E RNAi flies, although more than half of the flies are still rhythmic (Table A3.1). For period calculation, we usually exclude flies with P-S values below 10 as this is our threshold for rhythmicity and the periods of not rhythmic flies are often inaccurate. To confirm that the period lengthening phenotype in Hel25E RNAi flies is accurate, we also applied a more stringent threshold when selecting flies for period calculation. When flies with P-S over 40 are selected for period calculation (which is around 50% of all the timGAL4;Hel25E RNAi flies tested), the average period is 27.4 hr (data not shown), indicating that the effect on period is a reliable phenotype. In order to confirm the phenotype, we tested two additional independent RNAi lines from the other two RNAi collections, VDRC and NIG. Each of these RNAi lines increased period ~1hr with PdfGAL4;DCR2 and lengthening can be rescued by HEL25E overexpression. Unfortunately, flies expressing those two lines with timGAL4 are not viable.

We also addressed whether *Hel25E* is endogenously expressed in circadian neurons. Using a genomic *Hel25E* transgene with an in-frame GFP tag, we observed Hel25E-GFP

expression in clock neurons, consistent with its potential role in period determination. We observed a stronger expression of Hel25E-GFP in PDF neurons compared to labeling in brain regions containing other circadian neurons (LNds and DN1s, inferred from the location of the neurons, Figure A3.1). Besides circadian neurons, we found a strong GFP signal in the mushroom body. However, we were not able to address a functional role for Hel25E in this tissue because expression of the TRIP Hel25E RNAi line with mushroom body driver 247GAL4 leads to developmental lethality.

We also examined the effects of *Hel25E* RNAi on circadian gene expression in clock neurons. Interestingly, when we examined PER and PDF expression in the clock neurons, we found that the sLNv subset was not detectable after *Hel25E* knockdown, suggesting degeneration of these neurons. We found that sLNvs are absent in both PdfGAL4;Hel25E RNAi (Figure A3.2) and timGAL4;Hel25E RNAi flies (data not shown). We also find that PER levels are significantly decreased in the lLNvs in *Hel25E* RNAi flies compared to control (Figure A3.2). Notably, changes in period length are commonly accompanied by PER level alterations in circadian neurons, but such PER alterations are typically observed in the sLNv group, not the lLNv. In our data, it is not completely clear whether sLNvs degenerate during development or they are losing circadian gene expression. Notably, these neurons also lack mGFP signal driven by PdfGAL4 (Figure A3.2). As mentioned in Chapter 2 and 3, loss of sLNv (due to toxic ND genes), commonly leads to a severe reduction in rhythmicity without period change. Thus, the phenotypes observed in *Hel25E* knockdown flies are unique. In order to further demonstrate PER's role in Hel25E loss-of-function induced circadian defects, we tested PER overexpression in flies with Hel25E knocked down. Overexpression of PER (or other clock genes) did not restore normal period in PdfGAL4; Hel25E RNAi flies, while PER expression further lengthened the period phenotype caused by timGAL4;Hel25E RNAi (data not shown)

We then asked whether *Hel25E* mutant alleles exhibit a similar phenotype to *Hel25E* RNAi. However, most *Hel25E* homozygous mutant alleles are adult lethal. The only mutant combination viable in our hands is trans-heterozygous for f the UAP28 allele (5′ UTR deletion, reduced expression level) (Zhang et al., 2012) and the sz15' allele (point mutation, loss-of-function) (Meignin and Davis, 2008). We found that trans heterozygous mutant displayed no period lengthening but did show a significant reduction in DD rhythmicity (Figure A3.3, boxes). Moreover, in both genetic backgrounds, SZ15'/UAP28 heterozygotes display significantly reduced morning and evening anticipation as quantified by the anticipation index (indicated by arrows, Figure A3.3) compared to the single copy mutant controls in a corresponding genetic background. Future studies will be needed to determine the basis for the range of Hel25E circadian phenotypes observed.

Genotype	Period	P-S	n	R%
Pdf-Gal4/Ctrl (TRiP)	23.8±0.1	115±21	8	100%
Pdf-Gal4/+;Hel25E RNAi (TRiP)/+	25.5±0.1	55±6	36	86%
Pdf-Gal4/+;UAS-Hel25E	24.1±0.1	89±10	20	90%
Pdf-Gal4/+;Hel25E RNAi (TRiP)/UAS-Hel25E	24.7±0.2 ***	65±8	33	91%
tim-Gal4/Ctrl (TRiP)	24.3±0.1	80±9	8	100%
tim-Gal4/+;Hel25E RNAi (TRiP)/+	27.7±0.2	39±9	19	63%
tim-Gal4/+;UAS-Hel25E	24.3±0.1	56±7	24	96%
tim-Gal4/+;Hel25E RNAi (TRiP)/UAS-Hel25E	24.1±0.1***	34±7	18	94%
Pdf-dcr2/Ctrl (VDRC GD)	24.2±0.1	128±8	24	100%
Pdf-dcr2/Hel25E RNAi (VDRC GD)	25.1±0.1	55±5	31	94%
Pdf-dcr2/+;UAS-Hel25E/+	24.6±0.1	127±12	8	100%
Pdf-dcr2/Hel25E RNAi (VDRC GD);UAS-Hel25E/+	24.7±0.1*	105±10	20	100%
Pdf-dcr2/Ctrl (NIG)	24.2±0.1	78±6	28	93%
Pdf-dcr2/Hel25E RNAi (NIG)	25.0±0.1	74±7	34	97%
Pdf-dcr2/+;UAS-Hel25E/+	24.6±0.1	56±14	15	73%
Pdf-dcr2/Hel25E RNAi (NIG);UAS-Hel25E/+	24.3±0.1*	140±15	11	100%

Table A3.1. Knocking Down of *Hel25E* in Circadian Neurons Lengthens the Period

Different RNAi lines were tested with Pdf-Gal4 or time-Gal4. T-test was performed for testing rescue in period by compering Gal4,RNAi,UAS flies with Gal4, RANi flies. (*:p<0.05 **p<0.01, ***:p<0.005)

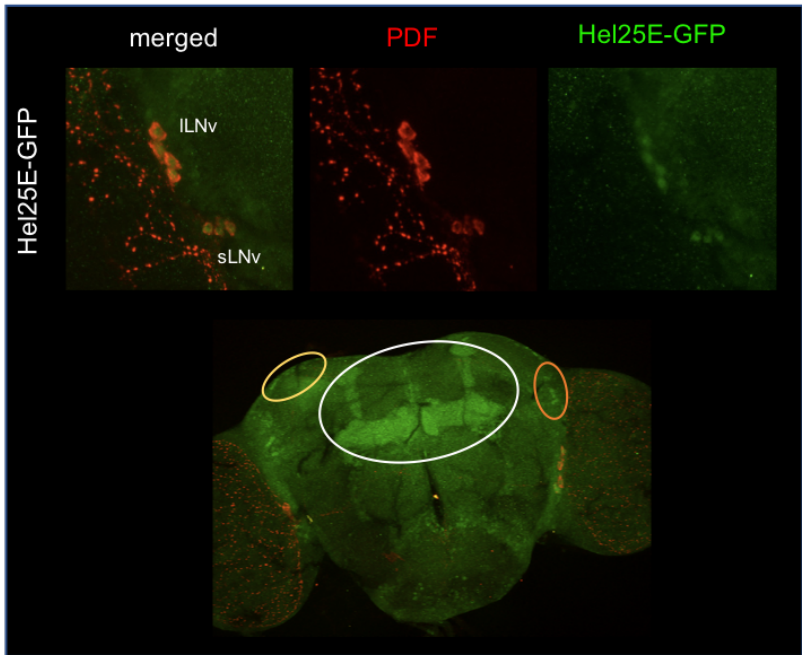

Figure A3.1. *HEL25E* Is Expressed in LNvs and Mushroom Body

Fly with genomic *Hel25E* tagged with GFP was used for dissection. HEL25E was stained with anti-GFP antibody (showed in green). GFP signals is detected in PDF positive neurons (small and large LNvs) and maybe LNds and DNs (in orange and yellow circles). GFP signal is also detected in mushroom body (white circle).

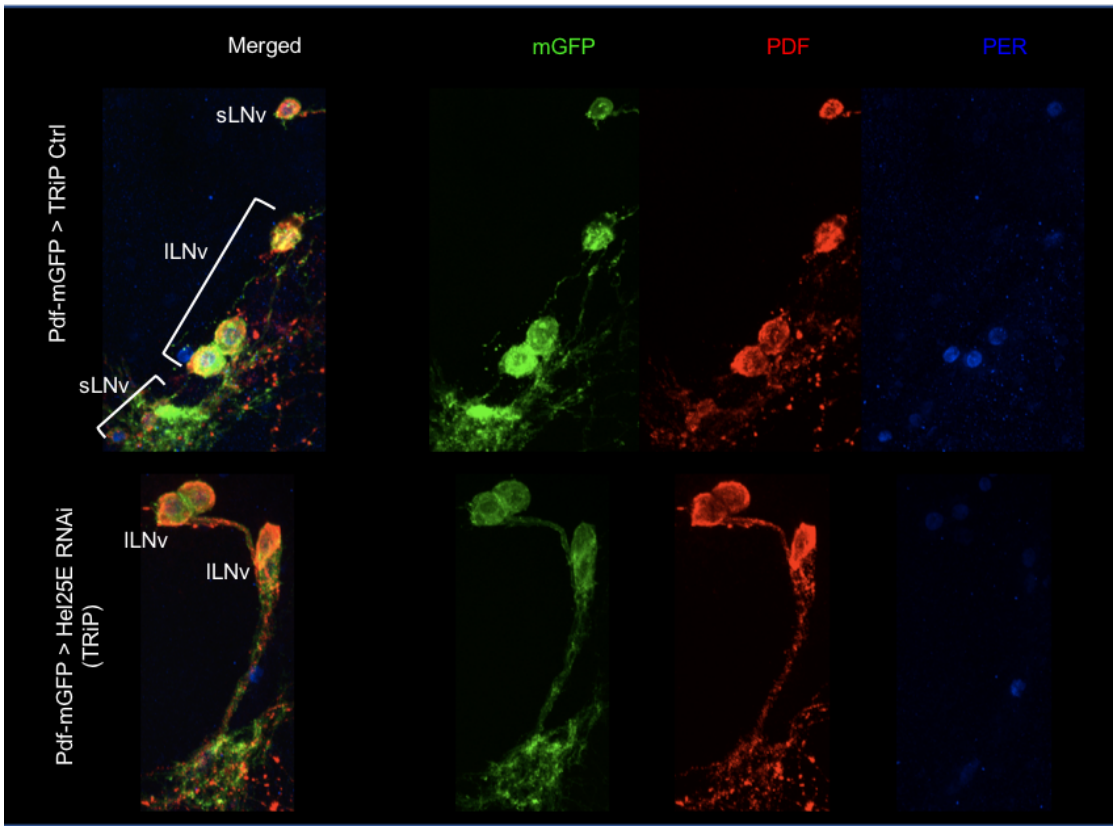

Figure A3.2. *Hel25E* Knock Down in PDF Neurons Reduces PDF Positive sLNv and PER in lLNv

Flies with PdfGal4 driving mGFP and control for RNAi or *Hel25E* RNAi were used for dissection. Flies were entrained to 12:12 LD prior to dissection and dissection was done at ZT2. sLNvs and lLNvs are labelled with mGFP (green) and stained with PDF (red). Brains are also stained with PER antibody to show PER level (blue). sLNvs are absence after Hel25E is knocked down. PER level is decreased in lLNvs when Hel25E is knocked down.

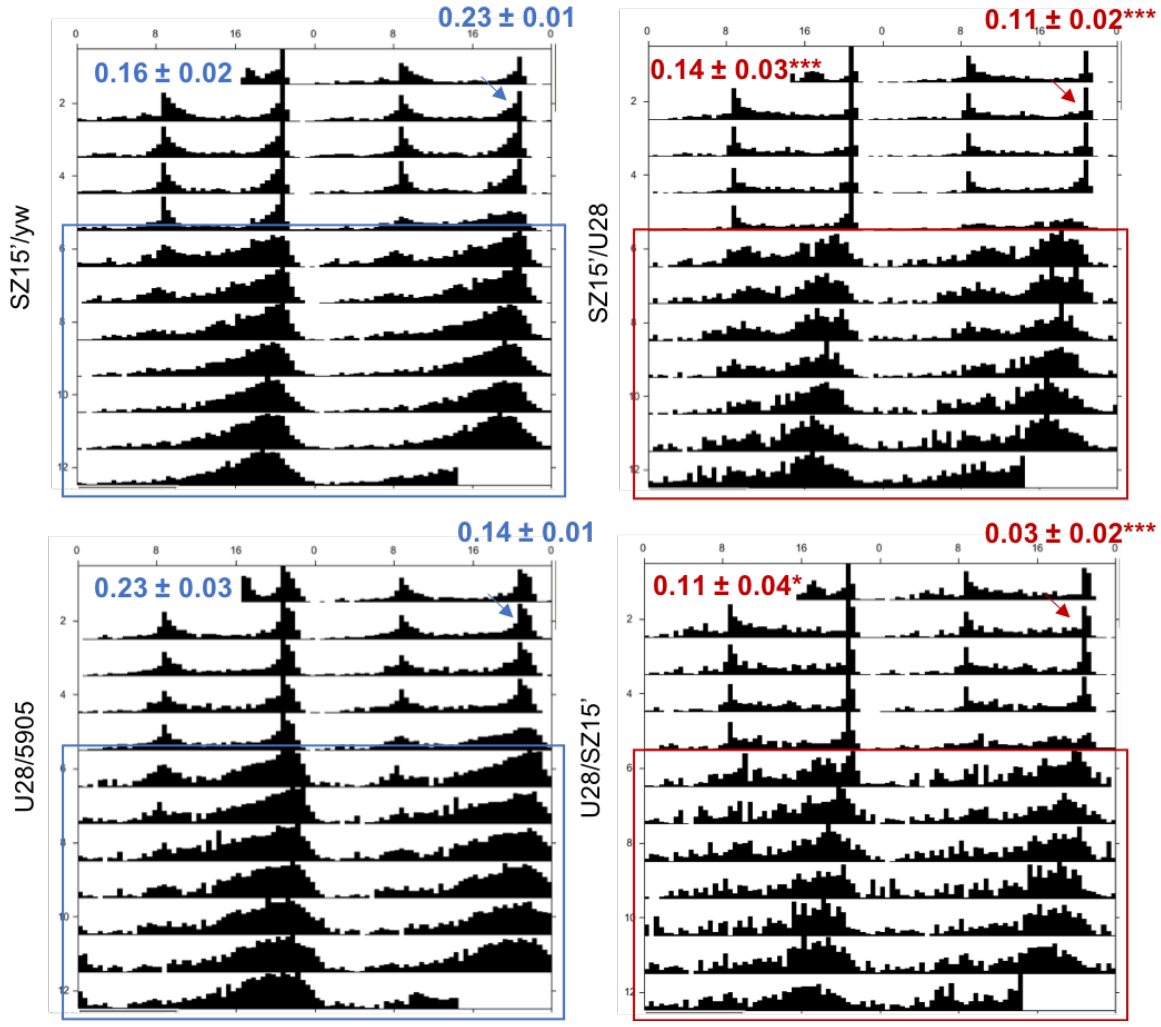

Figure A3.3. *Hel25E* Trans-heterozygous Mutant Flies Have Reduced Rhythmicity and Evening Anticipation

Flies were kept under 25 °C, 12:12LD cycle until loaded for behavior test. Flies went through 4 full days LD entrainment before released to 7 days constant darkness (total 5 days). Double plots of *Hel25E* heterozygous flies and trans-heterozygous mutant flies were shown. *Hel25E* trans-heterozygous mutant flies showed weaker rhythmicity under DD (surrounded by boxes). Evening anticipation is label with arrows. Quantification of morning or evening anticipation indexes are labelled at the morning or evening peaks. There is some reduction in the evening anticipations in trans-heterozygous mutants, especially in SZ15'/U28. Blue indicates mutant/WT control flies while red indicates mutant/mutant trans-heterozygous flies.

Reference

Kaneko, M., & Hall, J. C. (2000). Neuroanatomy of cells expressing clock genes in Drosophila: Transgenic manipulation of the period and timeless genes to mark the perikarya of circadian pacemaker neurons and their projections. *Journal of Comparative Neurology, 422*(1), 66-94. doi:Doi 10.1002/(Sici)1096-9861(20000619)422:1<66::Aid-Cne5>3.0.Co;2-2

Kota, K. P., Wagner, S. R., Huerta, E., Underwood, J. M., & Nickerson, J. A. (2008). Binding of ATP to UAP56 is necessary for mRNA export. *Journal of Cell Science, 121*(9), 1526-1537. doi:10.1242/jcs.021055

Lee, J., Yoo, E., Lee, H., Park, K., Hur, J. H., & Lim, C. (2017). LSM12 and ME31B/DDX6 Define Distinct Modes of Posttranscriptional Regulation by ATAXIN-2 Protein Complex in Drosophila Circadian Pacemaker Neurons. *Molecular cell, 66*(1), 129-+. doi:10.1016/j.molcel.2017.03.004

Lim, C., & Allada, R. (2013). ATAXIN-2 activates PERIOD translation to sustain circadian rhythms in Drosophila. *Science, 340*(6134), 875-879. doi:10.1126/science.1234785

Lin, H. F. (2012). Capturing the Cloud: UAP56 in Nuage Assembly and Function. *Cell, 151*(4), 699-701. doi:10.1016/j.cell.2012.10.026

Luo, M. J., Zhou, Z. L., Magni, K., Christoforides, C., Rappsilber, J., Mann, M., & Reed, R. (2001). Pre-mRNA splicing and mRNA export linked by direct interactions between UAP56 and Aly. *Nature, 413*(6856), 644-647. doi:Doi 10.1038/35098106

Meignin, C., & Davis, I. (2008). UAP56 RNA helicase is required for axis specification and cytoplasmic mRNA localization in Drosophila. *Developmental Biology, 315*(1), 89-98. doi:10.1016/j.ydbio.2007.12.004

Zhang, F., Wang, J., Xu, J., Zhang, Z., Koppetsch, B. S., Schultz, N., . . . Theurkauf, W. E. (2012). UAP56 Couples piRNA Clusters to the Perinuclear Transposon Silencing Machinery. *Cell, 151*(4), 871-884. doi:10.1016/j.cell.2012.09.040

Zhang, Y., Ling, J. L., Yuan, C. Y., Dubruille, R., & Emery, P. (2013). A Role for Drosophila ATX2 in Activation of PER Translation and Circadian Behavior. *Science, 340*(6134), 879-882. doi:10.1126/science.1234746

Zhao, J., Kilman, V. L., Keegan, K. P., Peng, Y., Emery, P., Rosbash, M., & Allada, R. (2003). Drosophila clock can generate ectopic circadian clocks. *Cell, 113*(6), 755-766. doi:Doi 10.1016/S0092-8674(03)00400-8

Zhao, R., Shen, J. P., Green, M. R., MacMorris, M., & Blumenthal, T. (2004). Crystal structure of UAP56, a DExD/H-Box protein involved in pre-mRNA splicing and mRNA export. *Structure, 12*(8), 1373-1381. doi:10.1016/j.str.2004.06.006

Appendix 4 Cover Design for Chapter 3

Mutant Huntingtin (devils) disrupts the circadian clock and is toxic to the circadian neurons (sLNv, the red neuron the devil is attacking). The perturbations of the circadian clock slow down the toxicity from mHtt, which is via reducing the level of a cycling gene regulated by the clock (*Hop*, shown as the bolded navy waves, dot line as reduced level).

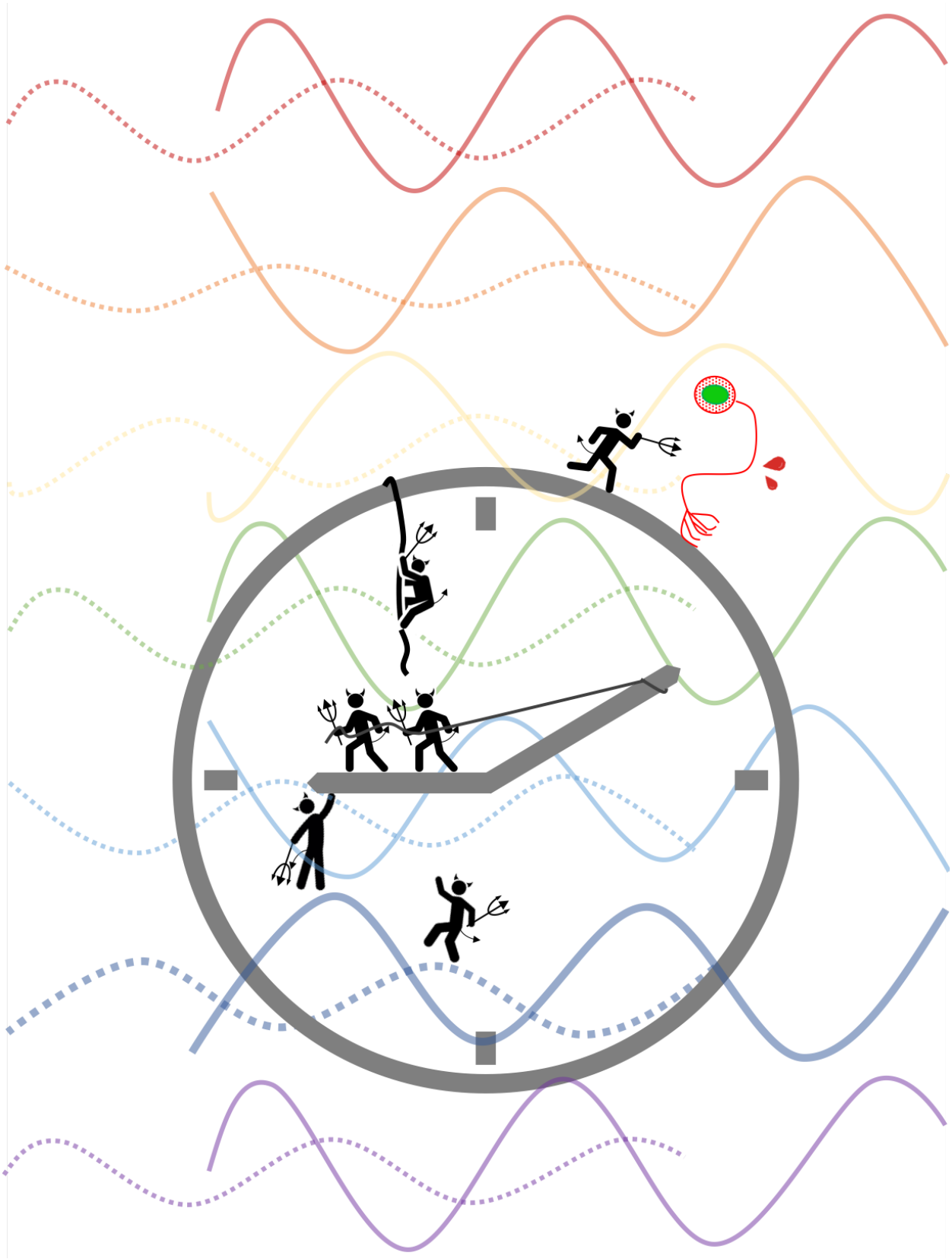

CV

Fangke Xu
1915 Maple Ave. Apt.618A Evanston, Il, 60201
E-mail: fangkexu2017@u.northwestern.edu
Mobile: 765-586-3058

Education

Northwestern University--PhD Candidate 2011-2019
Interdepartmental Biological Science PhD Program (Neuroscience)

Purdue University--Bachelor of Science (Graduation with Distinction) 2009-2011
Major: Biochemistry
Minor: Statistics

China Agricultural University--Bachelor of Science 2007-2009
Major: Biological Science

Research Experiences

Graduate Research
·2012 June -- Current, Northwestern University
Effect from Circadian Rhythms on Neurodegeneration in the Model of Drosophila

Fellowship

·2014 -- 2018, Training Grant under the Center for Sleep and Circadian Biology (CSCB), Northwestern University

Honors and Awards

·2016 Society for Research on Biological Rhythms (SRBR) Abstract Merit Award
·2015 Fellowship Award of Cold Spring Harbor Asia meeting on Biological Rhythms
·2015 TGS Travel Grant, Northwestern University
·2013 IBiS Travel Award, Northwestern University

Teaching Experience

·2012 Fall, BIOL216 Cell Biology, Teaching Assistant, Northwestern University
·2012 -- 2013, BIOL399 Independent Research, Undergraduate Student Mentor, Northwestern University
·2013 Spring, BIOL215 Genetics and Molecular Biology, Teaching Assistant, Northwestern University
·2015 -- 2017, BIOL398 and BIOL399 Independent Research, Undergraduate Student Mentor, Northwestern University

Poster Presentation

·Taichi Q Itoh, Alan Hutchison, Fangke Xu, Kevin White, Aaron Dinner, and Ravi Allada, Applications to Neurodegenerative Disease: Amyotrophic Lateral Sclerosis and Ataxin2, 2014, DARPA Biochronicity Midpoint Review, Biochronicity.
·Fangke Xu, Elzbieta Kula-Eversole, Alan Hutchison, Valerie Kilman, Aaron Dinner, Ravi Allada, Clock Control of the Heat Shock Protein Pathway Links Circadian Rhythm to Huntington's Disease in the *Drosophila* Model, 2015, Brain Research Foundation Neuroscience Day.
·Fangke Xu, Taichi Q Itoh, Elzbieta Kula-Eversole, Alan Hutchison, Peng Jiang, Kevin White, Aaron Dinner, Ravi Allada, Molecular Pathways Linking Circadian Clocks and Neurodegeneration Diseases, 2015, Cold Spring Harbor Asia Conference, Biological Rhythms.
·Fangke Xu, Taichi Q Itoh, Elzbieta Kula-Eversole, Alan Hutchison, Kevin White, Aaron Dinner, Ravi Allada, Circadian Clocks Modulate Huntington's Disease via Stress Response Pathways, 2016, Society for Research on Biological Rhythms meeting.
·Belinda S Pinto, Fangke Xu, Ravi Allada and Eric T. Wang. Understanding the Molecular Basis of Sleep Dysregulation in Myotonic Dystrophy. 2016, 4th RNA Metabolism in Neurological Disease Satellite Meeting, 11th Brain Research Conference.
·Belinda S Pinto, Fangke Xu, Ravi Allada and Eric T. Wang. Investigating the molecular basis of sleep dysregulation in Myotonic Dystrophy 2018, Society for Research on Biological Rhythms meeting.

Publications

·Fangke Xu, Elzbieta Kula-Eversole, Marta Iwanaszko, Alan L. Hutchison, Aaron Dinner, and Ravi Allada. Circadian Clocks Function in Concert with Heat Shock Organizing Protein to Modulate Mutant Huntingtin Aggregation and Toxicity. Cell Reports. 2019; 27: 59-70. (Cover)
·Bart van Alphen*, Samuel Stewart*, Marta Iwanaszko, Fangke Xu, Eugenie Bang, Sydney Rozenfeld, Anujaianthi Ramakrishnan, Taichi Q. Itoh, Rosemary, I. Braun, Ravi Allada. Glial Immune-related Pathways as Mediators of Closed Head TBI Effects on Behavior in *Drosophila*. (Submitted, preprint: doi: https://doi.org/10.1101/422535)
·Fangke Xu, Elzbieta Kula-Eversole, Marta Iwanaszko, Chunghun Lim, Ravi Allada. Ataxin2 functions via CrebA to Mediate Huntingtin Toxicity in Circadian Clock Neurons (PLOS Genetics, under revision)

Experiment Skills

·Fly genetics.
·Fly circadian and sleep test and analysis.
·Fly brain dissection, whole-mount immuno-staining.
·Confocal microscopy imaging.
·RNA extraction, amplification, qPCR, RNA immunoprecipitation.
·Genomic DNA extraction, genotyping PCR, inverse PCR.
·Molecular cloning.
·Western blot.
·RNA-seq library preparation.
·RNA-seq sequence alignment, quantification, differential expression analysis.